Groundwater flow and storage in weathered crystalline rock aquifer systems of Uganda: evidence from environmental tracers and aquifer responses to hydraulic stress

Thesis submitted for the Degree of Doctor of Philosophy of University of London

By

Callist Tindimugaya

Department of Geography
University College London

May 2008

ProQuest LLC
789 East Eisenhower Parkway
P.O. Box 1346
Ann Arbor, MI 48106-1346

I **Callist Tindimugaya**, confirm that the work presented in this thesis is my own. Where information has been derived from other sources, I confirm that this has been indicated in the thesis.

ACKNOWLEDGEMENTS

Many people and organizations have contributed in one way or another to the successful completion of this PhD research. First, I would like to thank the International Atomic Energy Agency (IAEA) for providing funding to cover tuition fees and supervision costs, my upkeep while in UK and isotope investigations in Uganda. I wish also to acknowledge the financial and material support provided by the Ministry of Water and Environment in Uganda during field data collection and for allowing me to be away from office for long periods. At University College London, I wish to acknowledge the high quality all round supervision provided by Dr Richard Taylor, Prof. John Barker and Prof. Tim Atkinson. I will always remember the many tips and suggestions they provided me especially during data analysis and writing up of the final thesis. Beyond purely academic aspects, I wish to wholeheartedly thank Dr Richard Taylor for the continuous valuable support and encouragement without which this research would not have been undertaken and completed to this standard and on record time. I would also like to thank John Chilton, Jeff Davies, Tamiru Alemayehu and Graham Brandly for independent reviews of some chapters of the thesis which helped improve the final product. Sincere thanks go to Pradeep, Kulkarni, Neil, Thoko and Andy from IAEA and Julie from British Council for their never ending encouragement and support which ensured that the research remained on course.

Within the Ministry of Water and Environment many colleagues particular Christine, Caroline, Rashid, Gastone, Francis and Leo assisted greatly in data collection and analysis and never got tired of my constant requests for additional data. I sincerely appreciate all their support and can only request them to keep up the good spirit. Many relatives and friends in London (Edith, Kenneth, Jackson, Ambrose) and

in Uganda (Milton, Lydia, Vincent, Bonny, Nicholas, John, Anthony, Connie, Aseka, Jackson, Patrick, Chris etc) kept me awake and motivated to push forward through regular emails, sms and phone calls for which I sincerely thank them all.

Undertaking PhD research while working puts high demands and extra pressure on the family. I therefore wish to sincerely thank my wife Harriet, children Bridget, Brian, Benjamin and Bruce for enduring my long absence from home and for supporting me when I needed them most. To all those who contributed to the successful completion of this research, whether mentioned or not, I salute you all and hope that you will not be disappointed by this final product.

ABSTRACT

Groundwater is widely developed for town water supplies in weathered crystalline rocks in sub-Saharan Africa but the sustainability of this abstraction is unknown. Groundwater flow and storage in aquifers underlying two towns in central (Wobulenzi) and southwestern (Rukungiri) Uganda are assessed using environmental tracers and aquifer responses to hydraulic stress. Stable isotope ratios ($^{2}H:^{1}H$, $^{18}O:^{16}O$) in precipitation and groundwater, the timely response of groundwater levels to bimodal rainfall, and short groundwater residence times of less than 22 years and big proportions of modern groundwater (5 to 100 %), derived from reconstructed atmospheric inputs of ^{3}H and anthopogenic gases (CFC-113, CFC-12, CFC-11), clearly indicate active rainfall-fed, groundwater recharge. Diagnostic plots (s versus t/r^2, log-log, log-linear, derivative, flow dimension) of drawdown responses are used to inform conceptual models of groundwater flow. In Wobulenzi, linear flow through individual bedrock fractures at early pumping times (between 600 and 1500 minutes) is succeeded by radial flow through interconnected fractures that induce vertical flow in a thick weathered (regolith) aquifer at late pumping times (approximately 1800 minutes). Groundwater abstraction from bedrock fractures of 12 $m^3 h^{-1}$ per borehole, has not significantly affected groundwater storage over the last 9 years due to vertical leakage from overlying weathered aquifers that is commensurate to rainfall-fed recharge. In Rukungiri, a highly productive aquifer comprising coarse-grained, fluvial sediments, is identified in palaeochannels of former westerly flowing river networks. Fluvial sediments can feature significant thicknesses in palaeochannels of major river networks truncated by Miocene to Pleistocene rifting but subsequent erosion in the intra-arch basin, draining to the downfaulted rift floor significantly constrains the extent and thickness of the aquifers and, hence, the sustainability of groundwater

abstraction. Depletion of groundwater storage over the last 8 years as a result of abstraction (12 m^3 h^{-1} per borehole), is indicated by water-level declines of 2.5 m a^{-1}. The identification of the palaeochannel aquifer provides new insight into the understanding of the relationship between the geomorphology and hydrogeology of deeply weathered environments and a new target for groundwater development in the humid tropics.

TABLE OF CONTENTS

LIST OF FIGURES

LIST OF TABLES

CHAPTER 1: INTRODUCTION

This chapter provides an introduction to weathered and fractured-bedrock aquifer systems and discusses the importance of the aquifers in meeting water supply needs of the rural and urban populations in developing countries with specific focus on sub-Saharan Africa. The chapter reviews the challenges of groundwater development in weathered crystalline rock aquifers and highlights the existing knowledge gaps in understanding groundwater flow and storage in these aquifers. The chapter concludes with a presentation of the rationale and aims of this research and the layout of the whole thesis.

1.1 Groundwater resources development in the weathered crystalline rock aquifer systems

Weathered crystalline rock aquifers are widely distributed thoughout the world and are vital sources of groundwater for many people in Africa, Asia and South America. Over most of sub-Saharan Africa, groundwater provides the only realistic water supply option for meeting dispersed rural demand (Macdonald *et al.*, 2005) and rapidly growing towns (Taylor *et al.*, 2004). This assertion is due, in part, to the high temporal and spatial variability in rainfall and surface water sources. Development of groundwater using low-cost, simple water-supply technologies is the focus of efforts to improve access to safe water supplies in rural areas (Republic of South Africa (RSA), 1999; Gyau-Boakye and Dapaah-Siakwan, 1999; Government of Uganda (GOU), 2001) and in small towns (Republic of South Africa (RSA), 2001; Government of Uganda (GOU), 2003). Groundwater development is however greatly influenced by variable climatic and geological conditions. About 40% of sub-Saharan

Africa is underlain by deeply weathered crystalline rocks of Precambrian age (Fig. 1.1) and is home to over 220 million people (Macdonald *et al.*, 2000).

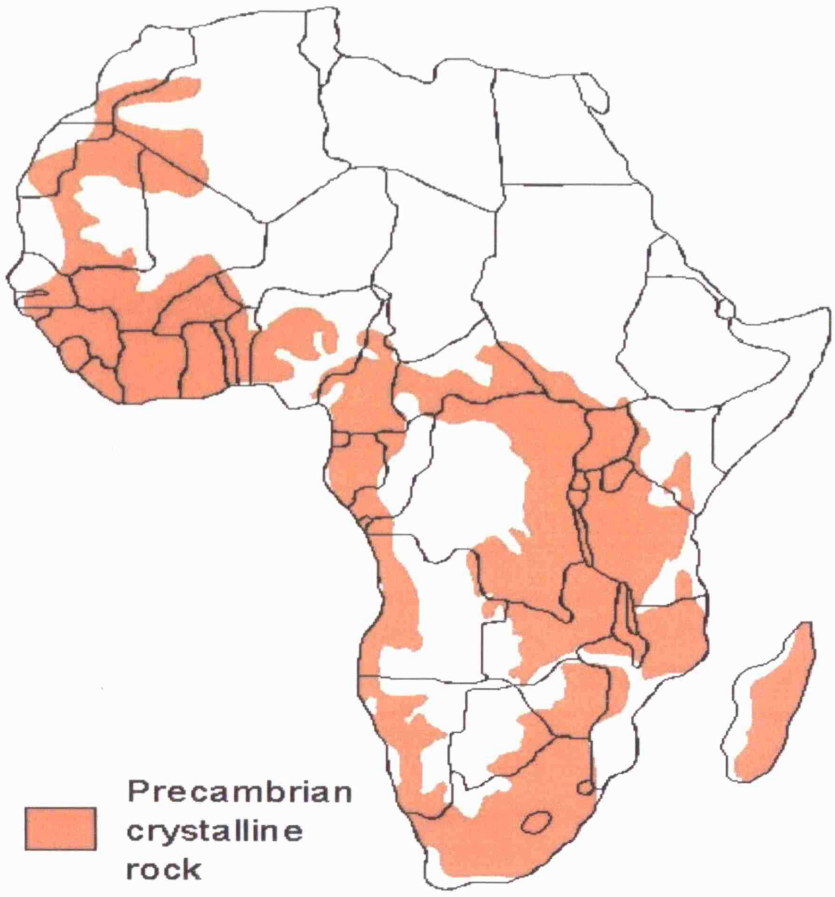

Figure 1.1. Distribution of crystalline rocks in sub-Saharan Africa (adapted from Key, 1992)

A lot of work has been carried out to understand the occurrence and movement of groundwater in crystalline rocks (e.g. Chilton and Smith-Carington, 1984; Clark, 1985; Acworth, 1985; Howard *et al.*, 1992; Howard and Karundu, 1992; Wright and Burgess, 1992; Owoade, 1995; Taylor and Howard, 1998; 1999a; 2000; Tindimugaya, 2000; Taylor *et al.*, 2001; Edet and Okereke, 2005). These studies indicate that the weathered aquifer is highly variable in thickness from a few metres to

over 90 m. It is anisotropic and characterised by permeability and porosity that vary with depth (Chilton and Foster, 1995). However, porosity and permeability of the bedrock depend on the nature of the formation and the extent of fracturing. The lithological profile of the weathered and fractured-bedrock indicates that close to the surface, there occurs a soil zone which has low porosity but high hydraulic conductivity. Although this zone may contain groundwater, its shallow nature makes it susceptible to seasonal weather changes and the water may not be available throughout the year (Chilton and Foster, 1995). Below the soil zone, a predominantly clay-rich zone exists that has high porosity but low hydraulic conductivity. This layer may form a minor aquifer if it contains sands and gravels, and can hence yield water for small water supplies. Where the thickness of this layer is fairly big, the clay layer may impede downward flow of water and hence affect recharge of the deeper aquifers. Below the clay zone and towards the base of the weathered overburden, there exists a zone of highly weathered and freshly fractured and brecciated material where the proportion of clay is very low. This zone remains poorly understood but is predicted to feature relatively low porosity but high hydraulic conductivity (Howard and Karundu, 1992; Hydrogeology-Uganda Phase II, 1994; Chilton and Foster, 1995; Owoade, 1995). The weathered overburden, whether in situ or transported, is sometimes refered to as the regolith. Below the weathered overburden and into the bedrock, fractures occur but their hydraulic conductivity depends on their aperture and interconnection. Where the fractures are wide and well interconnected, they have high hydraulic conductivity and therefore yield significant amounts of water (Hydrogeology-Uganda Phase II, 1994; Chilton and Foster, 1995; Owoade, 1995). Porosity generally decreases with depth whereas permeability is highest at the interface between the weathered overburden and the bedrock (Fig. 1.2).

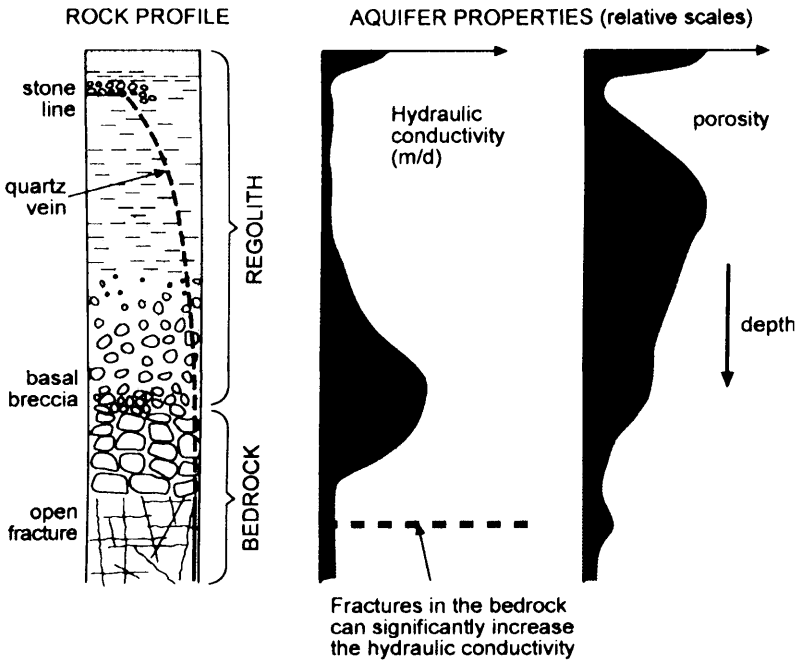

Figure 1.2. Conceptual model of the weathered and fractured bedrock aquifer system (from Chilton and Foster, 1995)

Significant well yields occur where the weathered zone is significantly developed and the bedrock is highly fractured (Wright, 1992). Key factors that contribute to the weathering of the bedrock include; geomorphology of the area, presence of fractures and lineaments, presence of water, temperature and mineralogy of the bedrock (Acworth, 1987; Macdonald *et al.*, 2001). The weathered zone therefore has generally low intrinsic hydraulic conductivity (0.5 to 10 $m \cdot d^{-1}$) but high storage (S_y = 0.20 to 0.25) (Taylor and Howard, 1998). The bedrock aquifer exhibits, on the other hand, high permeability but low bulk storage (S = 0.0001), that arise from secondary properties in the form of fractures, joints and faults (Acworth, 1987; Shapiro, 2002). A complex network of interconnected fractures in crystalline bedrock results from tectonic forces. Vertical flow is restricted by the dominance of

predominantly sub-horizontal fractures that are presumed to derive primarily from isostatic uplift associated with erosional unloading (Taylor and Howard, 2000). Packer testing of boreholes in Uganda indicates that bedrock permeability is greatest close to the interface between the bedrock and overburden but decreases with depth (Howard *et al.*, 1992; Taylor and Howard, 2000).

1.2 Conceptual models of aquifer units in weathered crystalline rocks

Groundwater development in weathered and fractured bedrock normally targets three zones: the minor aquifer formed by a mixture of sands, gravels and clays in the weathered zone, the interface between the weathered zone and bedrock, and the deeper fractured bedrock. The availability of groundwater resources within these aquifers depends on their thickness and their permeability both of which depend on the weathering histories (Macdonald *et al.*, 2001). Although occurrence of these aquifer zones is not uniform thoughout the weathered and fractured bedrock areas, Owoade (1995) proposes that the weathered- fractured bedrock aquifer generally comprises a sequence of three zones: an upper zone of weathered material, an intermediate zone of semi-weathered material, and a basal zone of fresh, but often fractured rocks. This is consistent with observations made in Uganda (Howard *et al.*, 1992; Hydrogeology-Uganda Phase II, 1994; Taylor and Howard, 2000, Tindimugaya, 2000) although the different aquifers are not universally present.

1.3 Challenges of groundwater resources development in Uganda

Uganda, like many other countries in sub-Saharan Africa is developing groundwater using low-cost, simple water-supply technologies in its efforts to improve access to safe water supplies in rural areas and small towns. The availability

of groundwater is, however strongly influenced by variable climatic and geological conditions. Aquifers primarily occur in the weathered zone and fractured crystalline bedrock of Precambrian age. Boreholes are typically installed into the fractured bedrock and the interface between the weathered zone and the bedrock; shallow wells are drilled in the weathered zone. Intensive groundwater abstraction (> 5 m^3 h^{-1} per borehole), especially for town water supplies, is restricted to areas where the bedrock is highly fractured and the weathered zone possesses moderate to high permeability and significant storage.

Although groundwater development is on a steep rise in Uganda like elsewhere in sub-Saharan Africa, it is not known whether the current, intensive abstractions (300 - 600 m^3 d^{-1}) from well fields within the weathered and fractured-bedrock aquifer systems is sustainable. Increases in population, per capita demand for water and pollution present serious challenges to the sustainability of groundwater abstraction for town water supplies. Considerable uncertainty also exists regarding vulnerability of weathered and fractured-bedrock aquifer systems to contamination from local land use practices such as sewage disposal.

1.4 Knowledge gaps and research objectives

Understanding the flow and storage properties of groundwater in the weathered and fractured-bedrock aquifer systems is key to their sustainable development and management. Current understanding of the weathered and fractured-bedrock aquifers is simplistic and largely conceptual. There is an urgent need for quantitative information regarding groundwater flow and storage. Specific knowledge gaps include circulation rates in weathered and fractured-bedrock aquifer systems and the response of weathered and fractured-bedrock aquifer systems to intensive

abstraction. Further research is required to improve understanding of the interactions between weathered and fractured-bedrock aquifers and to assess the impact of increased pumping rates from weathered and fractured-bedrock aquifer systems on the sustainability of groundwater abstraction. A major and novel contribution to the understanding of weathered and fractured-bedrock aquifers is proposed with the following aims:

1. to determine the source, timing and flow of recharge and groundwater residence times in the weathered, fractured-bedrock and fluvial aquifers;
2. to assess the flow of groundwater in weathered, fractured-bedrock and fluvial aquifers in response to hydraulic stress; and
3. to improve understanding of the relationship between observed hydrogeological characteristics and geomorphic evolution of weathered, fractured-bedrock and fluvial aquifers in Uganda.

1.5 Logical layout of dissertation

The thesis has been structured in a logical manner so that each chapter builds upon the former. Each chapter features a review of the literature relevant to its objectives and methodology. Chapter 1 provides an introduction to weathered and fractured-bedrock aquifer systems and highlights the aims of the research. Chapter 2 describes the overall methodological approach and study areas. Chapter 3 assesses the source, timing and dynamics of groundwater recharge using environmental isotopes and hydrochemistry. Chapter 4 assesses the geometry of the aquifers and the responses of groundwater levels to rainfall and intensive groundwater abstraction. Chapter 5 assesses the responses of the fluvial, weathered and fractured-bedrock aquifers to pumping, characterises the aquifer systems in terms of aquifer geometry and groundwater flow using Aquifer Diagnostic Methods and estimates aquifer

hydraulic properties using appropriate interpretation methods. Chapter 6 assesses groundwater residence times in weathered, fractured-bedrock and fluvial aquifers based on environmental tracers. Chapter 7 presents revised conceptual models of the evolution of weathered, fractured-bedrock and fluvial aquifers in Uganda. Chapter 8 presents the conclusions and recommendations of the study highlighting the key contributions to the understanding of the hydrogeology of weathered crystalline rock aquifers.

CHAPTER 2: RESEARCH METHODOLOGY AND CATCHMENT STUDY AREAS

This chapter provides an overview of the methods and datasets employed in this research and presents a rationale for the experimental design. The chapter also describes the catchment study areas reviewing their geology, climate, topography, and hydrology.

2.1 Methodology

This research employs diverse methodologies and develops a range of datasets to characterise both static and dynamic characteristics of groundwater flow and storage in weathered crystalline rock aquifers of Uganda (Fig. 2.1). Field data collection tasks carried out include; geophysical surveys to determine the lateral and vertical extent of aquifers; piezometer construction around production boreholes to assess responses of aquifers to recharge and abstraction; long duration pumping tests to assess groundwater flow and storage; monitoring and sampling of various water sources for environmental stable isotopes and hydrochemistry and spot sampling for chlorofluorocarbons (CFC) to assess groundwater flow and residence times. Borehole logs and geophysical survey data are used to determine the geometry of the aquifer ('aquifer architecture"). Pumping tests, borehole hydrographs and environmental tracers are employed to assess groundwater flow and storage in the aquifers. These data sets made it possible to test the reliability of the aquifer architecture and to develop conceptual models of groundwater flow. Knowledge of aquifer architecture and groundwater flow forms a basis for assessing the evolution of weathered and fractured-bedrock, and fluvial aquifers in Uganda. Combining all the information on aquifer architecture, groundwater flow and aquifer

evolution leads to evaluation of the implications for groundwater development and management in the weathered crystalline rock aquifers of Uganda.

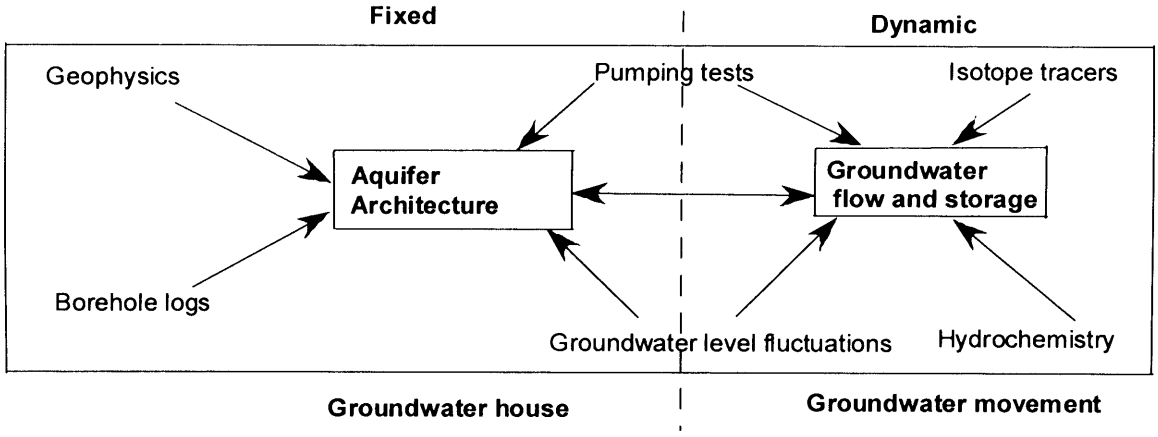

Figure 2.1. Methodological approach to the research

This doctoral research was undertaken within the framework of the International Atomic Energy Agency (IAEA) funded project "Isotopes in Management of Town Water Supplies in Southwestern Uganda", that was initiated in 2003 and will end in 2008. The PhD candidate executed all the research activities but substantial assistance in the execution of field activities was provided by staff of the Directorate of Water Resources Management. The doctoral research also takes advantage of datasets (borehole hydrographs, borehole drilling logs, isotope and hydrochemical data) recently generated through improved monitoring activities and infrastructure in Uganda funded by the Governments of Uganda and Denmark.

2.2 Study areas

2.2.1 Overview

The study has been carried out in two areas with contrasting geomorphic settings namely; River Kigwe catchment in central Uganda and River Mitano catchment in southwestern Uganda (Fig. 2.2). River Kigwe catchment is located in an area of low relief characterised by deep weathering of the bedrock whereas River Mitano catchment is located in an area of steep surface gradients characterised by erosion of weathered landsurfaces. The study has been carried out on two scales; sub-catchment and town scales. The sub-catchment scale assessment in River Kigwe catchment covers an area of approximately 50 km^2 whereas in River Mitano catchment, the sub-catchment occupies 220 km^2 out of 2095 km^2. The town scale studies were carried out in one major town in each of the catchments where groundwater is intensively abstracted for each town's water supply. Town-scale investigations in River Kigwe catchment were carried out in Wobulenzi town, around a production borehole used for town water supply. The area investigated covers approximately 800 m^2. The town scale investigations in River Mitano catchment were carried out in a wellfield in Rukungiri town, where boreholes for town water supply are constructed. The area investigated covers approximately 300,000 m^2.

The main aim of the sub-catchment scale studies was to assess groundwater recharge processes and flow so as to evaluate the sustainability of groundwater development in the catchments. The aims of the town scale studies were to assess in detail the geometry of the aquifers, their responses to precipitation and abstraction, and the nature of groundwater flow and storage in the aquifers. It was assumed that the results of detailed investigations at each specific site would be representative of the whole

catchment. Details of the catchment scale and town scale studies are presented in Chapter 3 and Chapter 4 respectively.

In addition to detailed studies carried out in the two towns, supplementary but less detailed studies were carried out in seven other areas (Ntungamo, Lukaya, Mubende, Hoima, Iganga, Aroca and Nyabisheki) with similar geomorphologic and hydrogeological conditions (Fig. 2.2). This was aimed at verifying and substantiating the findings of the detailed studies and placing them into a wider context.

2.2.2 River Kigwe catchment

The River Kigwe catchment is located approximately 60 km north of Kampala, the capital city of Uganda, at latitude 00°43'N and longitude 32°32'E. It is found in Katikamu County of Luwero District and covers an area of approximately 50 km^2. In June 2006, the population of Luwero District was estimated to be about 310,104 people (MWE, 2006) with the rural population constituting over 90% of this total whereas the urban dwellers constitute less than 10% of the population. Luwero district has a low population density (<100 people per km^2) with a population growth rate of 2.2% per annum and an urbanisation rate of 3.8%. The percentage of the population with access to improved water supply is estimated to be 77% (MWE, 2006). Safe water supplies are almost entirely based on groundwater from shallow wells, deep boreholes and a few springs. River Kigwe catchment has a population of about 40,000 people most of whom are concentrated around the major town, Wobulenzi and surrounding centres. River Kigwe catchment drains into Sezibwa River located at an elevation of 1050 mamsl which later flows into River Kafu. Catchment elevations between the mouth and source of River Kigwe vary between 1050 and 1160 mamsl. Mean daily minimum and maximum

temperatures range between 18 and 28^{0}C. Figure 2.2 shows the location in Uganda of the River Kigwe catchment.

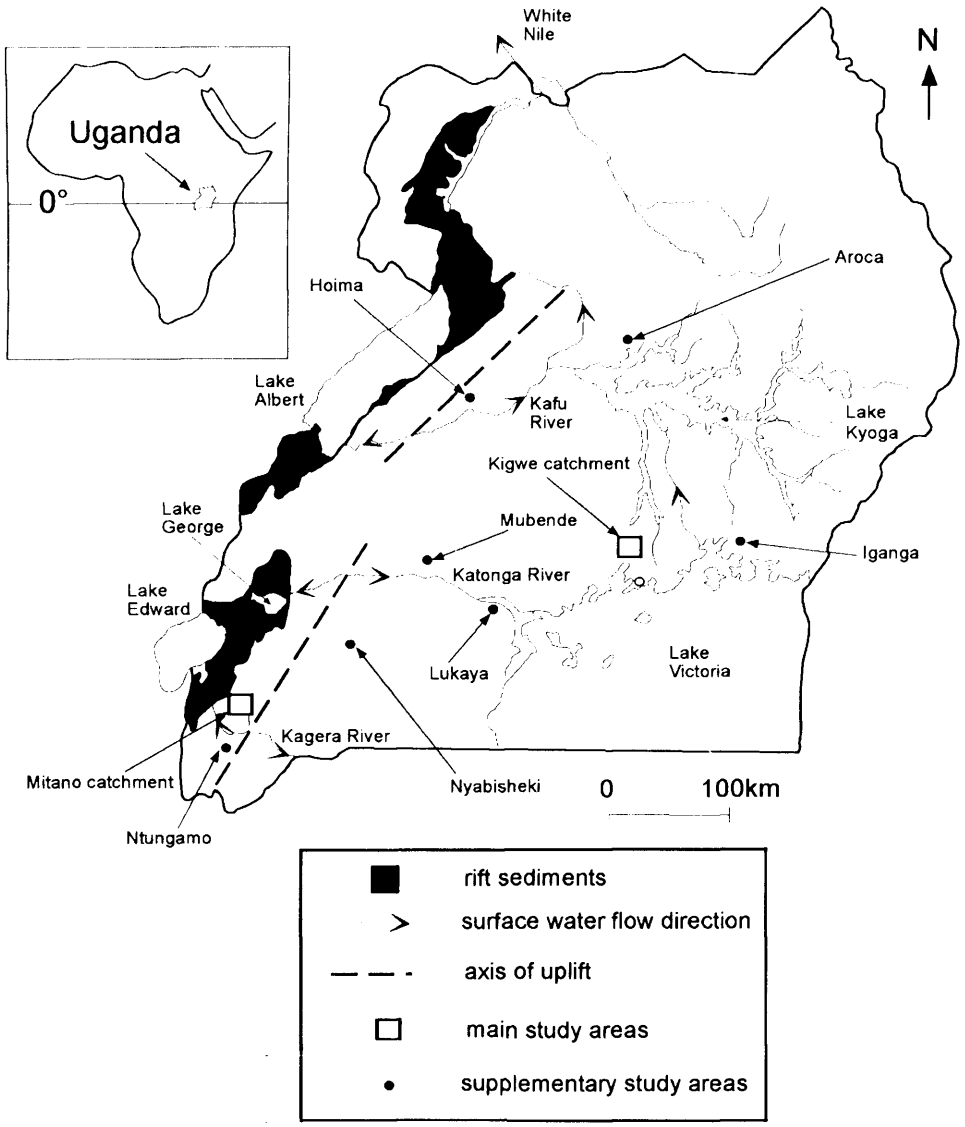

Figure 2.2. Location of the main study areas and supplementary study sites

2.2.3 River Mitano catchment

The River Mitano catchment is located approximately 400 km from Kampala, the capital city of Uganda, at latitude 00°43'S and longitude 30°E. The entire River Mitano catchment covers an area of approximately 2098 km^2 (Mileham, 2007). In this study, a sub-catchment of approximately 220 km^2 is the focus of detailed investigations. The sub-catchment is found in Rujumbura county of Rukungiri district. In June 2006, the population of Rukungiri district was estimated to be about 320,422 people (MWE, 2006) with the rural population constituting over 90% of this total. Rukungiri district has a population density of 220 people per km^2 with population growth rate of 2.5% per annum and an urbanisation rate, similar to the rest of the country, estimated to be 3.8%. The percentage of people with access to improved water supply is 88% (MWE, 2006) and depends almost entirely on groundwater from numerous springs and a few boreholes. The River Mitano sub-catchment has a population of about 80,000 people most of whom live in urban centres such as Rukungiri town and a few trading centres. The catchment drains into Lake Edward in the western (Albertine) rift valley at an elevation of 913 mamsl. The catchment elevations between the mouth and the source of River Mitano vary between 913 and 2,500 mamsl. Mean daily minimum and maximum temperatures range between 16 and 30 ^{0}C. Mean minimum temperatures are directly related to altitude and are lower on hills than in valleys. Figure 2.2 shows the location in Uganda of River Mitano catchment.

2.3 Geological setting

2.3.1 Geology of Uganda

The geology of Uganda is dominated by Archean and Proterozoic rocks which underlie more than two thirds of the country (Schlüter, 1997). Apart from archean rocks of high grade metamorphism, referred to by Schlüter (1997) as "Gneissic-Granulitic Complex", three major Proterozoic belts underlie Uganda: the Paleoproterozoic Buganda-Toro metasediments, the Mesoproterozoic Karagwe-Ankolean (Kibaran) and the Neoproterozoic Mozambique belt (Fig. 2.3). Tabular Neoproterozoic sediments are also widespread as are Tertiary to recent sediments that have filled parts of the down-faulted Albertine Rift Valley in the west of the country. Tertiary carbonatites and Cenozoic volcanics related to rifting occur along the eastern and western borders of the country.

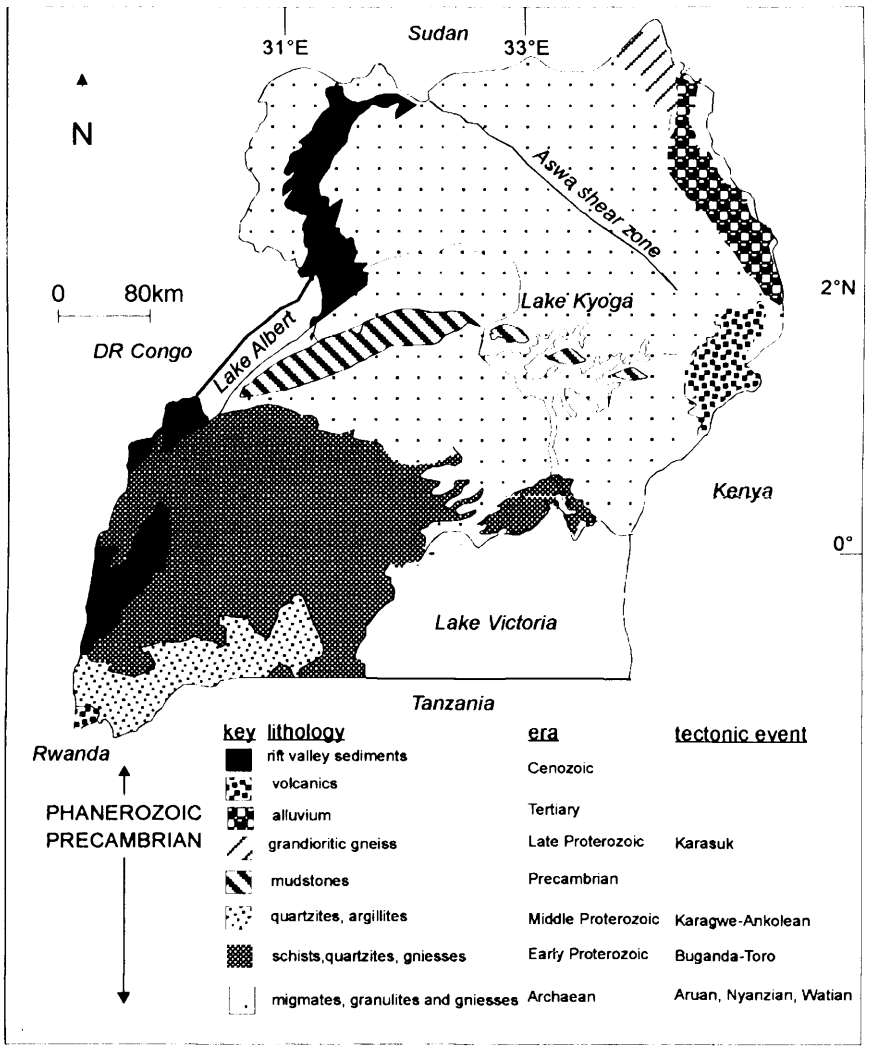

Figure 2.3. Generalised Geological map of Uganda (Modified after Schlüter, 1997, and Taylor and Howard, 1998)

The Archean "Gneissic-Granulitic Complex" rocks, also called the "Basement Complex" rocks, underlie most of the northern and central regions of the country (Bjørlykke, 1975; Schlüter, 1997). These rocks have smaller rock units embedded into them: the Watian, Aruan and Mirian Groups occurring in the north-western parts of the country and the Central Karamoja Gneiss Groups occurring in north-eastern Uganda. The rocks consist predominantly of biotite gneisses, banded, migmatic and granitic gneisses

with little hornblende gneiss, amphibolites, quartzites and very few ultrabasic rocks. The Neoarchean Nyanzian system, that is not appreciably regionally metamorphosed, occurs in south-eastern Uganda and comprises mainly of rhyolites, porphyrites, tuffs and basalts.

The Buganda-Toro system underlies much of the south-central and western parts of the country and is composed of phyllites, quartzites, schists and gneisses. The rocks of the Toro Group are characterised by a higher grade of metamorphism than the Buganda Group and metamorphism increases westwards (Schlüter, 1997). The Toro rocks are more complex and have different lithology compared with the Buganda Group. Prominent in the Buganda-Toro system are the Igara Schists in south-western Uganda composed mainly of quartzites, mica schists and gneisses; the Bwamba Pass series of the Rwenzori mountains, made up of grits, sandstones, slates and phyllites and the Kilembe series of Toro. The Karagwe- Ankolean system rests unconformably on the Buganda-Toro system in the south-west. Karagwe- Ankolean rocks are composed of quartzites, hematitic sandstones, conglomerates, shales, phyllites, gniesses and schists. The rocks are less metamorphosed than the Buganda-Toro system with many parts completely unmetamorphosed.

The Karasuk Group that is part of the Neoproterozoic Mozambique belt, occupies a small track of land in the north-east of the country, along the Uganda-Kenya border (Goodwin, 1991; Schlüter, 1997) and is composed of a mixture of gneisses, amphibolites, marbles, quartzites and utramafic rocks. The Tabular Neoproterozoic rocks include the Bunyoro series and the undeformed shallow water sediments of the Bukoban supergroup such as Singo and Mityana series (Schlüter, 1997). Bunyoro series rocks occupy a small part of the country in central Uganda and are predominantly argillaceous, with pebbly

beds occurring locally and tillite occurring at the base of the system (Bjørlykke, 1975). The Singo and Mityana series occur in the southern and western parts of the country and are both arenaceous and unmetamorphosed, possibly representing molasses-type deposits. Miocene volcanic rocks denoted topographically by prominent mountains of the southern Karamoja region outcrop in many areas in eastern Uganda along the Kenyan border. Carbonatite complexes representing eroded remnants of volcanoes occur in a number of locations in eastern Uganda. Other Cenozoic rocks are either sedimentary or volcanic in origin and are found in the western Albertine Rift Valley. These sediments are often fossiliferous and have thicknesses than exceed 4000 m.

2.3.2 Geology of the River Kigwe catchment

The River Kigwe catchment is found within the Archean "Gneissic-Granulitic Complex underlain by high-grade metamorphic rocks that are composed of biotite gneisses, banded, migmatic and granitic gneisses (Schlüter, 1997). Although the geology of the Archean belt is not well understood (Bjørlykke, 1975; Schlüter, 1997), previous studies based on geological maps, field mapping and borehole logging identified the main geological units in the River Kigwe catchment (Tindimugaya, 2000). Four major geological units were identified (Fig. 2.4): granites, schists, gneisses and quartzites. Granites and gneisses are distributed all over the catchment and occupy about 60 % of the total area. Small bands of quartzites are found in the eastern and north-western parts of the catchment and cover about 8% of the catchment. Schists are found in the eastern and north-western parts of the catchment alongside quartzites and cover approximately 15% of the catchment. Alluvium occupies approximately 17% of the catchment. According to

Tindimugaya (2000), fractured quartzite and weathered granite comprise the main aquifers of the area.

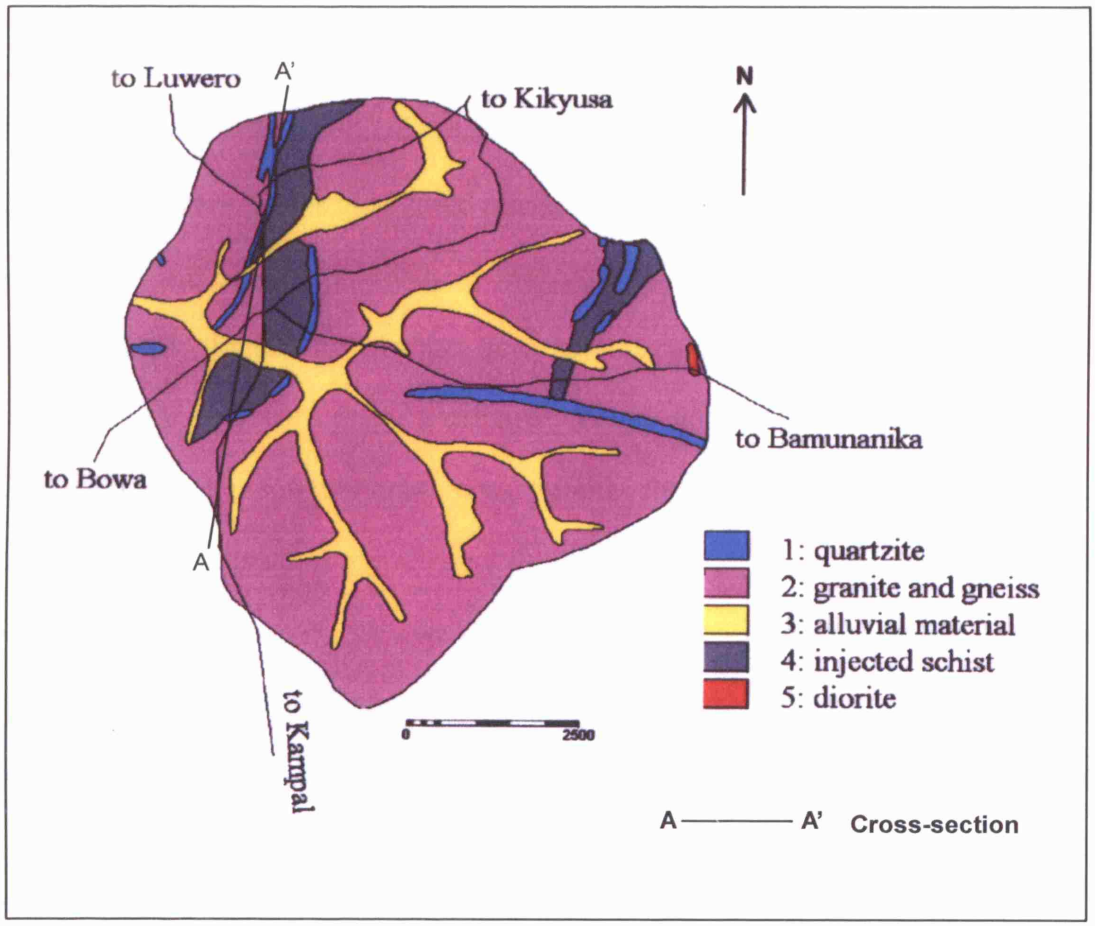

Figure 2.4. Distribution of geological units in the River Kigwe catchment (Adapted from Tindimugaya, 2000)

2.3.3 Geology of the River Mitano catchment

The River Mitano catchment is underlain by low-grade metasediments of Karagwe-Ankolean system. These rocks are characterised by phyllites, schists, gneisses, shales and quartzites (Doorkamp, 1968). Karagwe-Ankolean rocks are highly resistant to

weathering resulting in high topography. However, schists and gneisses are less resistant to weathering and form low lying areas where they are predominant in the catchment. Over 70% of the River Mitano catchment is underlain by refoliated gneisses that occur with localised pockets of quartzites and amphibolites probably derived from basaltic material (Fig. 2.5). The refoliated gneisses respond variably to weathering and form conspicuous hills and ridges around the catchment where pockets of quartzites occur. In western areas and along River Mitano, the catchment is underlain by more resistant bedrock probably formed by phyllites with quartizitic bands (Doorkamp, 1970) that occupy approximately 10% of the catchment. To the north-east and north-west of the catchment, schists composed of muscovites, sericites and quartz occupy about 10% of the catchment. These formations are resistant to weathering forming due to the presence of resistant quartz and so form conspicuous ridges. Alluvial sediments arising from the erosion of the weathered rock and deposition along river channels, valleys and wetlands occur all over the catchment and are composed of a mixture of sand, clays and gravels. They cover about 10% of the catchment.

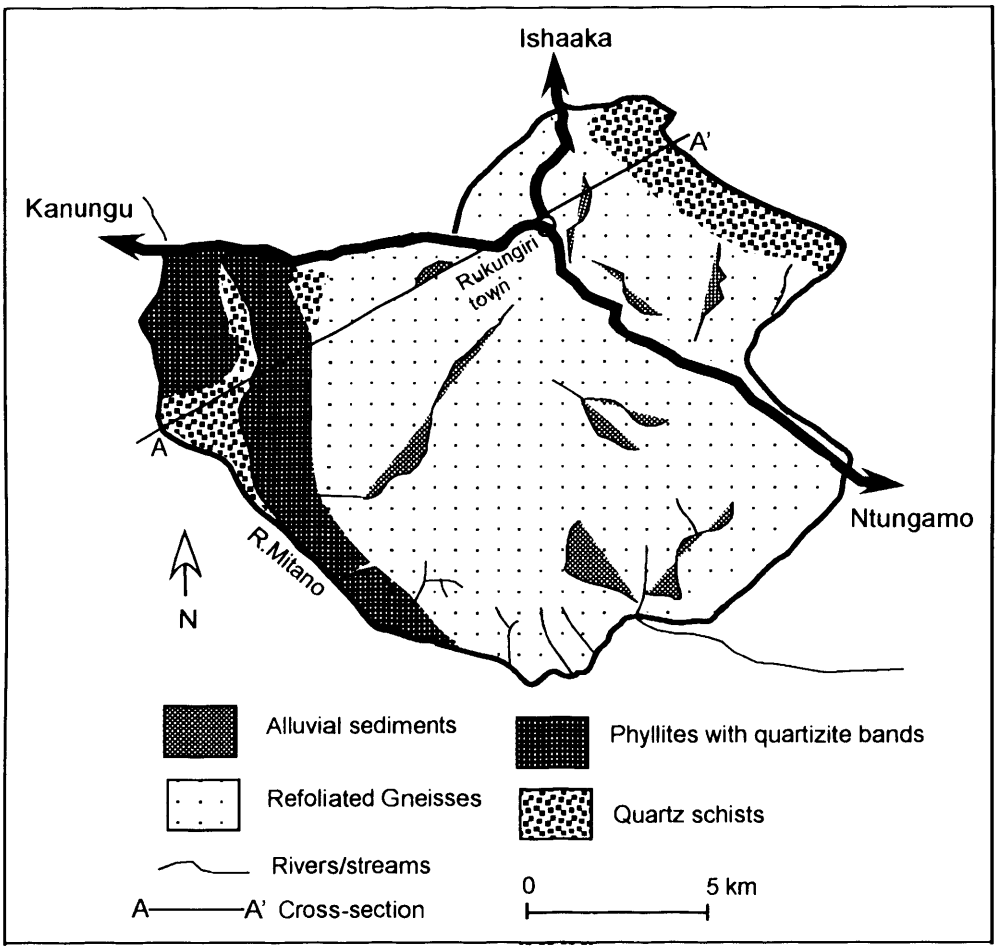

Figure 2.5. Distribution of geological units in the River Mitano catchment

2.4 Catchment hydrology

2.4.1 Rainfall

Rainfall in Uganda exhibits spatial and temporal variability due to changes in altitude and the influence of regional and local factors. Mean annual rainfall in Uganda is 1200 mm and rainfall is controlled by a number of systems that include the inter-tropical convergence zone (ITCZ), the subtropical anticyclones, monsoonal winds, the moist westerlies from Congo and several other regional and local factors (Basalirwa, 1995).

Basalirwa (1995) categorises the rainfall distribution patterns over Uganda and many parts of East Africa into four broad seasons with specific characteristics. Season 1 which is a dry period starts in December and ends in February of the following year and occurs when the ITCZ is south of East Africa. Precipitation during this period is associated with locally recycled moisture (e.g. Lake Victoria). Season 2 starts in March and ends in May when the northern movement of the ITCZ brings moist south-east monsoons from the Indian Ocean. Season 3 is generally dry except in the northern part of Uganda. It starts in June and ends in August when the ITCZ is just north of East Africa. Basalirwa (1995) suggests that the rains in northern Uganda that fall during this season originate from the moist westerly Congo air mass controlled by the St. Helena highs centred off south-west Africa. Season 4 starts in September and ends in November when southward movement of the ITCZ brings the north-east monsoons controlled by the subtropical anticyclones over the Azores and the Arabian peninsula. Basalirwa (1995) delineated Uganda into 14 homogeneous climatological zones based on spatial and temporal distribution of rainfall. The zones represent areas with similar temporal rainfall variability (Fig. 2.6).

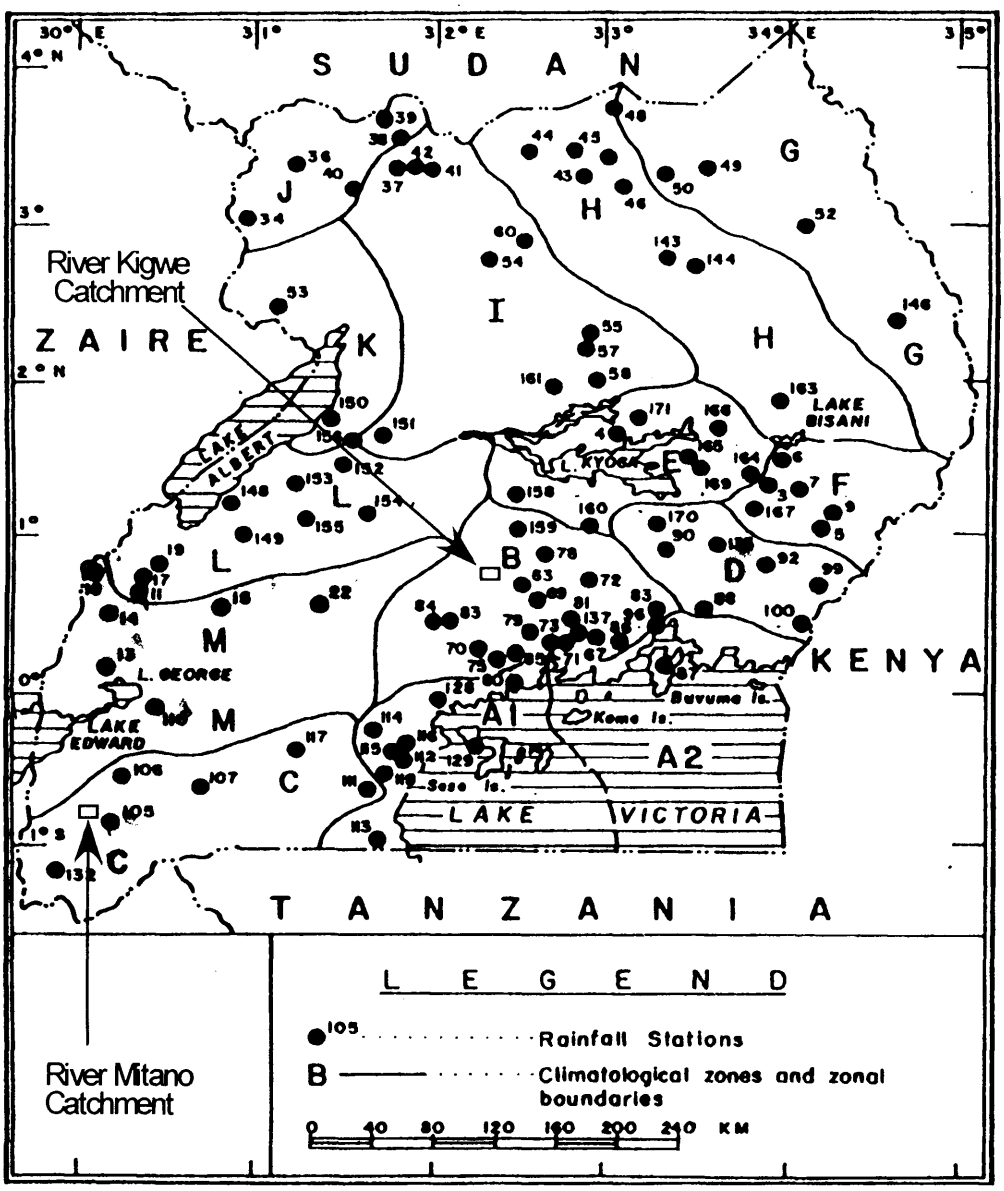

Figure 2.6. Climatological zones of Uganda (adapted from Basalirwa, 1995)

2.4.1.1 River Kigwe catchment

The mean annual rainfall in the River Kigwe catchment measured at Bukalasa Agricultural College (32°32'E, 00°44'N) for the period 1970 to 2000 is 1200 mm. Rainfall exhibits a bi-modal distribution (Fig. 2.7) with wet seasons occurring between

March and May and September and November. Mean annual pan evaporation measured at Namulonge Agricultural Research Station (32°30'E, 00°41'N) approximately 20 km to the southwest of the catchment, for the period 1970 to 1981 is 1500 mm. Monthly pan evaporation exceeds precipitation (Fig. 2.7) in almost all the months except a few wet season months.

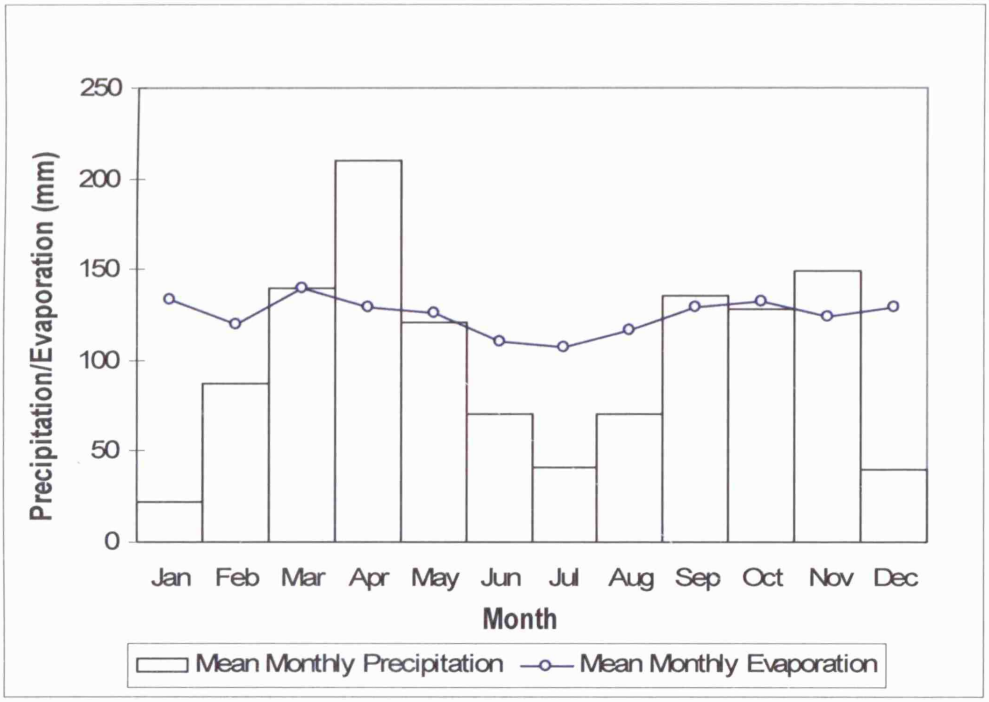

Figure 2.7. Distribution of rainfall and pan evaporation in the River Kigwe catchment

2.4.1.2 River Mitano catchment

The mean annual rainfall in the River Mitano catchment measured at a number of stations within in the catchment, for the period 1965 to 1979, is 1200 mm. Rainfall exhibits a bi-modal distribution (Fig. 2.8) with wet seasons occurring between March and May and September and November. Mean annual pan evaporation measured at Mbarara,

approximately 50 km to the east of the catchment is 1500 mm. Monthly pan evaporation exceeds precipitation (Fig. 2.8) in almost all the months except a few wet season months.

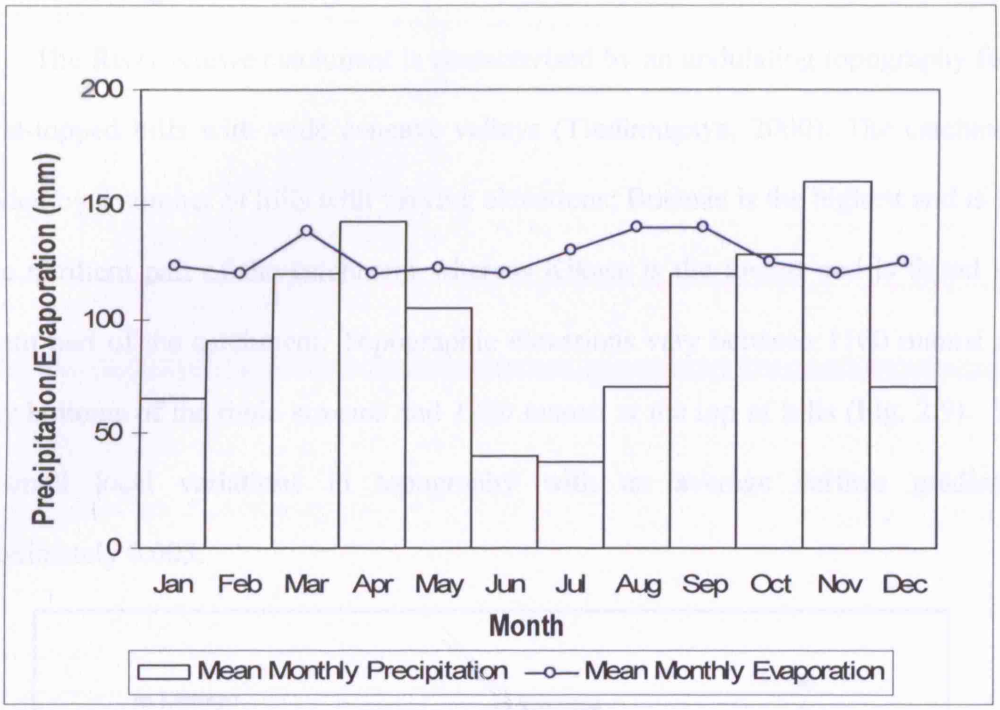

Figure 2.8. Distribution of rainfall and pan evaporation in the Mitano River catchment

The Rivers Kigwe and Mitano catchments fall in climatological zones B and C respectively (Fig. 2.6) where mean annual rainfall is around 1200 mm and the rainfall distribution exhibits a bimodal distribution. Thus, the two catchments are similar in terms of both total annual rainfall and seasonal distribution.

2.4.2 Topography

2.4.2.1 River Kigwe catchment

The River Kigwe catchment is characterised by an undulating topography formed by flat-topped hills with wide concave valleys (Tindimugaya, 2000). The catchment is bounded by a number of hills with varying elevations; Butanza is the highest and is found in the northern part of the catchment whereas Kikasa is the lowest and is found in the western part of the catchment. Topographic elevations vary between 1100 mamsl at the valley bottoms of the main streams and 1280 mamsl at the top of hills (Fig. 2.9). There are small local variations in topography with an average surface gradient of approximately 0.003.

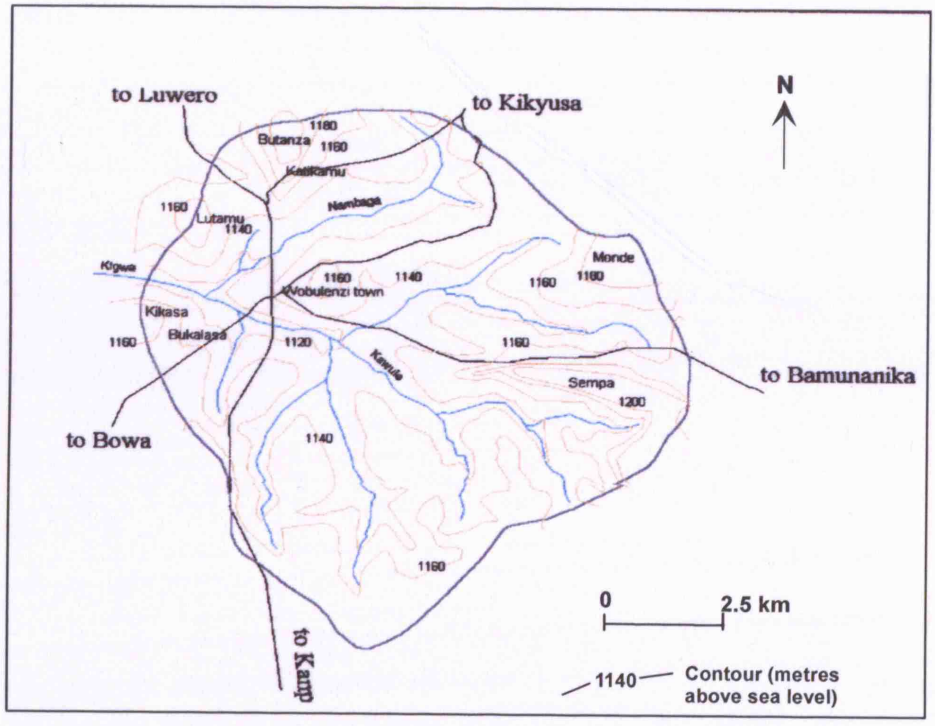

Figure 2.9. Topographic map of the River Kigwe catchment showing the drainage and road network

2.4.2.2 River Mitano catchment

The River Mitano catchment is characterised by an undulating topography with narrow convex valleys filled with swamp sediments and alluvium deposits of recent age. Topographic elevations in the catchment vary between 1190 and 1900 mamsl (Fig. 2.10). There are variations in topography with an average surface gradient of approximately 0.01. The topography in the north-eastern and western part of the catchment dips steeply in the south-western direction towards the River Mitano. Topography in the central and southern parts of the catchment varies gently and has lower topographic gradients. As a result of the steep topography, valley side springs are a very common phenomenon in this area as well as fast flowing streams.

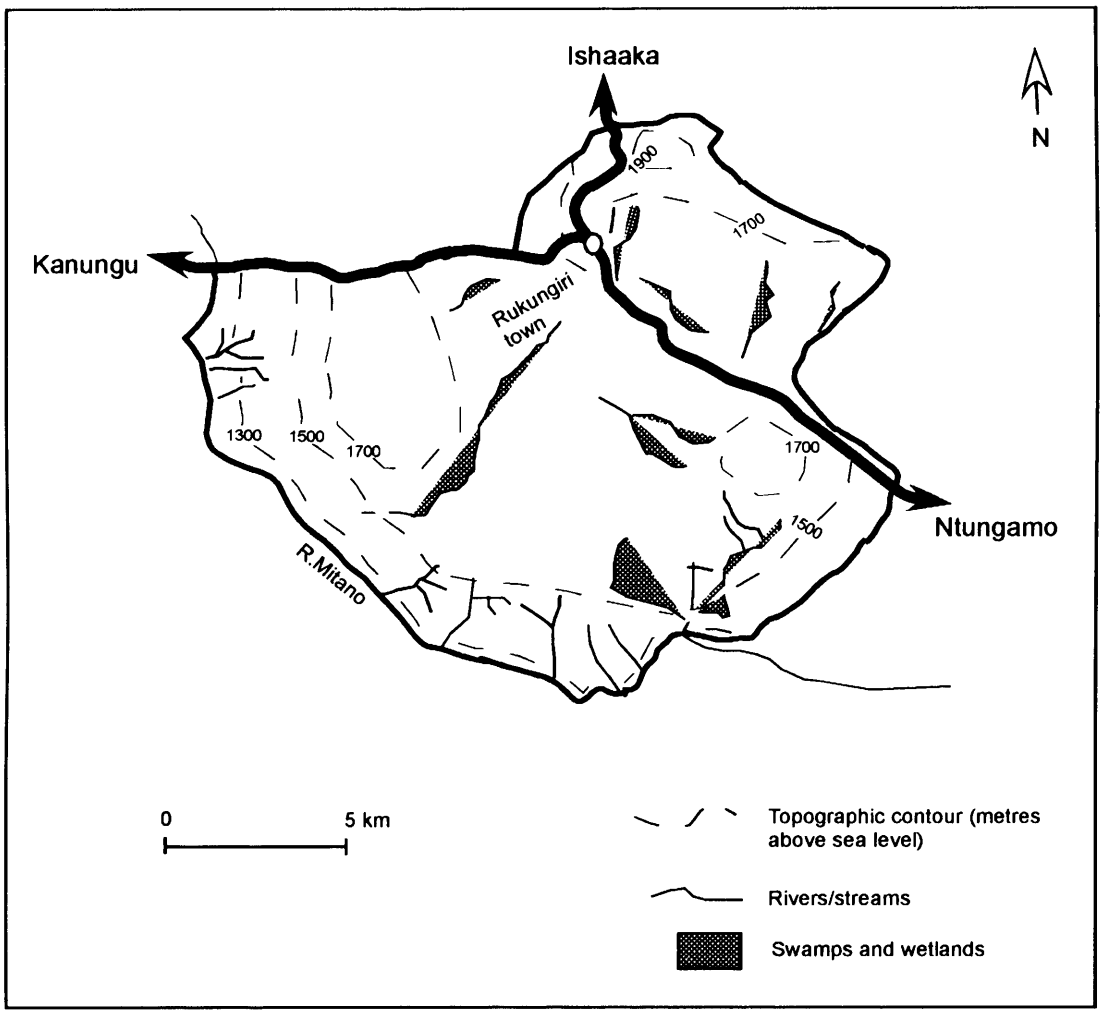

Figure 2.10. Topographic map of the River Mitano catchment showing the swamps and road network

2.4.3 Soils

Soils are strongly influenced by the underlying geology and geomorphic history. Soils in the River Kigwe catchment derive from Pre-Cambrian granitic gneiss and associated saprolite, with upland areas underlain by dismantled ferricrete (Brown, 2007). Groundwater level fluctuations result in a well-defined catenary soil color gradation associated with local elevation above the valley floor. Dark sandy clays are found in the seepage zones at the valley bottoms whereas grey loam sand overlying sandy clays are

found in areas of low reflief. Yellow sands are found on the sloping wetland margins whereas more weathered, kaolinitic, red sandy loam to clays are characteristic of the topographically raised grounds.

Soils in the River Mitano catchment are formed from the weathering of Karagwe-Ankolean rocks (Doorkamp, 1968). *In situ* weathering results in a well-defined soil color gradation whereas erosion and deposition result in a mixture of soil types. Weathered, kaolinitic, brown sandy loam and clays are found on raised grounds whereas sand, clays and gravels mixed in different proportions are found in valley bottoms, edges of wetlands and along river channels (Doorkamp, 1970).

2.4.4 Vegetation

Vegetation in Uganda varies greatly due to human influence. Apart from the protected forests, natural vegetation in many places has been modified due to agriculture and other economically driven landuse practices (Marchant and Taylor, 1997). Within the River Kigwe catchment, vegetation is dominated by grass, banana plantations, maize and coffee trees. On the edge of the hills around the catchment, thick vegetation can be found made up of broad-leaved hardwood trees. Eucalyptus trees are found in low lying areas close to the swamps. Along river channels and wetlands protected from human interference, mainly found in the lower parts of the catchment, papyrus is the dominant vegetation.

Within the River Mitano catchment, there is a lot of pressure on land due to high population density and much of the natural vegetation has been destroyed. Thus, the vegetation cover is dominated by grass, banana plantations and eucalyptus trees for

building poles and firewood. Papyrus swamps are found all over the catchment along river channels but many of these are being drained for agriculture and cattle rearing. Most of the wetlands are natural sponges and reservoirs in which run-off and seepage accumulate. Wetlands in the catchment are sources of many small rivers and streams and serve to regulate discharges resulting in small variations in discharges out of the catchment.

2.4.5 Surface water resources

2.4.5.1 River Kigwe catchment

The River Kigwe is the main drainage channel of the River Kigwe catchment and is the base level of drainage for the entire catchment. The drainage network is dendritic and supplied by two perennial streams; Kigwe and Nambaga that combine to form the River Kigwe. The discharge of the River Kigwe fluctuates greatly during the year and from year to year (Fig. 2.11) due to evapotranspiration from the papyrus swamps found upstream of the gauging station. The mean annual discharge of the River Kigwe measured at the gauging station at the outlet of the catchment is 0.05 $m^3 s^{-1}$.

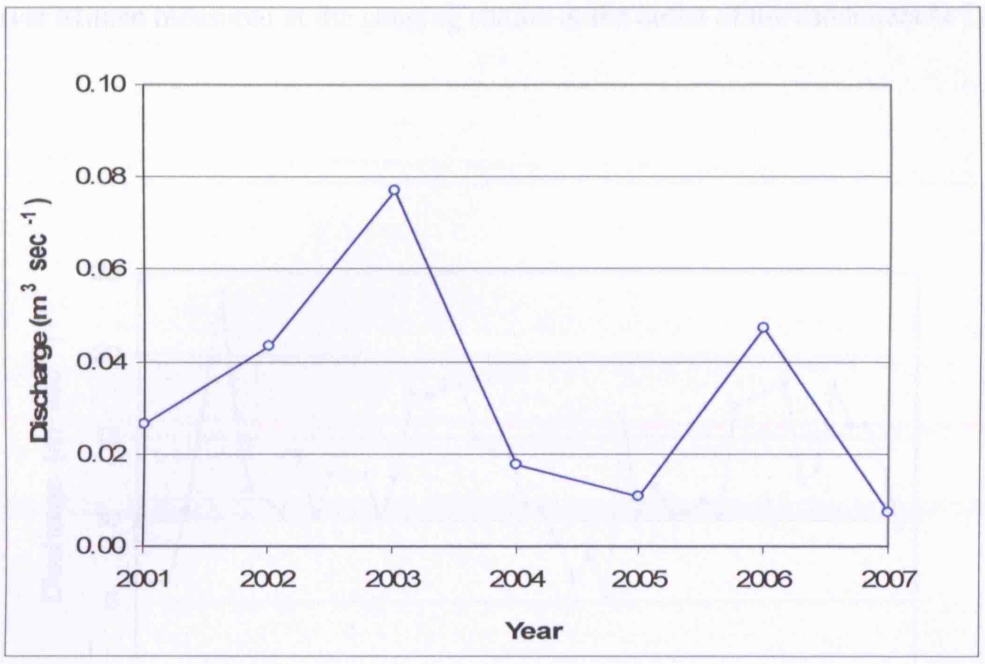

Figure 2.11. Mean annual discharge for the River Kigwe

2.4.5.2 River Mitano catchment

The River Mitano flows in a north-western direction and discharges into Lake Edward in the Albertine Rift Valley. Lake Edward is located at an elevation of 913 mamsl and is the base level of drainage for the whole catchment. With a mean topographic elevation of approximately 1740 mamsl for the River Mitano catchment, the difference between the catchment and the base level of drainage is over 800 m. The drainage pattern in the catchment is dendritic to semi-parallel and is a result of tectonic activity that has led to high topographic gradients. Most of the tributaries to the River Mitano flow in the northeast-southwest direction, almost parallel to the rift valley. The discharge of the River Mitano shows minor fluctuations during the year and from year to year (Fig. 2.12) suggesting that there is high basin storage. The mean annual discharge of

the River Mitano measured at the gauging station at the outlet of the catchment is 12.7 m^3 s^{-1}.

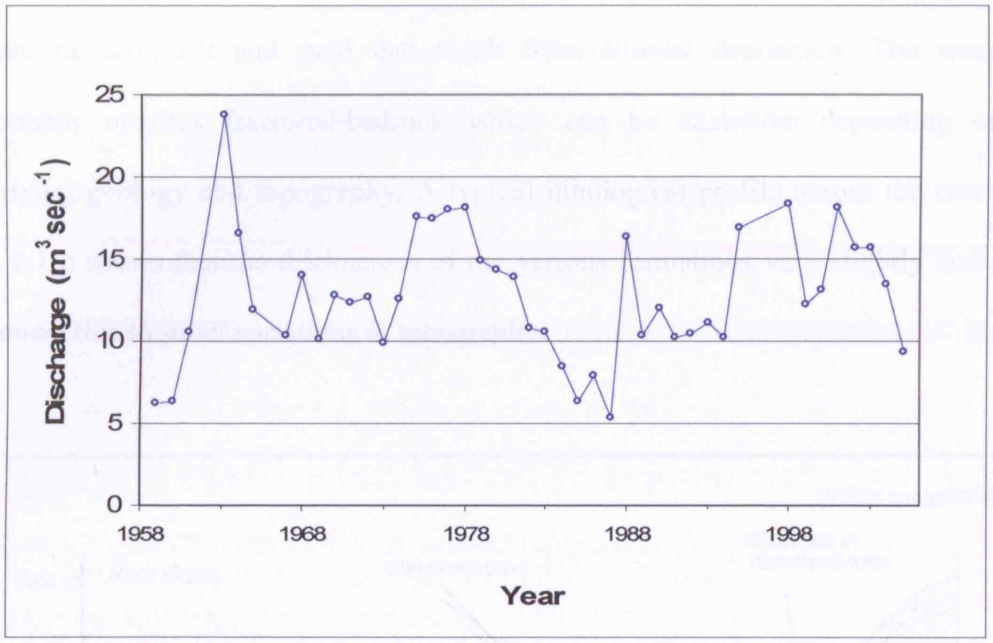

Figure 2.12. Mean annual discharge for the River Mitano in Western Uganda

2.5. Catchment groundwater resources

2.5.1 Lithology

2.5.1.1 River Kigwe catchment

Variation in lithology across the River Kigwe catchment is related to the underlying geology which determines the nature of weathering products. The eastern and north-western parts of the catchment are underlain by quartzites bands that are highly resistant to weathering, the lithology is dominated by coarse sands and quartz with small proportions of clay. In areas underlain by granites, schists and gneisses the lithology is

dominated by a clay-sized material mixed with silts and fine sands due to the increased susceptibility of these formations to weathering. These areas have fairly thick weathered overburdens. Along river channels and close to wetlands the lithology consists of a mixture of clay, silt and sand that result from alluvial deposition. The weathered overburden overlies fractured-bedrock which can be extensive depending on the underlying geology and topography. A typical lithological profile across the catchment (Fig. 2.13) shows that the thicknesses of the various formations vary slightly across the catchment due to small variations in topography.

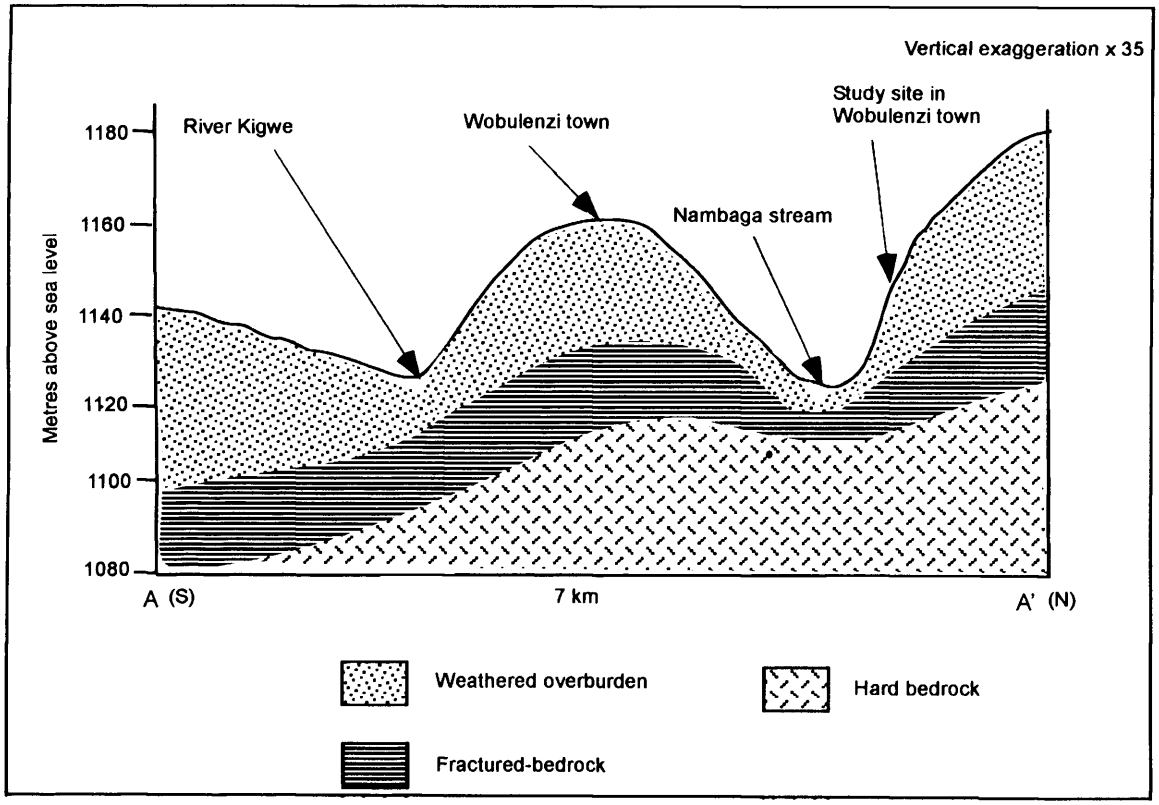

Figure 2.13. Cross-sectional profile of geology across the River Kigwe catchment. Locations of A and A' are indicated on Figure 2.4.

2.5.1.2 River Mitano catchment

Overburden lithologies in the River Mitano catchment are the result of variations in geology, weathering patterns and alluvial deposition. Areas underlain by gneisses and schists are highly susceptible to weathering and result in poorly sorted, bi-modal textures dominated by fine sand and clay. Due to the high topographic gradients in the catchment, weathered materials are eroded, transported and deposited along river channels and valleys resulting in thin and highly variable weathered overburdens. The lithology of the alluvial sediments depends on the nature of parent weathered material and erosion. Sediments transported over long distances consist of well sorted material dominated by coarse sands and gravels. In some locations, the weathered overburden and alluvial sediments overlie fractured-bedrock and hard bedrock. A typical lithological profile across the catchment (Fig. 2.14) shows that the thicknesses of the various formations vary greatly across the catchment.

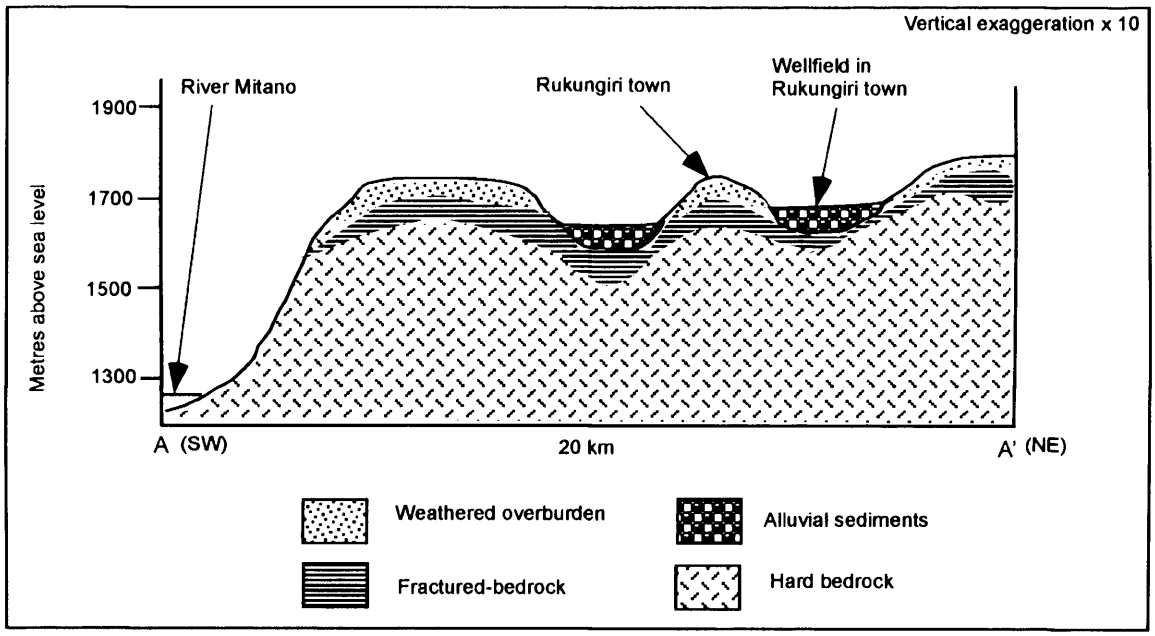

Figure 2.14. Cross-sectional representation of geology across the River Mitano catchment. Locations of A and A' are indicated on Figure 2.5.

2.5.2 Borehole yields

2.5.2.1 River Kigwe catchment

Borehole yields in the River Kigwe catchment range between 0.5 and 12 $m^3 h^{-1}$ based on data from 24 boreholes (Fig. 2.15). Only 26% of the boreholes have yields greater than 2 $m^3 h^{-1}$ suggesting that the catchment generally has low yielding aquifers. Only 12% of the boreholes have yields greater than > 4 $m^3 h^{-1}$. Borehole yields > 2 $m^3 h^{-1}$ are found where the bedrock is highly fractured, mostly in low lying areas and within the quartzite bands. The wide variation in borehole yields point to the role of geology and topography in the determination of aquifer properties. There is no relationship between borehole yields and regolith thicknesses in the River Kigwe catchment.

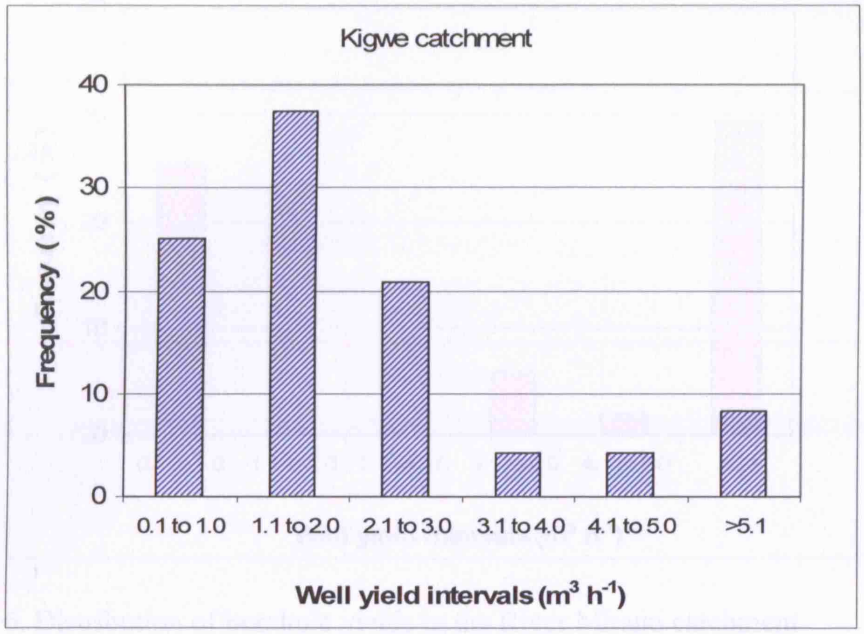

Figure 2.15. Distribution of borehole yields in the River Kigwe catchment

2.5.2.2 River Mitano catchment

Borehole yields in the River Mitano catchment range between 0.1 and 23 m^3 h^{-1} based on 51 boreholes (Fig. 2.16). Only 29% of the boreholes have yields >5 m^3 h^{-1} whereas 49% have yields <2 m^3 h^{-1}. Only 22% have borehole yields between 2 and 5 m^3 h^{-1}. Borehole yields suggest that there are two different aquifers units, one that exhibits very high yields (>5 m^3 h^{-1}) and one that has low yields (<2 m^3 h^{-1}). The low yielding boreholes are located where the overburden thickness is thin, mainly on topographically high areas whereas the high yielding boreholes are located in river channels and low lying areas underlain by coarse grained alluvial material and fractured-bedrock.

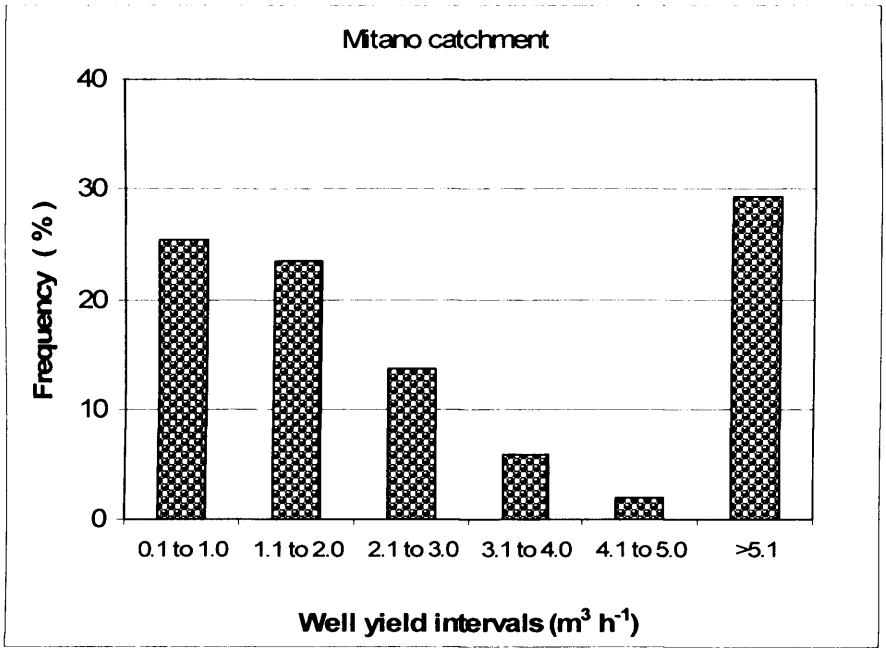

Figure 2.16. Distribution of borehole yields in the River Mitano catchment

2.6 Conclusions

The review of existing data indicates that the climate of the River Kigwe catchment is similar to that of the River Mitano catchment but there are large differences in geology and topography. The two catchments both have mean annual rainfall of 1200 mm that exhibits a bimodal distribution. The topographic gradients in the River Kigwe catchment are lower than those in the River Mitano and lead to lower surface run off as compared to the River Mitano catchment. The geology of both catchments is complex but the aquifer characteristics are influenced by topography which determines the nature of the weathering products. The thicknesses of the various formations in the River Kigwe catchment vary slightly across the catchment due to small variations in topography whereas the thicknesses of the formations vary greatly in the River Mitano catchment due to high variability in topography. Borehole yields are generally higher in the River

Mitano catchment than in the River Kigwe catchment due to coarser weathered material. The high variability in the various factors leads to high variability in the distribution and occurrence of groundwater resources in the two catchments as will be investigated further in the following chapters.

CHAPTER 3: CATCHMENT-SCALE GROUNDWATER RECHARGE AND FLOW CHARACTERISTICS

This chapter discusses groundwater recharge and flow in the River Kigwe and Mitano catchments. The source and timing of groundwater recharge and some aspects of groundwater flow are investigated using variations in stable isotope ratios of O ($^{18}O/^{16}O$) and H ($^{2}H/^{1}H$) of precipitation, groundwater and surface water. The hydrochemical study of groundwater flow also involves correlations between deuterium and chloride concentrations and trends in both tritium and electrical conductivity in groundwater. This preliminary assessment of groundwater recharge and flow characteristics on a catchment scale provides hydrogeological context for detailed town scale studies.

3.1 Groundwater recharge

3.1.1 Overview

Groundwater recharge is important in evaluating groundwater resources but is difficult to quantify (Alley *et al.*, 2002). Recharge can occur in response to individual precipitation events in regions with shallow water tables or can take many years in regions with deep water tables especially in semi-arid zones. Similarly, groundwater recharge can be diffuse or localised. Diffuse recharge refers to recharge that takes place from the land surface to the water table by infiltration and percolation though the unsaturated zone over large areas whereas localised recharge refers to recharge that is less uniform in space than diffuse recharge. Diffuse and localised recharge may occur together in groundwater systems although localised recharge is more common in arid regions.

Previous recharge studies in Uganda have employed a number of methods: soil moisture balance, water level fluctuation, isotope methods, chloride balance, flow modelling and baseflow separation (Howard and Karundu, 1992; Taylor and Howard, 1996, 1999a; Tindimugaya, 2000). Not all the water that infiltrates becomes recharge as some is stored in the soil zone and eventually lost to the atmosphere by evapotranspiration (Alley *et al.,* 2002). Recharge studies in Uganda (Howard and Karundu, 1992; Taylor and Howard, 1996, 1999a; Tindimugaya, 2000) show that upon reaching the land surface, most of the incoming rainfall (70-90 %) is recycled to the atmosphere by evapotranspiration and the reminder stays at the land surface and contributes to surface flow via runoff and to groundwater recharge via infiltration through the unsaturated zone. Taylor and Howard (1996) further show that groundwater is recharged by heavy rainfall and that recharge events are effectively restricted to periods of heavy rainfall so that the magnitude of recharge is controlled more by the number of heavy rainfall events (> 10 mm d^{-1}) during the monsoons than the total volume of rainfall. The percentage of rainfall that becomes recharge is highly variable and is influenced by a number of factors including weather patterns, properties of the soil, vegetation cover, topography, depths to the water table, and the size of the study areas and the time when recharge estimates are made (Alley *et al.,* 2002). The estimated annual groundwater recharge rates in Uganda are highly variable and amount to approximately 10% of annual rainfall in the zone of deep weathering in central Uganda (Taylor and Howard, 1996; Tindimugaya, 2000) whereas they are approximately 1% of annual rainfall in the zone of stripping in western Uganda (Taylor and Howard, 1999a). Estimation of groundwater recharge rates can however be complicated by preferential flow paths in the unsaturated zone as well as temporal and spatial variability of the various factors. Use of multiple

techniques is therefore normally recommended in view of uncertainties inherent in each method.

3.1.2 River Kigwe catchment

Groundwater recharge in the River Kigwe catchment was estimated in previous studies using the soil moisture balance model, EARTH (Van der Lee and Gehrels, 1990) and was verified though groundwater flow modelling (Tindimugaya, 2000). Recharge was found to exhibit spatial variability and thus point recharge estimates were regionalised using a weighted class method to obtain a long-term mean recharge of 161 $mm \cdot a^{-1}$ that accounted for approximately 13% of precipitation. Groundwater recharge estimates obtained using groundwater flow modelling was approximately 113 $mm \cdot a^{-1}$ and was considered to represent the lower limit of groundwater recharge in the catchment. The long-term recharge estimate of 161 $mm \cdot a^{-1}$ determined in the River Kigwe catchment is similar to estimates by Taylor and Howard (1996) of 120 $mm.a^{-1}$ in Aroca catchment also in central Uganda

3.1.3 River Mitano catchment

Ongoing studies in the River Mitano catchment (Mileham *et al.,* in prep.) have determined groundwater recharge using the soil moisture balance method. The studies show that groundwater recharge is approximately 104 $mm \cdot a^{-1}$, approximately 8 % of mean annual precipitation. This recharge estimate exceeds that determined by Taylor and Howard (1999a) for a nearby catchment (Nyabisheki) in southwestern Uganda (15 $mm \cdot a^{-1}$). Greater precipitation (1200 $mm \cdot a^{-1}$ versus 1000 $mm \cdot a^{-1}$) and a

larger basin storage offered by coarse-grained fluvial deposits in the River Mitano catchment likely account for the relatively greater recharge flux.

3.2 Investigating groundwater recharge processes and flow using isotopes and hydrochemistry

3.2.1 Overview

Isotopic methods have proved valuable in elucidating recharge processes and flow mechanisms in various aquifer environments and have been extensively utilised to characterise the source and timing of recharge and groundwater movement within catchments (Clark and Fritz, 1997; Kendal and Mcdonnel, 1998; Sukhija *et al.*, 2006). Groundwater recharge may derive from precipitation, surface water and palaeowater and may also occur due to rain falling at different times of the year. The different sources of recharge can be traced from contrasting isotopic signatures (Darling *et al.*, 1987; Gat, 1987). Distinct isotope signatures in groundwater enable identification of the source and timing of recharge (Taylor and Howard, 1999a). Rains falling during different periods have different isotope signatures due to differences in the effects of evaporation and the amounts of rainfall. Heavy precipitation is depleted in heavy isotopes whereas light precipitation is enriched in heavy isotopes.

Surface waters are enriched in heavy isotopes due to evaporation and comparison of their isotopic content with that of groundwater and precipitation enables characterisation of the basin outflow and the interactions between groundwater and surface water. Palaeowaters are characterised by strong depletion in heavy isotopes indicative of cooler climates as found by Darling *et al.* (1987) in the palaeowaters of Sudan ($-10‰ < \delta^{18}O < -5‰$, $-70‰ < \delta D < -40‰$).

The chemistry of groundwater primarily depends on the reactivity and mineral composition of the rocks forming the aquifer. The most important hydrochemical species in groundwater include calcium, sodium, bicarbonate, sulphate, nitrate, chloride and dissolved silica (Njitchoua *et al.,* 1997). The above parameters are derived mainly from water-rock interactions except nitrates which result entirely from anthopogenic inputs. Other processes such as evaporation or mixing may occur during infiltration and serve to change the concentrations of dissolved constituents in groundwater. Thus, a systematic hydrochemical investigation can provide information on the hydrogeological processes occurring in the aquifer (Tweed *et al.,* 2005). It is generally accepted that groundwater evolves from proportionately high concentrations of bicarbonates, though sulphates and finally to chloride along a groundwater flow path from recharge to discharge zones (Wilkes *et al.,* 2004). Thus, the longer the ground water remains within the subsurface system the more the groundwater will evolve from predominantly bicarbonate water to more mature, chloride rich water. Evolution of groundwater chemistry is often used to assess the movement of groundwater along a flowpath in order to determine recharge and discharge zones and hence the groundwater flow direction.

In this study, groundwater recharge processes and flow were investigated using environmental isotopes through four stages; (i) assessing the seasonal variation of isotopes in precipitation; (ii) comparison of isotopic composition of groundwater, precipitation and surface water to identify the source and timing of groundwater recharge; (iii) relating deuterium with chloride in groundwater to assess the mechanism of groundwater recharge; and (iv) relating the variation of tritium and electrical conductivity in the catchment to assess the movement of groundwater.

3.2.2 Groundwater sources

3.2.2.1 River Kigwe catchment

Thirty six water sources were mapped in the River Kigwe catchment using a hand held Global Positioning System (GPS) (Fig. 3.1). Two of the sources are springs, two are surface waters from Nambaga and Kigwe streams and the remaining thirty two are deep boreholes. Two of the boreholes are installed in the weathered aquifer, three are drilled in both the weathered and fractured aquifer whereas the remaining twenty seven are installed in only the fractured aquifer. The depths of the boreholes range between 32 and 94 m. All the water sources were sampled for environmental isotopes and hydrochemistry. In addition, the drilling records for the boreholes were used to assess the variation of key hydrogeological parameters across the catchment as discussed in the following sections.

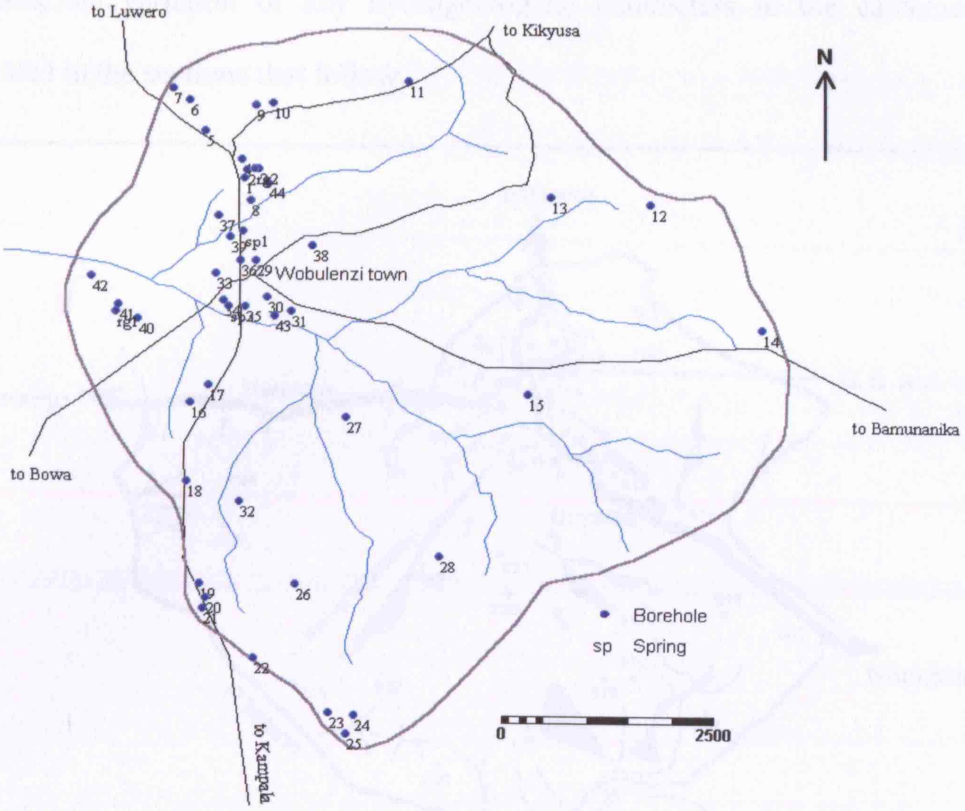

Figure 3.1. Location of water sources in the River Kigwe catchment. Numbers refer to water sources, details of which are presented in Appendices 1 and 2.

3.2.2.2 River Mitano catchment

Sixty water sources were mapped in the River Mitano catchment using a hand held GPS (Fig. 3.2). Twenty eight of the sources are springs, six are surface waters from the Rivers Mitano and Birira and the small streams in the catchment (Kyatoko, Nyakibale, Omuibare and Buhandagazi) whereas the remaining twenty six are deep boreholes. Nine of the boreholes are located in the alluvial aquifer in Rukungiri town. The depths of the boreholes in the alluvial aquifer ranged between 35 m and 89 m whereas the depths of the boreholes in the rest of the catchment range between 21 and 94 m. All the water sources were sampled for environmental isotopes and hydrochemistry. Available drilling records for some of the boreholes were also used

to assess the variation of key hydrogeological parameters in the catchment as elaborated in the sections that follow.

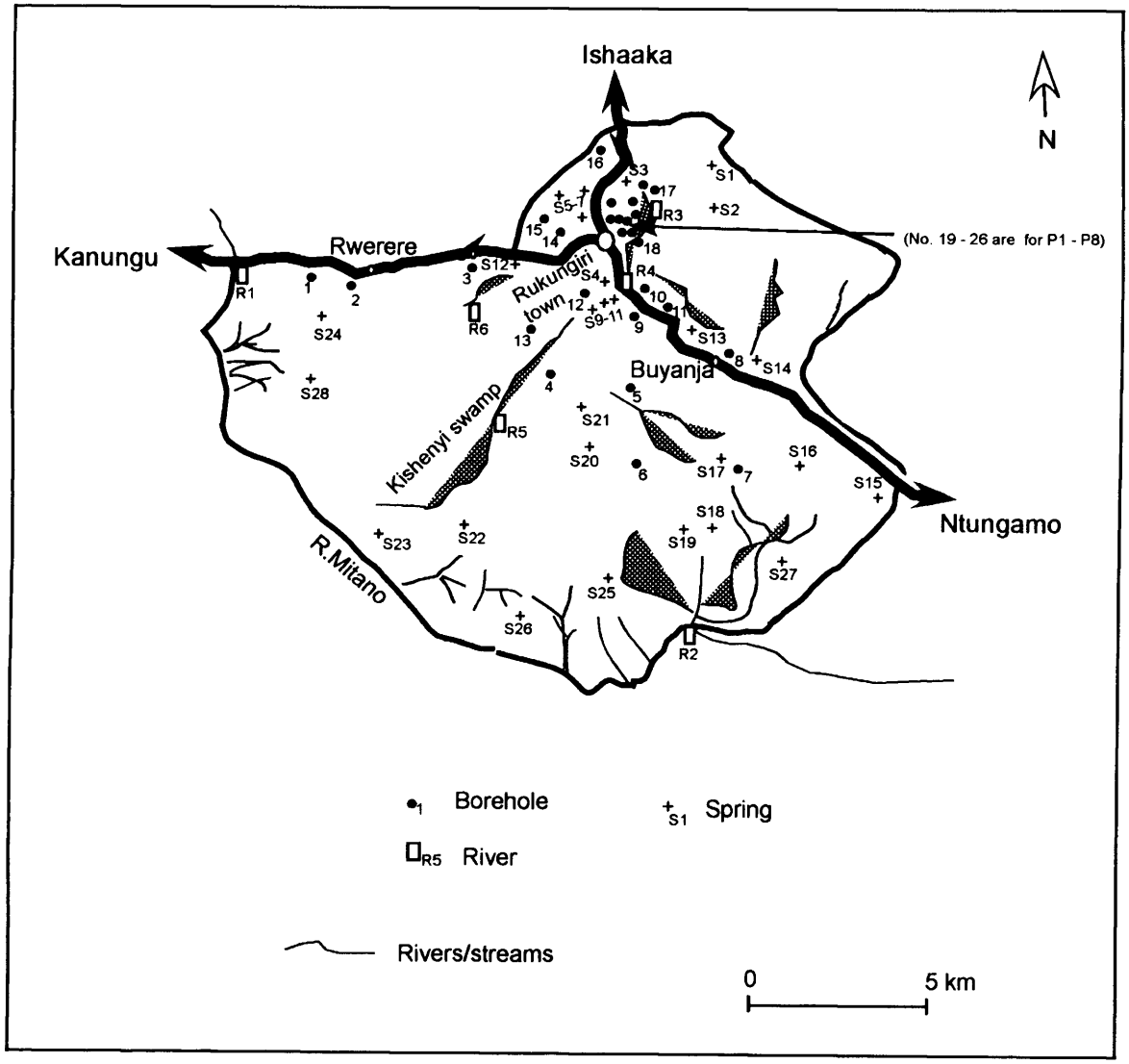

Figure 3.2. Location of water sources in the River Mitano catchment. Numbers refer to water sources, details of which are presented in Appendices 1 and 2.

3.2.3 Sample collection and analysis

Most of the sources sampled for isotopes and hydrochemistry are boreholes fitted with handpumps. In order to ensure that the samples collected were as representative as possible, samples were collected after extended periods of pumping after wellhead parameters such as pH, electrical conductivity (EC), and temperature

had stabilised. Wellhead parameters were monitored using a flow-through cell (Fig. 3.3) when sampling was carried out on motorized boreholes or during pump testing. Once the wellhead parameters stabilized, it was assumed that the water was derived directly from the aquifer. Samples for stable isotope analysis were collected in 50 ml bottles, those for tritium in 500 ml and those for hydrochemical analysis in 1 l bottles. Thirty six water sources were sampled for environmental isotopes and hydrochemistry in the River Kigwe catchment during three sampling campaigns carried out in both the dry and rainy seasons between 1999 and 2000. Sixty water sources were sampled in the River Mitano catchment during four sampling campaigns also carried out in both the dry and rainy seasons between 2003 and 2004. Rainfall sampling for stable isotope analysis is carried out on a monthly basis in both Wobulenzi and Rukungiri towns. The rainfall measured at each station everyday is stored in a container and at the end of the month a 50 ml bottle is filled for stable isotope analysis using the composite sample.

Figure 3.3. Sampling using a flow though cell while monitoring wellhead parameters

Samples for stable isotopes and tritium were analyzed using mass spectrometry and liquid scintillation counting respectively at the Schonland Research Center Isotope Laboratory in South Africa and the IAEA isotope laboratory in Vienna, Austria. Samples for hydrochemistry were analysed at the National Water Quality Laboratory in the Directorate of Water Development in Uganda using atomic absorption spectrometry, ion chomatography and titration methods. The isotope analysis results for the Rivers Kigwe and Mitano catchments are presented in Appendix 1A and 1B respectively whereas hydrochemical analysis results are presented in Appendix 2A and 2B respectively.

3.3 Evidence for recharge from stable isotopes

3.3.1 Seasonal variation of stable isotopes in precipitation

Stable isotope content in monthly precipitation recorded in Wobulenzi town (the River Kigwe catchment) from 1999 to 2000 and in Rukungiri town (River Mitano catchment) from 2003 and 2005 was used to examine the seasonal variation of stable isotopes in precipitation in the Rivers Kigwe and Mitano catchments. Monthly precipitation amounts and $\delta^{18}O$ values in precipitation for both catchments (Figs. 3.4 and 3.5) show a positive correlation between the amount of precipitation and the depletion in $\delta^{18}O$. The results clearly indicate that the relationship, commonly referred to as the "amount affect" (Dansgaard, 1964), exists between the amount of rainfall and depletion in $\delta^{18}O$ in the Rivers Kigwe and Mitano catchments. The amount effect is a result of the origin and history of the sources of precipitation (Gat, 1987). Various studies in the tropics suggest that depleted $\delta^{18}O$ values in precipitation correspond to the movement of the Intertropical Convergence Zones (ITCZ) and hence the occurrence of monsoonal rains (Salati *et al.,* 1979; Taylor and Howard, 1996).

Bimodal peaks in annual precipitation are thought to result from monsoons derived from the movement of the ITCZ and coincide with the most depleted isotopic signatures. Taylor and Howard (1996) also show that monsoonal rains in Uganda originate from the Indian Ocean which is a more depleted source in stable isotopes than the less intense conventional rains that originate from regional surface waters. The above observations regarding the source of precipitation are consistent with the findings of Basalirwa (1995) which suggest that the two rainfall peaks (heavy precipitation) in March to May and September to November are due to the convergence into the ITCZ of the moist south-east monsoons from the Indian Ocean and the north-east monsoons controlled by the subtropical anticyclones over the Azores and the Arabian peninsula. Although the isotopic composition of precipitation depends on the properties of the advecting air masses, local conditions can greatly modify the isotopic signature of precipitation (Gat, 1987). Comparison of isotopic composition of heavy and light rainfall (Figs. 3.4 and 3.5) show that heavy rain falling in March and May and September and November is depleted in heavy isotopes whereas the light rainfall that falls between June and August and December and February is enriched in heavy stable isotopes due to evaporation of the lighter isotopes.

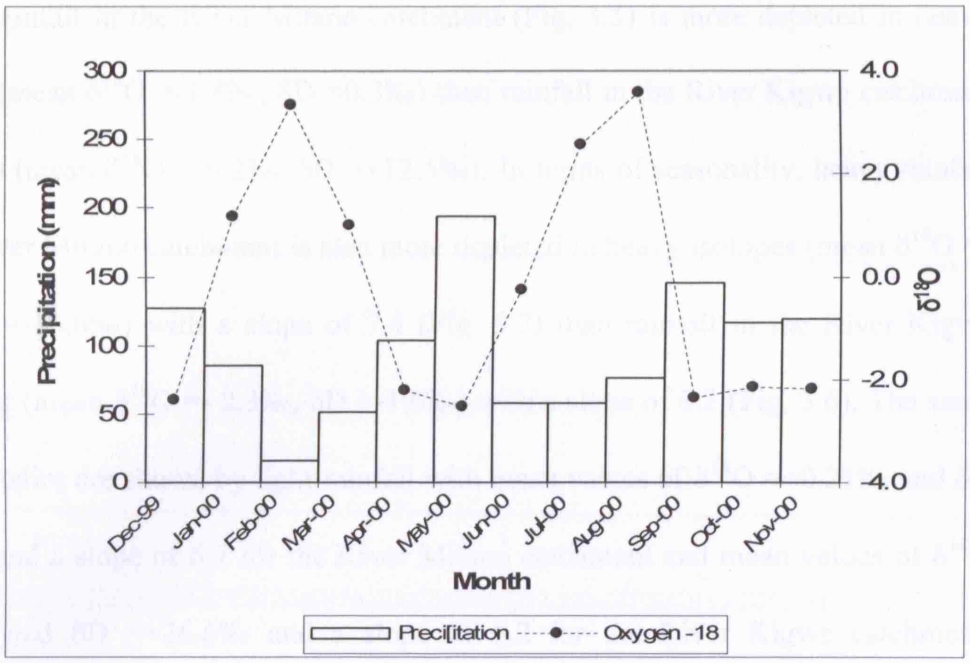

Figure 3.4. Variation of stable isotopes with rainfall amount in the River Kigwe catchment.

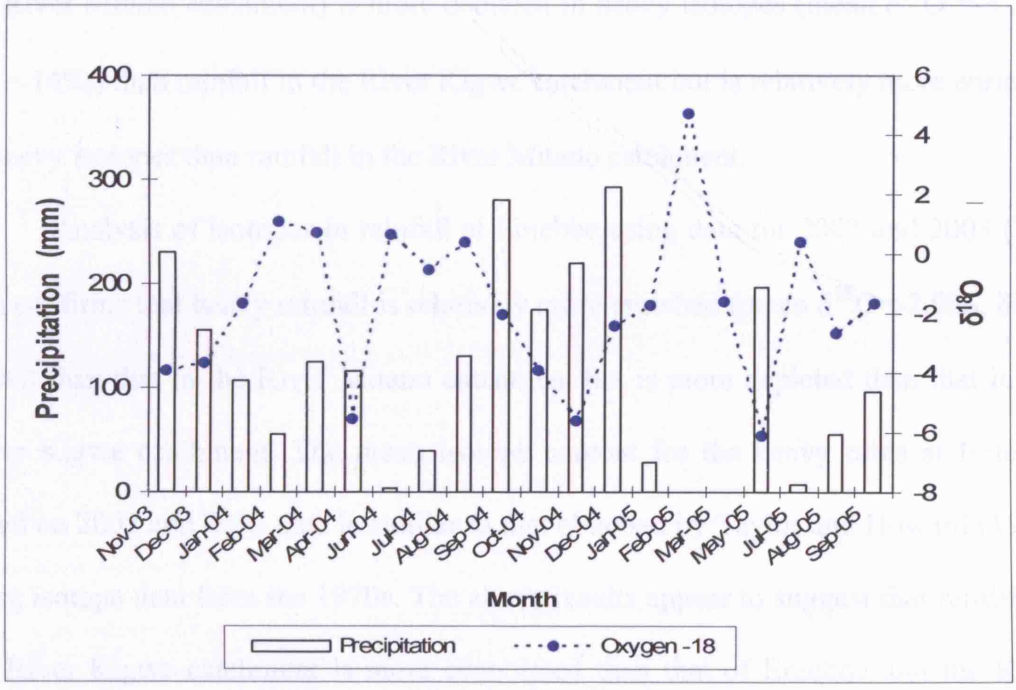

Figure 3.5. Variation of stable isotopes with rainfall amount in the River Mitano catchment.

Rainfall in the River Mitano catchment (Fig. 3.5) is more depleted in heavy isotopes (mean $\delta^{18}O$ =-1.8‰, δD =0.3‰) than rainfall in the River Kigwe catchment (Fig. 3.4) (mean $\delta^{18}O$ =-0.2‰, δD =+12.5‰). In terms of seasonality, heavy rainfall in the River Mitano catchment is also more depleted in heavy isotopes (mean $\delta^{18}O$ =-6‰, δD =-16.6‰) with a slope of 7.4 (Fig. 3.7) than rainfall in the River Kigwe catchment (mean $\delta^{18}O$ =- 2.3‰, δD =-1.6‰) with a slope of 6.2 (Fig. 3.6). The same characteristics are shown by light rainfall with mean values of $\delta^{18}O$ =+0.21‰ and δD =+14‰ and a slope of 6.7 for the River Mitano catchment and mean values of $\delta^{18}O$ =+1.9‰ and δD =+26.6‰ and a slope of 6.2 for the River Kigwe catchment. Previous studies in Uganda (Taylor and Howard, 1996) show that heavy rainfall for the 1970s at Entebbe (60 km south of the River Kigwe catchment and 350 km east of the River Mitano catchment) is more depleted in heavy isotopes (mean $\delta^{18}O$ =-3.3‰, δD =-14‰) than rainfall in the River Kigwe catchment but is relatively more enriched in heavy isotopes than rainfall in the River Mitano catchment.

Analysis of isotopes in rainfall at Entebbe using data for 2002 and 2003 (Fig. 3.8) confirms that heavy rainfall is relatively more enriched (mean $\delta^{18}O$=-2.9‰, δD=-9.6‰) than that in the River Mitano catchment but is more depleted than that in the River Kigwe catchment. The mean isotope content for the heavy rains at Entebbe based on 2002 and 2003 data is similar to that obtained by Taylor and Howard (1996) using isotope data from the 1970s. The above results appear to suggest that rainfall in the River Kigwe catchment is more evaporated than that of Entebbe and the River Mitano catchment.

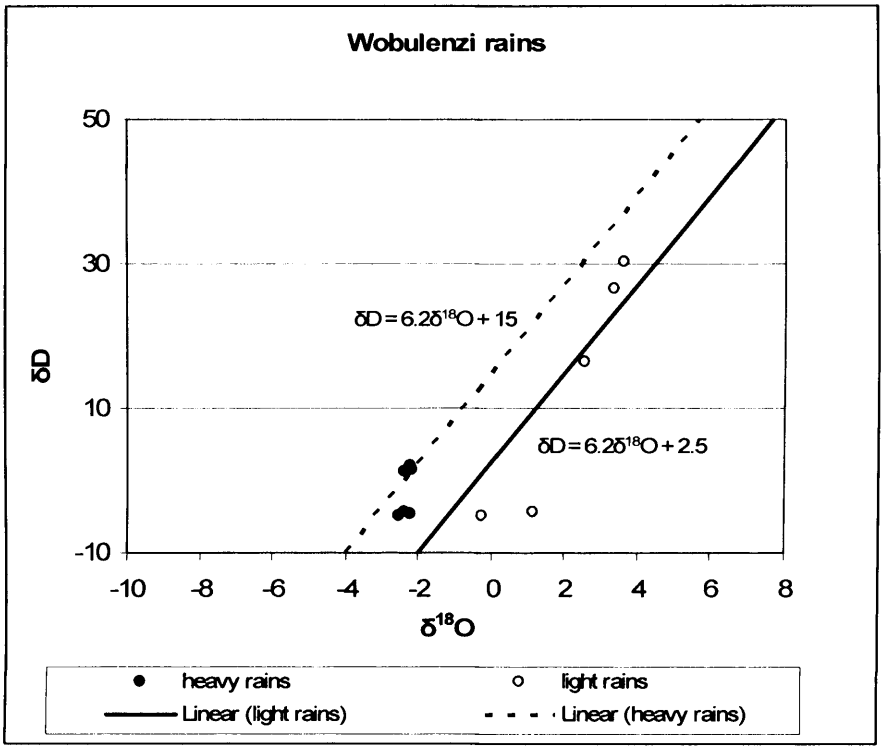

Figure 3.6. Plot of $\delta^{18}O$ versus δD for Wobulenzi rainfall based on monthly data from 1999 to 2000. Linear regressions of observations for light and heavy rainfall are shown. Light rains are those which fall in the dry season whereas heavy rains are those which fall during the rainy season.

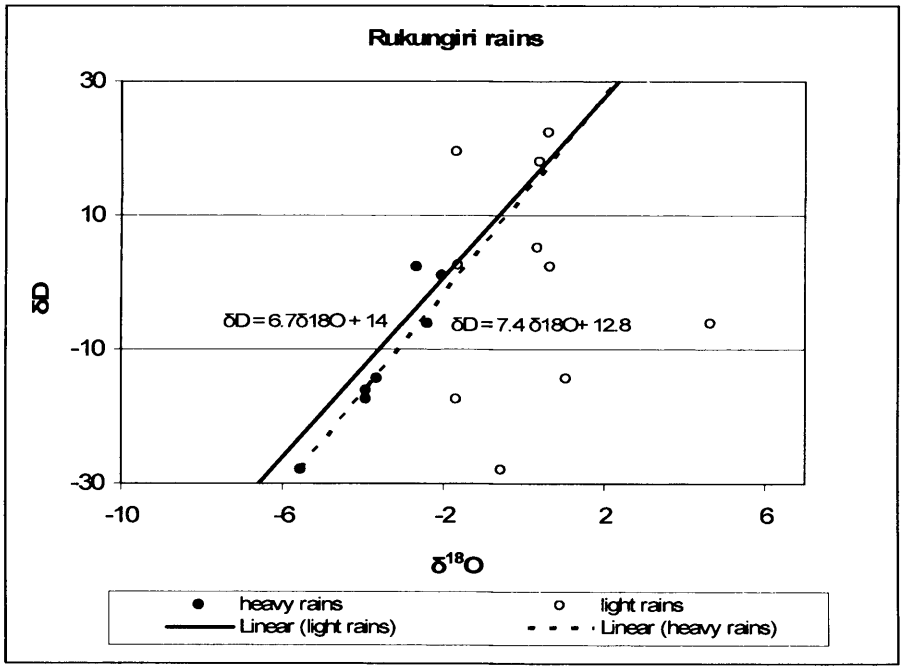

Figure 3.7. Plot of $\delta^{18}O$ versus δD for Rukungiri rainfall based on monthly data from 2003 to 2005. Linear regressions of observations for light and heavy rainfall are shown. Light rains are those which fall in the dry season whereas heavy rains are those which fall during the rainy season.

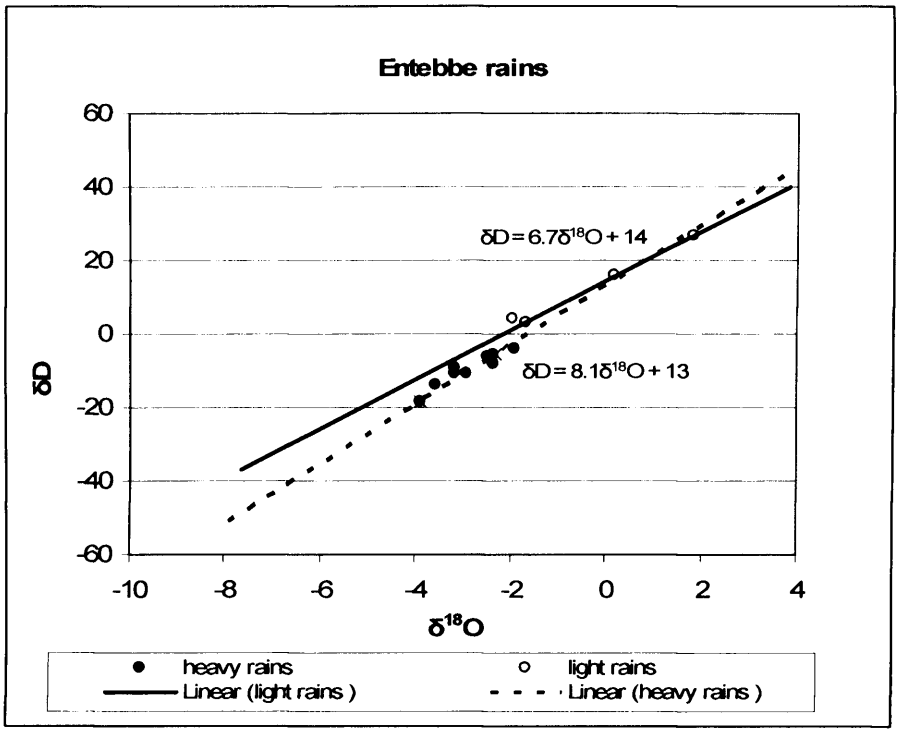

Figure 3.8. Plot of $\delta^{18}O$ versus δD for Entebbe rainfall based on monthly data from 2002 to 2003. Linear regressions of observations for light and heavy rainfall are shown. Light rains are those which fall in the dry season whereas heavy rains are those which fall during the rainy season.

The LMWL at Wobulenzi ($\delta D = 7.6\delta^{18}O + 11.7$) derived from mean stable isotope values in precipitation has a slope of 7.6 with a deuterium excess of 11.7 (Fig. 3.9) whereas that at Rukungiri ($\delta D = 7.5\delta^{18}O + 13.7$) has a slope of 7.5 with a deuterium excess of 13.7 (Fig. 3.10). The LMWL for Wobulenzi and Rukungiri have higher slopes and deuterium excess than those of Entebbe ($\delta D = 7.3\delta^{18}O + 11$), derived by Taylor and Howard (1996). The slopes of the LMWL in Uganda are lower than that of the global meteoric water line ($\delta D = 8\delta^{18}O + 10$) whereas the deuterium excess for the global meteoric water line is lower that those of rainfall in Uganda. Craig (1961) suggests the relationship between deuterium and oxygen-18 with a slope of 8 is characteristic of meteoric waters that have undergone minimum evaporation whereas evaporated waters have a slope of 5. Thus, the lower slopes and higher

deuterium excess of the meteoric water lines in Uganda and indeed the rest of East Africa (Taylor and Howard, 1996) reflect the influence of evaporation on the isotopic composition of rainfall. The stable isotope content in light rains in Wobulenzi (Fig. 3.6), Rukungiri (Fig. 3.7), and Entebbe (Fig. 3.8) have lower slopes than heavy rains thus confirming the effect of evaporation on meteoric water lines. The above results therefore show that heavy rainfall in Uganda in depleted in heavy isotopes due to what is commonly known as the "amount effect" whereas light rainfall is enriched in heavy isotopes due to re-evaporation of falling raindrops. The meteoric water line in Uganda has a slope that is lower than that of the global meteoric water line due to the influence of evaporation of light rains.

3.3.2 Relationship between isotopic composition of precipitation, groundwater and surface water

A plot of oxygen-18 and deuterium content in precipitation and groundwater is normally utilised to identify the source of recharge and the mixing of groundwater from different sources. In addition to precipitation, groundwater recharge can result from surface water bodies or leakage from other aquifers. Surface water can contain a distinct stable isotope composition due to enrichment in heavy isotopes caused by evaporation which aids in the identification of recharge from surface water bodies. Groundwaters that are recharged by surface water plot along an evaporation line that deviates from the LMWL with a slope that tends to 5 whereas groundwaters that are recharged by precipitation plot along the LMWL with a slope that tends to 8.

3.3.2.1 River Kigwe catchment

Stable isotope content of groundwater collected from 32 sources and surface water collected from 2 sources in the River Kigwe catchment is plotted relative to the

LMWL (Fig. 3.9). All the stable isotope values cluster quite closely suggesting uniform and active recharge conditions. $\delta^{18}O$ content ranges between -2.6 and -2.0 ‰ whereas δD content ranges between -8.0 and -2.5 ‰. Groundwater samples show no evidence of evaporation suggesting that recharge is solely from precipitation. Stable isotope content of river/stream water sampled in both rainy and dry seasons are similar to those of groundwater and also do not show any evidence of evaporation. This appears to indicate that stream water is directly contributed by groundwater.

The rain falling in the months of April, May and December has isotopic compositions similar to that of groundwater ($\delta^{18}O$ content ranges between -2.5 and -2.2 ‰ and δD content ranges between -4.9 and +2.1) whereas rain falling in other months has more enriched stable isotope content ($\delta^{18}O$ content ranges between -0.3 and +3.6‰ and δD content ranges between +16 and +37) than that of groundwater. The results therefore appear to indicate that groundwater recharge results primarily from heavy, isotopically depleted rainfalls associated with the monsoons. These observations are consistent with the findings of Taylor and Howard (1999b) which indicate that groundwater recharge in Nyabisheki and Aroca catchments, found in western and central Uganda respectively, occurs primarily during periods of heavier, monsoonal rainfall and not in the months of lighter rainfall.

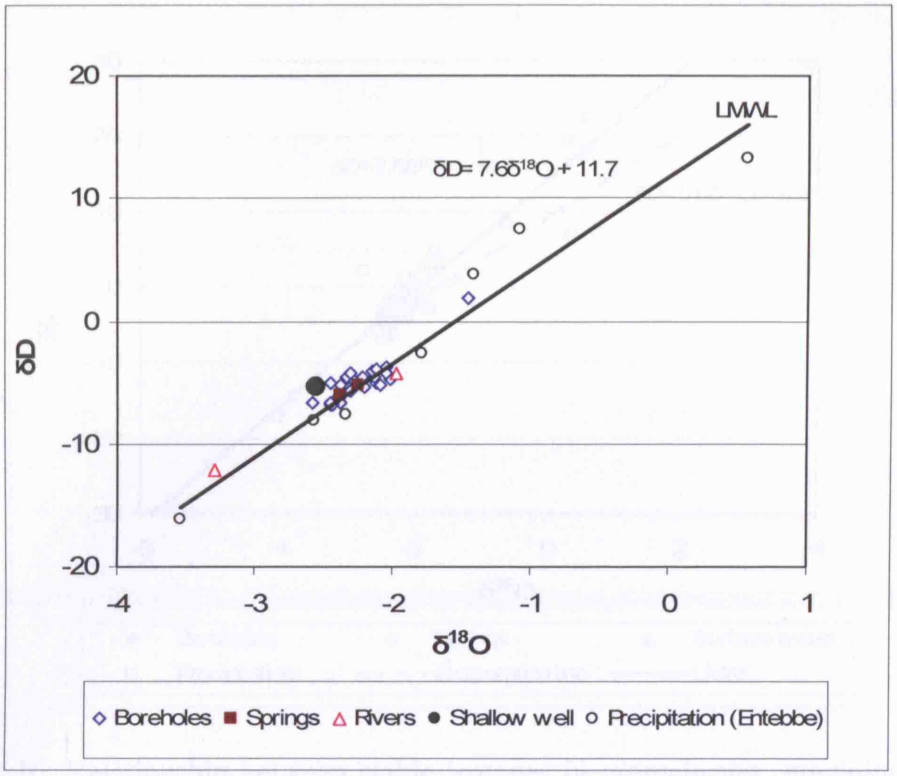

Figure 3.9. Relationship between stable isotopes in groundwater, precipitation and surface water in the River Kigwe catchment

3.3.2.2 River Mitano catchment

A plot of stable isotope content, relative to the LMWL at Rukungiri, of groundwater collected from 54 sources and surface water collected from 6 sources in the River Mitano catchment (Fig. 3.10) shows that all groundwater samples plot along the LMWL suggesting that recharge is principally meteoric in origin. The $\delta^{18}O$ content ranges between -2.6 and -1.6 ‰ whereas δD content ranges between -6.8 and +3.6 ‰. There are minor differences in stable isotope content of groundwaters collected at different times from the same sources suggesting that stable isotopes in groundwater remain relatively constant with time. The isotope content of boreholes tapping deep aquifers and springs tapping shallow aquifers are similar suggesting that groundwater recharge has occurred under similar climatic conditions.

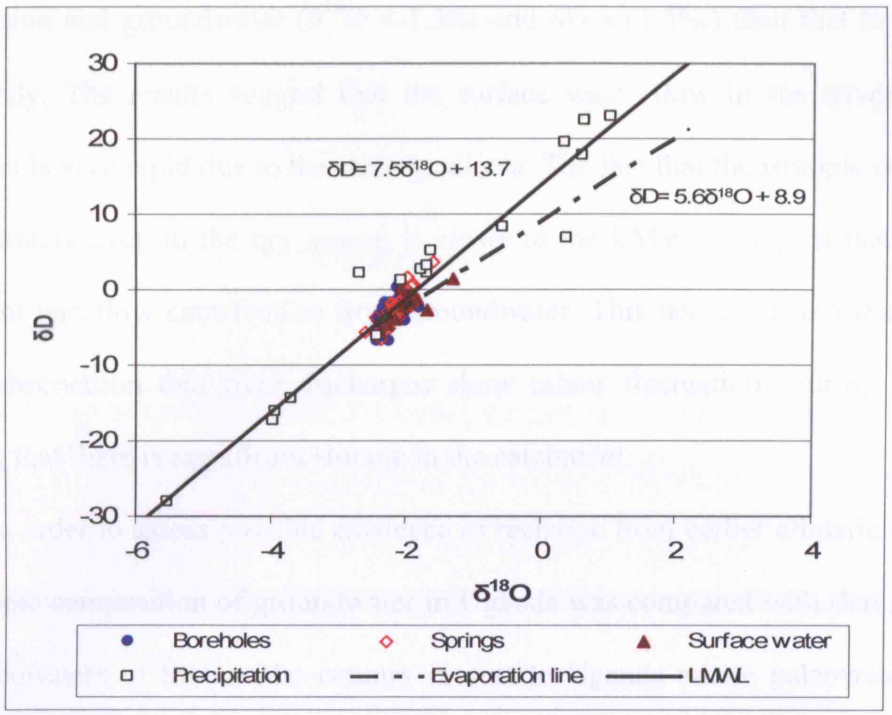

Figure 3.10. Relationship between stable isotopes in groundwater, precipitation and surface water in the River Mitano catchment

Despite the fact that there are many surface water bodies in the catchment, stable isotope content of groundwaters shows no evidence of evaporation suggesting that surface water does not recharge groundwater. Rivers in the catchment (the Rivers Mitano and Birira) plot along an evaporation line with a slope of 5.6 that is close to that for evaporated open waters (Craig, 1961). Surface waters from the small rivers and streams cluster together with groundwater sources along the LMWL suggesting that they are not evaporated due probably to rapid flow that is enhanced by high topographic gradients. Significant isotopic enrichment in regional surface water bodies and slight isotopic enrichment in river waters relative to groundwaters have also been observed by Taylor and Howard (1996) in Nyabisheki and Aroca catchments. Although the surface waters of the big rivers in the River Mitano catchment are evaporated, their stable isotope signature is closer to that of

precipitation and groundwater ($\delta^{18}O$ <-1.3‰ and δD <+1.5‰) than that to an open water body. The results suggest that the surface water flow in the River Mitano catchment is very rapid due to the steep gradients. The fact that the isotopic content of surface waters even in the dry season is closer to the LMWL suggests that there is significant baseflow contribution from groundwater. This deduction is substantiated by the observation that river discharges show minor fluctuations during the year implying that there is significant storage in the catchment.

In order to assess possible existence of recharge from earlier climatic regimes, the isotopic composition of groundwater in Uganda was compared with that found in the palaeowaters of Sudan (the country closest to Uganda where paleowaters have been found) (-10‰ < $\delta^{18}O$ < -5‰, -70‰ < δD< -40‰) by Darling *et al.* (1987). The isotopic content of groundwater in River Mitano catchment shows much more enrichment (-2.6‰ < $\delta^{18}O$ < -1.6‰, -6.8‰ < δD < 3.6‰) in heavy isotopes than the paleaowaters suggesting that groundwater recharge is recent.

The relationship between stable isotopes in groundwater, heavy rains, light rains and seasonal weighted mean precipitation was assessed in order to investigate the timing of groundwater recharge. The results indicate that the mean isotope content of heavy rains ($\delta^{18}O$=-4‰ and δD=-17‰) and light rains ($\delta^{18}O$=+0.2‰ and δD=+14‰) are very different from the mean isotopic content of groundwater ($\delta^{18}O$=-2.5‰ and δD=-2.2‰). The seasonal weighted mean isotope content of precipitation ($\delta^{18}O$=-1.8‰ and δD=0.3‰) is close to the mean isotope content of groundwater ($\delta^{18}O$=-2.5‰ and δD=-2.2‰). Based on the limited sampling of precipitation, the results suggest that groundwater recharge tends to occur consistently thoughout the year. The presence of a more permeable sandy unsaturated zone in the River Mitano catchment favours infiltration of isotopically lighter conventional rainfall.

3.3.3 Correlation of deuterium with chloride in groundwater

Stable isotopes are conservative in low-temperature groundwater environments so groundwater retains the isotopic signature of recharging waters as long as there are no processes altering the isotopic content in the soil zone before reaching the water table or there are no other sources of recharge (Clark and Fritz, 1997). Evaporation is the main process that can affect the isotopic content of recharging precipitation before it reaches the water table. This process can be assessed though correlation of the stable isotope content of groundwater with concentrations of chloride. Chloride is conservative but its concentration can increase alongside enrichment of stable isotopes due to evaporation. Thus, a positive correlation between chloride and stable isotopes suggests that there was significant evaporation before recharge whereas lack of any correlation may indicate that groundwater recharge was rapid (Darling *et al.,* 1987; Taylor and Howard, 1996). Investigations of the main flowpaths of groundwater recharge in the Rivers Kigwe and Mitano catchments was carried out through correlating the deuterium content and chloride concentration in groundwater.

Two contrasting pathways were investigated; slowly via steady (piston) flow through the regolith matrix, and rapidly via preferential pathways in the regolith or directly to aquifer units in outcrop. Any correlation between deuterium and chloride would indicate that groundwater recharge occurs slowly via piston flow thus allowing evaporation of recharging precipitation to occur. Lack of a correlation would imply that groundwater recharge is rapid through preferential pathways and there is very limited time for evaporation to occur. A plot of deuterium versus chloride for the River Kigwe catchment (Fig. 3.11) shows no correlation ($r^2<0.01$) implying that groundwater recharge in the area is spontaneous and evaporation before recharge is

not a major factor. Similar to the plot of the River Kigwe catchment, the plot of deuterium versus chloride for the River Mitano catchment (Fig. 3.12) also shows poor correlation (r^2=0.07) implying that groundwater recharge in the catchment is spontaneous. Correlation of deuterium and chloride therefore shows that evaporation is not a significant process in the two catchments.

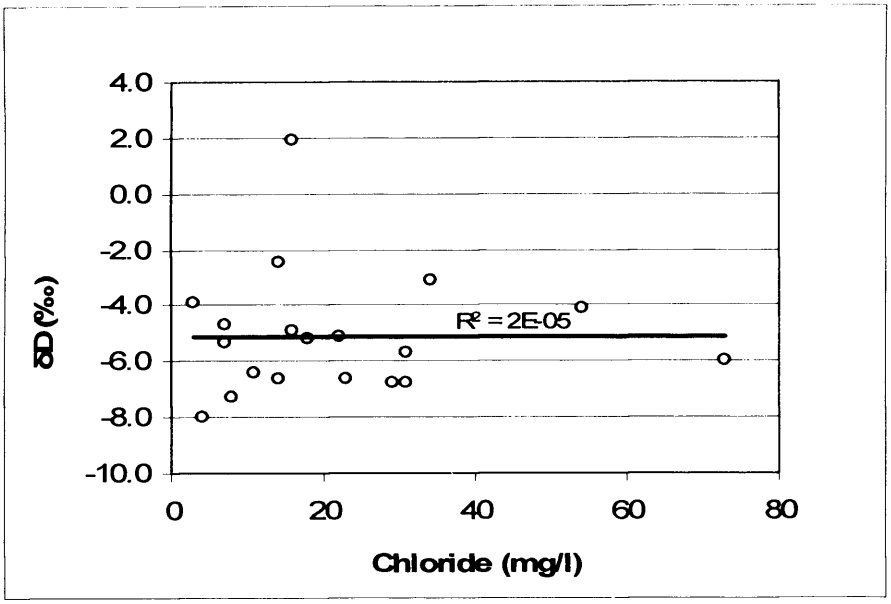

Figure 3.11. Plot of deuterium versus chloride in groundwater in the River Kigwe catchment.

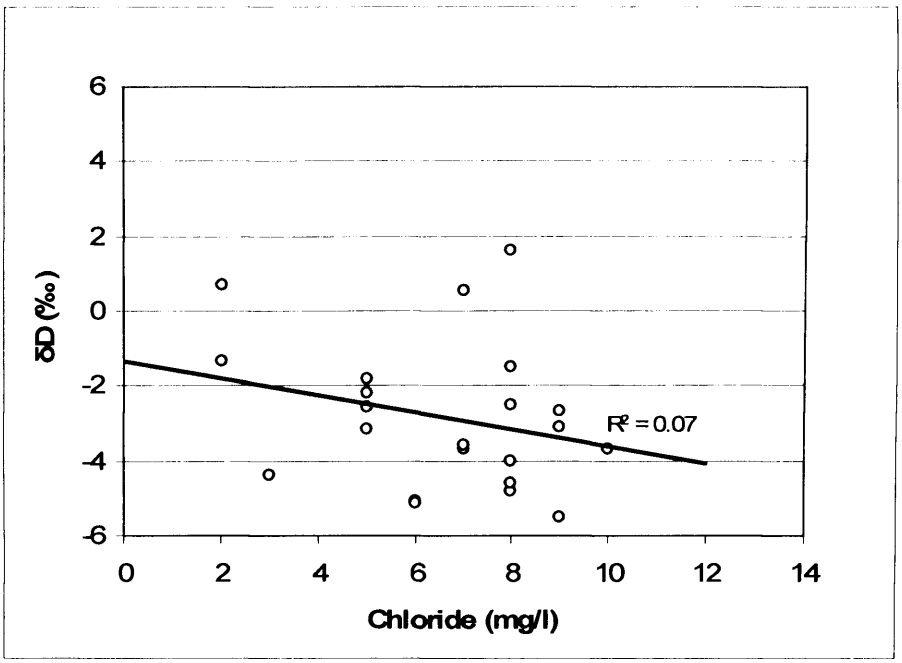

Figure 3.12. Plot of deuterium versus chloride in groundwater in the River Mitano catchment

3.3.4 Correlation of tritium and electrical conductivity

The distribution of tritium and electrical conductivity (EC) values in a catchment can highlight areas of more rapid recharge and discharge and presence of active groundwater flow paths. The evolution of groundwater along a flowpath is characterised by tritium content that decreases from the recharge to the discharge zone and EC values that increase from the recharge to the discharge zone. Recharge areas are expected to have relatively high tritium content and low EC values whereas discharge areas should have low tritium content and high EC values. The method also assumes that there is no contamination of EC which could raise its value.

3.3.4.1 River Kigwe catchment

The tritium content for most boreholes in the River Kigwe catchment lies between 1.1 and 3.5 TU, although there are some boreholes with 0 TU. The areas where there is 0 TU in groundwater may be indicative of restricted movement of groundwater and hence little weathering, whereas those areas where there is high tritium content may be indicative of high turnover times and thus high weathering/fracturing. Although there is no clear trend in the distribution of tritium, high tritium content is observed in the hills around the catchment. It is not possible to differentiate springs from deep boreholes using tritium, as the values are similar. This may be an indication that the shallow aquifer though which spring water flows is in direct hydraulic connection with the deep fractured aquifer that is tapped by the boreholes. Tritium values of the streams are similar to those of groundwater, suggesting that both surface water and groundwater are actively replenished by precipitation.

EC values range between 90 and 450 μs/cm. The distribution of EC values does not show any specific pattern and thus the parameter is unable to indicate a regional groundwater flow pattern. Relatively low EC values are found in the hills around the catchment possibly due to the presence of quartzites that do not have sufficient amounts of soluble minerals. The results suggest that groundwater recharge is diffuse and that there is no distinct groundwater flow paths. Furthermore, the correlation between tritium and EC values for the River Kigwe catchment (Fig. 3.13) is weak ($r^2 = 0.42$). Samples that have high EC and low tritium likely reflect locations where groundwater turnover is low. The results also show that the groundwater in the River Kigwe catchment has low mineralisation suggesting that it is fresh and actively recharged.

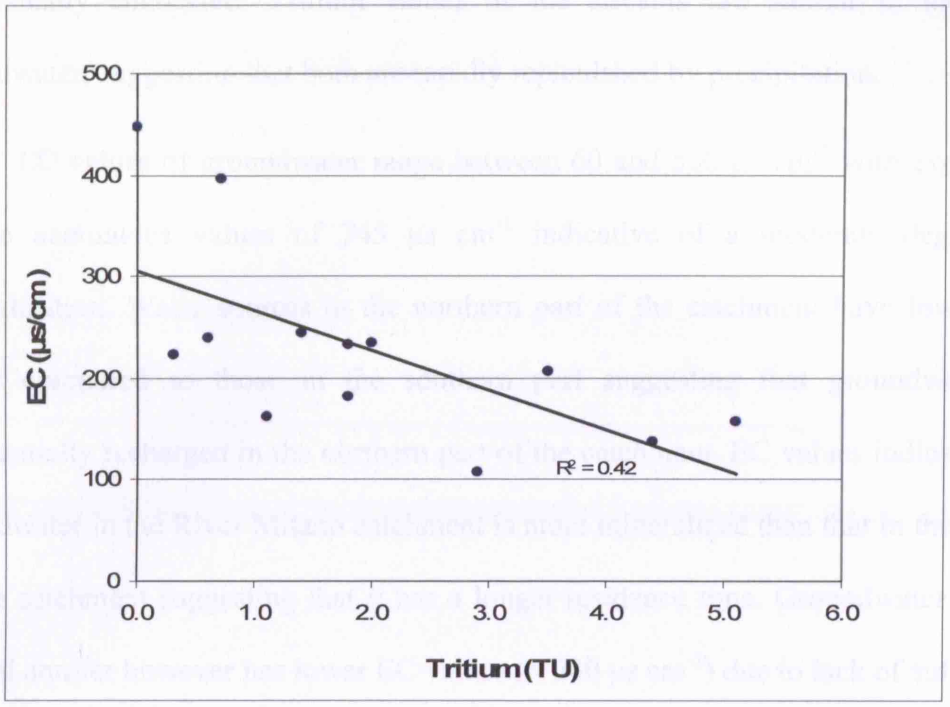

Figure 3.13. Plot of electrical conductivity versus tritium in the River Kigwe catchment

3.3.4.1 River Mitano catchment

Tritium content for all groundwater sources in the River Mitano catchment lies between 0.36 and 3.1 TU. Although there is no clear trend in the distribution of tritium, highest values are observed in the northern part of the catchment whereas the lowest values are observed in the southern part. Similarly, higher tritium values (>2 TU) are found in the topographically high areas around the catchment underlain by weathered and fractured-bedrock aquifers whereas lower tritium values (<1.5 TU) are found in boreholes constructed in alluvial sediments in valleys. The results appear to indicate that there is preferential recharge in the topographically high areas and most especially in the northern part of the catchment. It is also not possible to differentiate springs from deep boreholes using tritium, as the values are similar further suggesting

that groundwater is rapidly turned over and that the shallow and deep aquifer units are hydraulically connected. Tritium values of the streams are similar to those of groundwater, suggesting that both are rapidly replenished by precipitation.

EC values of groundwater range between 60 and 500 μs cm^{-1} with exception of one anomalous values of 745 μs cm^{-1} indicative of a moderate degree of mineralisation. Water sources in the northern part of the catchment have lower EC values compared to those in the southern part suggesting that groundwater is preferentially recharged in the northern part of the catchment. EC values indicate that groundwater in the River Mitano catchment is more mineralized than that in the River Kigwe catchment suggesting that it has a longer residence time. Groundwater in the alluvial aquifer however has lower EC values (< 200 μs cm^{-1}) due to lack of sufficient amounts of soluble cation bearing minerals. Mineralisation is exhibited by boreholes installed in the fractured aquifer which have EC values > 200 μs cm^{-1}. EC can therefore aid in differentiating boreholes installed in the alluvial aquifer from those constructed in the fractured-bedrock. Similar to the River Kigwe catchment, the plot of tritium versus EC values for the River Mitano catchment (Fig. 3.14) shows no clear correlation (r^2 = 0.27) between tritium and EC suggesting that there is no distinct groundwater flowpath. Most of the samples show low EC and high tritium suggesting that the groundwater in the catchment is fresh and is actively recharged.

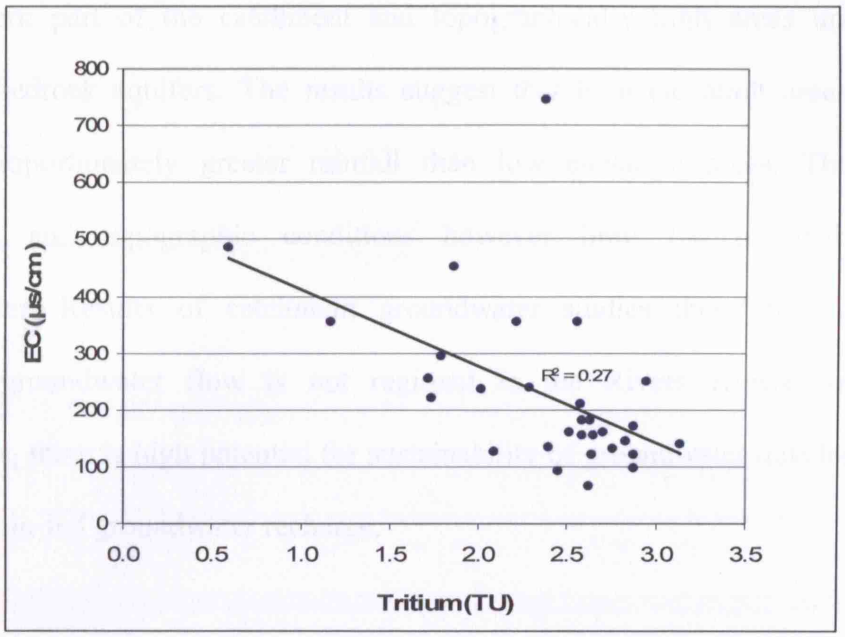

Figure 3.14. Plot of tritium versus electrical conductivity values in the River Mitano catchment

3.4 Conclusions

Previous studies of groundwater recharge in both the Rivers Kigwe and Mitano catchments assume that it derives principally from precipitation and accounts for between 8 to 13% of precipitation. Stable-isotope ratios in precipitation, groundwater and surface water confirm that recharge results primarily, if not solely, from precipitation with no evidence of recharge from surface water. Stable-isotopes further show that groundwater resources in the River Kigwe catchments are actively recharged by monsoonal rainfall associated with the two rainy seasons whereas recharge in the River Mitano catchment results from mixing in the unsaturated zone, of rain falling throughout the year. Although recharge occurs everywhere in the two catchments, zones of preferential recharge are indicated by high tritium and low EC values. In the River Kigwe catchment, these zones are found around the hills surrounding the catchment whereas in the River Mitano catchment they are found in

the northern part of the catchment and topographically high areas underlain by fractured-bedrock aquifers. The results suggest that high elevation areas generally receive proportionately greater rainfall than low elevation areas. The complex geological and topographic conditions however limit the regional flow of groundwater. Results of catchment groundwater studies therefore suggest that although groundwater flow is not regional in the Rivers Kigwe and Mitano catchments, there is high potential for sustainability of groundwater development due to active rain-fed groundwater recharge.

CHAPTER 4: TOWN WATER RESOURCES

This chapter describes the development of groundwater-fed town water supplies within the River Kigwe and River Mitano catchments. Specifically, the chapter discusses the current groundwater abstraction patterns in two towns, Wobulenzi in the River Kigwe catchment and Rukungiri in the River Mitano catchment, and the groundwater level monitoring conducted to closely monitor and assess the impacts of intensive groundwater abstraction for town water supply. The chapter reviews the construction of piezometer networks around the production boreholes and the use of lithological profiles and geophysical surveys to assess the extent of aquifers in view of localised groundwater flow systems as observed in Chapter 3. The chapter also assesses the responses of the aquifers to rainfall and intensive groundwater abstraction and the impact this has on groundwater storage.

4.1 Introduction

4.1.1 Groundwater-fed town water supplies in Uganda

Groundwater is the main source of piped water supply for private, domestic and industrial use in many urban areas in the developing world because of its widespread occurrence, good natural quality and relatively low cost of development compared to surface water (Foster *et al.,* 1998). In addition, the need for water supply systems that can easily be operated and managed by the users makes groundwater a preferred source for piped water supplies.

Groundwater development for town water supplies in Uganda effectively began in the early 1990s with the formulation of the Rural Towns Water and Sanitation Programme under which 60 urban centres in the country were identified for piped water supply (MWLE, 2006a). The initiative, supported by the World Bank, aimed at developing mechanisms for providing water supply to the growing number of small towns thoughout Uganda and led to the implementation of water supply and sanitation activities in eleven towns. Detailed hydrogeological investigations confirmed availability of adequate groundwater resources in eight out of the eleven towns which were subsequently developed based on groundwater. Additional towns have since been developed based on groundwater. By July 2006, there were 180 small towns in the country already considered for piped water supply, out of which 98 had functional water supply systems whereas 24 and 44 were at construction and design stages respectively (MWLE, 2006a). Out of the 98 operational water supply systems, 73 are based on groundwater, which is approximately 74% of the towns (MWLE, 2006a). The total number of groundwater sources supplying piped water to the 98 towns is 90 (66 deep boreholes and 24 springs).

In order to improve provision of water supply and sanitation services, a comprehensive urban water supply and sanitation reform study was carried out between 1999 and 2000 that resulted in wide-ranging policy and institutional reform proposals including formulation of a strategic and investment plan covering the period 2000 to 2015. The reform study recognised the need for a coherent strategy for implementing the reforms in small towns' water and sanitation facilities and identified the small towns that need to be provided with piped water during the next 15 year period. By June 2006, a

total number of 782 small towns in the whole country including the 98 that already have operational piped water supply schemes, had been identified for provision of piped water (MWLE, 2006a). It is estimated that over 70% of these towns (550) will be based on groundwater mainly though deep boreholes. Thus, intensive groundwater development for town water supply in Uganda based on high yielding deep boreholes has been ongoing since the mid 1990s and is slated to increase drastically as the Uganda Government intensifies its efforts of providing safe drinking water to urban populations.

Although large investments have been put into infrastructure development for both rural and urban water supply, insufficient attention has been given to assessment of the sustainability of the water supply systems. In an effort to assess the impact of heavy groundwater abstraction on surrounding water resources in urban areas, groundwater resources monitoring and assessment studies were initiated in small towns in Uganda in mid-1990s. Groundwater resources monitoring and assessment studies in Wobulenzi town were initiated in 1997 and were the first in the country. Studies in Rukungiri town were initiated in 2003. The studies have generated a large volume of hydrogeological, isotope and hydrochemical data. Current efforts seek to transform these data into useful information to guide optimum and sustainable groundwater development. Similar investigation techniques were employed in Wobulenzi and Rukungiri towns for purposes of comparing the results and generating information that is representative of the whole country. It was assumed that the results in the two contrasting towns would provide information that is applicable to the two dominant geomorphic settings in Uganda; the zone of deep weathering in central Uganda, and the zone of stripping in western Uganda.

4.1.2 Water supply in Wobulenzi town

Wobulenzi town relies entirely on groundwater for its piped water supply. Motorised groundwater abstraction based on a single deep borehole located in the centre of the town has been ongoing for over 20 years. The borehole was supplemented by 4 additional deep boreholes in the mid 1990s to increase access to piped water. Three of the boreholes are equipped with motorised pumps whereas the fourth is yet to be installed. More intensive groundwater development for town water supply has occurred since 1997 and demand for water continues to increase (MWLE, 2006b). In addition to the piped water supply, there are approximately 20 hand-pumped boreholes and 2 springs that provide a supplementary water supply. Wobulenzi town has a population of about 21,500 people living within the town itself and surrounding institutions. The percentage of the population with access to safe water in the town is 61% out of which 54% are supplied by the piped water supply system whereas 7% are supplied by point water sources (MWE, 2006). Based on the most recent performance monitoring report on town water supplies (MWLE, 2006b) it is estimated that daily abstraction from the four boreholes is 250 m^3. The report notes that the water supply system in Wobulenzi town is inadequate for meeting the current water demand and recommends that additional boreholes be installed to augment the supply from existing boreholes.

Figure 4.1. Production borehole (DCL725) used for piped water supply to Wobulenzi town together with one of the piezometers. The production borehole is in the background whereas the piezometer is in the foreground.

4.1.3 Water supply in Rukungiri town

Rukungiri town relies on groundwater for its piped water supply which is based on two high yielding deep boreholes. An additional borehole drilled in 1998 is currently not installed with a pump. Motorised groundwater development has been ongoing since 1998 but has greatly increased since 2003 due to the increase in demand (MWLE, 2006b). To supplement the piped water supply system, there are approximately 14 hand-pumped boreholes and 47 springs in the town in addition to one production borehole privately operated by Nyakibale Hospital. Rukungiri town has a population of about 18,600 people living within the town itself and surrounding institutions. The percentage

of the population with access to safe water in the town is 71%. Of this, 56% are supplied by the piped water supply system whereas 15% are supplied by point water sources (MWE, 2006). In the most recent performance monitoring report on town water supplies (MWLE, 2006b) it is estimated that daily abstraction from the two boreholes is 150 m^3 although there is over reliance on one of the boreholes (Fig. 4.2) with the highest yield. The water supply system in Rukungiri town like that in Wobulenzi town is singled out as being inadequate for meeting the current town water demand. The report (MWLE, 2006b) recommends that an existing borehole that is currently not operational should be installed to augment the water supply from the existing boreholes.

Figure 4.2. Production borehole (Ruk 8) used for piped water supply to Rukungiri town. The town water supply depends heavily on this borehole due to its high yield.

4.2 Monitoring of groundwater levels in town water supplies

4.2.1 Overview

Groundwater levels are lowered when water is removed from storage in aquifers. Groundwater level measurements enable the effects of recharge and abstraction on groundwater systems to be monitored. Groundwater level monitoring has been enhanced by recent advances in instrumentation which allow collection of very accurate and real-time water level data making it possible to accurately determine diurnal and seasonal variations in water levels (Alley *et al.*, 2002). Understanding the nature of changes in groundwater systems and differentiating between natural and human induced changes however requires long-term water level measurements.

Monitoring groundwater levels in town water supplies in Uganda was initiated in 1998 as part of the national groundwater monitoring network. The aim was to monitor the impact of intensive groundwater abstraction in urban areas on surrounding water resources. Dedicated monitoring wells were established close to production boreholes in a few towns to monitor continuously the response of groundwater levels to abstraction. In addition, piezometers have been constructed around production boreholes in three towns including Wobulenzi and Rukungiri with two aims; (i) to closely monitor the responses of different aquifers to pumping, and (ii) to provide an opportunity to assess in detail the groundwater flow and storage in weathered crystalline rock aquifers so as to effectively guide optimum and sustainable groundwater development in the country.

Groundwater level monitoring is carried out using water level transducers (divers) and automatic water level recorders in order to monitor continuously small changes in water levels. Rainfall is also monitored alongside groundwater levels in the these towns

in order to assess the response of the aquifer systems to rainfall events and be able to differentiate between natural and human induced changes in groundwater levels. In addition to the purposely drilled monitoring wells, groundwater level monitoring is carried out in production boreholes on a weekly basis as part of the conditions attached to groundwater abstraction permits. All owners of motorised boreholes are required by law to obtain groundwater abstraction permits though compliance to this requirement remains low. Details of monitoring well (piezometer) construction and groundwater monitoring in Wobulenzi and Rukungiri towns are discussed below.

4.2.2 Site construction and layout of the piezometers

4.2.2.1 Wobulenzi town

A network of four monitoring wells (piezometers) was constructed at increasing radial distances around one of the production boreholes (DCL725) in Wobulenzi town (Fig. 4.3) using the air rotary drilling method. The production borehole was drilled to a depth of 94 mbgl into the fractured-bedrock aquifer. Two piezometers (P1 and P2) were drilled to depths of 39 and 32 mbgl respectively in the shallow weathered aquifer. Two other piezometers (P3 and P4) were drilled to depths of 71 and 65 mbgl respectively in the fractured-bedrock aquifer. A set of shallow and deep piezometers are located 13 m (P1 and P4) and 42 m (P2 and P3) from the production borehole.

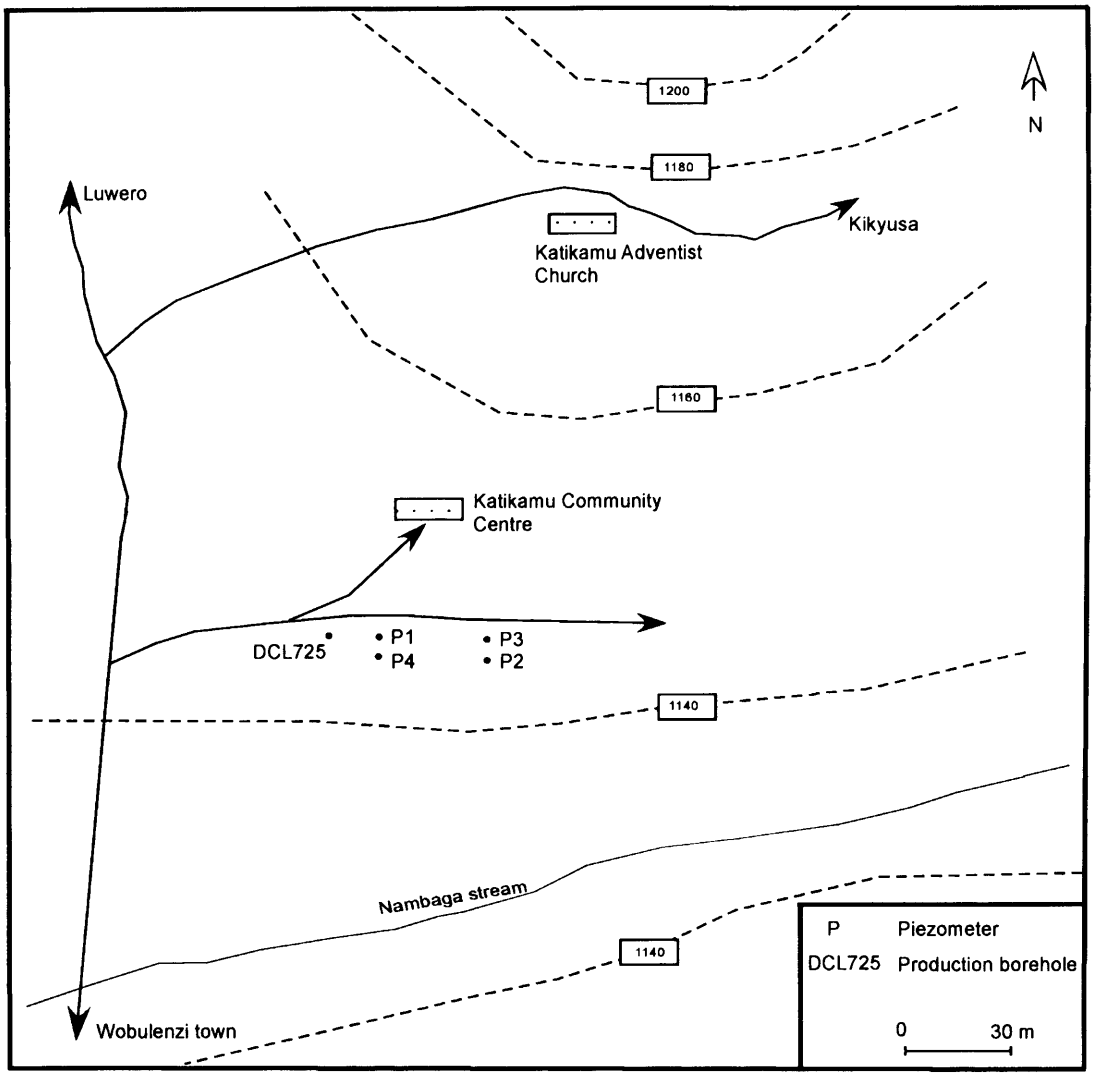

Figure 4.3. Study site layout indicating positions of piezometers around the production borehole in Wobulenzi town. The map also shows topographic contours which indicate that the site slopes towards Nambaga stream.

The production borehole was drilled in 1997 using 10" (254 mm) boring diameter in the overburden and 6.5" (165 mm) in the bedrock. It was completed with an open hole in the bedrock and a 6" (152 mm) plastic (uPVC) casing lining in the weathered bedrock down to the competent bedrock at a depth of 60 mbgl. The first 7 m from the bedrock were lined with plain casings above which 6 m of screened casings with 1.5 mm slot sizes were installed. The rest of the hole was lined with plain uPVC casings up to the

ground surface. A sand and gravel filter (2 to 6 mm in size) was placed around the screen casings and was extended 1 m above the depth of the screen casings to allow for settling during well development and completion. The top of the gravel was sealed using cement slurry. Clay cuttings obtained during drilling were backfilled above the cement slurry up to 2 m below the ground level where a seal was installed using cement slurry. A concrete slab was cast above the cement seal to limit any contaminants entering the borehole. The borehole was developed by air lift method using a compressor until the water cleared.

Piezometers were drilled using 8" (203 mm) boring diameter and lined with 5" (127 mm) plastic (uPVC) casings. P1 installed in the weathered aquifer, was drilled to a depth of 68 mbgl into the fractured-bedrock but later backfilled with fine-grained drilling cuttings to 39 mbgl. Each of the shallow piezometers (P1 and P2) was designed with 6 m of screen casings with 2 mm slot sizes, above a 1 m plain casing starting from the bottom of the well. Plain uPVC casings were installed over the remaining depths of the piezometers up to the ground level. The piezometers were completed following procedures similar to those used when drilling the production borehole. The piezometers drilled in the fractured-bedrock (P3 and P4) were completed with an open hole in the bedrock and were lined with 5" plastic plain casings in the weathered overburden, starting at the interface with the bedrock. The deep piezometers were designed in a similar manner to the production borehole except that no screen casings and gravel pack were used. The piezometers thus tapped only the fractured-bedrock aquifer. All the piezometers were developed by air lift method using a compressor until the water cleared. Table 4.1 presents the construction details of the piezometers and production borehole.

Table 4.1. Construction details of the piezometers and the production borehole in Wobulenzi town

Piezometer no.	Piezometer name	Aquifer type	Distance from PW (m)	Depth (mbgl)	Main water strike depth (mbgl)	Screen casing depth (mbgl)
P1	WRMD –5	Weathered	13	39	34	31 - 37
P2	WRMD –6	Weathered	42	32	28	25 - 31
P3	WRMD –7	Fractured	42	71	57	n.a
P4	WRMD –8	Fractured	13	65	63	n.a
PW	DCL725	Weathered – fractured	0	94	65, 79	53 - 59

PW- production borehole; mbgl: metres below ground level; n.a: not applicable

4.2.2.2 Rukungiri town

A dense array of eight monitoring wells (piezometers) was constructed around one of the production boreholes (Ruk 8) in Rukungiri town (Fig. 4.4) using air rotary and mud-drilling methods. Originally, it had been planned to construct a set of 3 piezometers each at 20 and 40 m from the production borehole to monitor the shallow, intermediate and deep fractured aquifer units. Two piezometers in each of the 3 aquifer units would thus enable monitoring of the response of the aquifer units to pumping at varying distances from the production borehole. However, as drilling progressed the anticipated 3 aquifer units could not be encountered and so the study site construction design was modified. During construction of the first 6 piezometers only alluvial material was encountered a maximum depth of 61 mbgl. Drilling could not go deeper than 61 mbgl because of highly collapsing sands and gravels. Drilling was extended beyond the 40 m radius in an effort to reach the underlying bedrock. The bedrock was encountered in P7 and P8, located 66 and 60 m from the production well respectively.

The production borehole (Ruk 8) around which the piezometer network is constructed is installed to a depth of 64 mbgl into the alluvial sediments. It was drilled in 1998 using 10" (254 mm) boring diameter and was completed with a 6" (152 mm) plastic (uPVC) casing lining up to the bottom. The first 3 m from the bottom were lined with a plain casing above which 6 m of screened casings with 1.5 mm slot sizes were installed. The rest of the borehole was lined with plain uPVC casings up to the ground surface. Similar to the production borehole in Wobulenzi, a sand and gravel filter (2 to 6 mm in size) was placed around the screen casings and extended 1 m above the depth of the screen casings to allow for settling during well development and completion. The top of the gravel was sealed using a cement slurry. Clay cuttings obtained during drilling were backfilled above the cement slurry up to 2 m below the ground level where a seal was installed using cement slurry. A concrete slab was cast above the cement seal to limit any contaminants entering the borehole. The borehole was developed by air lift method using a compressor until the water cleared.

Piezometers in Rukungiri were located at a range of radial distances from the production borehole (Fig. 4.4). Six piezometers (P1, P2, P3, P4, P5 and P6) were constructed in the alluvial sediments whereas two piezometers (P7 and P8) were constructed in the fractured-bedrock. P1, P2 and P3 installed to depths of 45, 36 and 35 mbgl respectively are located 40 m in the north-west direction from the production borehole and are about 6 m from each other (Fig. 4.5). It had originally been planned to drill P3 to a depth deeper than 35 m to explore the aquifer further but there was continuous loss of drilling air into P2 (Fig. 4.6). Drilling therefore could not go deeper because the drill cuttings could not be flushed out. P4 and P5 installed to depths of 61 and

48 mbgl respectively are located 20 m in the north-west direction from the production borehole and are about 10 m from each other. P6 originally constructed to a depth of 51 mbgl but backfilled to 19 mbgl due to highly collapsing formation is located 140 m in the north-west direction from the production borehole. P7 installed to a depth of 48 mbgl is located 66 m to the west of the production borehole. P8 installed to a depth of 81 mbgl is located 60 m to the north of the production borehole. The varying depths and distances of the piezometers from the production borehole made it possible to investigate vertical and radial responses of the aquifer units to pumping.

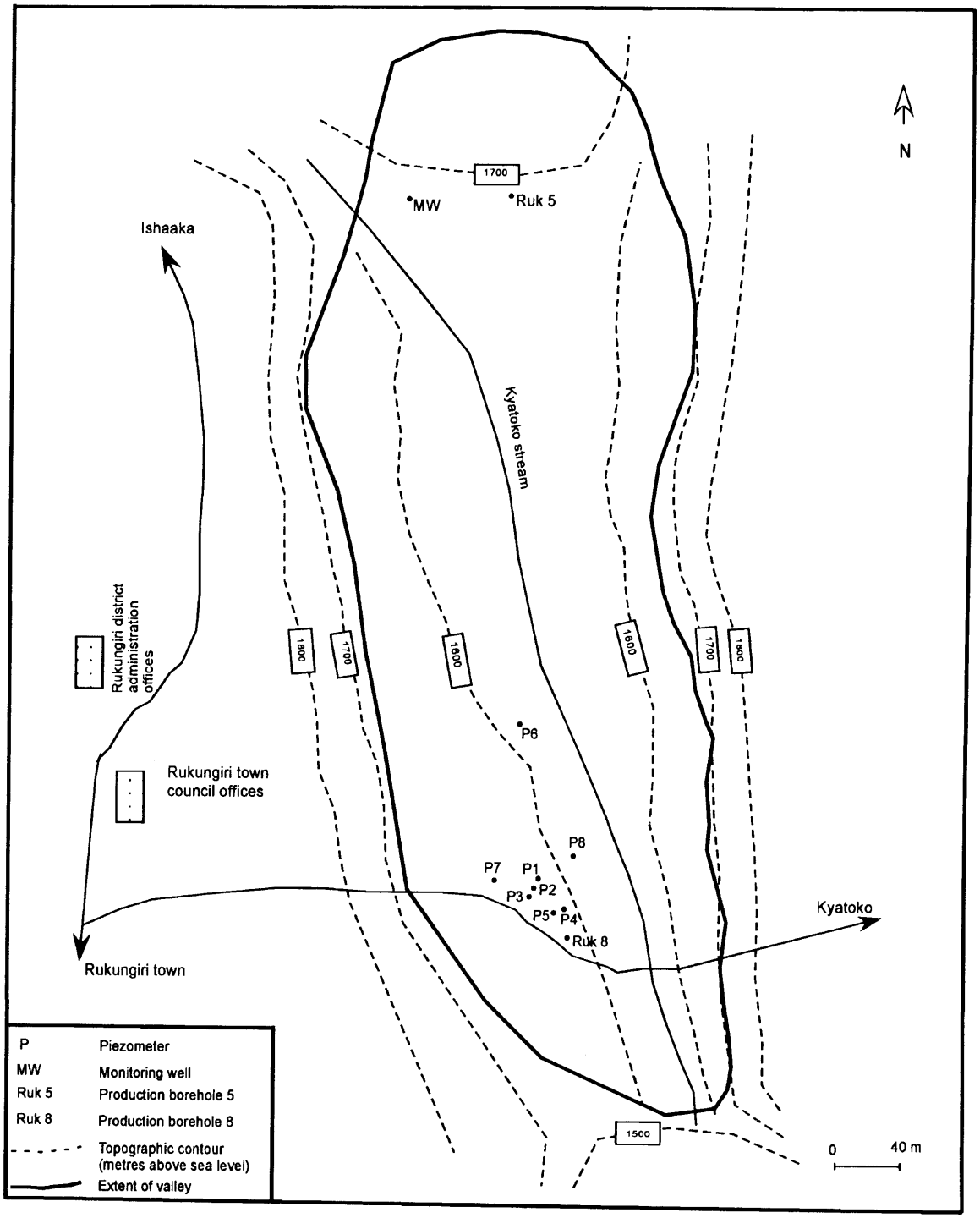

Figure 4.4. Study site layout indicating the position of the piezometers around the production borehole, Ruk 5 and the monitoring well. Topographic contours are shown indicating that the study site lies in a valley.

Figure 4.5. Location of Piezometers 1, 2 and 3 around the production borehole in Rukungiri town.

All the piezometers in Rukungiri town were drilled using an 8" (203 mm) boring diameter and were lined with 5" (127 mm) plastic (uPVC) casings. Each of the piezometers drilled in the alluvial sediments was designed in a similar manner to the production borehole but the length of the plain casing at the bottom below the screen casings varied between 1 and 3 m. The piezometers drilled in the fractured-bedrock (P7 and P8) were completed with an open hole in the bedrock and plain casings in the alluvial sediments similar to the fractured-bedrock piezometers in Wobulenzi town. All the piezometers were developed by air lift method using a compressor and later during test pumping. Table 4.2 presents construction details of the piezometers and the production borehole.

Figure 4.6. Drilling of the piezometers in Rukungiri town. Photo above shows water gushing out of P2 while drilling P3. Continuous loss of drilling air to P2 could not allow drilling in P3 to go deeper.

Table 4.2. Construction details of the piezometers and the production borehole in Rukungiri town

Piezometer No.	Piezometer Name	Aquifer Type	Distance from PW (m)	Depth (mbgl)	Main water strike depth (mbgl)	Screen casing depth (mbgl)
P1	DWD20335	Alluvial	40	45	39	38 - 44
P2	DWD20336	Alluvial	40	36	31	27 - 33
P3	DWD20337	Alluvial	40	35	28	26 - 32
P4	DWD20338	Alluvial	20	61	54	52 - 58
P5	DWD20339	Alluvial	20	48	43	41 - 47
P6	DWD20340	Alluvial	140	19	15	10 - 16
P7	DWD20341	Fractured	66	48	44	n.a
P8	DWD20342	Fractured	60	81	71	n.a
Ruk 8	DCL1016	Alluvial	0	64	56	55 - 61
Ruk 5	DCL1015	Alluvial	600	89	55, 69	44 - 51
MW	MW	Alluvial	600	66	56	45 - 52

MW- monitoring well; mbgl: metres below ground level; n.a: not applicable

4.2.3 Groundwater level monitoring

4.2.3.1 Wobulenzi town

Groundwater level monitoring was initiated in Wobulenzi town in 1997 immediately after the commissioning of the water supply system. Groundwater levels are monitored in the four piezometers, located around one of the production boreholes (DCL725), on a daily basis using automatic water level recorders (Fig. 4.7) which are supplemented by manual measurements using water level dip meters. A rainfall measurement station using a rain gauge is located next to the monitoring wells and has been monitoring rainfall daily since 2000.

Figure 4.7. Groundwater level monitoring using an automatic water level recorder in Wobulenzi town. The charts on the recorder are set to measure water levels daily and are changed every month.

4.2.3.2 Rukungiri town

Groundwater monitoring in Rukungiri was initiated in 1998 immediately after the commissioning of the water supply system. Groundwater abstraction was from two motorised boreholes (Ruk 5 and Ruk 8) and thus a groundwater monitoring borehole was located close to one of the production boreholes (Ruk 5). Ruk 5 is approximately 100 m from the monitoring well whereas Ruk 8 is located approximately 600 m both the monitoring well and Ruk 5 (Fig. 4.4). In 2005, groundwater level monitoring was initiated in seven of the eight piezometers drilled around Ruk 8 and is done continuously using water level transducers (divers) in two of the piezometers (Fig. 4.8) and automatic water level recorders in the remaining five piezometers. Manual measurements using a water level dip meter is done on a monthly basis to supplement the measurements from the divers and automatic water level recorders. Monitoring of groundwater level in the old monitoring well has been done on a daily basis since 1998 using an automatic water level recorder supplemented by manual measurements using a water level dip meter. A rainfall measurement station is located next to the monitoring well and has been in use since 2000 using a rain gauge. Rainfall measurement was automated in 2003 and is currently being done using an automatic recorder located next to Ruk 5.

Figure 4.8. Downloading of groundwater level data from a water level transducer (diver) in Rukungiri town. The divers were set to measure water levels every 10 minutes and data is retrieved every 3 months.

4.3 State of groundwater resources in Wobulenzi town

4.3.1 Lithological profiles

Information on the lithology underlying the study site in Wobulenzi town was obtained from the drilling logs of the four piezometers and the production borehole. Soil sample collection and description was carried out every metre or when there was a change in lithology. Based on lithological logs, the study site is underlain by a thin brown top soil layer of about 1 m below which there is a reddish brown clay layer with a thickness of about 5 m. A brown layer of sand mixed with small amounts of clay occurs below the clay layer, with an average thickness of 16 m. The water table is found in this clayey sand layer at a depth of about 15 mbgl. The clayey sand layer is underlain by a coarse-grained quartz sand layer with an average thickness of 27 m in which the quartz

fragments are big and angular. The quartz sand layer is underlain by weathered-fractured bedrock dominated by big quartz fragments whose frequency and size increase with depth. The weathered-fractured bedrock is approximately 35 m thick and is underlain by hard but fractured bedrock. A lithological profile across the study site (Fig. 4.9) shows that the average thickness of the weathered aquifer is 27 m.

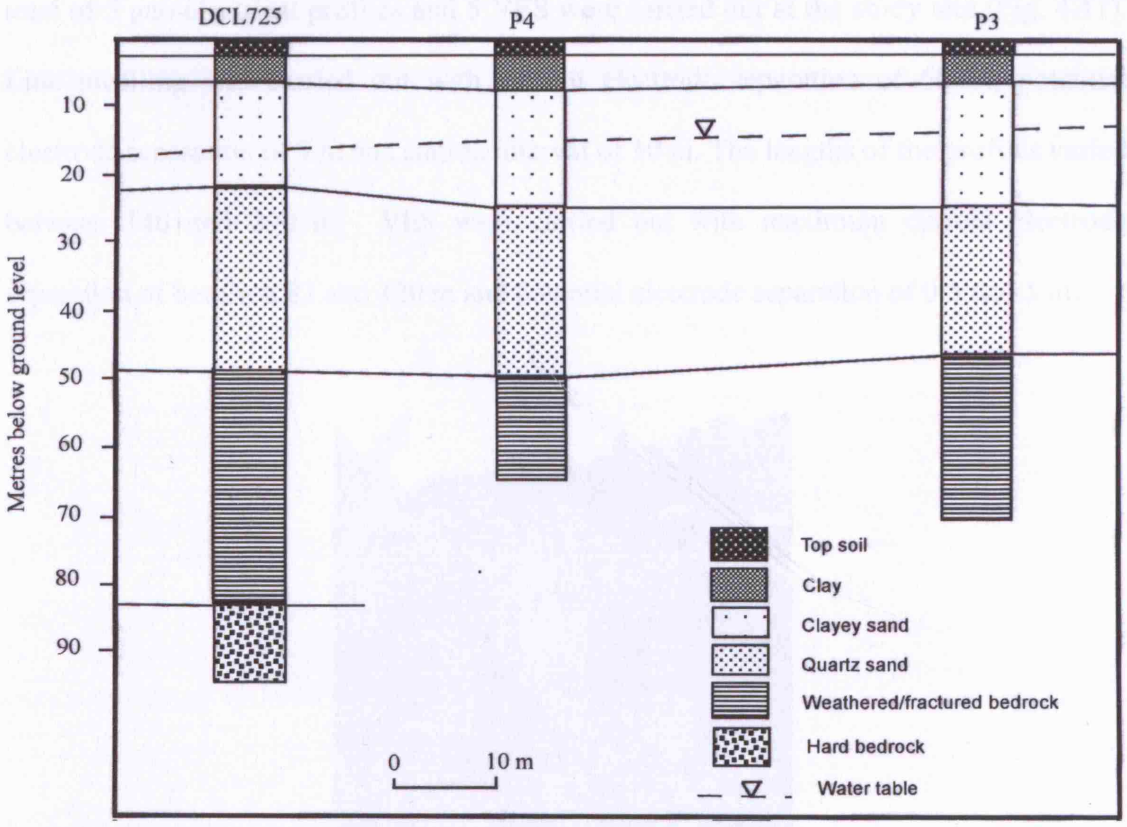

Figure 4.9. Lithological profile across the study site in Wobulenzi town

4.3.2 Geophysical surveys

Surface geophysical surveys were employed to assess the lateral and vertical variations of aquifers units at the study site. The surveys involved resistivity geo-electrical profiling and Vertical Electrical Soundings (VES) using the Schlumberger configuration (Fig. 4.10). Geo-electrical profiles were used to assess the lateral variation of the aquifer whereas VES were used to assess the vertical variation of the aquifer. A total of 5 geo-electrical profiles and 5 VES were carried out at the study site (Fig. 4.11). Line profiling was carried out with current electrode separation of 60 m, potential electrode separation of 5 m and station interval of 10 m. The lengths of the profiles varied between 140 and 290 m. VES were carried out with maximum current electrode separation of between 83 and 120 m and potential electrode separation of 0.5 and 5 m.

Figure 4.10. Resistivity surveys by geo-electrical profiling and Vertical Electrical Soundings using an ABEM terrameter in Rukungiri wellfield

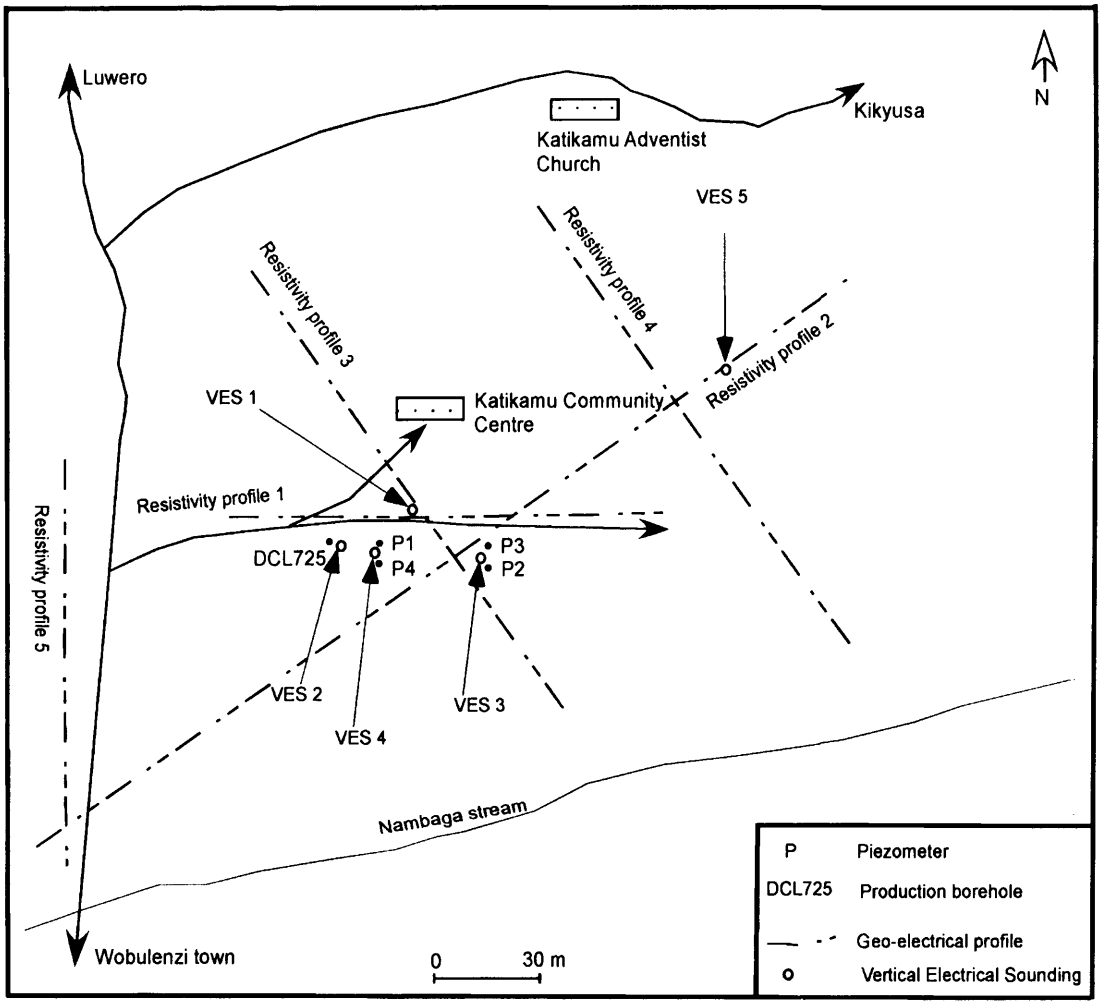

Figure 4.11. Location of geo-electrical profiles and Vertical Electrical Soundings in Wobulenzi town

Result of profiling indicate that the quartzites exhibit the highest resistivities (>200 ohm-m) with steep peaks whereas the schists exhibit low (<100 ohm-m) and uniform resistivity values (Figs. 4.12 and 4.13). The observed resistivity of granites and gneisses lie between those of quartzites and schists and varies from 100 to 200 ohm-m. The results of profiling suggest that the quartzite unit at the wellfield is approximately 50 m wide and is surrounded to the west by granites and gneisses and to the east by schists.

The production borehole and the piezometers at the study site are constructed in the quartzite and deeper boreholes extend into the granites and gneisses.

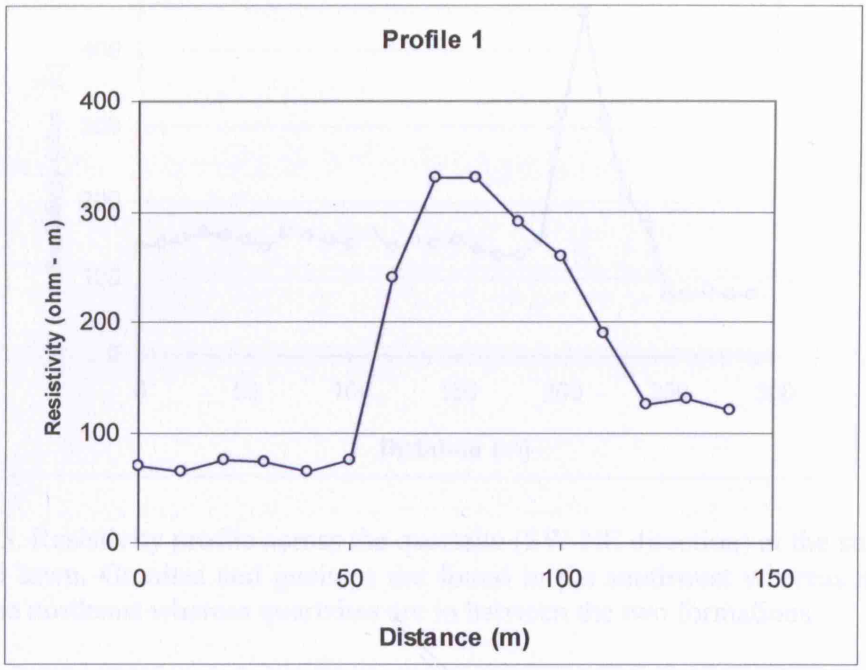

Figure 4.12. Resistivity profile perpendicular to the quartzite (E-W direction) at the study site in Wobulenzi town. Low resistivity values (<100 ohm-m) are characteristic of schists, intermediate resistivity values (100-200 ohm-m) are characteristic of granites and gneisses whereas high resistivity values (>200 ohm-m) are characteristic of quartzites.

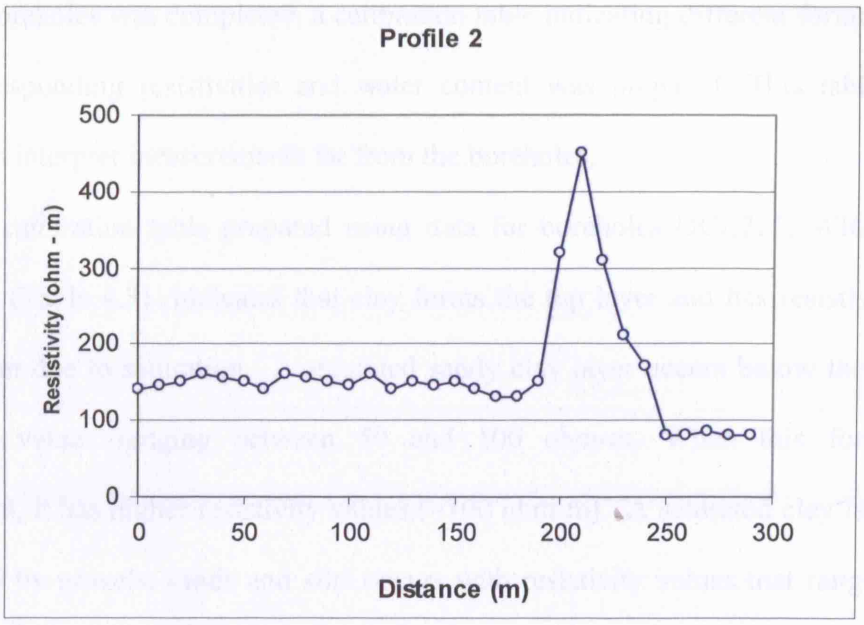

Figure 4.13. Resistivity profile across the quartzite (SW-NE direction) at the study site in Wobulenzi town. Granites and gneisses are found in the southwest whereas schists are found in the northeast whereas quartzites are in between the two formations.

The VES measurements were quantitatively interpreted using GEWIN V1.01 (NileSoftware, 1999). It is worth noting though that the assignment of a geophysical property value to a specific geological material is rather complicated and to a certain extent site specific. One resistivity value might correspond to many different materials depending on, for example, the water content, nature and thickness of the overburden, water chemistry, degree of weathering etc. Similarly, from the principle of equivalence there is no unique solution to an interpretaion of a geo-electrical measurement. Any combination of aquifer depth and resistivity can produce the best fitting curve resulting in many solutions for a single measurement. In order to improve interpretation of geophysical data, it is essential to correlate this data with borehole records. Thus, interpretation of VES results (Fig. 4.14) used borehole drilling logs to assign a resistivity value to a specific geological formation. Once interpretation of measurements near

existing boreholes was completed, a calibration table indicating different formations with their corresponding resistivities and water content was prepared. This table made it possible to interpret measurements far from the boreholes.

A calibration table prepared using data for boreholes DCL725, WRMD-5 and WRMD-6 (Table 4.3) indicates that clay forms the top layer and has resistivity values <50 ohm-m due to saturation. A saturated sandy clay layer occurs below the clay with resistivity values ranging between 50 and 100 ohm-m. When this formation is unsaturated, it has higher resistivity values (>100 ohm-m). A saturated clay layer that is dominated by gravels, sands and silts occurs with resistivity values that range between 100 and 200 ohm-m and is underlain by saturated weathered and fractured-bedrock with resistivities that range between 100 and 300 ohm-m. Resistivity values are higher when the weathered and fractured-bedrock is formed by quartzites (>200 ohm-m) and lower when it is formed by granites and gneisses (<200 ohm-m). Dry bedrock or sands and gravels layers have resistivity values >200 ohm-m. Resistivity values are relatively high because the study site is underlain by quartzites.

Table 4.3. Calibration table for resistivity measurements in Wobulenzi town based on drilling logs of the production borehole and the piezometers

Formation Resistivity (ohm-m)	Rock type	Water content
<50	Clay, weathered schist	Saturated
50 – 100	Sandy clay	Saturated
100 – 300	Sandy clay	Dry
100 – 200	Sand, silt, gravel with clay	Saturated
100 - 300	Weathered granite/gneiss	Saturated
200 - 400	Fractured quartzite	Saturated

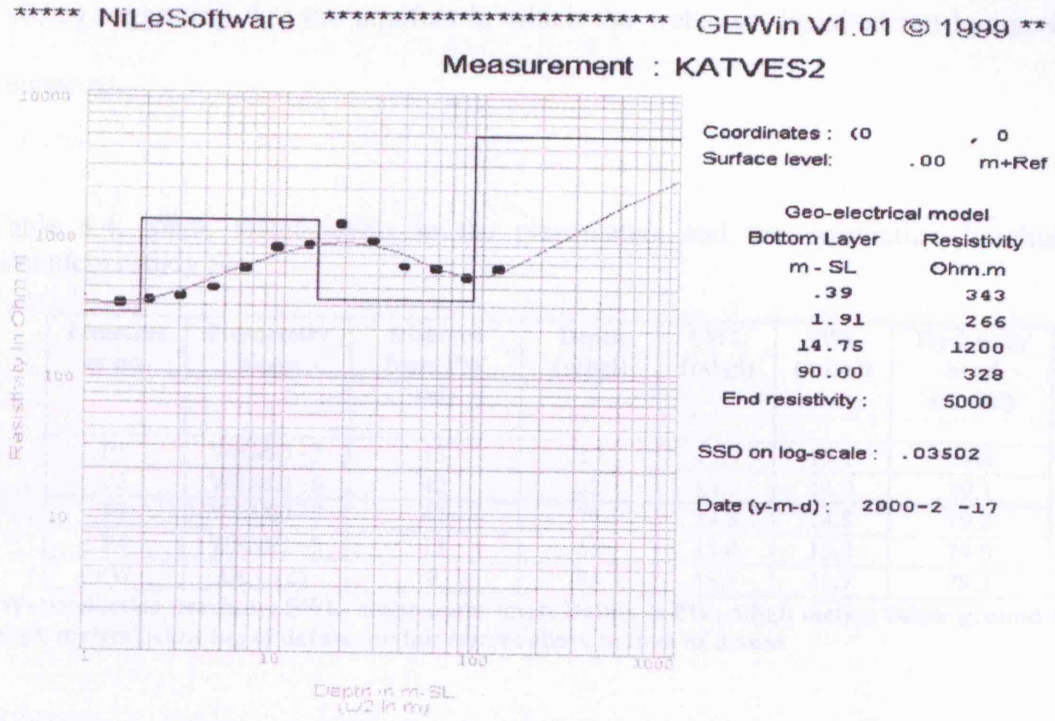

Figure 4.14: An example of a field apparent resistivity curve with modelled layers

4.3.3 Groundwater level trends

Static water levels in the various piezometers and the production borehole were compared with respect to a common datum. The bottom of the production borehole was used as the datum to convert static water levels in the piezometers into hydraulic heads (Table 4.4). The results indicate that hydraulic head in P4 is higher than in P1 at the same location. Similarly, hydraulic head in P2 is lower than in P3 at the same location. The hydraulic heads in all the piezometers are higher than in the PW suggesting that groundwater flow direction is towards the pumping well. The hydraulic gradients between the piezometers and the production borehole at the study site are very small

(<0.05) suggesting that the aquifers in which the wells are installed are hydraulically connected.

Table 4.4. Static water levels in the piezometers and the production borehole at Wobulenzi study site

Piezometer no.	Piezometer Name	Distance from PW (m)	Depth (mbgl)	SWL (mbgl)	SWL (mbtd)	Hydraulic head (mabd)
P1	WRMD –5	13	39	15.3	15.1	78.9
P2	WRMD –6	42	32	14.7	14.9	79.1
P3	WRMD –7	42	71	14.8	14.8	79.2
P4	WRMD –8	13	65	15.0	15.0	79.0
PW	DCL725	0	94	15.7	15.7	78.3

PW- production borehole; SWL- static water level; Datum is PW; mbgl: metres below ground level; mbtd: metres below top of datum; mabd: metres above bottom of datum

Groundwater levels measured in the piezometers at Wobulenzi study site were smoothened using a 5-day moving average for purposes of plotting. The data were plotted together with rainfall to assess the impact of rainfall on water levels (Figs. 4.15 and 4.16). Water levels in both the weathered and fractured-bedrock aquifer exhibit a seasonal pattern and responds to the onset and amount of rainfall. The time-lag between the onset of rainfall and the rise in groundwater levels in both the weathered and fractured aquifers is between 10 and 15 days suggesting that the vertical flow of infiltration precipitation is in the order of 1 m d^{-1}. The shallow and deep aquifers respond in a similar manner to rainfall and there appears to be no time lag in the response of the two aquifers. This suggests that the weathered and fractured-bedrock aquifers are directly connected. Preferential flowpaths within the regolith (e.g. stonelines) and bedrock (subvertical fractures) are assumed to enable relatively rapid responses to recharge events (Taylor and Howard, 1999b; Tindimugaya, 2000).

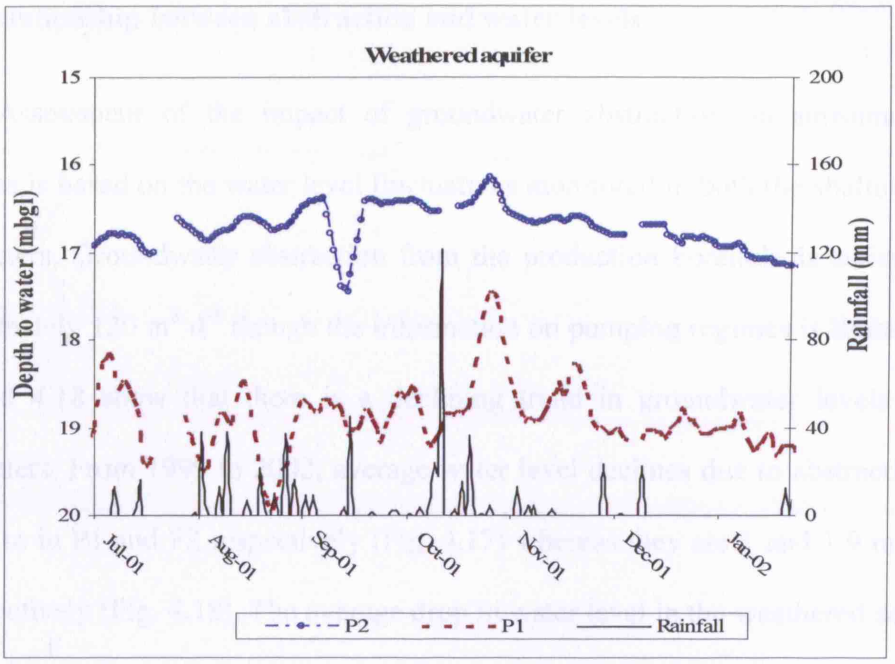

Figure 4.15. Response of groundwater levels to precipitation in P1 and P2 in the weathered aquifer in Wobulenzi town

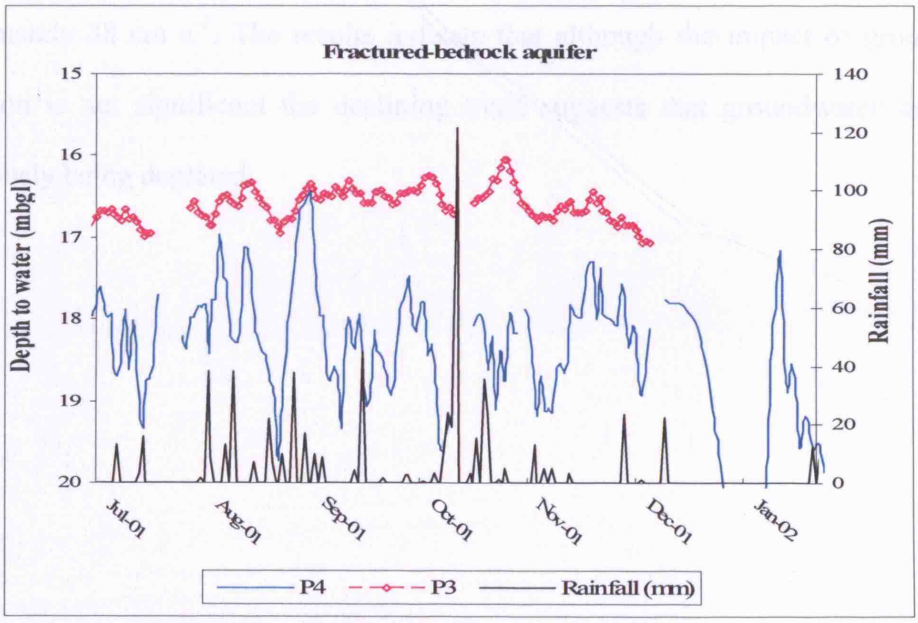

Figure 4.16. Response of groundwater levels to precipitation in P3 and P4 in the fractured-bedrock aquifer in Wobulenzi town

4.3.4 Relationship between abstraction and water levels

Assessment of the impact of groundwater abstraction on surrounding water resources is based on the water level fluctuations monitored in both the shallow and deep piezometers. Groundwater abstraction from the production borehole is estimated to be approximately 120 $m^3 d^{-1}$ though the information on pumping regimes is limited. Figures 4.17 and 4.18 show that there is a declining trend in groundwater levels in all the piezometers. From 1999 to 2002, average water level declines due to abstraction are 0.8 and 1.0 m in P1 and P2 respectively (Fig. 4.17) whereas they are 1 and 1.9 m in P3 and P4 respectively (Fig. 4.18). The average drop in water level in the weathered aquifer over a 4 year period is 90 cm which is approximately 23 cm a^{-1}. Similarly, the average drop in water level in the fractured-bedrock aquifer over a 4 year period is 1.5 m which is approximately 38 cm a^{-1}. The results indicate that although the impact of groundwater abstraction is not significant the declining trend suggests that groundwater storage is continuously being depleted.

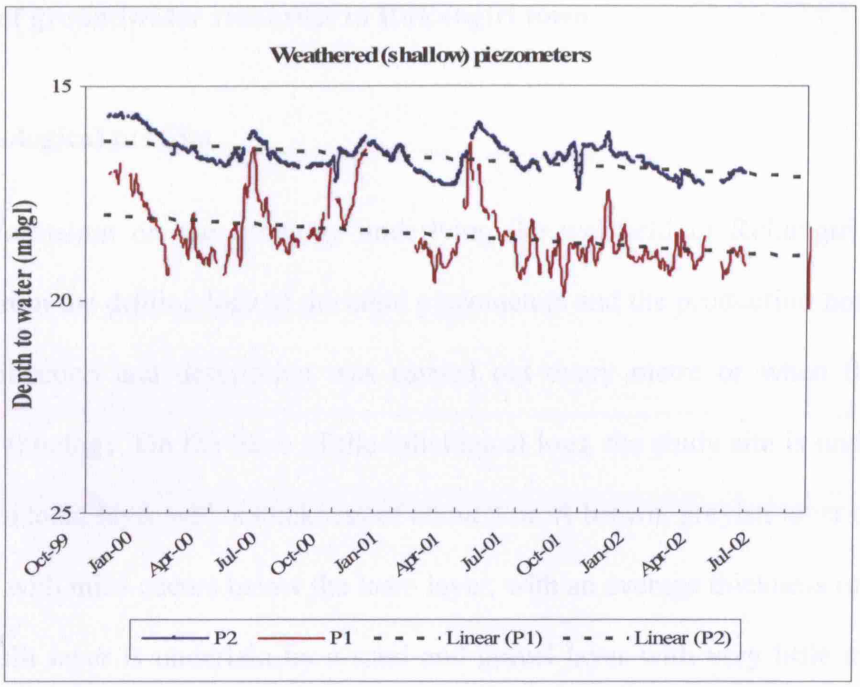

Figure 4.17. Response of groundwater levels to abstraction in P1 and P2 in the weathered (shallow) aquifer in Wobulenzi town

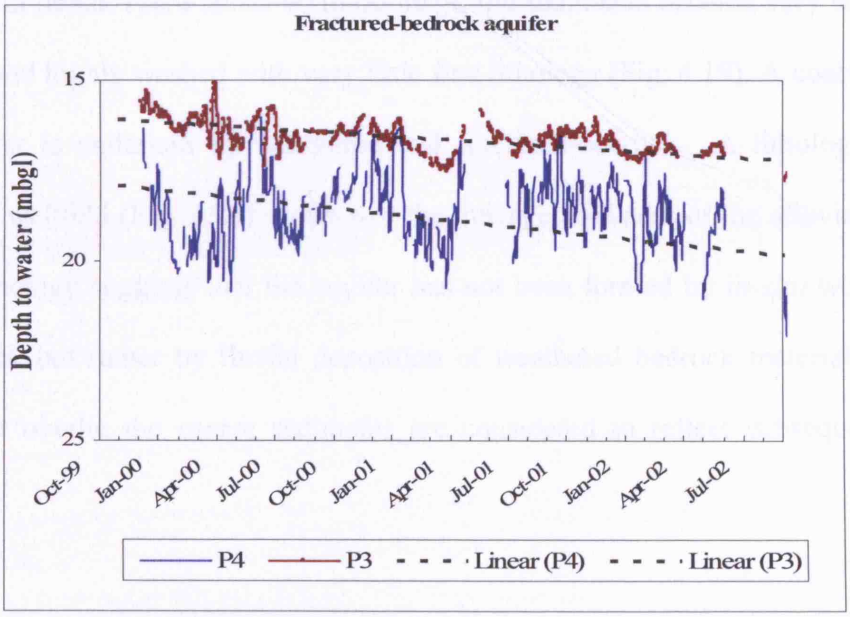

Figure 4.18. Response of groundwater levels to abstraction in Piezometers 3 and 4 in the fractured-bedrock (deep) aquifer in Wobulenzi town

4.4 State of groundwater resources in Rukungiri town

4.4.1 Lithological profiles

Information on the lithology underlying the wellfield in Rukungiri town was obtained from the drilling logs of the eight piezometers and the production borehole. Soil sample collection and description was carried out every metre or when there was a change in lithology. On the basis of the lithological logs, the study site is underlain by a dark brown loam layer with a thickness of about 3 m. A brown, greyish layer of sand and silt mixed with mica occurs below the loam layer, with an average thickness of 21 m. The sand and silt layer is underlain by a sand and gravel layer with very little mica with a thickness that ranges between 10 and 40 m. The water table is found in the sand and gravel layer at a depth of about 28 mbgl. The texture of the sand and gravel becomes coarser with depth. From about 40 to 60 mbgl, the sediments become very coarse, more rounded, and highly washed with very little fine lithology (Fig. 4.19). A coarse sand and gravel layer is underlain by weathered and fractured-bedrock. A lithological profile across the wellfeld (Fig. 4.20) shows that the average thickness of the alluvial aquifer is 30 m. Lithology suggests that the aquifer has not been formed by *in-situ* weathering of the bedrock but rather by fluvial deposition of weathered bedrock material. The finer layers that overlie the coarse sediments are considered to reflect subsequent alluvial deposition.

Figure 4.19. Coarse sands and gravels encountered during drilling of the piezometers in Rukungiri town. The sediments are distinct from in situ weathered regolith due to the near absence of fine-grained (clay) sediments (i.e Unimodal as opposed to bimodal particle size distribution) between 40 and 60 mbgl.

Figure 4.20. Lithological profile across the wellfield in Rukungiri town

4.4.2 Geophysical surveys

A total of nine geo-electrical profiles and seven VES were carried out in the wellfield. Line profiling was carried out at a depth of approximately 60 m and station interval of 10 m. The lengths of the profiles varied between 200 and 420 m and were determined mainly by the topographical setting and in a few instances by inability to go further due to presence of barriers such as swamps, thick forests and gardens. Four line profiles were carried out in the southwest-northeast direction across the wellfield while five profiles were carried out in the southeast-northwest direction between the piezometers and the production boreholes details of which are presented in Appendix 3. VES were carried out at locations selected based on results of geo-electrical profiling. Locations of the profiles and VES are presented in Fig. 4.21.

Figure 4.21. Direction of line profiles and locations of VES in the wellfield in Rukungiri town.

Line profiling (Figs. 4.22 and 4.23) shows that resisitivity values in and around the study area range between 50 and 4000 ohm-m. Resistivity values <200 ohm-m are found in the wellfield where the production boreholes are constructed whereas resistivity

values greater than 200 ohm-m are exhibited by the geological formations surrounding the wellfield. The high resistivity values are indicative of a dense unfractured crystalline geology. The driller's logs for the two boreholes and the piezometers confirm that the wellfield is underlain by unconsolidated alluvial material with low resistivity values.

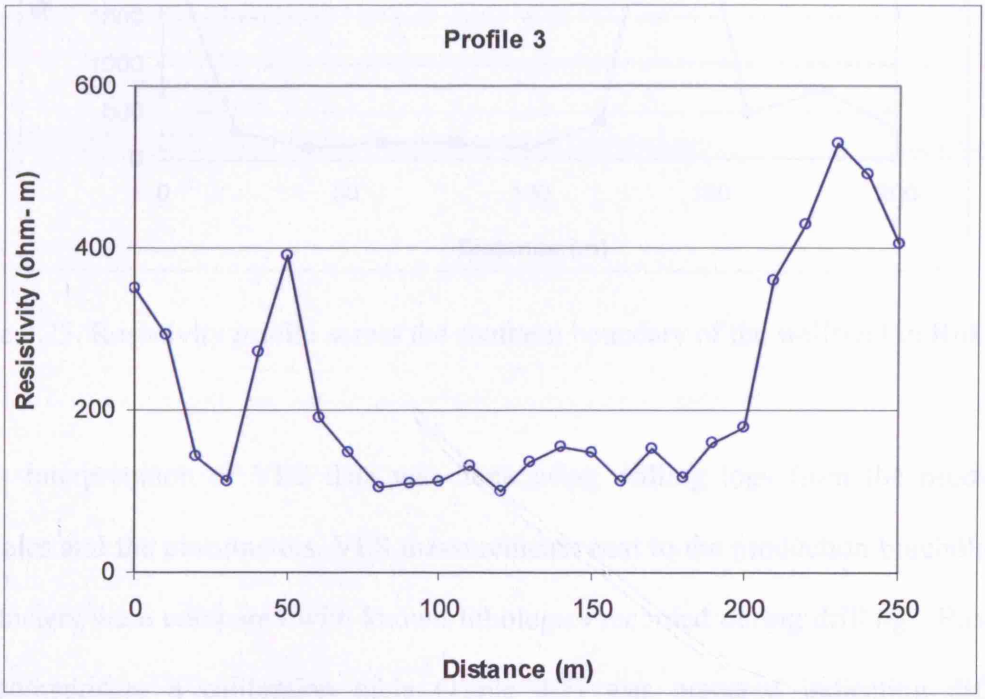

Figure 4.22. Resistivity profile in the W-E direction though the wellfield in Rukungiri town. Low resistivity values (<200 ohm-m) are characteristic of the alluvial sediments whereas high resistivity values (>200 ohm-m) are characteristic of the bedrock surrounding the alluvial sediments.

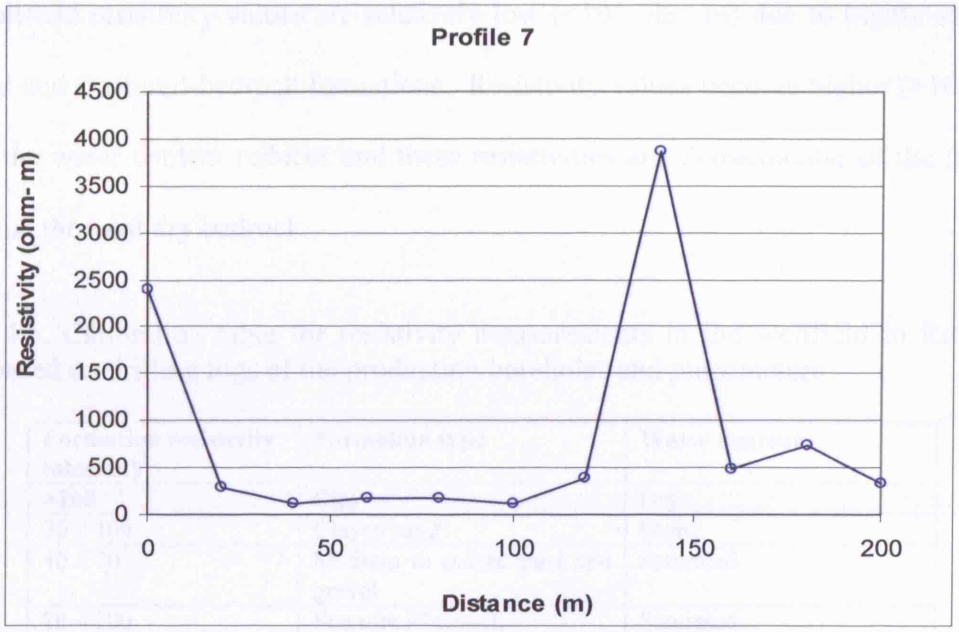

Figure 4.23. Resistivity profile across the southern boundary of the wellfield in Rukungiri town.

Interpretation of VES data was done using drilling logs from the production boreholes and the piezometers. VES measurements next to the production boreholes and piezometers were compared with known lithologies recorded during drilling. Based on this comparison, a calibration table (Table 4.5) was prepared indicating different formations with their corresponding resistivities and water content. The table was used to interpret VES measurements done far from the boreholes. Table 4.5 indicates that clay forms the top layer in the wellfield and has resistivity values >100 ohm-m because it is dry. A layer formed by mixture of sand and clay that occurs below the clay is moist and has resistivity values ranging between 70 and 100 ohm-m. Medium to coarse sands and gravels are saturated and have resistivity values ranging between 40 and 70 ohm-m. A saturated fractured-bedrock layer occurs below the coarse sands and gravels with resistivity values ranging between 70 and 100 ohm-m. VES results indicate that within

the wellfield resistivity values are relatively low (<100 ohm-m) due to highly saturated alluvial and fractured-bedrock formations. Resistivity values become higher (>100 ohm-m) as the water content reduces and these resistivities are characteristic of the top clay layer and the hard dry bedrock.

Table 4.5. Calibration table for resistivity measurements in the wellfield in Rukungiri town based on drilling logs of the production boreholes and piezometers

Formation resistivity (ohm-m)	**Formation type**	**Water content**
>100	Clay	Dry
70 – 100	Clayey sand	Moist
40 – 70	Medium to coarse sand and gravel	Saturated
70 – 100	Fractured-bedrock	Saturated
>200	Hard bedrock	Dry

The distribution of resistivity values in and around the wellfield is presented based on results of profiling (Fig. 4.24) using a contour interval of 100 ohm-m. The resistivity values at the wellfield range between 50 and 300 ohm-m and are lowest (<100 ohm-m) within the valley underlain by the alluvial material and are highest (>200 ohm-m) on the hills that surround the valley. Resistivity values higher than 100 ohm-m are characteristic of dry clay and hard unfractured bedrock whereas resistivity values <100 ohm-m are characteristic of moist to saturated alluvial sediments and weathered-fractured bedrock. Based on the distribution of resistivity values it can be concluded that the two production boreholes Ruk 5 and Ruk 8 are located in the same wellfield. The wellfield's southern boundary is approximately 100 m south of Ruk 8 (Fig. 4.24). The northern part of the boundary could not be established due to the presence of a thick forest (deciduous plantation), which interfered with the profiling. However, based on topographic expressions the boundary is expected to be between 100 and 200 m north of Ruk 5. The

average width of the valley is approximately 300 m. Based on geophysical survey results, the area covered by the alluvial aquifer is approximately 0.24 km^2 (0.8 km x 0.3 km).

Figure 4.24. Distribution of resistivity values in and around the wellfield in Rukungiri town

4.4.3 Groundwater level trends

4.4.3.1 Hydraulic heads

Static water levels in the various piezometers and the production boreholes were referenced to a common datum (Table 4.6). The bottom of Ruk 8 was used as a local datum to covert static water levels into hydraulic heads. The results indicate that there are minor differences in hydraulic head measured in the piezometers and the production borehole (Ruk 8) at the study site. The shallowest piezometers (P1, P2, P3, P5 and P7) installed <50 mbgl have slightly lower hydraulic heads whereas deeper piezometers (P4 and P8) and the production borehole installed >50 mbgl have higher hydraulic heads. The differences in hydraulic heads suggest that the aquifer is under some pressure at deep depths and exhibits slight semi-confined conditions. The fact that the differences in hydraulic heads are very small suggests that the piezometers and the production borehole are hydraulically connected. However, P6 is located in the valley close to the swamp and has a very shallow static water level, very different from those of the other piezometers and Ruk 8. The aquifer at this site appears to be perched and hydraulically isolated and influenced by the water in the nearby swamp. The hydraulic heads in Ruk 5 and adjacent monitoring well are much higher than those in Ruk 8 and the piezometers. The lower hydraulic heads around Ruk 8 appears to be due to intensive groundwater abstraction. By September 2005, the SWL in Ruk 8 had fallen by 10 m since its construction in April 1998.

Table 4.6. Static water levels and hydraulic heads in the piezometers, production boreholes and monitoring wells in the wellfield in Rukungiri town

Piezometer no.	Piezometer name	Distance from Ruk 8 (m)	Depth (mbgl)	SWL (mbgl)	SWL (mbtd)	Hydraulic head (mabd)
P1	DWD20335	40	45	30.4	31.2	33.4
P2	DWD20336	40	36	31.3	31.4	33.2
P3	DWD20337	40	35	32.3	31.8	32.8
P4	DWD20338	20	61	29.6	30.8	33.9
P5	DWD20339	20	48	31.1	31.3	33.3
P6	DWD20340	140	19	9.0	15.2	49.5
P7	DWD20341	66	48	34.4	31.3	33.3
P8	DWD20342	60	81	26.5	30.5	34.1
Ruk 8	DCL1016	0	64.6	30.2	30.2	34.4
Ruk 5	DCL1015	600	89	18.1	13.5	51.1
MW	MW	600	66	22.2	12.2	52.6

Ruk 8- production borehole no.8; Ruk 5- production borehole no.5; MW – monitoring well; SWL- static water level; Datum is Ruk 8; mbgl: metres below ground level; mbtd: metres below top of datum; mabd: metres above bottom of datum

4.4.3.2 Response of groundwater levels to rainfall

When groundwater level monitoring started in the monitoring well near Ruk 5 in 1999, this borehole was non-functional so groundwater level fluctuations in the monitoring well primarily reflect recharge events. Ruk 5 was pump tested in October 2002 and intensive pumping began in February 2003 resulting in large groundwater level fluctuations. Thus, groundwater level measurements in the monitoring well during the period between 2001 and 2003 provide an opportunity to assess the response of groundwater levels to rainfall-fed recharge. Figure 4.25 shows the response of groundwater levels to rainfall events. Recharge occurs only during periods of excessive rainfall due to the high evapotranspirative flux at other times. These observations are consistent with the findings of Taylor and Howard (1996) who show that recharge events are restricted to periods of heavy rainfall and that the magnitude of recharge is controlled by the number of heavy rainfall events (10 $mm \cdot d^{-1}$).

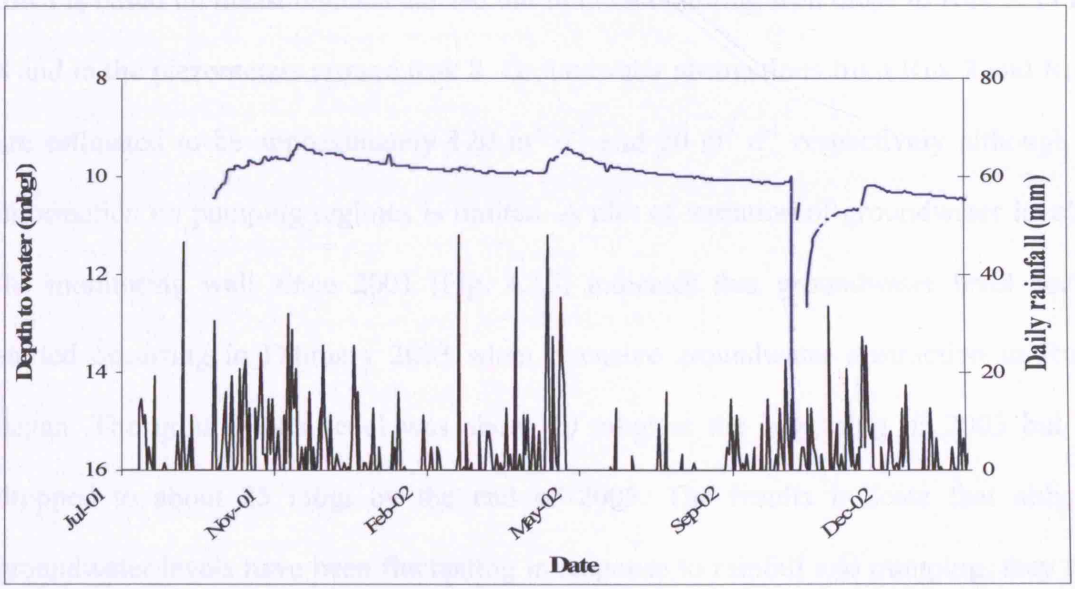

Figure 4.25. Response of groundwater levels to precipitation in the monitoring well in Rukungiri town.

Alley *at al.* (2002) suggest that the aquifer response time is illustrated by the time required for hydraulic head (water levels) in a groundwater system to approach equilibrium following a hydraulic perturbation, such as well pumping or a recharge event. The time-lag between the onset of rainfall and the rise in groundwater levels was determined through relating the main rainfall peaks with groundwater level peaks. The date when the rainfall peak occurred was related to that when the groundwater level peak occurred. Based on this comparison, the estimated time-lag between the onset of rainfall and the rise in groundwater levels is approximately 14 days suggesting that the vertical velocity is in the order of 0.5 m d^{-1}. A time-lag of 15 days was also estimated by Mileham *et al.* (in review) for the River Mitano catchment based on water balance studies.

4.4.4 Response of groundwater levels to abstraction

The response of groundwater levels to abstraction in the wellfield in Rukungiri town is based on measurements carried out in the monitoring well close to Ruk 5, in Ruk 8 and in the piezometers around Ruk 8. Groundwater abstractions from Ruk 8 and Ruk 5 are estimated to be approximately 120 m^3 d^{-1} and 70 m^3 d^{-1} respectively although the information on pumping regimes is limited. A plot of variation of groundwater levels in the monitoring well since 2001 (Fig. 4.26) indicates that groundwater level decline started occurring in February 2003 when intensive groundwater abstraction in Ruk 5 began. The groundwater level was about 10 mbgl at the beginning of 2003 but had dropped to about 25 mbgl by the end of 2005. The results indicate that although groundwater levels have been fluctuating in response to rainfall and pumping, they have been declining by about 2.6 m a^{-1}.

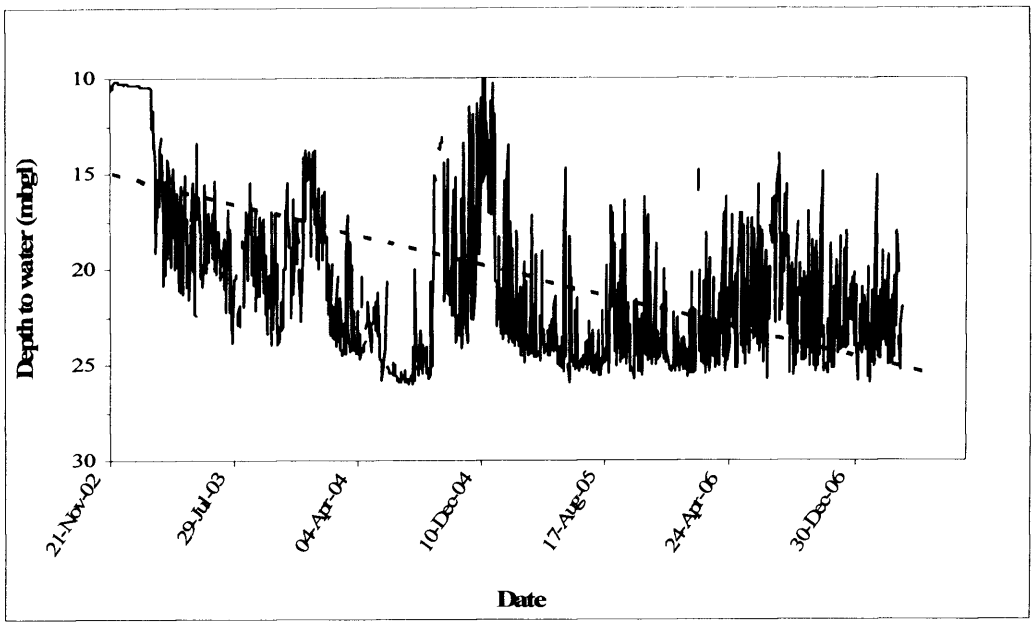

Figure 4.26. Response of groundwater levels in the monitoring well to abstraction in Ruk 5. Peaks in water levels correspond to periods when there is no pumping

Groundwater level measurements that have so far been carried out in the piezometers also provide indications of the response of groundwater levels to abstraction. Groundwater levels in the piezometers show fluctuations (Fig. 4.27) in response to rainfall and abstraction. Average fluctuations due to abstraction are approximately 1 m and water levels show a declining trend. A broad peak in water levels of approximately 3 m is observed from May to November 2006 as a result of heavy rainfall. The water levels start declining thereafter as a result of abstraction and reduced rainfall. The rate of decline in groundwater levels is estimated to be about 2 m a^{-1} which is consistent with the estimate obtained using data for the monitoring well located 600 m from the piezometers.

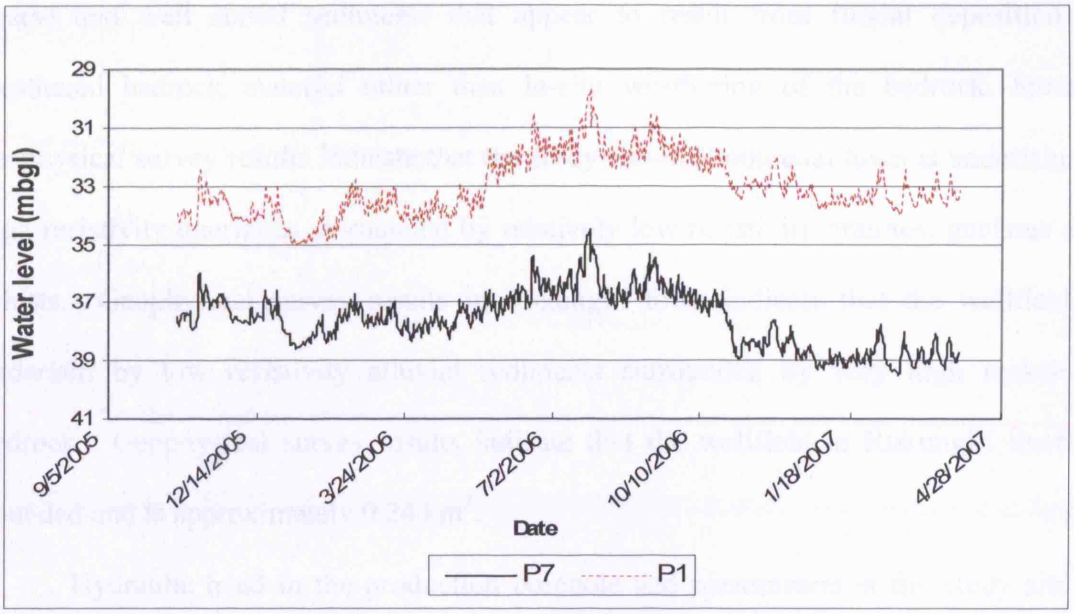

Figure 4.27. Response of groundwater levels in P1 and P7 to abstraction in Ruk 8 in Rukungiri town.

Groundwater level in the production borehole (Ruk 8) at the study site was found to have dropped by approximately 20 m (from 10 m to 30 mbgl) between 1998 and 2005. This drop is equivalent to 2.5 m a^{-1}. Based on groundwater level fluctuations in the monitoring well, the piezometers and Ruk 8 it can be concluded that abstraction in Rukungiri town is rapidly depleting groundwater storage and the average rate of groundwater level decline is 2.5 m a^{-1}.

4.5 Conclusions

Findings of this study indicate that the study site where the production borehole and the piezometers are installed in Wobulenzi town is underlain by a weathered and fractured-bedrock aquifer. However, the wellfield in Rukungiri town where the production boreholes and the piezometers are drilled is underlain by an aquifer formed by

coarse and well sorted sediments that appear to result from fluvial deposition of weathered bedrock material rather than in-situ weathering of the bedrock. Surface geophysical survey results indicate that the study site in Wobulenzi town is underlain by high resistivity quartzites surrounded by relatively low resistivity granites, gneisses and schists. Geophysical survey results in Rukungiri town indicate that the wellfield is underlain by low resistivity alluvial sediments surrounded by very high resistivity bedrock. Geophysical survey results indicate that the wellfield in Rukungiri town is bounded and is approximately 0.24 km^2.

Hydraulic head in the production borehole and piezometers at the study site in Wobulenzi town are similar suggesting that the weathered and fractured-bedrock aquifers are hydraulically connected. The differences in hydraulic heads in the production borehole (Ruk 8) and the piezometers in Rukungiri town are very small suggesting that they are all installed in a hydraulically connected aquifer. The hydraulic heads in Ruk 5 and the nearby monitoring well are much higher than those in Ruk 8 and the piezometers indicating that groundwater storage is more depleted around Ruk 8. The 20 m difference in hydraulic heads in Ruk 8 measured in 1998 and 2005 indicates that there is significant depletion of groundwater storage in the wellfield in Rukungiri town. Groundwater levels in both Wobulenzi and Rukungiri towns respond to rainfall and the time-lag between the onset of rainfall and the rise in groundwater levels range between 10 and 15 days and 8 and 14 days in Wobulenzi and Rukungiri towns respectively. The response of groundwater levels to abstraction in Wobulenzi town shows a declining trend suggesting that groundwater storage is continuously being depleted but at low rate estimated to be 23 cm a^{-1} and 38 cm a^{-1} in the weathered and fractured-bedrock aquifers respectively.

However, the response of groundwater levels to abstraction in Rukungiri town shows a sharp declining trend suggesting that groundwater storage is heavily depleted at a rate estimated to be 2.5 m a^{-1}. Groundwater abstraction in Rukungiri town is therefore unsustainable.

CHAPTER 5: AQUIFER SYSTEM RESPONSES TO PUMPING

This chapter investigates the responses of aquifers to pumping in order to assess aquifer geometry and models of groundwater flow in weathered crystalline rocks of Uganda. Research is conducted primarily in the two study towns (Chapter 4) and involves the application of four different but complementary Aquifer Diagnostic Methods (ADMs) (plots of drawdown (s) versus time divided by square of radial distance (t/r^2), log-log/semi-log plots of drawdown versus time, derivative analysis, and flow dimension analysis). The ADMs are used to determine aquifer geometry and groundwater flow mechanisms and this information is summarised in conceptual models of the aquifer systems. The developed conceptual models are then used to select appropriate pumping test analysis solutions and to evaluate estimates of aquifer hydraulic properties determined without knowledge of aquifer geometry and models of groundwater flow.

5.1 Determining aquifer geometry and models of groundwater flow in weathered crystalline rock aquifer systems

5.1.1 Rationale for determining aquifer geometry and groundwater flow

Knowledge of groundwater flow and storage is required for the sustainable development of groundwater. This understanding is especially important in weathered crystalline rocks where groundwater resources are limited by the low permeability and extent of weathered and fractured-bedrock aquifers (Rushton and Weller, 1985; Marechal *et al.*, 2003). A considerable volume of data pertaining to the responses of weathered

crystalline rock aquifers to pumping is available in developing countries but is rarely used to infer groundwater flow and storage characteristics. Aquifer flow geometry, boundary conditions and hydraulic properties can be obtained though hydraulic testing if drawdown responses are systematically interpreted (Marechal *et al.*, 2003; Walker and Roberts, 2003). Ever since the publication of Darcy's law in 1856 (Renard, 2005), analytical and numerical techniques have been developed to analyse aquifer responses to pumping. Estimation of groundwater flow and storage typically involves the fitting of analytical models for head changes to field observations.

Various analytical models and their modifications (Thiem, 1906; Theis, 1935; Cooper-Jacob, 1947; van Everdingen, 1953; Boulton, 1954; Hantush and Jacob, 1955; Hantush, 1961; Papadopulos and Cooper, 1967; Warren and Root, 1963; Gringarten *et al.*, 1974) are described in several texts (e.g. Kruseman and de Ridder, 2000). The first analytical techniques to interpret steady-state and transient (non-steady state) pumping-test data were developed by Thiem and Theis. Theis's analytical solution provides a basis for most transient, pumping-test interpretation techniques (Serrano, 1997; Kuusela-Lahtinen *et al.* 2003; Walker and Roberts, 2003) and has subsequently undergone further development. The solution was extended to analyse: (1) flow boundaries by Theis, (2) non-linear head losses within the pumping well during step drawdown tests by Jacob, (3) skin effects to assess the performance of a pumping well by van Everdingen, and (4) the effect of unsaturated zone in an unconfined aquifer by Boulton. As discussed by Kruseman and de Ridder (2000), further refinements include the analysis of: (1) leakage from an adjacent aquifer by Hantush and Jacob, (2) partially penetrating wells by Hantush, (3) large-diameter wells by Papadopulos and Cooper, (4) dense network of

fractures in porous matrix by Warren and Root, and (5) a single fracture intersecting the well by Gringarten *et al.* in 1974. The development of analytical solutions has progressed alongside development of interpretation techniques involving straight-line analysis and type-curve matching, the most notable of which is the Jacob's straight-line method that utilises late time- drawdown data based on the Theis solution.

Hydraulic-test data analysis is commonly based on Theis solution because it is built on the most simplifying assumptions. These assumptions include cylindrical, radial flow as well as homogeneous and isotropic aquifer conditions. Although analytical solutions are useful in characterizing aquifers, numerous studies (Barker, 1985; 1991; Rushton and Weller, 1985; Walker and Roberts, 2003; Marechal *et al.*, 2003) have observed that weathered crystalline rock aquifer systems are complex and type-curve methods of pumping test analysis are unsuitable because many of the underlying assumptions are invalid.

The condition that confined aquifers are bounded by impermeable layers may not be encountered in real situations in weathered crystalline rocks (Marechal *et al.,* 2003; Vandenbohede and Lebbe, 2003). Confined aquifer solutions employed in such situations tend to underestimate the flow from adjacent semi-permeable layers (Marechal *et al.,* 2003; Vandenbohede and Lebbe, 2003) and therefore overestimate transmissivity and hydraulic conductivity of the tested aquifer. Analytical methods for the interpretation of data for unsteady flow in a semi-confined aquifer can be used to address the problem of leakage (Vandenbohede and Lebbe, 2003). Chilton and Smith-Carington (1984) show that interpretation of reduced, late-time drawdowns as the effect of leakage rather than other recharge boundaries, results in a regional transmissivity that is about half of

apparent transmissivity. Rushton (2003) demonstrates that use of leaky-aquifer analytical solutions for early and medium times, when aquitard storage is significant, generates aquifer drawdowns that are typically half an order of magnitude less than when aquitard storage is ignored. Aquitard storage may be significant in semi-confined aquifers but its significance is not always apparent (Rushton, 2003) when fitting time-drawdown data to type curves. Although use of numerical models has been proposed for analysis of hydraulic test data because they provide a more realistic representation of the aquifer system than type-curve methods (Rushton and Weller, 1985; Renard, 2005), there is still the limitation of the assumption in some models that the hydraulic conductivities are radially symmetrical, a condition that may not consistently be met in weathered crystalline rocks.

Despite inconsistencies in the use of analytical solutions, various aquifer analysis methods and software continue to be used without careful reflection (Vandenbohede and Lebbe, 2003; Renard, 2005; Yeh and Lee, 2007). Many computer software packages (AquiferTest, Aqtesolv, Adept, Aquiferwin etc) are available for interpretation of pumping-test data using a wide range of analytical models. Each model employs assumptions that may be invalid and unknown to the users (Johnson *et al.*, 2001). Automated curve-matching programs have exacerbated this situation as estimates of aquifer parameters can be generated by users with little or no understanding of groundwater flow in the aquifer (Johnson *et al.*, 2001). Identification of aquifer geometry and appropriate models of groundwater flow is an important step in the interpretation of pumping-test data (Kruseman and de Ridder, 2000; Yeh and Lee, 2007) as invalid conceptual and numerical models lead to erroneous estimates of hydraulic properties of

the aquifer. Erroneous estimates of aquifer parameters can, in turn, lead either to underestimation or overestimation of available groundwater resources (Yeh and Lee, 2007). Simple diagnostic methods can assist the determination of aquifer geometry and appropriate models of groundwater flow in groundwater systems and hence guide detailed pumping test data analysis and modelling (Kruseman and de Ridder, 2000; Renard, 2005).

5.1.2 Diagnostic methods for determining aquifer geometry and models of groundwater flow

Use of diagnostic methods to identify aquifer geometry and models of groundwater flow is now possible (Hamm and Bidaux, 1996; van Tonder *et al.*, 2001; Renard, 2005) following the development of a number of interpretation techniques developed over the last 25 years. Families of curves formed by plots of drawdown versus time/square of distance (s versus t/r^2) can be used to show the degree of heterogeneity within the cone of depression of the aquifer (Osiensky *et al.*, 2006; Tumlinson *et al.*, 2006). Knowledge of the degree of heterogeneity of the subsurface aids in the identification of appropriate models of groundwater flow and selection of analytical methods for the interpretation of pumping-test data. Use of log-log and semi-log plots to identify aquifer geometry and models of groundwater flow has been suggested by various workers (Rushton and Weller, 1985; Kruseman and de Ridder, 2000; Gernand and Heidtman, 1997) and characteristic responses proposed. More recently, logarithmic plots of the derivative of drawdown with respect to time (Horne, 1997; van Tonder *et al.*, 2001; Renald, 2005) have been used to diagnose groundwater flow characteristics (well-bore storage, skin, linear flow, radial flow, double porosity etc) that would otherwise be

difficult to detect on linear time-drawdown plots. Added to this, a generalised radial flow approach developed by Barker (1988) that relates cross-sectional area of flow and distance from the pumping well has been successfully employed (Kuusela-Lahtinen *et al.*, 2003; Marechal *et al.*, 2003; Walker and Roberts, 2003) to determine groundwater flow dimension.

In this study, four different but complementary aquifer diagnostic methods (drawdown (s) versus time divided by square of radial distance (t/r^2) plot, log- log/semi-log plots, derivative analysis and flow dimension analysis) are used to assess aquifer geometry and models of groundwater flow in weathered crystalline rock aquifer systems in Uganda and to develop conceptual models of the aquifer systems. The developed conceptual models are then used to select appropriate pumping test analysis solutions and to evaluate estimates of aquifer hydraulic properties determined without knowledge of aquifer geometry and models of groundwater flow.

5.2 Performance of constant-discharge pumping tests

5.2.1 Wobulenzi, central Uganda

A network of four monitoring wells (piezometers) was constructed around a production borehole in Wobulenzi town of central Uganda (Fig. 4.3 in Chapter 4). The production borehole was drilled to a depth of 94 m into the fractured-bedrock aquifer. Two piezometers (P1 and P2) were drilled to depths of 39 m and 32 m in the shallow weathered aquifer. Two other piezometers (P3 and P4) were drilled to depths of 71 m and 65 m in the fractured-bedrock aquifer. A set of shallow and deep piezometers was located 13 m (P1 and P4) and 42 m (P2 and P3) from the production borehole respectively. The

construction details of the piezometers and lithological cross-section are presented in Table 4.1 and Fig. 4.9 respectively in Chapter 4. The production borehole was pumped for 48 hours at a constant rate of 12 m^3 h^{-1} while water levels in the four surrounding piezometers were monitored using a water level dip meter. Water level measurements were conducted in incremental time steps; every 1 minute during the first 10 minutes, every two minutes during the next 10 minutes, every 5 minutes during the next 40 minutes, every 10 minutes during the next 1 hr, every 30 minutes during the next 10 hrs and every 1 hr up to the end of the test. Recovery was monitored in all the wells immediately after cessation of pumping for a maximum period of 3 hrs. Details of the test are presented in Tables 5.1 and 5.2.

Table 5.1. Summary of results from constant-discharge pumping test of the production borehole in Wobulenzi (pumped for 48 hrs at a rate of 12 m^3 h^{-1})

Piezometer No.	Piezometer Name	Aquifer	Distance from PW (m)	Time before drawdown occurred (min)	Maximum drawdown (m)	Duration of drawdown after pump stop (min)
P1	WRMD –5	Weathered	13	80	1.46	70
P2	WRMD –6	Weathered	42	180	0.26	20
P3	WRMD –7	Fractured	42	7	1.37	3
P4	WRMD –8	Fractured	13	10	4.69	<1
PW	DCL725	Fractured	0	0	38.19	0

PW – production borehole; P1, P2, P3 and P4- Piezometers 1, 2, 3 and 4 respectively

Table 5.2. Summary of recovery results after cessation of pumping in the production borehole in Wobulenzi

Piezometer No.	Piezometer name	Aquifer	Maximum drawdown (m)	Duration of recovery (min)	Recovery (%)
P1	WRMD –5	Weathered	1.46	180	94
P2	WRMD –6	Weathered	0.26	180	-
P3	WRMD –7	Fractured	1.37	180	99
P4	WRMD –8	Fractured	4.69	180	96
PW	DCL725	Fractured	38.19	180	100

PW – production borehole; P1, P2, P3 and P4– Piezometers 1, 2, 3 and 4 respectively

5.2.2 Rukungiri, southwestern Uganda

Eight monitoring wells (piezometers) were constructed around a production borehole in Rukungiri town (Fig. 4.4 in Chapter 4). The production borehole was drilled to a depth of 64 m into an alluvial aquifer. Piezometers were located at a range of radial distances from the production borehole (20 m to 140 m). Six piezometers (P1, P2, P3, P4, P5 and P6) were constructed in an alluvial aquifer at depths varying from 36 to 61 m. Two piezometers (P7 and P8) were installed into the underlying fractured-bedrock at depths of 48 and 81 m respectively. The varying depths and distances of the piezometers from the production borehole enabled assessment of the relative responses of the aquifers to pumping. The construction details of the piezometers and lithological cross-section are presented in Table 4.2 and Fig. 4.19 respectively in Chapter 4.

Constant-discharge pumping tests were carried out in each of the 8 piezometers and the production borehole for durations ranging between 6 and 72 hrs. The production borehole was pumped for 72 hrs at a rate of 12 $m^3 h^{-1}$ while water levels in P1, P2, P3, P4 and P5 were monitored (Table 5.3). Each piezometer was also pumped at a constant rate while water levels in the surrounding non-pumping piezometers and the production borehole were monitored using pressure transducers (divers) and water level dip meters (Table 5.4). P1, P2, P4 and P5 drilled in the alluvial aquifer were each pumped for 24 hrs at constant rates varying from 1 to 11 $m^3 h^{-1}$. P6 drilled in the shallow weathered aquifer was pumped for 12 hrs at a constant rate of 6 $m^3 h^{-1}$. P8 drilled in the fractured aquifer was pumped for 48 hrs at a constant rate of 12 $m^3 h^{-1}$. P3 drilled in the alluvial aquifer and P7 drilled in the fractured aquifer were pumped at constant rates of 1.2 and 1 $m^3 h^{-1}$ respectively. Recovery was monitored in all the wells after cessation of pumping for

periods ranging between 1.5 and 18 hrs. In Rukungiri, pressure transducers equipped with dataloggers ("divers") were installed in the piezometers before the start of each test and recorded water levels continuously every 10 seconds during the pumping and recovery phases. To set and test the divers, water-level measurements using dip meters were conducted in incremental time steps as was done in Wobulenzi.

Table 5.3. Summary of results from constant-discharge pumping test of the production borehole in Rukungiri (pumped for 72 hrs at a rate of 12 $m^3 h^{-1}$)

Piezometer No.	Piezometer Name	Aquifer	Distance from PW (m)	Time before drawdown occurred (min)	Maximum drawdown created (m)	Duration of drawdown after pump stop (min)
P1	DWD20335	Alluvial	40	2	2.02	2
P2	DWD20336	Alluvial	40	10	2.02	2
P3	DWD20337	Alluvial	40	190	1.86	0
P4	DWD20338	Alluvial	20	2	1.98	2
P5	DWD20339	Alluvial	20	2	2.07	2
P7	DWD20341	Fractured	66	2	1.97	3
P8	DWD20342	Fractured	60	2	2.08	2
Ruk 8	Production borehole	Alluvial	0	0	8.03	0

Ruk 8 – production borehole no.8; P1, P2, P3, P4, P5, P7 and P8 – Piezometers 1, 2, 3, 4, 5, 7 and 8 respectively

Table 5.4.Summary of results from constant-discharge and recovery test in piezometers and production boreholes in Rukungiri

Piezometer No.	Piezometer Name	Depth (mbgl)	Duration of test (hrs)		Pumping rate ($m^3 h^{-1}$)	Maximum drawdown (m)	Specific capacity ($m^2 d^{-1}$)
			Discharge	Recovery			
P1	DWD20335	45	24	1.5	6	4.86	29.6
P2	DWD20336	36	24	1.5	1.1	1.96	13.5
P3	DWD20337	35	7	1.5	1.2	1.35	21.3
P4	DWD20338	61	24	1.6	11.2	3.51	76.6
P5	DWD20339	48	24	2	5.6	5.15	26.1
P6	DWD20340	19	12	3	6	4.09	35.2
P7	DWD20341	48	7	2	1	1.52	15.8
P8	DWD20342	81	48	18	12	4.82	59.8
Ruk 8	DCL1016 (2005 test)	64	72	12	12	8.03	35.9
Ruk 8	DCL1016 (1998 test)	64	24	12	23	15.09	36.6
Ruk 5	DCL1015 (1998 test)	88.9	24	12	10	30.55	7.9
Geralds	DCL1011 (1998 test)	61	36	12	7.6	22.01	8.3

mbgl: metres below ground level ; Ruk 5, Ruk 8 and Geralds – production boreholes no. 5, 8 and Geralds; P1, P2, P3, P4, P5, P6, P7 and P8 – Piezometers 1, 2, 3, 4, 5, 6, 7 and 8 respectively.

5.3 Aquifer responses to pumping

5.3.1 Overview

Drawdown responses of idealised aquifers follow the Theis curve. Boundaries can cause deviations from the Theis curve (Kruseman and de Ridder, 2000; Marechal *et al.*, 2003; Vandenbohede and Lebbe, 2003). When the cone of depression expands and intersects a geological boundary or a surface water body, a change in slope on the time-drawdown curve occurs. Interactions with a constant-head boundary (e.g. surface water) increase flow and result in a decrease in the rate of drawdown. Conversely, interactions with a no-flow boundary reduce flow and induce an increase in the rate of drawdown.

5.3.2 Weathered and fractured-bedrock aquifers- Drawdown and recovery responses in Wobulenzi

The production borehole (Fig. 5.1) shows an initial sharp decline in water level that is followed by a stabilisation in water level from ~12 hrs after pumping up to the end of the test. Drawdown responses of the weathered and fractured-bedrock aquifers to pumping are, however, variable (Fig. 5.2). The fractured-bedrock aquifer responds much faster to pumping than the weathered aquifer. The responses of P3 and P4 demonstrate heterogeneity in flow within the fractured-bedrock aquifer over very short distances. Drawdown in P3, which is the farthest (42 m) from the production borehole, was observed after only 7 minutes of pumping (Table 5.1) whereas in P4 which is the closest to the production borehole, it was observed after 10 minutes of pumping. Although P3 responded more quickly to pumping than P4, P3 showed a steady decline in water level during pumping whereas P4 experienced a more rapid decline in water level as pumping proceeded. Unlike the production borehole, both P3 and P4 show a sharp decline in water level initially that was followed by fluctuations in water level between 8 and 24 hrs of pumping. This was followed by a steady decline of water level to the end of the test. The fluctuations in water level between 8 and 24 hrs of pumping are not observed in either the production borehole or the shallow piezometers (P1 and P2). The fluctuations may suggest that, as the cone of depression increases, productive fractures are intercepted and these contribute to reduce drawdown. Where productive fractures are limited, drawdown increases rapidly. Drawdown in P3 continued for 3 minutes after cessation of pumping whereas it stopped immediately in P4 on cessation of pumping. The results suggest that the fractures intercepted by P3 are more permeable that those intercepted by P4.

Drawdown responses of P1 and P2, installed in the weathered aquifer, differ slightly. P1, located 13 m from production borehole, responded after 80 minutes of pumping (Table 5.1) but P2 located 42 m from production borehole responded after 180 minutes of pumping. Although P1 (weathered aquifer) responded to pumping much later than P3 (fractured-bedrock aquifer), it exhibited a steady decline in water level that is fairly similar to that of P3 but very different from that of P2. The drawdown response of P2 is more subdued and gradual than other piezometers. Interestingly, drawdown increased in P1 for 70 minutes after cessation of pumping but continued for only 20 minutes in P2. Increased drawdown by the weathered aquifer after cessation of pumping reflects leakage from this aquifer to the underlying fractured-bedrock aquifer as a result of the induced downward hydraulic gradient. The results confirm that the weathered and the fractured-bedrock aquifers are hydraulically connected and act therefore as an integrated aquifer system.

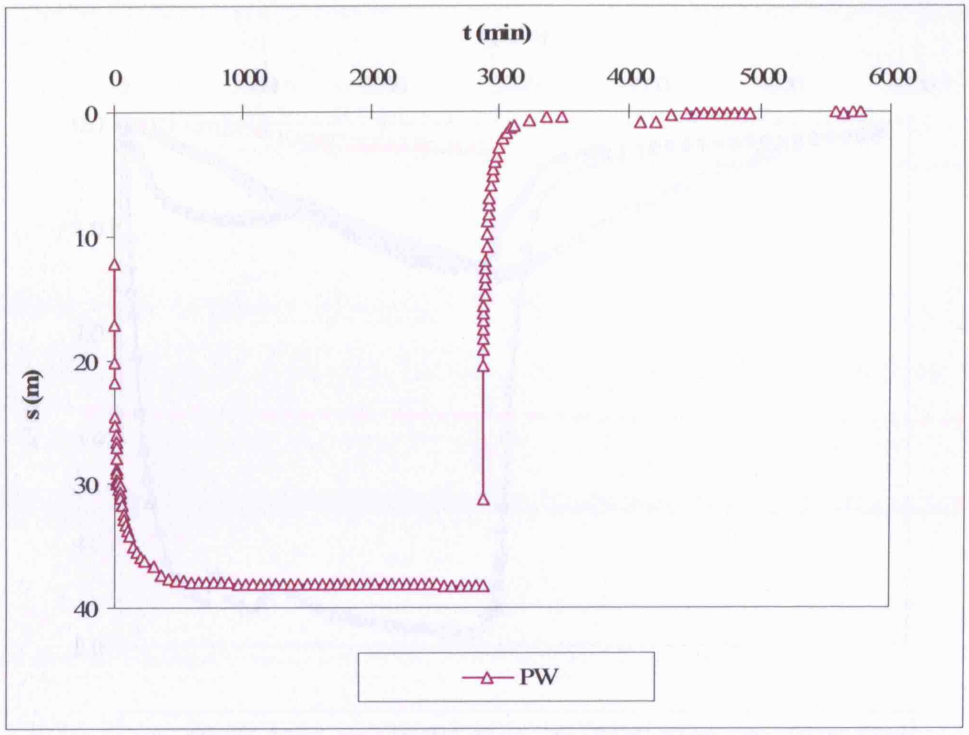

Figure 5.1. Time-drawdown and recovery curve for the production borehole in the weathered and fractured-bedrock aquifer in Wobulenzi while pumping at a constant-discharge rate of 12 $m^3 h^{-1}$ for 48 hrs (2880 minutes).

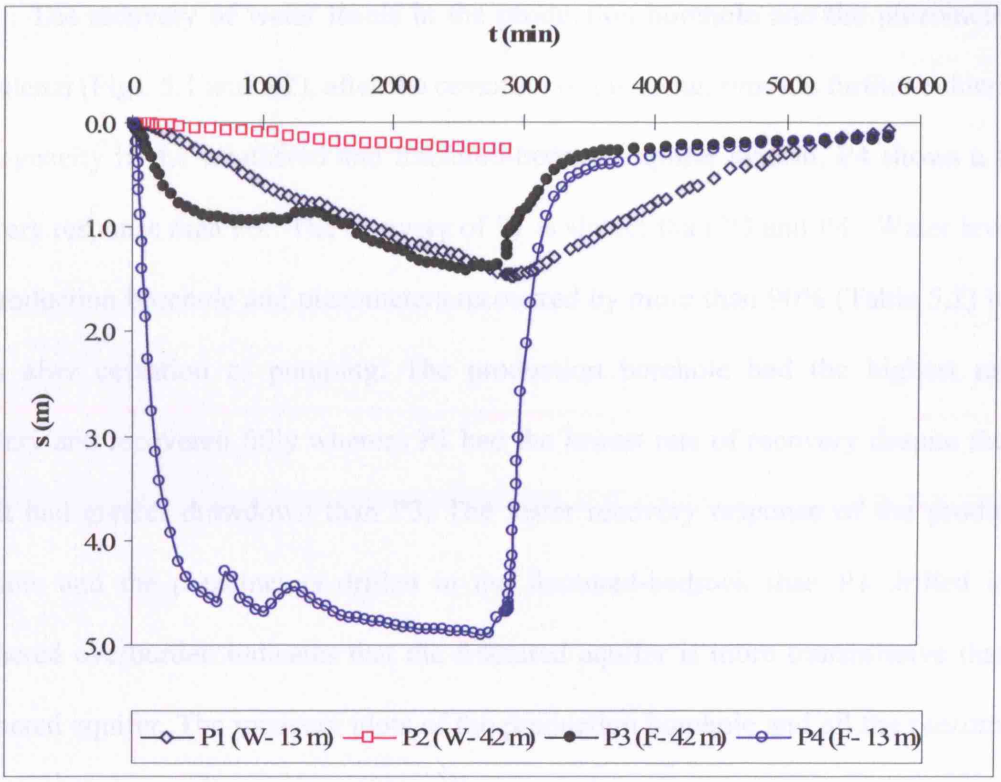

Figure 5.2. Time-drawdown and recovery curves for the piezometers in the weathered (W) and fractured-bedrock (F) aquifers at various distances from the production borehole in Wobulenzi while pumping at a constant-discharge rate of 12 $m^3 h^{-1}$ for 48 hrs (2880 minutes).

Observed drawdown in the weathered and fractured-bedrock aquifer system decreases with increasing distance from the production borehole (pumping well) consistent with radial-flow conditions. P1 and P4, located 13 m from the production borehole, experienced the greatest maximum drawdowns, 1.46 m and 4.69 m respectively. P2 and P3, located 42 m from the production borehole, had the smallest maximum drawdowns, 0.26 m and 1.37 m respectively.

The recovery of water levels in the production borehole and the piezometers in Wobulenzi (Figs. 5.1 and 5.2), after the cessation of pumping, provide further evidence of heterogeneity in the weathered and fractured-bedrock aquifer system. P4 shows a faster recovery response than P3. The recovery of P1 is slower than P3 and P4. Water levels in the production borehole and piezometers recovered by more than 90% (Table 5.2) in just 3 hrs after cessation of pumping. The production borehole had the highest rate of recovery and recovered fully whereas P1 had the lowest rate of recovery despite the fact that it had greater drawdown than P3. The faster recovery response of the production borehole and the piezometers drilled in the fractured-bedrock than P1 drilled in the weathered overburden indicates that the fractured aquifer is more transmissive than the weathered aquifer. The recovery plots of the production borehole and all the piezometers converge almost to the same level (Figs. 5.1 and 5.2) providing further evidence that the weathered and fractured-bedrock aquifers, in which they are installed, are hydraulically connected.

5.3.3 Alluvial aquifer - Drawdown and recovery responses in Rukungiri

Each piezometer in Rukungiri town responded rapidly to pumping in the production borehole (less than 2 minutes) except P2 and P3 which responded after 10 minutes and 190 minutes respectively. Each piezometer shows a consistent and steady decline in water level (Fig. 5.3) irrespective of its distance from the production borehole and its depth (Table 5.3). Drawdown in all the piezometers ceased quickly (<3 minutes) after cessation of pumping in the production borehole. Similarity in responses of the piezometers installed to different depths suggests that the aquifer in which they are

installed is relatively isotropic and homogeneous in comparison to the tested aquifer in Wobulenzi.

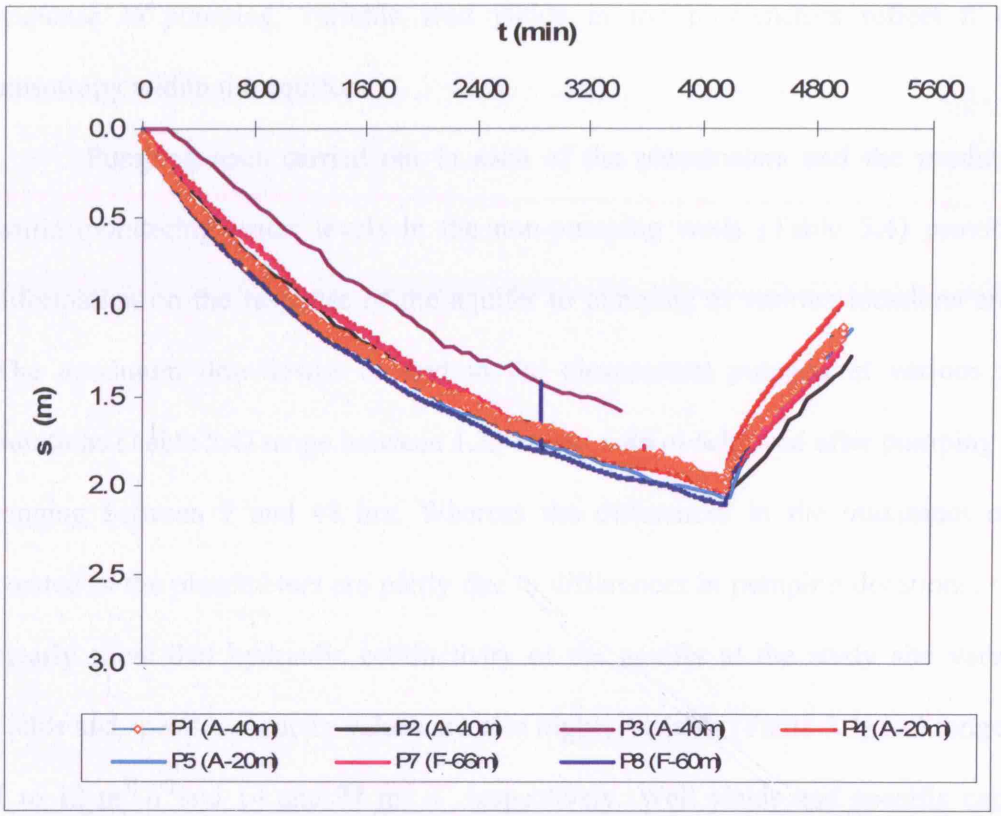

Figure 5.3. Time-drawdown and recovery curves for the piezometers in the alluvial (A) and fractured-bedrock (F) aquifers at various distances from the production borehole in Rukungiri

The maximum drawdowns observed in each piezometer (Table 5.3) are remarkably consistent (1.86 to 2.08 m) differing by less than 10% irrespective of the depth or distance from the production borehole. Although there are small differences in drawdown, the well yields of the piezometers are highly variable (Table 5.4). For example, the observed maximum drawdowns in the three shallowest piezometers (P1, P2

and P3), installed in the alluvial aquifer at 40 m from the production borehole are 2.02, 2.02 and 1.86 m respectively but well yields vary. Well yields are higher in P1 (6 $m^3 h^{-1}$) and lower in P2 and P3 (1.1 and 1.2 $m^3 h^{-1}$ respectively). Thus, despite a consistent response to pumping, variable well yields in the piezometers reflect a degree of anisotropy within the aquifer.

Pumping tests carried out in each of the piezometers and the production well while monitoring water levels in the non-pumping wells (Table 5.4) provide further information on the response of the aquifer to pumping at various locations and depths. The maximum drawdowns created in the piezometers pumped at various rates and durations (Table 5.4) range between 1.35 m and 4.86 m achieved after pumping durations ranging between 7 and 48 hrs. Whereas the differences in the maximum drawdown created in the piezometers are partly due to differences in pumping durations, the results clearly show that hydraulic conductivity of the aquifer at the study site varies. Wells yields and specific capacity values are also highly variable (Table 5.4) and range between 1 to 12 $m^3 h^{-1}$and 14 and 77 $m^2 d^{-1}$ respectively. Well yields and specific capacity are highest in the piezometers constructed at the base of the alluvial aquifer and in the fractured aquifer.

Drawdown responses to pumping (Fig. 5.4) of the production boreholes individually tested just after drilling in 1998 and located within and close to the study site provide further evidence of groundwater flow in the Rukungiri wellfield. Each production borehole (Ruk 8, Ruk 5 and Geralds) shows a rapid and sharp decline in water levels at early pumping times. The rate of change in drawdown slows after pumping times of between 0.5 and 3.5 hrs. The production boreholes feature similar drawdown curves but

the curve for Ruk 5 becomes steeper as pumping proceeds. Maximum drawdowns observed after 24 hrs of pumping are 15.09, 39.55 and 20.35 m for Ruk 8, Ruk 5 and Geralds respectively. Ruk 8 and Geralds have drawdown curves with similar slopes but the drawdown in Ruk 8 is smaller despite the fact that it was pumped at a higher rate (Table 5.4). The above results indicate that despite the fact that Ruk 5 and Ruk 8 are only 600 m apart the transmissivity of the aquifers in which they are installed varies significantly.

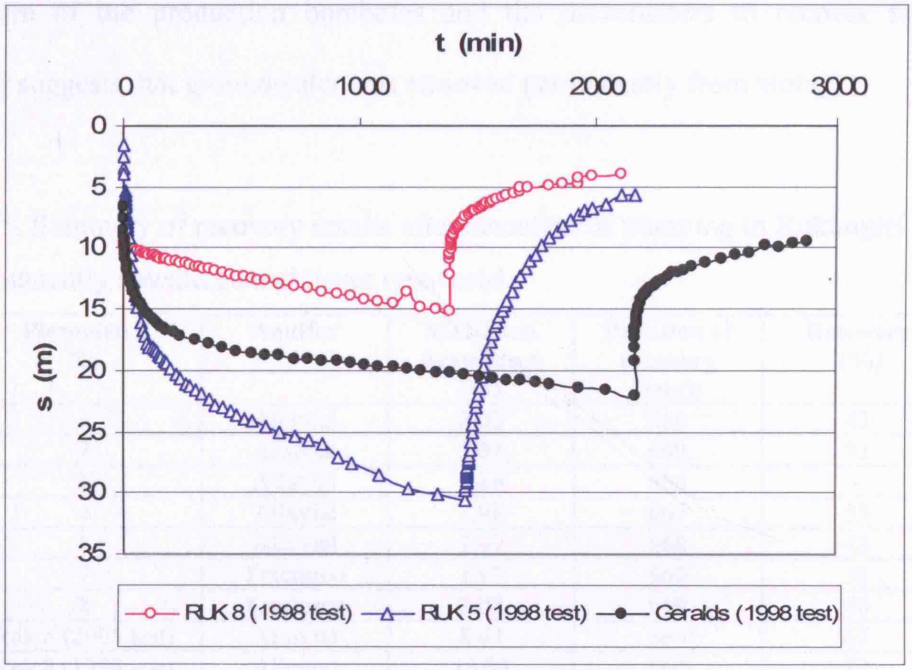

Figure 5.4. Time-drawdown and recovery curve for the production boreholes drilled in Rukungiri town in 1998

Recovery responses of the piezometers and production boreholes (Figs. 5.3 and 5.4) in Rukungiri provide further information about the groundwater flow in the aquifer. The recovery responses are remarkably consistent and none of the piezometers or the

production boreholes recovered completely 11 hrs after cessation of pumping (Table 5.5). The highest recovery of water levels in the piezometers observed in P4 was only 53%. The poorest recovery was 33% observed in P2. Recovery of water levels in the production boreholes was greater than in the piezometers. Ruk 5, approximately 500 m from the wellfield had the best recovery (81%) whereas Geralds, located about 5 km from the study site had the least recovery (56%). Ruk 8, around which the piezometers are installed, had recovery of 73 and 67% for the 1998 and 2005 tests respectively. However, the failure of the production boreholes and the piezometers to recover fully from pumping suggests that groundwater was removed permanently from storage.

Table 5.5. Summary of recovery results after cessation of pumping in Rukungiri town. P3 was permanently dewatered and never recovered.

Piezometer No.	Aquifer	Maximum drawdown (m)	Duration of recovery (min))	Recovery (%)
1	Alluvial	2.02	660	43
2	Alluvial	2.02	660	33
3	Alluvial	1.86	660	-
4	Alluvial	1.98	660	53
5	Alluvial	2.07	660	43
7	Fractured	1.97	660	38
8	Fractured	2.08	660	46
Ruk 8 (2005 test)	Alluvial	8.03	660	67
Ruk 8 (1998 test)	Alluvial	15.09	660	73
Ruk 5 (1998 test)	Alluvial	30.55	660	81
Geralds (1998 test)	Alluvial	22.01	660	56

5.4 Determining hydraulic properties based on commonly used pumping test analysis solutions

5.4.1 Overview

A number of analytical models; Theis, Cooper- Jacob, Theis recovery, Hantush, Neuman and PTFIT program developed by Barker (2000) etc are commonly used to determine aquifer hydraulic properties. These analytical solutions are based on governing equations and assumptions as presented in Table 5.6. In this study, the above methods were applied manually and using computer software to determine aquifer hydraulic properties in Wobulenzi and Rukungiri towns before knowledge of aquifer geometry and models of groundwater flow. Through this approach the importance of understanding aquifer geometry and models of groundwater flow in pumping test data interpretation was assessed. The best fits of the models to the data are presented in Appendix 5.

Table 5.6. Commonly used pumping test analysis solutions and their basic assumptions

Method	Governing Equation	Assumptions
Theis	$s(r,t)=\frac{Q}{4\pi T}\mathrm{W}(u);$ $u=\frac{Sr^2}{4Tt}$	Unsteady groundwater flow; homogeneous and isotropic confined aquifer of infinite areal extent; pumping at a constant rate by a fully penetrating well of a very small diameter.
Cooper-Jacob	$T=\frac{2.3Q}{4\pi\Delta s};$ $S=\frac{2.25Tt_0}{r^2}$	Same as Theis. In addition, function, u, in the Theis equation is very small due to small distance of the piezometers from the pumping well and long pumping time.
Theis recovery	$T=\frac{2.3Q}{4\pi\Delta s^*}$	Same as Cooper-Jacob

Hantush	$s = \frac{Q}{4\pi T} W(u, \frac{r}{B})$; $B = \sqrt{\frac{bT}{K_v}}$	The aquifer is bounded by semi-permeable layers with outer constant head boundaries; flow in the confined aquifer is horizontal; water table (in the overlying layer) remains at a constant level; there is no loss of water from storage in the confining layer.
Neuman	$s = \frac{Q}{4\pi T} W(u_B, \beta)$	Aquifer is isotropic or anisotropic, infinite and homogeneous; unsteady state flow; influence of the unsaturated zone on the drawdown in the aquifer is negligible; observation well screen covers the full thickness of the aquifer; diameter of the pumped and observation wells are small; pumping is done at a constant discharge rate, and one part of the water comes from storage in the aquifer and the other from gravitational drainage at the free surface.
PTFIT5 Model	Based on Theis equation	One or more pumping wells with same characteristics (diameter in the aquifer, diameter of casing, well-loss coefficients; constant pumping rates over fixed intervals; single homogeneous, isotropic, semi-confined aquifer below a single homogeneous aquitard; flow in the aquitard is vertical and the aquitard is characterised by its thickness, hydraulic conductivity, specific storage and specific yield.

s is drawdown in the well; Δs is drawdown difference per log cycle; Δs^* is residual drawdown difference per log cycle; Q is constant discharge rate in the pumping well; T is transmissivity of the aquifer; S is dimensionless storativity of the aquifer; t is time since pumping started; r is radial distance from pumping well; t_o is the time where straight line though drawdown data intercepts x-axis; W(u) is Theis well function; B is leakage; W(u, r/B) is well function for u and r/B; K_v is the vertical hydraulic conductivity of the leaky layer; b is the thickness of aquitard; $W(u_B, \beta)$ is well function for u_B and β

5.4.2 Weathered and fractured-bedrock aquifers

Interpretation of pumping-test data from the weathered and fractured-bedrock aquifers in Wobulenzi, employing commonly used analytical methods shows that the transmissivity and storage coefficient estimates are highly variable, varying by over one order of magnitude between the different methods (Fig. 5.5). Transmissivity estimates for the weathered aquifer (P1 and P2) range between 14 $m^2 d^{-1}$ derived from PTFIT without aquitard and 170 $m^2 d^{-1}$ obtained using Hantush method. Similarly, specific yield estimates for the weathered aquifer range between 0.01 obtained using PTFIT with aquitard and 0.4 derived from PTFIT without aquitard. Transmissivity estimates for the fractured-bedrock aquifer (P3, P4 and production well) range between 3.4 $m^2 d^{-1}$ obtained using Theis method and 150 $m^2 d^{-1}$ obtained using Theis recovery method. Similarly, storage coefficient estimates for the fractured-bedrock aquifer range between 0.003 obtained using Cooper-Jacob method and 0.036 obtained using Hantush method. The results clearly show that estimates of hydraulic properties are sensitive to the employed model and selection of appropriate pumping test interpretation models is essential for determination of accurate estimates of aquifer hydraulic properties.

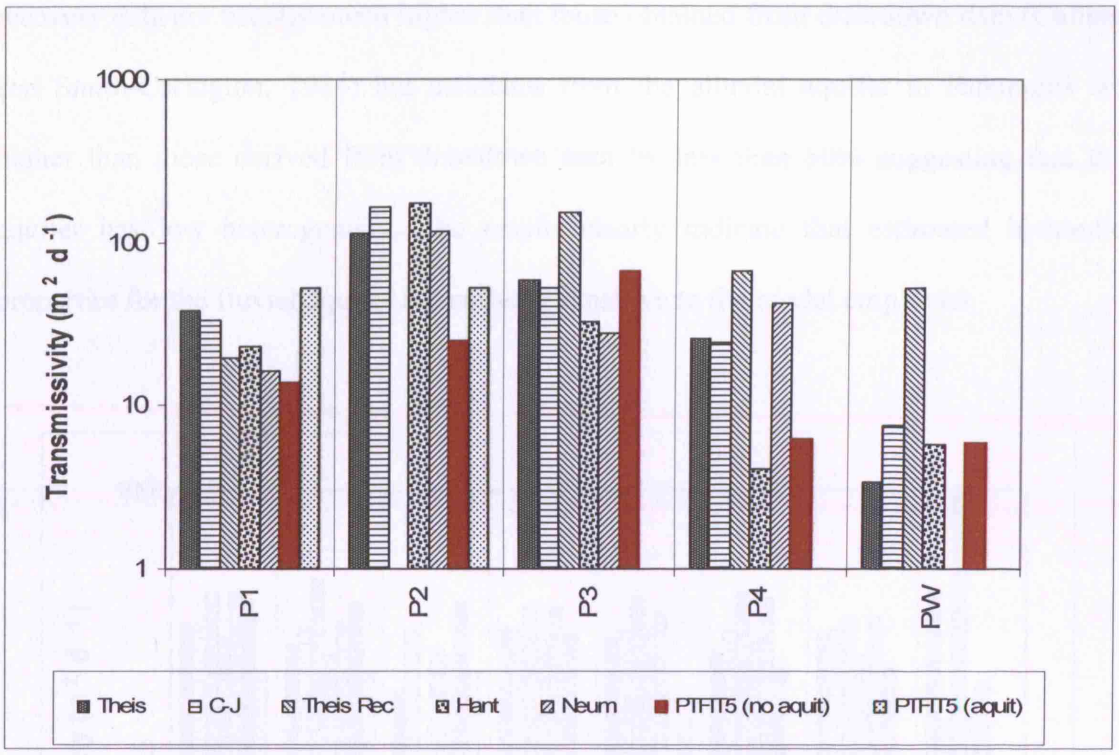

Figure 5.5. Plot of transmissivity estimates obtained using various analytical methods for the weathered and fractured-bedrock aquifers in Wobulenzi

5.4.3 Alluvial aquifers

Interpretation of pumping-test data from the alluvial aquifer in Rukungiri employing commonly used analytical models shows that the transmissivity and storage coefficient estimates are relatively consistent (Fig. 5.6). Transmissivity estimates range between 18 m^2 d^{-1} derived from PTFIT with aquitard and 39 m^2 d^{-1} obtained using Theis recovery method. The estimated storage coefficient values range between 0.006 derived from Cooper-Jacob method and 0.1 obtained using PTFIT5 with aquitard. Transmissivity estimates derived from Cooper-Jacob are identical for all the piezometers and are similar to those derived from Theis and Hantush methods. Transmissivity estimates derived from

recovery data are usually much higher than those obtained from drawdown data (Chilton and Smith-Carington, 1984) but estimates from the alluvial aquifer in Rukungiri are higher than those derived from drawdown data by less than 50% suggesting that the aquifer has low heterogeneity. The results clearly indicate that estimated hydraulic properties for the fluvial aquifer are not very sensitive to the model employed.

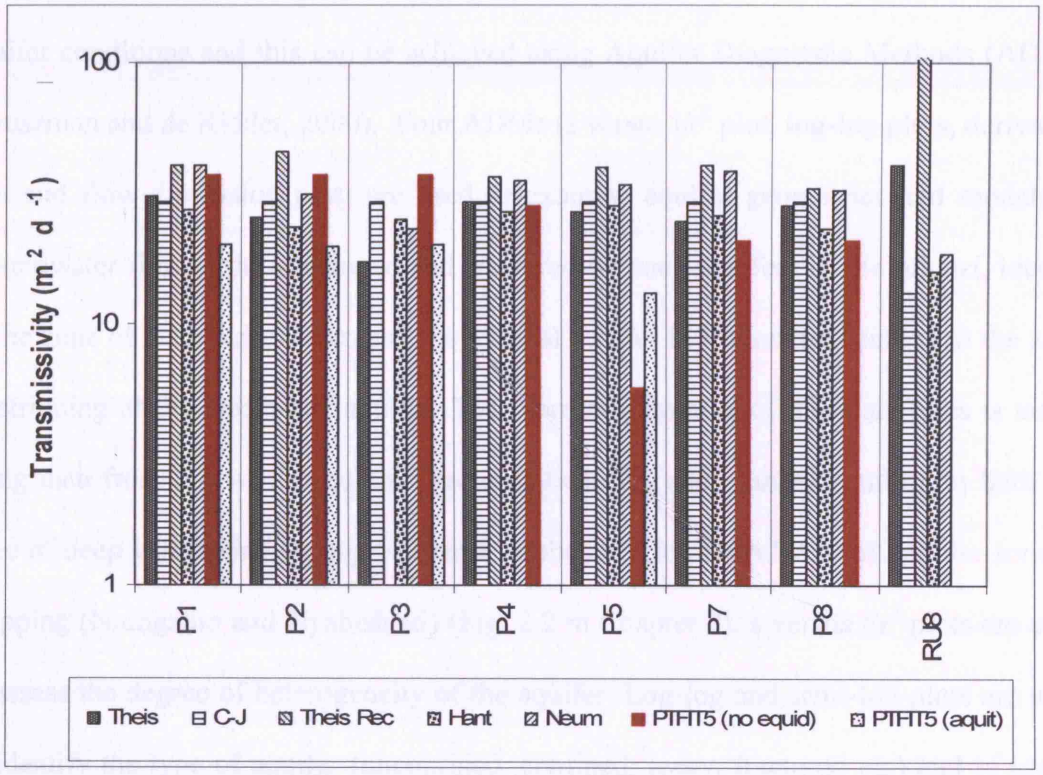

Figure 5.6. Plot of transmissivity estimates obtained using various analytical methods for the alluvial aquifer in Rukungiri

5.5 Aquifer Diagnostic Methods

5.5.1 Overview

Identification of dominant aquifer geometries and models of groundwater flow is complicated by the fact that different aquifer models can generate similar hydraulic responses (Kruseman and de Ridder, 2000). Comparison of field data with theoretical aquifer models can, therefore, greatly assist in identifying the models that match the aquifer conditions and this can be achieved using Aquifer Diagnostic Methods (ADMs) (Kruseman and de Ridder, 2000). Four ADMs (s versus t/r^2 plot, log-log plots, derivative plot and flow dimension plot) are used to examine aquifer geometries and models of groundwater flow in the weathered and fractured-bedrock aquifers in Wobulenzi, located in the zone of deep weathering, and the alluvial aquifer in Rukungiri, located in the zone of stripping of the weathered aquifer. The representativeness of these analyses is tested using data from the weathered and fractured-bedrock, and alluvial aquifers in both the zone of deep weathering (Iganga, Lukaya, Mubende, Hoima and Aroca) and the zone of stripping (Ntungamo and Nyabisheki) (Fig. 2.2 in Chapter 2). s versus t/r^2 plots are used to assess the degree of heterogeneity of the aquifer. Log-log and semi-log plots are used to identify the type of aquifer (unconfined, confined, leaky, fractured etc) and to assess the nature of groundwater flow in the aquifer (linear or radial). Derivative plots are used to identify the aquifer geometry (presence of boundaries, leakage, nature of flow (linear, radial etc) whereas the determination of flow dimension is used to understand the nature of groundwater flow (linear, radial or spherical).

5.5.2 Drawdown versus t/r^2 plots

5.5.2.1 Overview

Families of curves formed by plots of drawdown versus time divided by square of the distance from pumping well (s versus t/r^2) indicate the degree of heterogeneity within the cone of depression of the aquifer (Osiensky *et al.*, 2006; Tumlinson *et al.*, 2006). Any separation between drawdown curves in a family provides a measure of the degree of heterogeneity within the aquifer and all the drawdown curves in a family should converge on a single curve at a large value of t/r^2. Plotting s versus log t/r^2 makes the separation between the drawdown curves more visible. Insight regarding the distribution of heterogeneity in the subsurface facilitates identification of aquifer geometry and selection of appropriate analytical methods for the interpretation of pumping test data (Osiensky *et al.*, 2006; Tumlinson *et al.*, 2006). It also enables appropriate evaluation of aquifer parameters obtained from drawdown curves.

5.5.2.2 Weathered and fractured-bedrock aquifer – Wobulenzi results

Piezometers drilled in the weathered and fractured-bedrock aquifers are plotted together to compare the responses of their drawdown curves and assess the distribution of heterogeneity in the aquifers. The drawdown curves for the shallow piezometers (P1 and P2) drilled into the weathered aquifer show small divergence at both small and large t/r^2 values (Fig. 5.7) suggesting that the weathered aquifer has uniform heterogeneity in the cone of depression. Drawdown curves for the deep piezometers (P3 and P4) drilled into the fractured-bedrock aquifer have similar shapes at low t/r^2 values (Fig. 5.7) but exhibit large diverge at large t/r^2 suggesting that the aquifer is heterogeneous but heterogeneity increases as the cone of depression increases. The drawdown curves for the weathered

aquifer and the fractured-bedrock aquifer at the same location have similar shapes at small t/r^2 but diverge at large t/r^2 (Fig. 5.7). The big divergence of the drawdown curves of the piezometers at the same location (P1 and P4, and P2 and P3) indicates that the weathered and fractured-bedrock aquifers exhibit strong heterogeneity as the cone of depression increases.

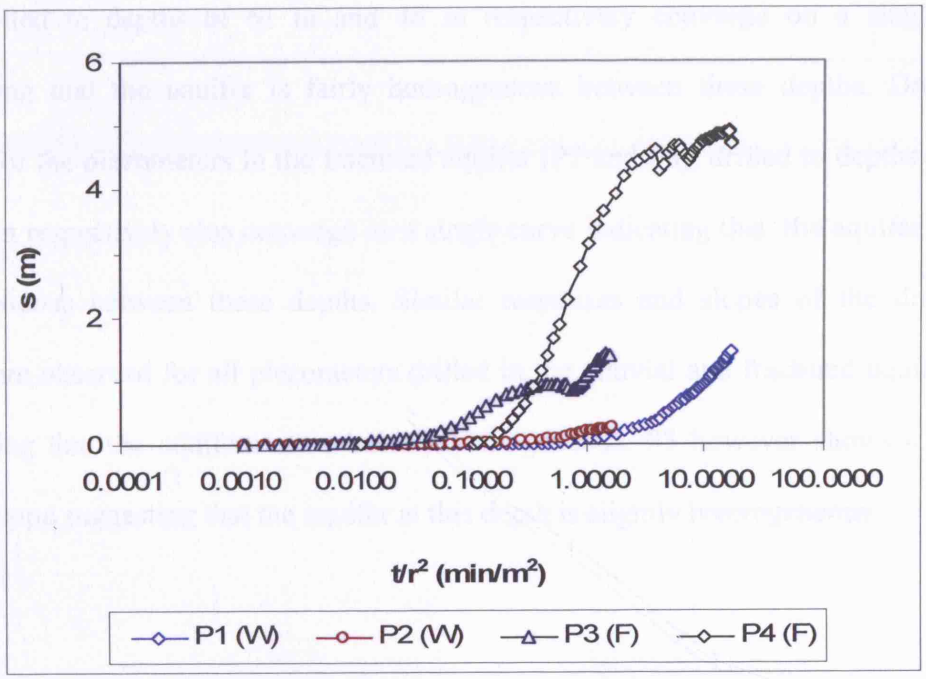

Figure 5.7. Plot of s versus log t/r^2 for the piezometers in the weathered (W) and fractured-bedrock (F) aquifer in Wobulenzi

5.5.2.3 Alluvial aquifer – Rukungiri

Drawdowns in piezometers drilled in the alluvial and fractured-bedrock aquifers in Rukungiri are plotted together (Fig. 5.8) to compare the responses of their drawdown curves and assess the distribution of heterogeneity in the aquifer. Drawdown curves for the shallowest piezometers in the alluvial aquifer (P1, P2 and P3), installed at 40 m from the production borehole have similar shapes. Curves for P1 and P2 drilled to depths of 45

and 36 m respectively converge on a single curve suggesting that the aquifer between these depths is relatively homogeneous. The curve for the shallowest piezometer (P3) diverges from those of P1 and P2 suggesting that the aquifer characteristics at shallower depth (35 m) are different from those at greater depths.

The drawdown curves for the deeper piezometers in the alluvial aquifer (P4 and P5), drilled to depths of 61 m and 48 m respectively converge on a single curve suggesting that the aquifer is fairly homogeneous between these depths. Drawdown curves for the piezometers in the fractured aquifer (P7 and P8), drilled to depths of 48 m and 81 m respectively also converge on a single curve indicating that the aquifer is fairly homogeneous between these depths. Similar responses and slopes of the drawdown curves are observed for all piezometers drilled in the alluvial and fractured aquifer units suggesting that the aquifers are relatively homogeneous. P3 however shows a slightly higher slope suggesting that the aquifer at this depth is slightly heterogeneous.

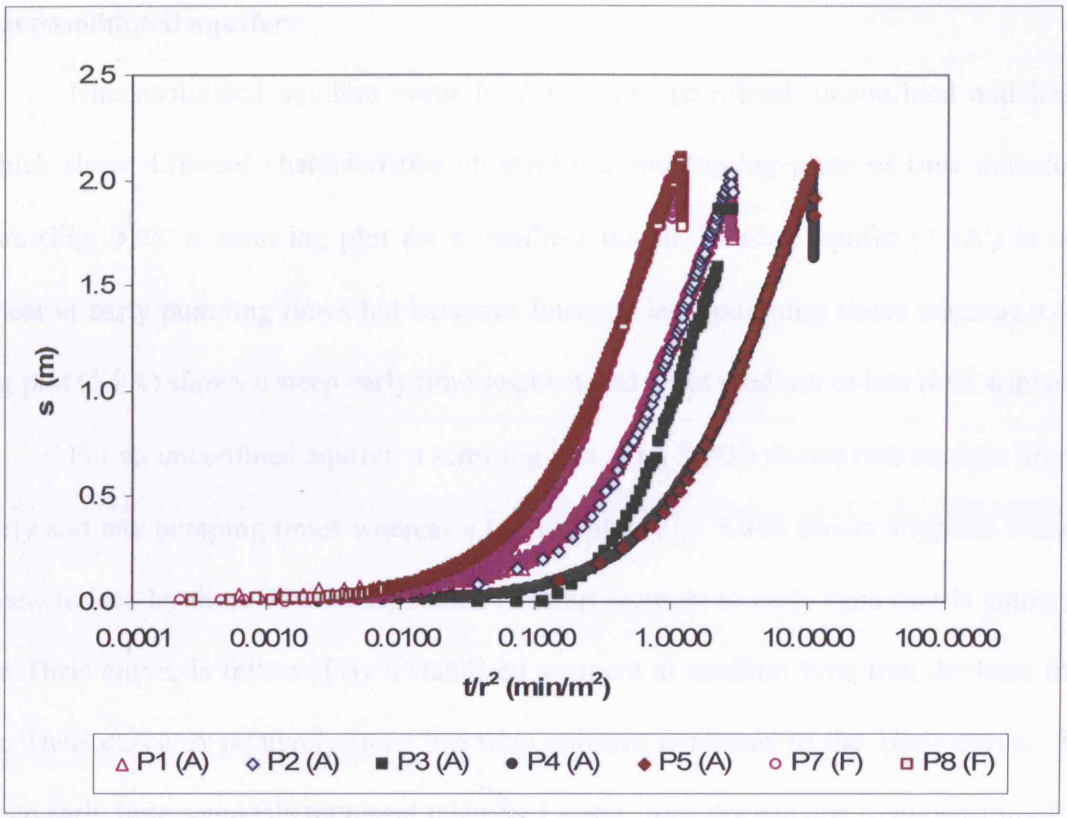

Figure 5.8. Plot of s versus t/r^2 for the piezometers in the alluvial (A) and fractured bedrock (F) aquifers in Rukungiri

5.5.3 Log-log and semi-log plots of time- drawdown data

5.5.3.1 Overview

Log-log and semi-log plots of theoretical time-drawdown data for unconsolidated and consolidated aquifers provide a good means of diagnosing aquifers (Kruseman and de Ridder, 2000). Different aquifer characteristics are exhibited on log-log and semi-log plots and the combined use of the plots makes it possible to identify the dominant aquifer geometries and flow regimes.

Unconsolidated aquifers

Unconsolidated aquifers occur in three types (confined, unconfined and leaky) which show different characteristics on semi-log and log-log plots of time-drawdown data (Fig. 5.9). A semi-log plot for a confined unconsolidated aquifer (5.9A′) is non-linear at early pumping times but becomes linear at later pumping times whereas a log-log plot (5.9A) shows a steep early time segment and a flat medium to late time segment.

For an unconfined aquifer, a semi-log plot (Fig. 5.9B′) shows two straight lines at early and late pumping times whereas a log-log plot (Fig. 5.9B) shows a typical S-shape characterised by three distinct segments. A steep segment at early time that is similar to the Theis curve, is followed by a stabilised segment at medium time that deviates from the Theis curve. A relatively steep late time segment conforms to the Theis curve. The steep early time segments represent release of water from storage due to expansion of the water and compaction of the aquifer whereas the flat medium time segments represent the effects of dewatering of the aquifer that follows the falling water table (Kruseman and de Ridder, 2000). The steep late time segments represent the condition when the flow in the aquifer is sub-horizontal.

A semi-log plot for a leaky aquifer (Fig. 5.9C′) at early pumping times is similar to that of a confined aquifer and is therefore not linear, but shows stabilization at medium to late pumping times. A log-log plot (Fig. 5.9C) is also similar to that of a confined aquifer at early pumping times and is thus characterised by a steep early time segment, and shows stabilization at medium to late pumping times. Leaky-aquifer responses arise from the flow of water into the aquifer from the overlying aquitard, starting from medium to late pumping times, and leads to steady-state flow.

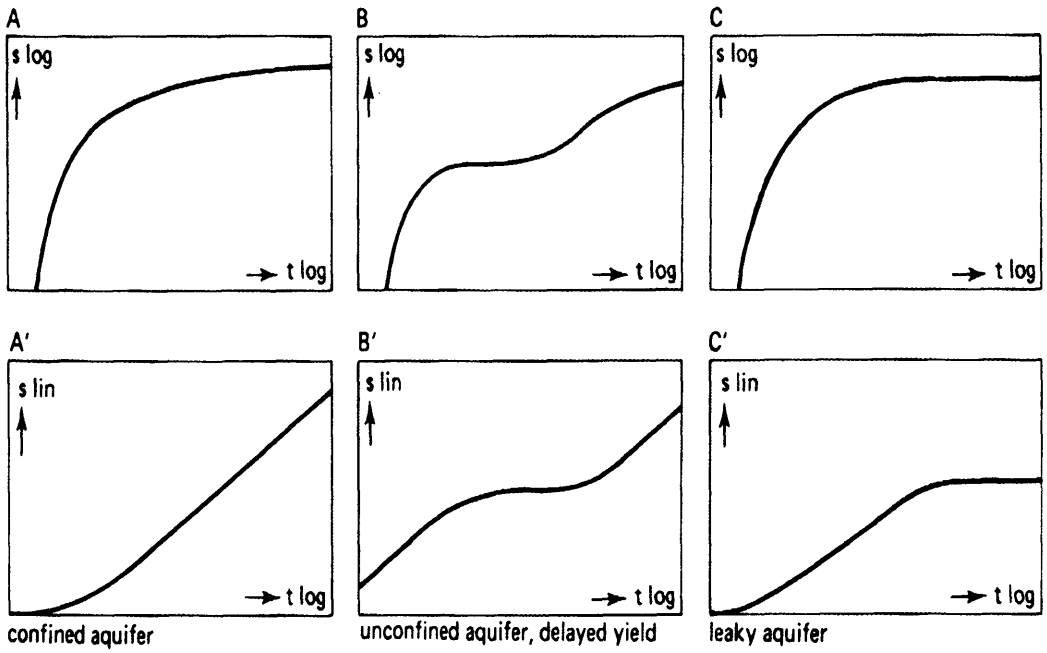

Figure 5.9. Theoretical drawdown curves for unconsolidated aquifers (from Kruseman and de Ridder, 2000).

Consolidated fissured aquifers

The conceptual characteristics of confined, consolidated fractured aquifers are also described using both semi-log and log-log plots of time-drawdown data (Fig. 5.10). Semi-log and log-log plots for confined densely fractured consolidated aquifers of double porosity type (Fig. 5.10A) are similar to those of unconfined unconsolidated aquifers with delayed yield. A semi-log plot (Fig. 5.10A') shows two straight lines at early and late pumping times whereas a log-log plot (Fig. 5.10A) show an S-shape characterised by three distinct segments (Rushton and Weller, 1985; Kruseman and de Ridder, 2000; van Tonder *et al.*, 2001). Two systems are recognized in double porosity aquifers; the high

permeability and low storage capacity fractures, and the low permeability and high storage matrix blocks. Flow to wells in double porosity systems is commonly considered to take place through the fractures, is radial, and unsteady (e.g. Rushton and Weller, 1985; Kruseman and de Ridder, 2000; van Tonder *et al.,* 2001) whereas the flow from matrix blocks to fractures is in a pseudo-steady state. The three segments on log-log plots represent characteristics of flow in the two systems. At early pumping time, groundwater flow comes from storage in the fractures thus exhibiting a steep rise of the time-drawdown curve (Rushton and Weller, 1985; Kruseman and de Ridder, 2000; van Tonder *et al.,* 2001). At medium-term pumping times, the matrix blocks recharge the fractures and stabilize the drawdown. At late pumping times, groundwater derives from storage in both the fractures and matrix blocks and gives rise to a slow but steady increase in drawdown.

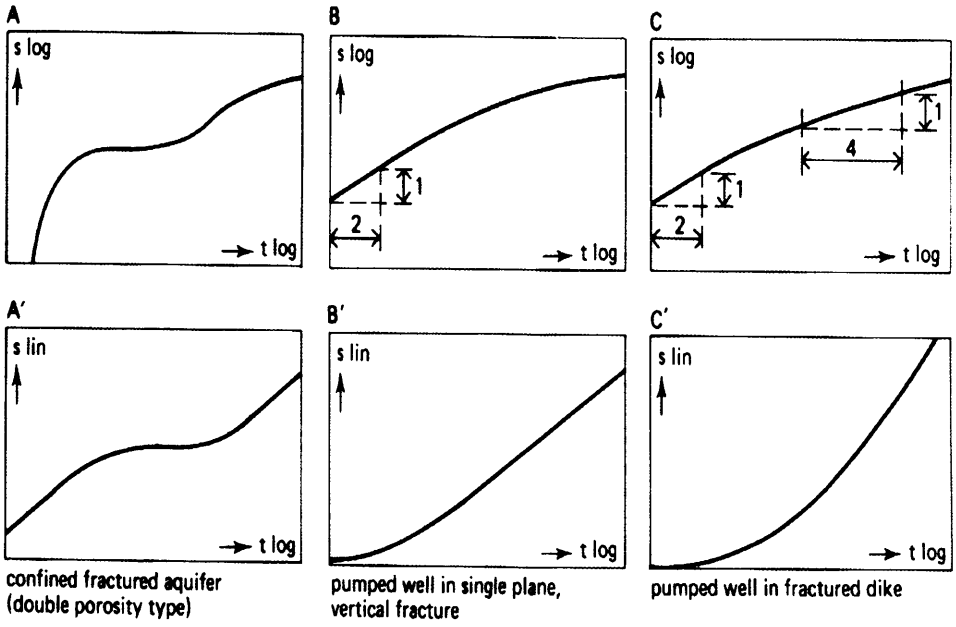

Figure 5.10. Theoretical drawdown curves for consolidated fractured aquifers (from Kruseman and de Ridder, 2000).

A conceptual semi-log plot for a single plane vertical fracture in a confined, homogenous and isotropic aquifer of low permeability (Fig. 5.10B′) resembles that of a confined unconsolidated aquifer, and is not linear at early pumping times but become linear at later pumping times. The log-log plot for a well that draws groundwater from a single plane vertical fracture (Fig. 5.10B) however shows straight lines for early pumping times. The slopes of the straight lines vary between 0.25 and 0.5 (Rushton and Weller, 1985; Kruseman and de Ridder, 2000) depending on the conductivity of the fracture. A slope of 0.25 is attributed to a relatively low permeability fracture whereas a slope of 0.5 is attributed to a high permeability fracture (Rushton and Weller, 1985). As the flow regime gradually changes to radial at late pumping times the drawdown response follows the Theis curve and resembles a confined, unconsolidated aquifer.

A log-log plot of theoretical time-drawdown data for a pumping well in a densely fractured, high permeability dike of infinite length and finite width in a confined, homogeneous, isotropic, consolidated aquifer of low hydraulic conductivity and high storage capacity (Fig. 5.10C) shows two straight lines for early and medium pumping times. The first segment of the straight line has a slope of 0.5 and thus resembles that of a high permeability vertical fracture (Rushton and Weller, 1985; Kruseman and de Ridder, 2000) and flow to the well is entirely though the dike. At medium pumping time, the adjacent aquifer matrix supplies water to the dike reducing the rate of drawdown (i.e, slope of 0.25 on a log-log plot). At late pumping times, the dominant flow is radial and follows the Theis curve. This behaviour shows as a straight line on a semi-log plot (Fig.

5.10C). Kruseman and de Ridder (2000) observe that the slope of 0.25 sometimes does not appear on the log-log plot.

Further means of identifying groundwater flow characteristics in weathered and fractured-bedrock aquifers have been proposed by Rushton and Weller (1985). Wells that intersect the "extended well" (same aquifer) typically have drawdown responses similar or identical to that of the pumping well. If the early time data in a monitoring well have a higher slope than the pumping well (Rushton and Weller, 1985; Kruseman and de Ridder, 1991), the observation well is in proximity to the fracture tapped by the pumping but does not intersect it. Similarly, if early time data of an observation well has a lower slope than the pumping well it indicates that the observation well intersects the fracture tapped by the pumping well (Rushton and Weller, 1985). Based on extensive interpretation of pumping tests data in weathered and fractured-bedrock aquifers, Rushton and Weller (1985) assert that early time-drawdown responses in weathered and fractured-bedrock aquifers usually indicate linear flow though a single fracture whereas late time-drawdown responses indicate flow though interconnected fractures. They argue that all the wells outside the zone of linear flow after a long period of pumping are interpreted by radial flow methods.

Based on the above discussion, the two types of flows in the weathered and fractured-bedrock aquifer can be conceptualised as shown in Fig. 5.11.

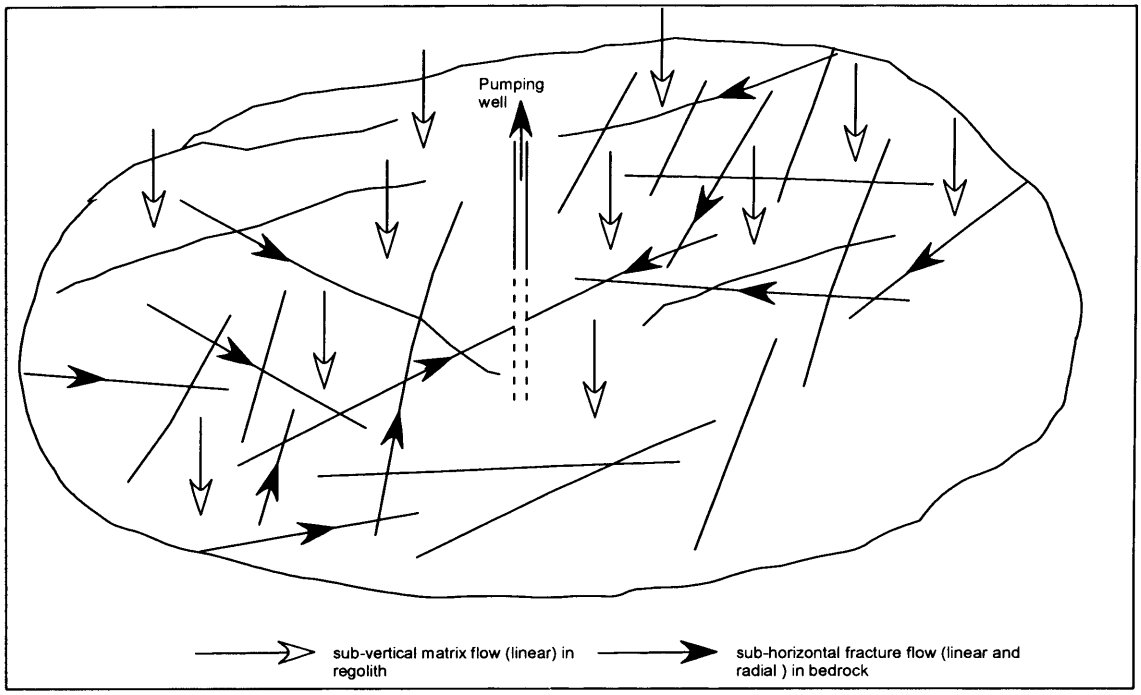

Figure 5.11. Types of flows in the weathered and fractured-bedrock aquifer system

Boundary conditions

Specific boundary conditions such as partial penetration of the well, well-bore storage, recharge boundaries and impermeable boundaries also cause curves of field time-drawdown data to deviate from the theoretical curves of the main types of aquifer (Kruseman and de Ridder, 2000). These boundary conditions can occur individually or in combination.

5.5.3.2 Weathered and fractured-bedrock aquifers – Wobulenzi results

Log-log plots of time-drawdown data for the pumping well, P3 and P4 in the fractured-bedrock aquifer show steep rises at early pumping times and stabilized

segments at medium to late pumping times (Fig. 5.12 and 5.13). The semi-log plots however show non linear rises at early pumping times and stabilized segments at medium and late pumping times (Fig. 5.12 and 5.13). The steep rises at early pumping times (approximately 20 minutes) on log-log plots could be due to wellbore storage and later linear flow whereas the stabilized segments at medium to late pumping times (approximately 400 minutes) are indicative of inflow of recharge to the aquifer. These drawdown responses are characteristic of leaky aquifer conditions (Fig. 5.9).

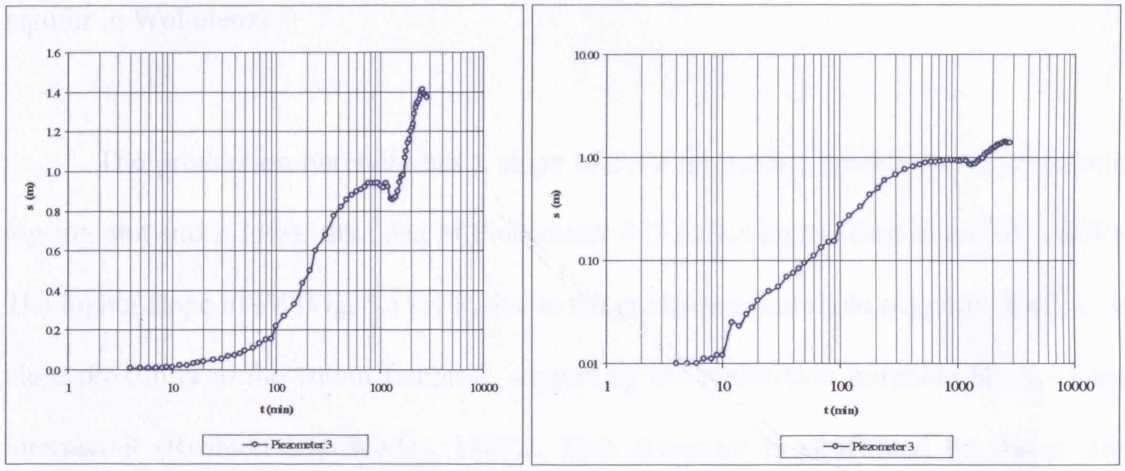

Figure 5.12. Semi-log and Log-log plots for Piezometer 3 in the fractured-bedrock aquifer in Wobulenzi

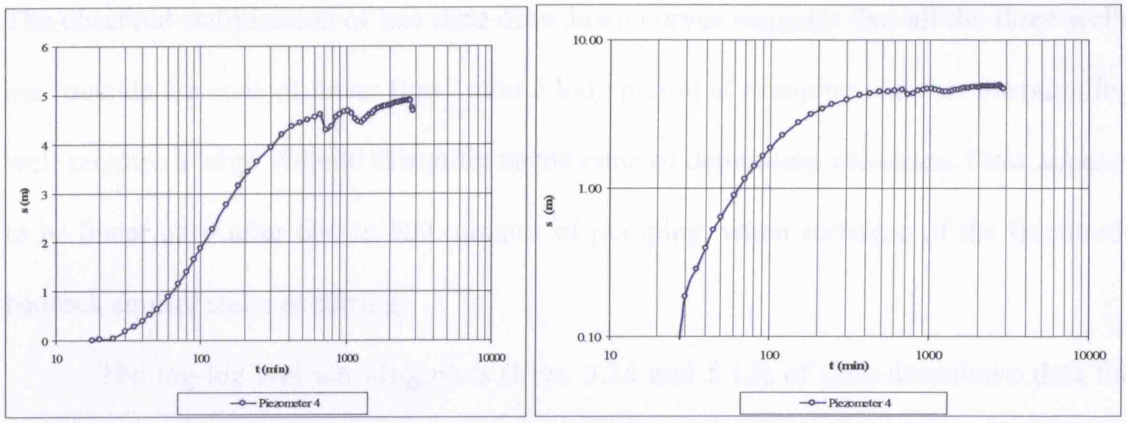

Figure 5.13. Semi-log and Log-log plots for Piezometer 4 in the fractured-bedrock aquifer in Wobulenzi

The production borehole has a slope of 0.19 for early time-drawdown data on a log-log plot and is lower than that of Piezometer 4 (3.6) but higher than that of P3 (0.07). The higher slope of P4 (Fig. 5.13) relative to the production borehole suggests that it is in close proximity to the "main fracture" tapped by the production borehole but does not intersect it (Rushton and Weller, 1985). This inference is confirmed by the slower response of P4 (10 minutes) to pumping compared to P3 (7 minutes). P3 has a lower slope than the production borehole for early time-drawdown data (Fig. 5.12) indicating that it intersects the main fracture tapped by the pumping well (Rushton and Weller, 1985). Field observations which show that P3 located further away from the pumping well responded to pumping faster and in a more 'linear' manner than P4 confirms that there is a good hydraulic connection between P3 and the production borehole. Time-drawdown responses in the fractured-bedrock aquifer therefore indicate that flow is complex but is predominantly linear though individual fractures at early pumping times.

The observed stabilization of late time-drawdown curves suggests that all the three wells are "outside the zone of linear flow" after a long period of pumping and that the pumping well samples a large volume of aquifer as the cone of depression increases. Flow appears to be linear until after 600 to 800 minutes of pumping, when recharge of the fractured-bedrock aquifer starts occurring.

The log-log and semi-log plots (Figs. 5.14 and 5.15) of time-drawdown data for P1 and P2 in the weathered aquifer show characteristics similar to those of a pumped well in a single plane (Fig. 5.10C). The log-log plots show two steep lines; one with a slope >0.5 at early pumping times and the other with a slope of about 0.5 at late pumping times. However, the semi-log plots are not linear at early pumping times but become linear at late pumping times with slopes greater than 1 (Figs. 5.14 and 5.15). The straight lines of high slopes on the log-log and semi-log plots at late time-drawdown times for P1 and P2 indicate uni-dimensional flow (Rushton and Weller, 1985) that could be due to vertical hydraulic gradient in the weathered aquifer that is induced by pumping in the fractured-bedrock aquifer. The reduction in slope on log-log plots at late pumping times suggests that there is inflow of groundwater in the aquifer. The results suggest that as the vertical hydraulic gradient increases, it induces horizontal flow in the weathered aquifer that serves to reduce the slope of the late drawdown curve. The data indicate that horizontal flow in the weathered aquifer starts occurring after 800 to 1000 minutes of pumping which is consistent with the periods when recharge of the fractured-bedrock aquifer emerges. The weathered aquifer therefore exhibits unconfined aquifer conditions that are dominated by downward vertical flow. Thus, consistent with the observations of Rushton and Weller (1985), the stabilization of the time-drawdown curves for the

fractured-bedrock aquifer at late pumping times results from groundwater flow though a network of interconnected fractures and recharge from the overlying weathered aquifer. The weathered and fractured-bedrock aquifers are therefore hydraulically connected and form one aquifer system.

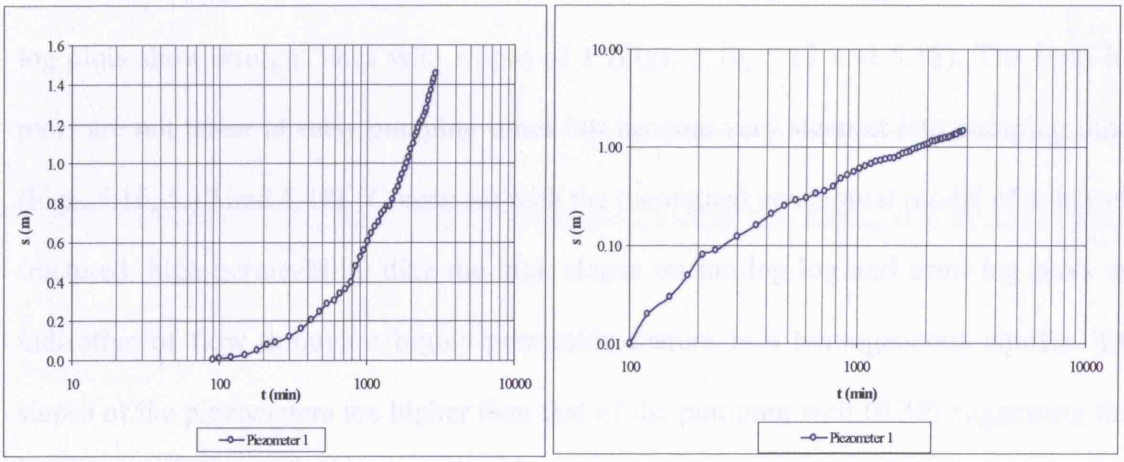

Figure 5.14. Semi-log and log-log plots for Piezometer 1 in the weathered aquifer in Wobulenzi

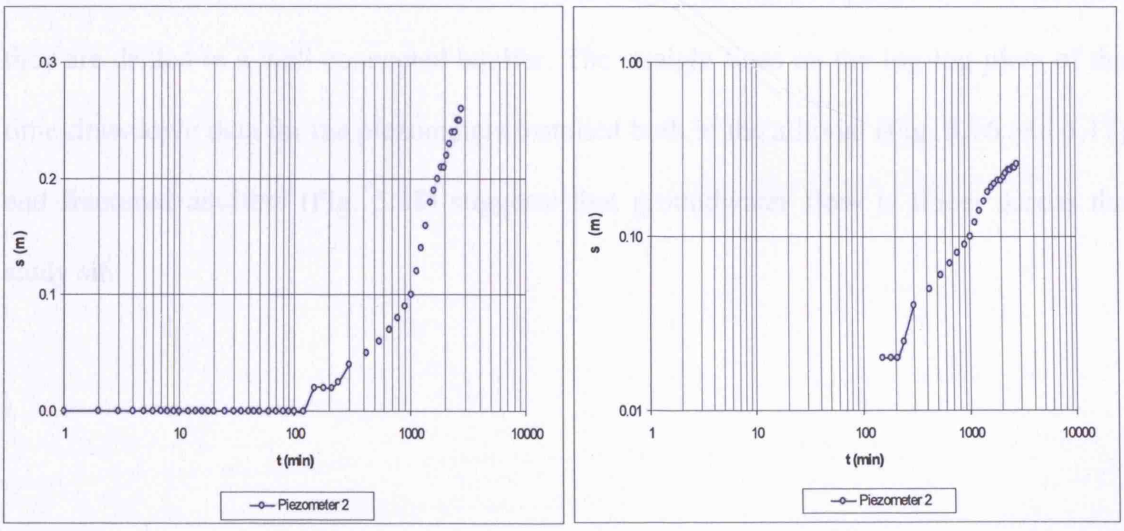

Figure 5.15. Semi-log and log-log plot for Piezometer 2 in the weathered aquifer in Wobulenzi

5.5.3.3 Alluvial aquifer – Rukungiri

The log-log and semi-log plots for all the seven piezometers (P1, P2, P3, P4, P5, P7 and P8) show characteristics similar to those of a densely fractured, high permeability dike in a homogeneous aquifer of low conductivity but high storage capacity. The log-log plots show straight lines with slopes of 1 (Figs. 5.16, 5.17 and 5.18). The semi-log plots are not linear at early pumping times but become very steep at late pumping times (Figs. 5.16, 5.17 and 5.18). Consistent with the theoretical conceptual model of a densely fractured, high permeability dike the high slopes on the log-log and semi-log plots are indicative of flow through a highly permeable feature in a homogeneous aquifer. The slopes of the piezometers are higher than that of the pumping well (0.39) suggesting that all the piezometers are in close proximity to the aquifer tapped by the pumping well (Rushton and Weller, 1985). The almost identical maximum drawdowns in the seven piezometers irrespective of their depths and distances from the pumping well confirm that they are drilled in a well-connected aquifer. The straight lines on the log-log plots of the time-drawdown data for the piezometers installed both in the alluvial (Fig. 5.16 and 5.17) and fractured aquifers (Fig. 5.18) suggests that groundwater flow is linear across the study site.

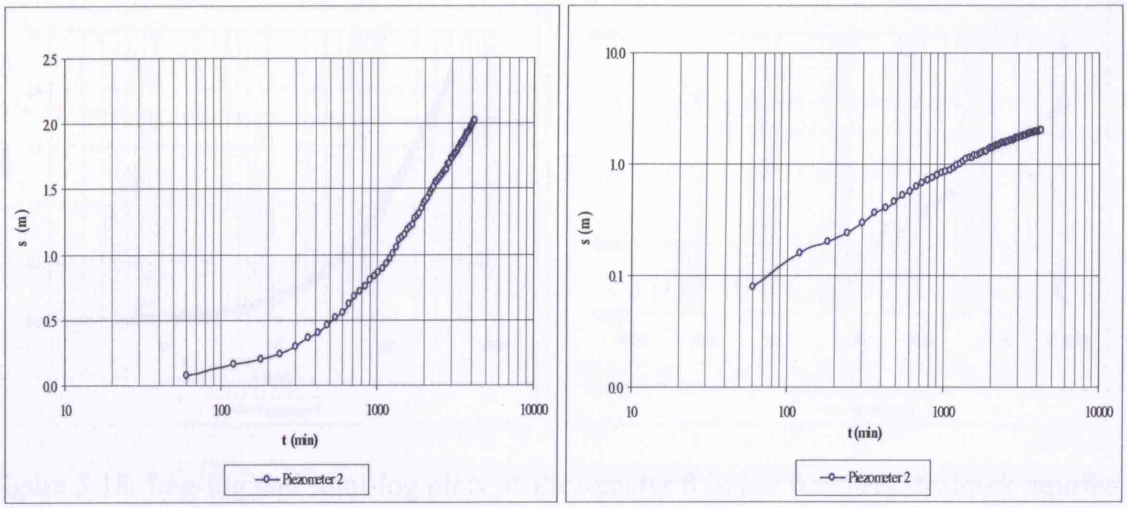

Figure 5.16. Log-log and semi-log plots of Piezometer 2 in the alluvial aquifer in Rukungiri

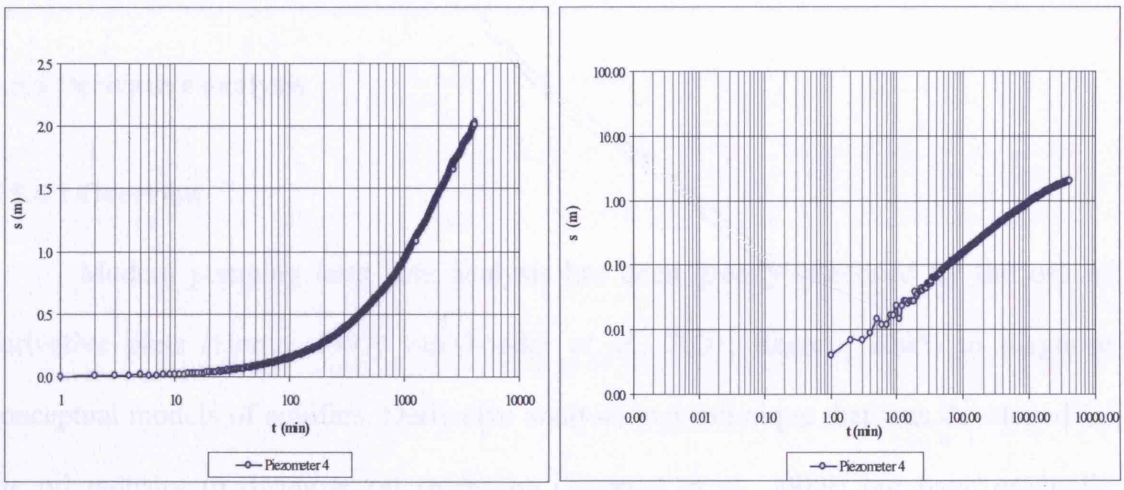

Figure 5.17. Log-log and semi-log plots of Piezometer 4 in the alluvial aquifer in Rukungiri

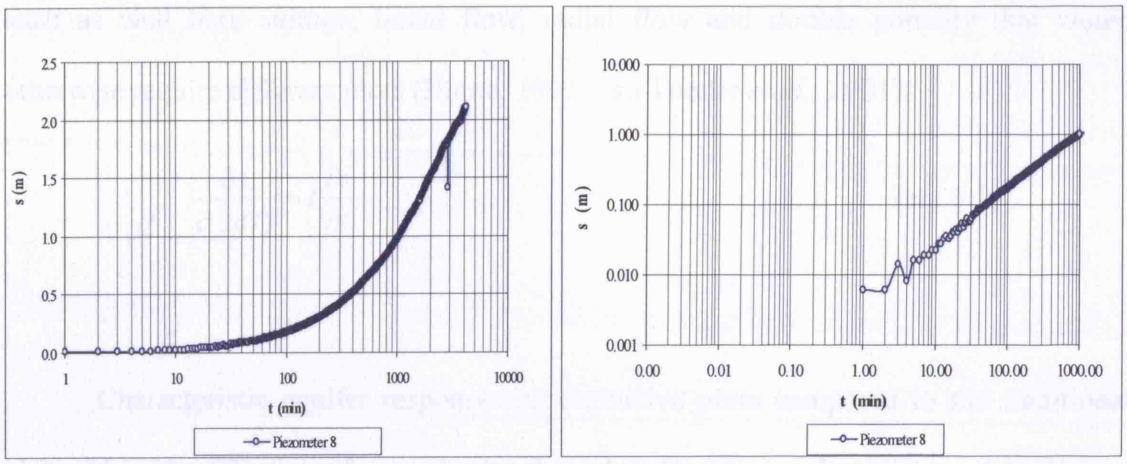

Figure 5.18. Log-log and semi-log plots of Piezometer 8 in the fractured-bedrock aquifer in Rukungiri

All the log-log and semi-log plots are presented in Appendix 4.

5.5.4 Derivative analysis

5.5.4.1 Overview

Modern pumping tests data analysis has been greatly enhanced by the use of derivative plots (Horne, 1997; van Tonder *et al.,* 2001; Renard, 2005) to diagnose conceptual models of aquifers. Derivative analysis is a technique that was developed by the oil industry to diagnose oil reservoirs (Bourdet et al., 1989) but have gradually become adopted by the water industry. The derivative of drawdown (eq. 5.1) when plotted against time on logarithmic scale is more sensitive to variations in drawdown response than the plot of the drawdown alone (van Tonder *et al.,* 2001; Renard, 2005) and can show characteristic responses of an aquifer depending on the hydraulic constraints. Derivative plots are able to display in a single graph separate characteristics

such as well bore storage, linear flow, radial flow and double porosity that would otherwise require different plots (Horne, 1997; van Tonder *et al.,* 2001).

$$\frac{\partial s}{\partial \ln(t)} = t\frac{\partial s}{\partial t} \qquad \text{(eq. 5.1)}$$

Characteristic aquifer responses on derivative plots compared to the traditional plots aid in identification of groundwater flow characteristics and aquifer models (Horne, 1997; van Tonder *et al.,* 2001). Radial flow in characterised by a horizontal stabilization (slope = 0) on the log-log derivative plot (Fig. 5.19) but exhibits a straight line on a semi-log plot. It is therefore often easier to identify deviations from radial flow behaviour on the derivative plot. Well-bore storage is characterised by a slope of 1 on the derivative plot and a curve of low gradient on the semi-log plot (Fig. 5.19). Linear flow is characterised by a slope of 0.5 on a derivative plot (Fig. 5.19) and the same slope is exhibited on a log-log plot. The double porosity condition manifests as two parallel semi-log straight lines on a semi- log plot and as a minimum on a derivative plot (Fig. 5.19). A constant head boundary (recharge boundary) leads to a 'flat' region on s versus t plots at late pumping times and as a continuously decreasing line on a derivative plot (Fig. 5.19). Horne (1997) and van Tonder *et al.* (2001) maintain that double-porosity response is much easier to identify on a derivative plot even when the first semi-log straight line is obscured by wellbore storage.

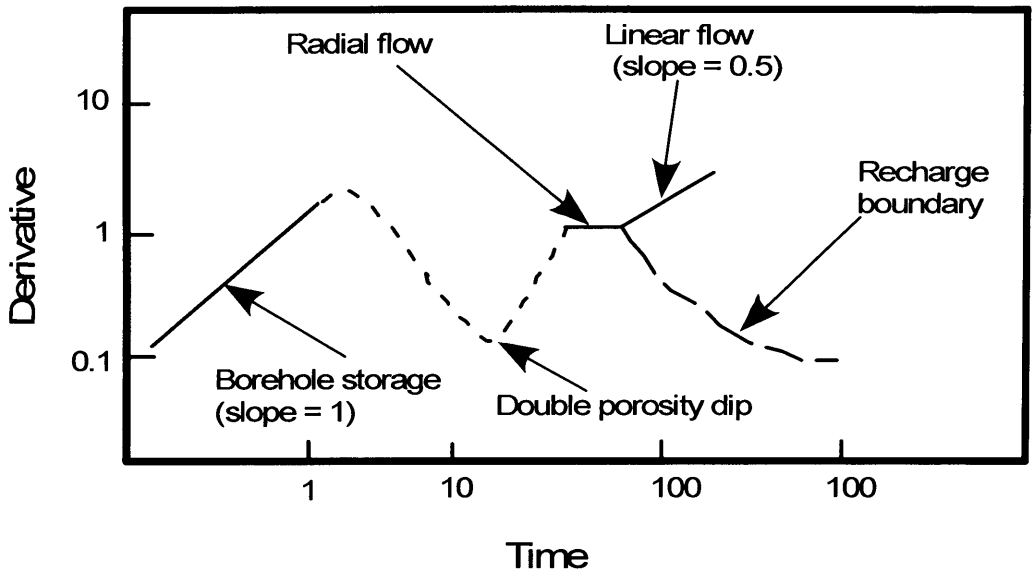

Figure 5.19. Typical shapes of drawdown responses on a derivative plot (modified from Horne, 1997 and van Tonder *et al.*, 2001).

Groundwater flow characteristics and aquifer models in Wobulenzi and Rukungiri were investigated through comparison of the derivative plots of the field data with the theoretical curves. Derivative analysis is very sensitive to noise in observed water level (van Tonder et al., 2001) and should therefore be applied to observed drawdowns that are free of noise. The drawdown data used to generate derivatives plots was smoothed using a least squares approximation method, details of which are provided in van Tonder *et al.* (2001) and Barker (2006).

5.5.4.2 Weathered and fractured-bedrock aquifer – Wobulenzi

The derivative plot of time-drawdown data for the production borehole drilled in the fractured-bedrock aquifer shows a hump and a minimum at medium pumping times that is characteristic of double-porosity conditions (Fig. 5.20). This is followed by a steep curve with a slope ~1 characteristic of storage-dominated "linear flow" that evolves to a stabilized segment that indicates radial flow. At late pumping times, the plot shows a continuously decreasing curve that is characteristic of a recharge boundary. The derivative plots for P3 and P4 drilled in the fractured-bedrock do not show double porosity response but rather a continuously increasing curve with a slope that varies between 0.5 and 1 which is characteristic of linear flow dominated by storage in the fractures. The steep curve is followed by a small stabilized segment with zero slope indicative of radial flow that is followed by a continuously decreasing curve at late pumping times that is characteristic of a recharge boundary (Fig. 5.21). The log-log plots and time-drawdown curves for the piezometers installed in the fractured-bedrock aquifer and the production borehole show that changes in the rate of drawdown slow considerably or cease at late pumping times further confirming the presence of a recharge boundary (section 5.3.2 and 5.5.3.2). The stabilized segments on derivative plots of the production borehole, P3 and P4 appear after ~1500 minutes of pumping whereas a continuously decreasing curve occurs at approximately 1800 minutes of pumping. Recharge boundary response at late pumping times is consistent with the earlier observation that recharge is from a dense network of interconnected fractures and the overlying weathered aquifer (section 5.5.3.2).

The derivative plots of time-drawdown data for P1 and P2 drilled in the weathered aquifer show a slope ~1 at early pumping times that is characteristic of storage, a slope of zero at intermediate pumping times that is characteristic of radial flow and a slope of 0.5 at late pumping times that is characteristic of linear flow (Fig. 5.22). The results suggest that for a sufficiently long period (approximately 1800 minutes), flow in the weathered aquifer is dominated by storage in the well and the aquifer surrounding the well resulting in a slope of 1. This response indicates that the weathered aquifer has high storage. After approximately 1800 minutes of pumping radial flow evolves due to horizontal flow of groundwater in the aquifer and changes to linear flow after approximately 2400 minutes of pumping due to increased hydraulic gradient in the weathered aquifer due to pumping in the fractured-bedrock aquifer. A linear response is also shown on the log-log plots of late time-drawdown data for the two piezometers confirming that flow is linear at late pumping times. The evolution of the different flow regimes in the weathered and fractured-bedrock aquifers coincide further confirming that the two aquifers are hydraulically connected and form one aquifer system.

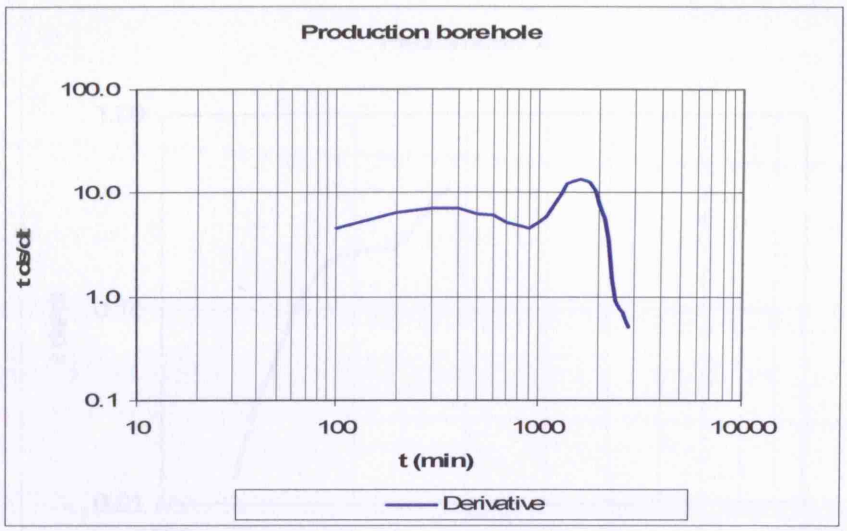

Figure 5.20. Derivative plot for the production borehole drilled in the fractured-bedrock aquifer

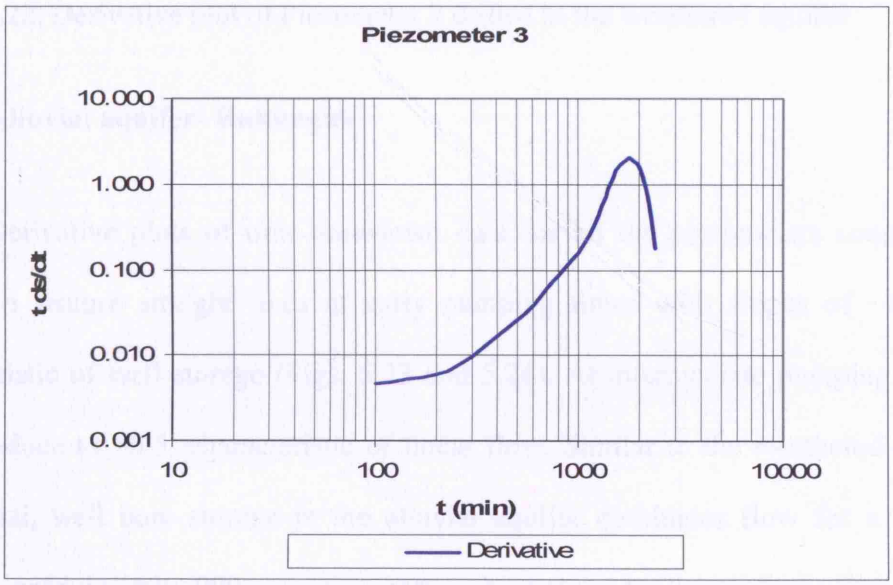

Figure 5.21. Derivative plot for Piezometers 3 drilled in the fractured-bedrock aquifer

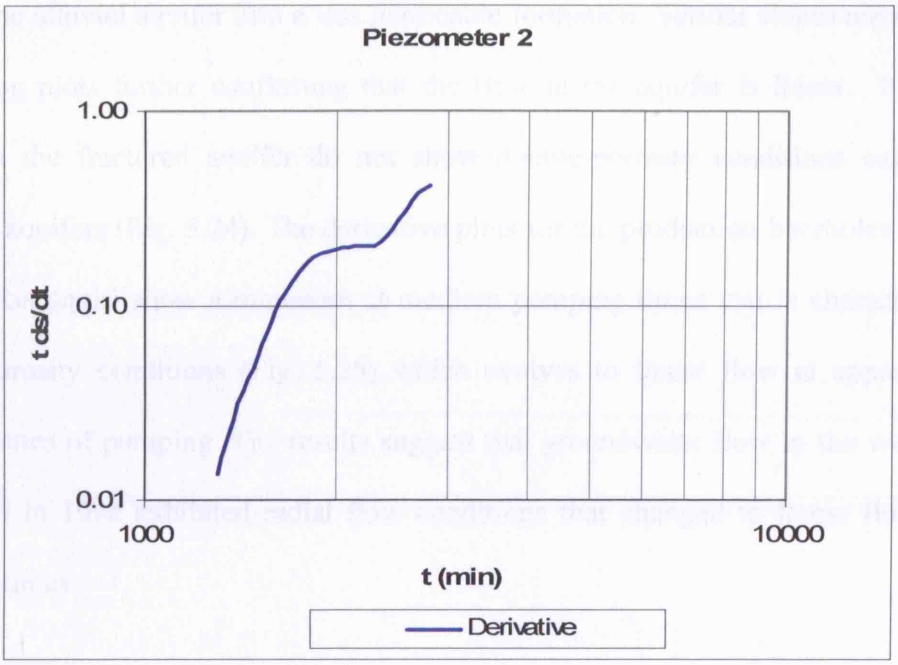

Figure 5.22. Derivative plot of Piezometer 2 drilled in the weathered aquifer

5.5.4.3 Alluvial aquifer- Rukungiri

Derivative plots of time-drawdown data for all the piezometers constructed in Rukungiri feature straight lines at early pumping times with slopes of ~1 that are characteristic of well storage (Figs. 5.23 and 5.24). At intermediate pumping times the slopes reduce to ~0.5, characteristic of linear flow. Similar to the weathered aquifer in Wobulenzi, well bore storage in the alluvial aquifer dominates flow for a very long period (approximately 900 minutes) before it evolves to linear flow. This response appears to suggest that the alluvial aquifer responds as would a well of very high storage possibly because the aquifer is fairly homogeneous with high permeability. At late pumping times (approximately 1500 minutes) the slopes of the curves gradually reduce to less than 0.5 possible due to reduction in transmissivity as the cone of depression goes

beyond the alluvial aquifer into a less permeable formation. Similar slopes are shown on the log-log plots further confirming that the flow in the aquifer is linear. P7 and P8 drilled in the fractured aquifer do not show double-porosity conditions expected of fractured aquifers (Fig. 5.24). The derivative plots for the production boreholes drilled in 1998 in Rukungiri show a minimum at medium pumping times that is characteristic of double-porosity conditions (Fig. 5.25) which evolves to linear flow at approximately 1200 minutes of pumping. The results suggest that groundwater flow in the wellfield in Rukungiri in 1998 exhibited radial flow conditions that changed to linear flow at late pumping times.

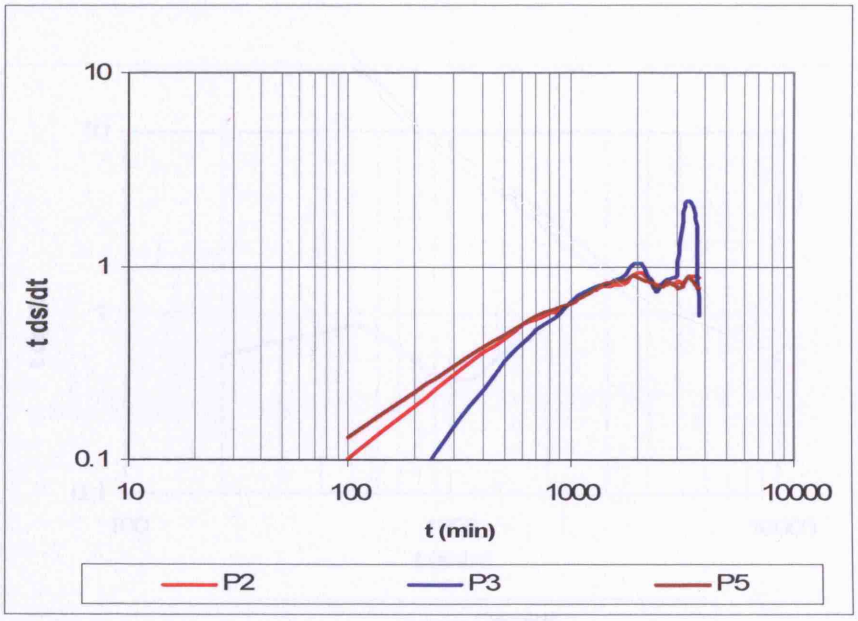

Figure 5.23. Derivative plots of Piezometers 2, 3 and 5 drilled in Rukungiri

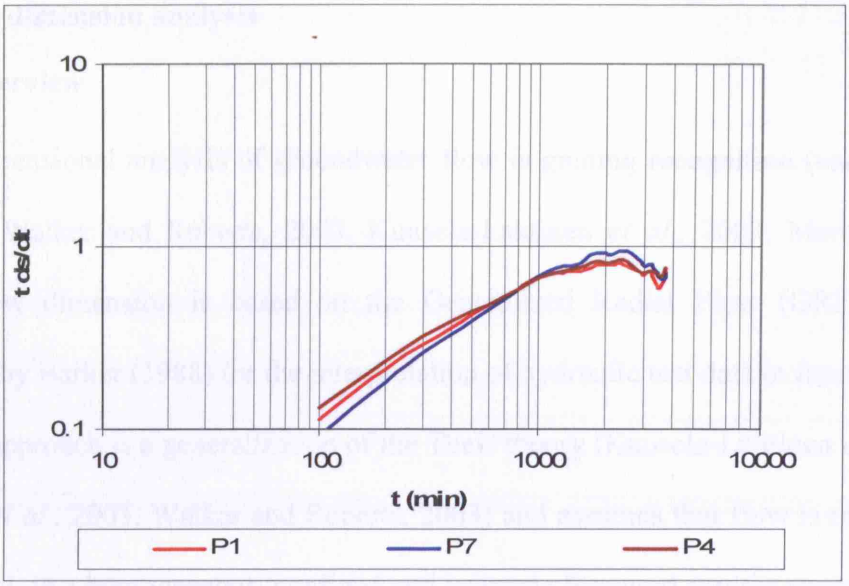

Figure 5.24. Derivative plot of Piezometers 1, 4 and 7 drilled in Rukungiri

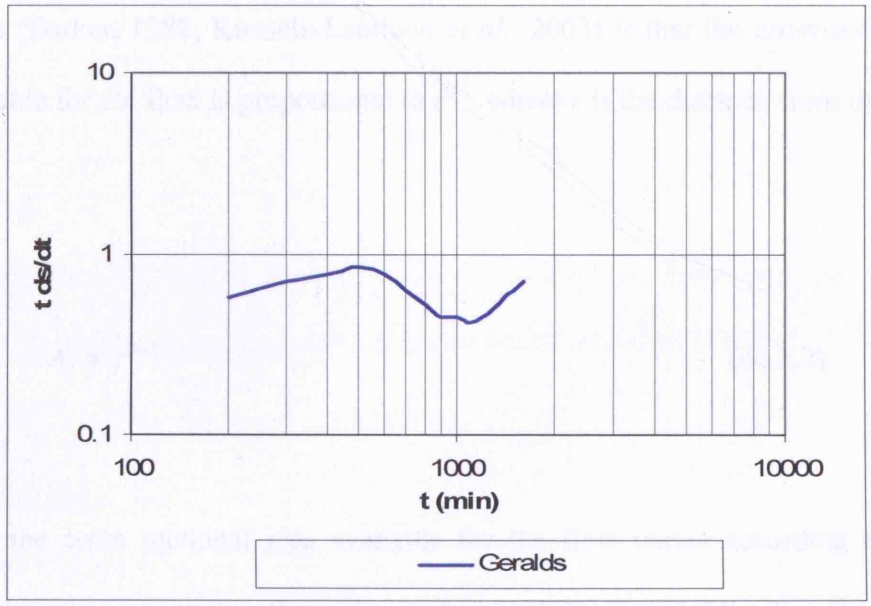

Figure 5.25. Derivative plot for one of the production boreholes drilled in 1998 in Rukungiri

5.5.5 Flow dimension analysis

5.5.5.1 Overview

Dimensional analysis of groundwater flow is gaining recognition (van Tonder *et al.,* 2001; Walker and Roberts, 2003; Kuusela-Lahtinen *et al.,* 2003; Merechal et al., 2003). Flow dimension is based on the Generalized Radial Flow (GRF) approach developed by Barker (1988) for the interpretation of hydraulic test data in fractured rocks. The GRF approach is a generalization of the Theis theory (Kuusela-Lahtinen *et al.,* 2003; Merechal *et al.,* 2003, Walker and Roberts, 2003) and assumes that flow is radial and n-dimensional, in a homogeneous, confined and isotropic fractured aquifer characterised by a hydraulic conductivity K_f and specific storage S_{sf}. Thus, the GRF model introduces the fractional dimension of flow, n, which varies from 0 to 3. The physical meaning of flow dimension (Barker, 1988; Kuusela-Lahtinen *et al.,* 2003) is that the cross-sectional area (A_r) available for the flow is proportional to r^{n-1}, where r is the distance from the well (eq. 5.2).

$$A_r \propto r^{n-1} \qquad \text{(eq.5.2)}$$

If n = 1, the cross sectional area available for the flow varies according to $A_c \propto r^0$ implying that the cross-sectional area is constant with increase in distance from the well. The flow is therefore described as one dimensional channel flow. If n = 2, the cross sectional area for the flow varies according to $A_c \propto r^1$ implying that the cross-sectional area will vary linearly with distance from the well. The flow is therefore described as two

dimensional radial flow and corresponds to the Theis model (Kuusela-Lahtinen *et al.*, 2003). If n = 3, the cross sectional area available for the flow varies according to $A_c \propto r^2$ and implies that the cross-sectional area will vary with the square of the distance from the well. The flow is therefore described as three-dimensional, spherical flow. Flow dimension is estimated directly from the second derivative of drawdown versus log time (Kuusela-Lahtinen *et al.*, 2003; Barker, 2006). A flow dimension plot is based on the asymptotic result that drawdown is proportional to time to a power dependent on the flow dimension, D_f (Barker, 2006):

$$s(t) \sim t^{1-D_f/2} \quad as \quad t \to \infty \qquad \text{(eq. 5.3)}$$

Based on eq. 5.3, flow dimension is given by eq. 5.4 below:

$$D_f = 2\left(1 - \frac{\partial \ln(s)}{\partial \ln(t)}\right) = 2\left(1 - \frac{t}{s}\frac{\partial s}{\partial t}\right) \qquad \text{(eq. 5.4)}$$

The interpretation of flow dimension is carried out based on type curve analysis for n-dimension flow. The early part of the curve is not normally considered reliable for detailed type curve fitting and the analysis is based mainly on later parts of the data.

Flow-dimension of a hydraulic test may reflect several characteristics of a system that includes heterogeneity, boundaries and leakage (Walker and Roberts, 2003; Kuusela-Lahtinen *et al.*, 2003; Marechal *et al.*, 2003). Walker and Roberts (2003) demonstrate that a stationary transmissivity field with a modest level of heterogeneity has a flow dimension of two whereas highly heterogeneous systems have higher flow dimensions. Kuusela-Lahtinen *et al.* (2003) maintain that the main characteristics of the formation

such as linear flow can easily be distinguished from dimensions higher than two. Both integer and non-integer dimensions are possible (Barker, 1988; Walker and Roberts, 2003; Kuusela-Lahtinen *et al.,* 2003; Merechal *et al.,* 2003). Non-integer values observed in fractured rocks may result from radial diffusion in a fractal network of fractures (Barker, 1988; Hamm and Bidaux, 1996; Walker and Roberts, 2003). Walker and Roberts (2003) show that flow dimension for radial flow in an infinite, homogeneous domain is 2 and that the plot will remain horizontal and constant when flow dimension is plotted on a graph.

Walker and Roberts (2003) caution about the difficulties with unique interpretation of apparent flow dimension because heterogeneity and flow geometry are interchangeable and both can influence the flow dimension of a system. Flow dimension of a hydraulic test can therefore reflect several hydrogeological conditions. Barker (1988) notes that the observed flow dimension in fractured rocks is not necessarily a simple function of radial distance as it is in the homogeneous system. It should be considered as a relative measure that depends on the geometry and flow area of an aquifer and several possible geometrical interpretations exist to a flow dimension (Kuusela-Lahtinen *et al.,* 2003). Non-uniqueness of flow dimension might be viewed as a limitation of the GRF approach (Hamm and Bidaux, 1996; Walker and Roberts, 2003) but it enables consideration of alternative hydrogeological conceptual models. Similarly, even though the effects of multiple hydrogeological conditions can limit interpretation of pumping-test data, flow dimension constrains admissible combinations of conceptual models for a groundwater system. Walker and Roberts (2003) therefore recommend that interpretation of hydraulic testing data should be done based on an understanding of the

hydrogeological context rather than on assumptions made in the models used in data interpretation. Despite the above limitations, flow dimensions observed during hydraulic tests assist in identifying suitable hydrogeological conceptual models (Kuusela-Lahtinen *et al.*, 2003; Walker and Roberts, 2003) and promote sound interpretations of hydraulic testing data.

5.5.5.2 Weathered and fractured-bedrock aquifer – Wobulenzi

The production borehole and P3 and P4 in the fractured-bedrock exhibit a flow dimension, D_f, of 2 (Fig. 5.26). D_f of 2 confirms that flow in the fractured-bedrock aquifer is radial and that the cross-sectional area available for the flow will vary linearly with distance from the well (Walker and Roberts, 2003; Kuusela-Lahtinen et al., 2003; Merechal et al. 2003). Confirmation of radial flow in the fractured-bedrock aquifer implies that pumping test data can be appropriately interpreted using a Theis model.

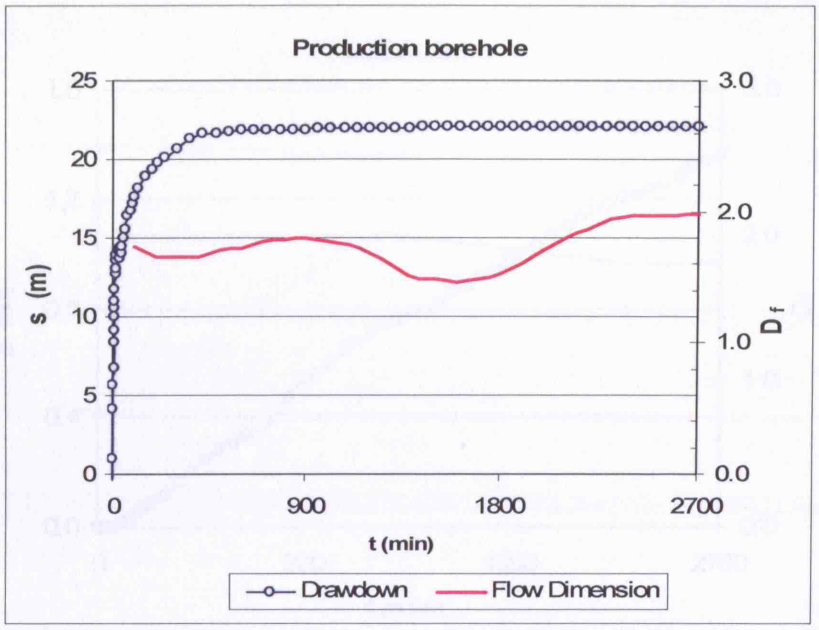

Figure 5.26. Plot of drawdown and flow dimension for the production borehole in the fractured-bedrock aquifer in Wobulenzi

P1 and P2 in the weathered aquifer also exhibit a flow dimension, D_f, of 2 suggesting that the weathered aquifer also exhibits radial flow conditions and that the cross-sectional area of flow varies linearly with distance from the production borehole (Fig. 5.27). The D_f for P2 is 2 at late pumping times whereas for P1 it reduces to about 1.8 at late pumping times. The reduction in D_f for P1 could be due to the higher hydraulic gradient between the weathered and fractured-bedrock aquifers that induced more vertical flow. The higher drawdown observed in P1 than those observed in either P3 or P2 confirms presence of higher vertical flow from the weathered aquifer to the fractured-bedrock aquifer.

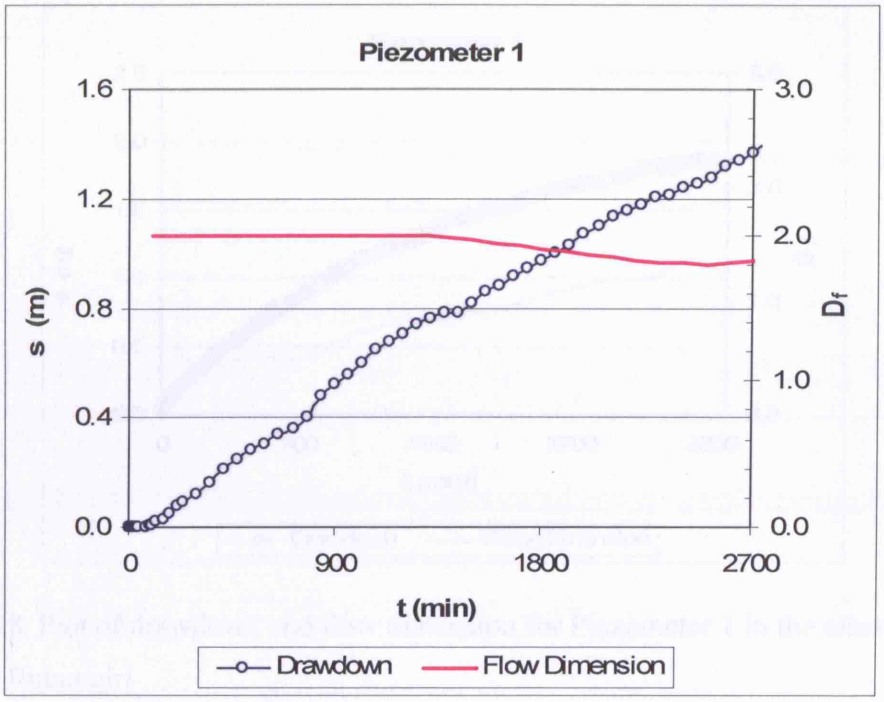

Figure 5.27. Plot of drawdown and flow dimension for Piezometer 1 in the weathered aquifer in Wobulenzi

5.5.5.3 Alluvial aquifer- Rukungiri

All piezometers and the production borehole (Ruk 8) in Rukungiri exhibit a flow dimension of about 1.2 (Figs. 5.28, 5.29 and 5.30) suggesting that the cross-sectional area of flow is constant with increase in distance from the well. There are no significant differences between the piezometers in the alluvial aquifer (Figs. 5.28 and 5.30) and those in the fractured aquifer (Fig. 5.29). Flow in the wellfield in Rukungiri is therefore considered to be one-dimensional (channel) flow. The uniform flow dimension of 1.2 is consistent with the observations of the linear flow response on both log-log and derivative plots and weak heterogeneity on the s versus t/r^2.

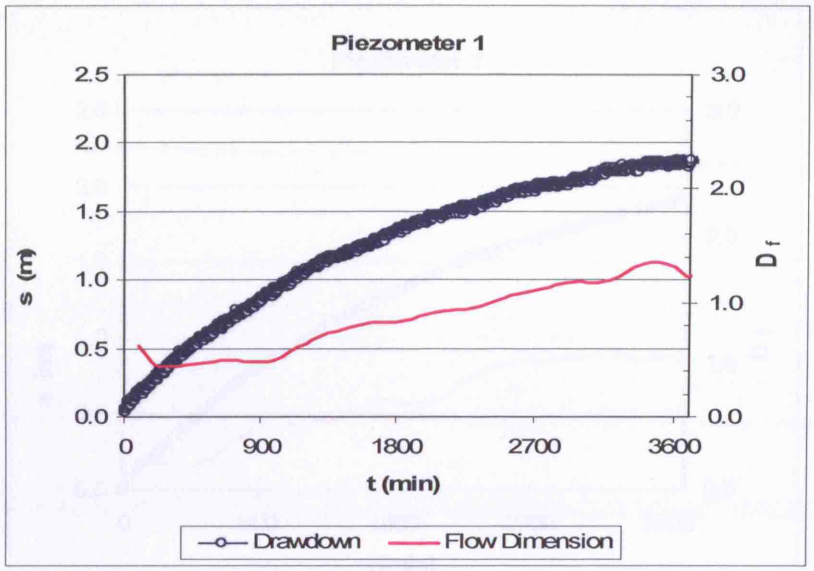

Figure 5.28. Plot of drawdown and flow dimension for Piezometer 1 in the alluvial aquifer in Rukungiri

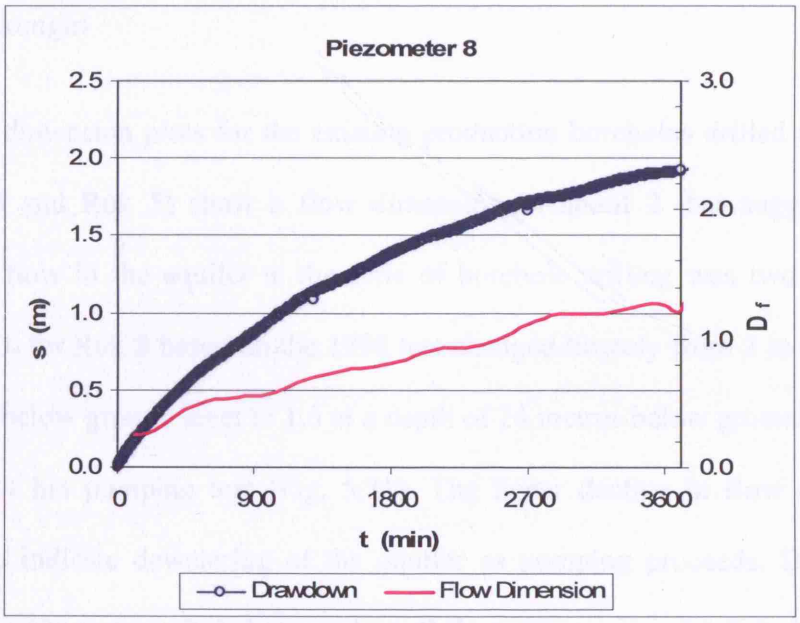

Figure 5.29. Plot of drawdown and flow dimension for Piezometer 8 in the fractured aquifer in Rukungiri

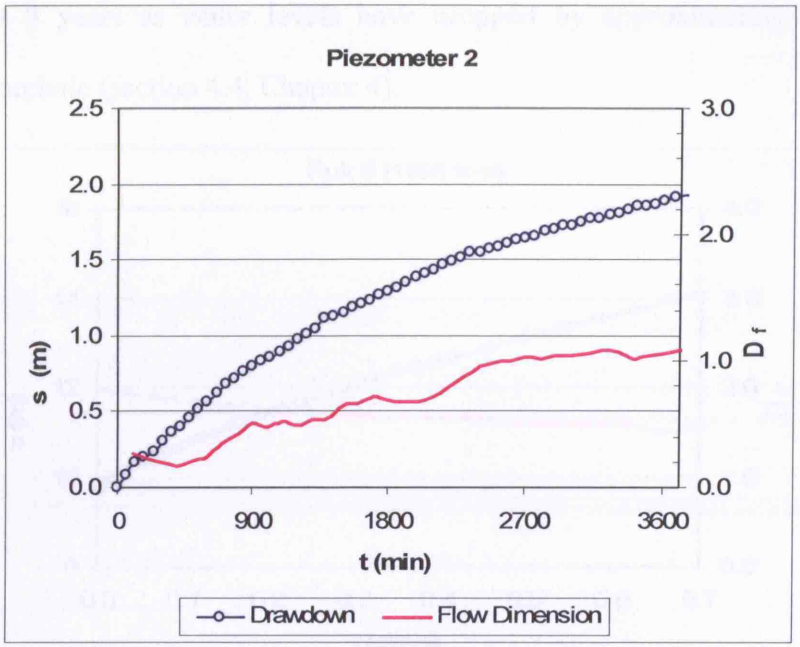

Figure 5.30. Plot of drawdown and flow dimension for Piezometer 2 in the alluvial aquifer in Rukungiri

Flow dimension plots for the existing production boreholes drilled and tested in 1998 (Ruk 8 and Ruk 5) show a flow dimension of about 2 that suggests that the groundwater flow in the aquifer at the time of borehole drilling was two dimensional radial flow. D_f for Ruk 8 based on the 1998 test changed linearly from 2 at a water level of 22 metres below ground level to 1.6 at a depth of 24 metres below ground level by the end of the 24 hrs pumping test (Fig. 5.31). The linear decline in flow dimension is considered to indicate dewatering of the aquifer as pumping proceeds. D_f for Ruk 5, approximately 600 m from Ruk 8 showed small fluctuations around 1.8 during the 24 hrs pumping test suggesting limited dewatering of the aquifer (Fig. 5.32). D_f for Ruk 8 based on the 2005 test fluctuates about 1 (Fig. 5.33). The transition from radial flow field to linear flow between 1998 and 2005 coincides with a rapid decline in groundwater storage

over the last 8 years as water levels have dropped by approximately 20 m in the production borehole (section 4.4, Chapter 4).

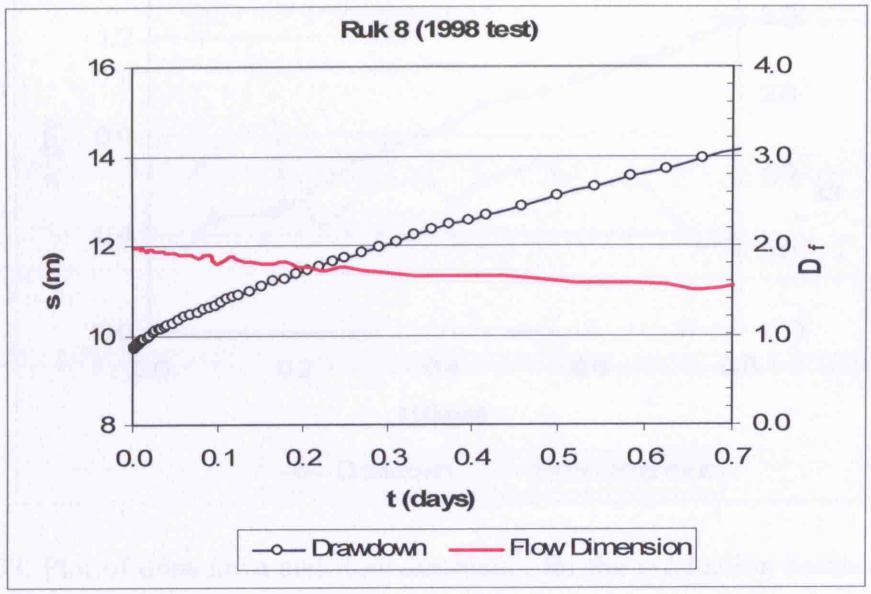

Figure 5.31. Plot of drawdown and flow dimension for the production borehole (Ruk 8) based on 1998 test

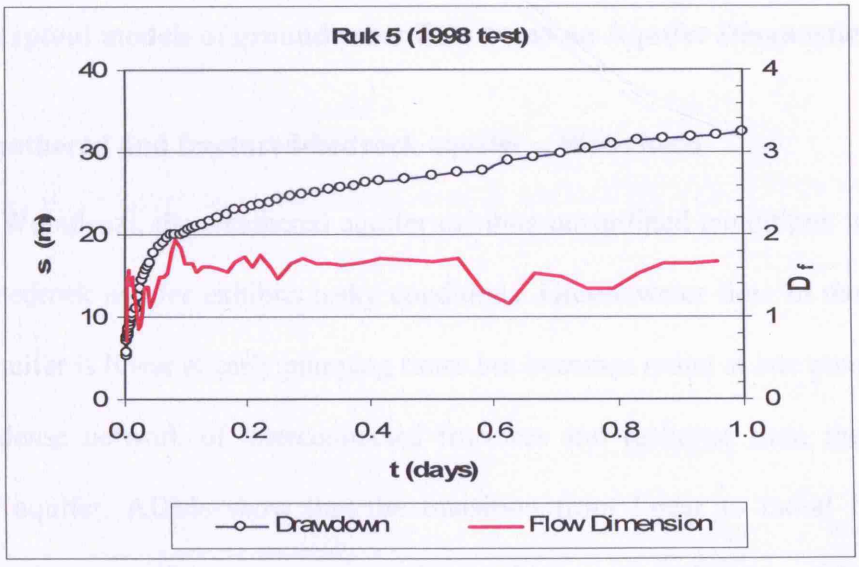

Figure 5.32. Plot of drawdown and flow dimension for the production borehole (Ruk 5) based on 1998 test

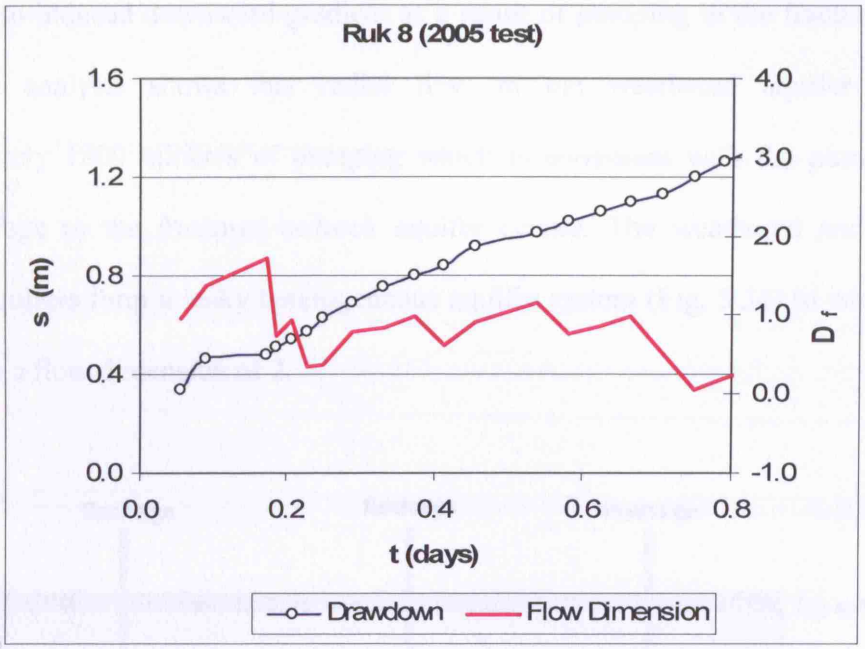

Figure 5.33. Plot of drawdown and flow dimension for the production borehole (Ruk 8) based on 2005 test

5.5.6 Conceptual models of groundwater flow based on Aquifer Diagnostic Methods

5.5.6.1 Weathered and fractured-bedrock aquifer – Wobulenzi

In Wobulenzi, the weathered aquifer exhibits unconfined conditions whereas the fractured-bedrock aquifer exhibits leaky conditions. Groundwater flow in the fractured-bedrock aquifer is linear at early pumping times but becomes radial at late pumping times due to a dense network of interconnected fractures and recharge from the overlying weathered aquifer. ADMs show that the transition from linear to radial flow in the fractured-bedrock aquifer occurs at pumping periods ranging between 600 and 1500 minutes whereas leakage from the overlying weathered aquifer starts after 1800 minutes of pumping. Flow in the weathered aquifer is radial but becomes linear at late pumping

times due to induced downward gradient as a result of pumping in the fractured aquifer. Derivative analysis shows that radial flow in the weathered aquifer occurs at approximately 1800 minutes of pumping which is consistent with the pumping times when leakage to the fractured-bedrock aquifer occurs. The weathered and fractured-bedrock aquifers form a leaky heterogeneous aquifer system (Fig. 5.34) in which flow is radial with a flow dimension of 2.

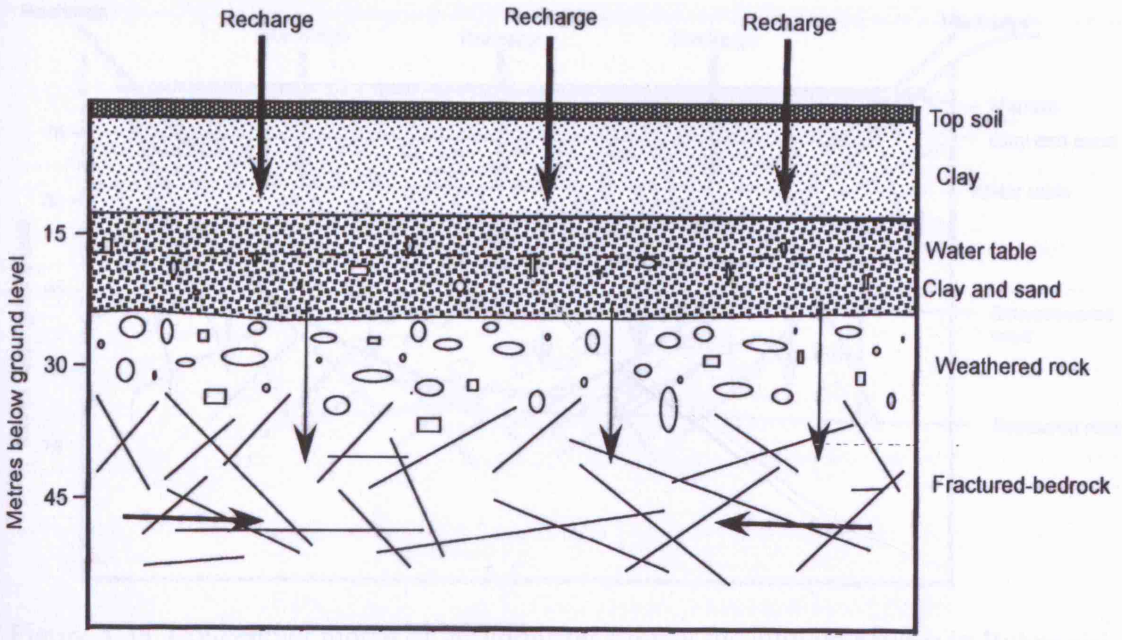

Figure 5.34. Conceptual model of groundwater flow in the weathered and fractured-bedrock aquifer system in Wobulenzi

5.5.6.2 Alluvial aquifer – Rukungiri

The alluvial aquifer in Rukungiri is unconfined and highly permeable. The consistency in the drawdown responses unlike the heterogeneity observed in the in-situ weathered overburden in Wobulenzi is an indication of sorted, relatively homogeneous

formations associated with alluvial deposition. Groundwater flow in the aquifer has changed from radial to linear (Fig. 5.35) at a depth of approximately 22 metres below ground level. This corresponds to a change in flow dimension from 2 to 1 due to the rapid decline in groundwater storage over the last 8 years. The alluvial aquifer has high storage and this dominates groundwater flow at early pumping times resulting in delay in the linear response. Derivate analysis shows that aquifer/well storage evolves into linear flow after approximately 900 minutes of pumping.

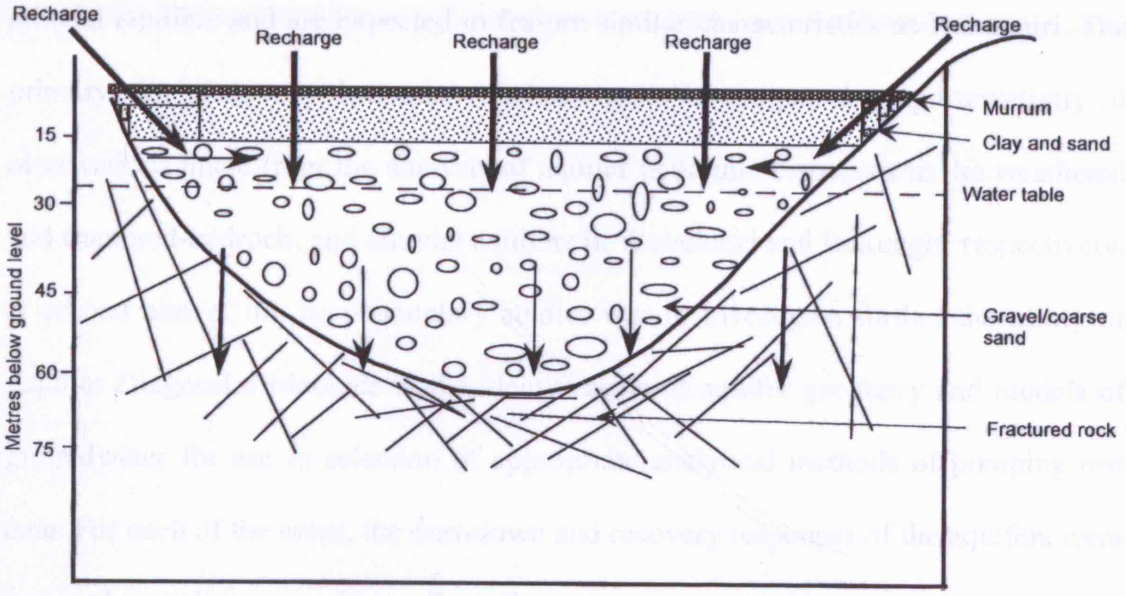

Figure 5.35. Conceptual model of groundwater flow in the alluvial aquifer in Rukungiri

5.6 Investigations into the representativeness of observations in Wobulenzi and Rukungiri

Supplementary studies were carried out in seven areas that have similar hydrogeological conditions as Wobulenzi and Rukungiri, underlain by weathered and fractured-bedrock, and alluvial aquifers respectively. Iganga, Aroca and Nyabisheki (Fig. 2.2 Chapter 2) are underlain by the weathered and fractured-bedrock aquifers and are therefore expected to feature similar characteristics as Wobulenzi whereas Ntungamo, Lukaya, Mubende and Hoima (Fig. 2.2 Chapter 2) are underlain by alluvial aquifers and are expected to feature similar characteristics as Rukungiri. The primary aim of the supplementary studies was to investigate the representativity of observations made from the analysis of aquifer hydraulic responses in the weathered and fractured-bedrock, and alluvial aquifers in Wobulenzi and Rukungiri respectively. A second aim of the supplementary studies was to investigate further the utility of Aquifer Diagnostic Methods in the identification of aquifer geometry and models of groundwater for use in selection of appropriate analytical methods of pumping test data. For each of the areas, the drawdown and recovery responses of the aquifers were assessed as well as groundwater flow dimension as presented in Appendix 4.

Results of supplementary studies highlight the representativeness of the analyses in Wobulenzi and Rukungiri. The applicability of these conceptual models is a significant advance in the understanding of this heterogeneous hydrogeological terrain. Water levels in weathered and fractured bedrock aquifers decline sharply during early and medium pumping times resulting in very big drawdowns, normally greater than 20 m after 72 hrs of pumping. The recovery responses are however much faster and full recovery is achieved in a few hrs, normally less than 3 hrs suggesting that sufficient storage exists in the weathered aquifer to recharge the deeper fractured

aquifer. Water levels in alluvial aquifers decline gradually during the whole test resulting in small drawdowns, normally less than 10 m after 72 hrs of pumping. The recovery is however poor and full recovery takes over 10 hrs to be achieved, if at all it is achieved, suggesting that the aquifers have poor storage. Groundwater flow dimension in the weathered and fractured bedrock aquifers is about 2. The flow dimension in alluvial aquifers is less than 2 and varies during the test and sometimes shows a declining trend from medium to late pumping times suggesting that the aquifer is dewatered as pumping proceeds. The actual value of D_f appears to depend on the duration of groundwater pumping in the aquifer and the extent of the alluvial formation. Extensive alluvial formations appear to exhibit D_f that is closer to 2 whereas alluvial formations of limited extent in which groundwater abstraction has been on-going for some years exhibit D_f closer to 1.

5.7 Determining hydraulic properties based on aquifer geometry and models of groundwater flow

5.7.1 Overview

Aquifer hydraulic properties (transmissivity and storage coefficient) derived from pumping test data analysis solutions without considering the appropriate aquifer geometry and models of groundwater flow can vary widely depending on the methods employed. Variations in aquifer hydraulic properties provide an indication of the potential errors associated with using analytical solutions without considering the aquifer geometry and the model of groundwater flow. The need to identify appropriate pumping test interpretation models becomes apparent when the hydraulic properties vary widely whereas the need is less apparent if the hydraulic properties show small variations. The variability in aquifer hydraulic properties determined

using different analytical methods has been demonstrated in Section 5.4 by comparison of estimates obtained through application of commonly used analytical models; Theis, Cooper- Jacob, Theis recovery, Hantush, Neuman and PTFIT program developed by Barker (2000). Information on aquifer geometry and model of groundwater flow derived from ADMs is used to select appropriate analytical methods for determining hydraulic properties for the aquifers in the two study areas.

5.7.2 Weathered and fractured-bedrock aquifers

5.7.2.1 Weathered aquifer

Aquifer Diagnostic Methods (ADMs) show that the weathered aquifer exhibits unconfined radial flow conditions that become uni-dimensional (vertical) at late pumping times due to induced downward gradient resulting from pumping in the fractured-bedrock aquifer. Interpretation of hydraulic test data from such an aquifer requires use of an unconfined aquifer analytical model that accounts for horizontal and vertical flow in the aquifer. Based on the assumptions of the various analytical solutions (Table 5.6), the solution that meets the above criteria is the Neuman method which accounts for radial horizontal permeability and vertical permeability in an unconfined aquifer. PTFIT with aquitard would have also been appropriate but it assumes that the flow in the weathered aquifer is only vertical which is contrary to radial flow conditions exhibited by the aquifer in Wobulenzi.

Detailed work in weathered and fractured-bedrock aquifers in India (Marechal *et al.,* 2003) demonstrates that when observed drawdowns are very small (<25%) compared to the aquifer thickness, the application of analytical solutions for confined aquifers to the unconfined aquifers is possible without introducing significant

inaccuracies. The studies found that the differences between the average values obtained by the confined and unconfined aquifer solutions for both specific yield and hydraulic conductivity were less than 30%. Based on the above observation and considering that the drawdowns in the weathered aquifer in Wobulenzi (average 0.86m) are very small (<10%) compared to the aquifer thickness (~22 m), unconfined aquifer properties can be estimated using confined aquifer analytical solutions. Thus, Theis and Cooper- Jacob methods were employed purely for purposes of comparing their estimates with those of Neuman method and for evaluating the assumptions made by Marechal *et al.* (2003).

Aquifer hydraulic properties determined using Theis, Cooper-Jacob and Neuman methods for the weathered aquifer are presented in Table 5.7. Transmissivity estimates for P1 are much lower than those for P2. The specific yield estimate from Cooper-Jacob method (0.14) is slightly lower than those from Theis and Hantush methods (0.18 and 0.21). The average transmissivity estimates for the weathered aquifer are 75, 99 and 66 m^2 d^{-1} for Theis, Cooper- Jacob and Neuman methods respectively whereas average specific yield estimates are 0.19, 0.11 and 0.16 for Theis, Cooper- Jacob and Neuman methods respectively. The average transmissivity estimates for the weathered aquifer are too high and estimates for P2 are anomalous. Transmissivity and specific yield estimates for P1 appear to be more reasonable as they are consistent with estimates from previous studies in Uganda (Taylor and Howard, 2000). Theis and Cooper-Jacob methods appear to overestimate transmissivity and underestimate specific yield. The transmissivity estimates from Neuman method are more consistent with estimates from similar environments (Chilton and Smith-Carington, 1984; Taylor and Howard, 2000) confirming that this method is the most appropriate for estimating aquifer hydraulic properties. The

estimated transmissivity values from previous studies in Uganda (Taylor and Howard, 2000; Taylor *et al.,* in prep) and Southern Africa (Chilton and Smith-Carington, 1984) for the weathered aquifer range between 5 and 20 m^2 d^{-1} whereas average specific yield values range between 0.18 and 0.23. The transmissivity and specific yield estimates for the weathered aquifer based on PI and obtained using the Neuman method are 16 m^2 d^{-1} and 0.21 respectively.

Table 5.7. Aquifer hydraulic properties obtained using appropriate solution methods for the weathered aquifer in Wobulenzi

Piezometer	Theis		Cooper - Jacob		Neuman	
	T (m^2 d^{-1})	S	T (m^2 d^{-1})	S	T (m^2 d^{-1})	S_y
P1	39	0.18	33	0.14	16	0.21
P2	112	0.19	165	0.07	115	0.10

5.7.2.2 Fractured-bedrock aquifer

ADMs show that the fractured-bedrock aquifer is heterogeneous but exhibits leaky aquifer conditions at late pumping times due to recharge from the overlying weathered aquifer. The aquifer exhibits a radial flow response with a flow dimension of 2. Interpretation of hydraulic test data from such an aquifer requires use of a confined aquifer analytical model that accounts for leakage from an overlying aquitard. Based on the assumptions of the various analytical solutions (Table 5.6), the Hantush method features a more realistic approach to interpretation of pumping test data from a leaky aquifer (Vandenbohede and Lebbe, 2003) but assumes a constant head in an overlying aquifer, which is inconsistent with the conceptual model of the fractured-bedrock aquifer in Wobulenzi. Although, Theis and Cooper-Jacob methods are confined aquifer solutions, they do not account for leakage and hence ignore flow

from adjacent semi-permeable layers (Marechal *et al.,* 2003; Vandenbohede and Lebbe, 2003). PTFIT5 with aquitard is not appropriate because it assumes that the flow in the overlying aquitard is only vertical whereas PTFIT5 without aquitard assumes that there is no aquitard. The drawdown due to pumping in an aquifer depends on the hydrogeological properties of the aquifer as well as the properties of the overlying layers (Marechal *et al.,* 2003; Vandenbohede and Lebbe, 2003). The estimated flow properties are therefore influenced by the amount of water that leaks from the overlying layers. Vandenbohede and Lebbe (2003) show that interpretation methods based on models that underestimate or neglect leakage towards a pumped permeable aquifer result in overestimation of horizontal conductivity of the aquifer. Thus, the Theis and Cooper-Jacob methods, and to some extent the Hantush method, tend to overestimate transmissivity of the leaky aquifer (Marechal *et al.,* 2003; Vandenbohede and Lebbe, 2003). The overestimation increases with distance from the pumping well. Vandenbohede and Lebbe (2003) show that drawdowns from observation wells at large distances from the pumping well will lead to larger transmissivity estimates derived from the Theis method than drawdowns from an observation well close to the pumping well. This implies that a large amount of leakage between the observation well and pumping well is ignored for an observation well located very far from the pumping well. Marechal *et al.* (2003) demonstrate, using data from the hard-rock terrain of India that classical techniques such as Theis and Cooper- Jacob methods cannot properly interpret drawdown data after 470 minutes of pumping. They subsequently employ the methods of Gringarten, Warren and Root, and Barker that account for the complex groundwater flow in fractured rocks to estimate aquifer parameters.

The above observations indicate that none of the methods employed in this study is appropriate for estimating hydraulic properties in the leaky fractured-bedrock aquifer of Wobulenzi. Although Theis, Cooper-Jacob and Hantush methods overestimate transmissivity values they are used to determine aquifer hydraulic properties (Table 5.8) because they are closest to the conceptual model of groundwater flow in the fractured-bedcrock aquifer in Wobulenzi but the results have to be used with caution. Transmissivity estimates derived from Theis and Cooper-Jacob methods for P3 and P4 are higher than those obtained using the Hantush method possibly because they completely ignore leakage. However, estimates of storage coefficient are similar for the three methods and are consistent with estimates obtained elsewhere in similar hydrogeological environments (Chilton and Smith-Carington, 1984; Taylor and Howard, 2000; Tindimugaya, 2000; Marechal *et al.,* 2003). The transmissivity estimates in the production borehole are much lower than those of the piezometers based on the Theis and Cooper-Jacob methods. The transmissivity estimate for the production borehole derived from Hantush method is however slightly higher than that for P4. Consistent with the observations that the overestimation of transmissivity by the Theis, Cooper-Jacob and Hantush methods increases with distance from the pumping well (Marechal *et al.,* 2003; Vandenbohede and Lebbe, 2003) the transmissivity estimates derived from all the 3 methods for P3 could be slightly overestimated due its greater distance from the production borehole. The average transmissivity estimates for the fractured-bedrock aquifer in Wobulenzi based on the Theis, Cooper- Jacob and Hantush methods are 29, 28 and 14 m^2 d^{-1} respectively whereas the average storage coefficient estimates are 0.004, 0.003 and 0.014 for the Theis, Cooper- Jacob and Hantush methods respectively. Transmissivity estimates derived from the Hantush method appear to be more realistic than those

derived from the Theis and Cooper-Jacob methods because the error in underestimation of leakage is lower than those from the Theis and Cooper-Jacob methods. Consistent with the above observations, the average transmissivity and specific yield estimates for the fractured-bedrock aquifer based on the Hantush method are are 14 $m^2 d^{-1}$ and 0.014 respectively.

Table 5.8. Aquifer hydraulic properties obtained using selected solution methods for the fractured-bedrock aquifer in Wobulenzi

Piezometer	Theis		Cooper - Jacob		Hantush	
	T ($m^2 d^{-1}$)	S	T ($m^2 d^{-1}$)	S	T ($m^2 d^{-1}$)	S
P3	58	0.0040	52	0.003	32	0.004
P4	26	0.0038	24	0.003	4.1	0.004
PW	3.4		7.5	0.012	5.8	0.036

Previous studies in fractured-bedrock aquifers in sub-Saharan Africa (Chilton and Smith-Carington, 1984, Taylor and Howard, 2000, Tindimugaya, 2000) show that transmissivity estimates for the fractured-bedrock aquifer are less than 1 $m^2 d^{-1}$ unless there are local high permeability features that serve to increase the transmissivity of the aquifer. Thus, the transmissivity estimates for the fractured-bedrock aquifer at the study site in Wobulenzi are much higher than average values for this aquifer and indicate presence of highly conductive fractures tapped by the production boreholes. Transmissivity estimates from 19 boreholes in Wobulenzi show that 47% of the boreholes have values greater than 1 $m^2 d^{-1}$ and are all found near the site where the current study has been carried out confirming that the higher estimates than average are due to presence of local high conductivity features (Tindimugaya, 2000). Storage coefficient values obtained else where in similar geological environments (Chilton and Smith-Carington, 1984, Taylor and Howard, 2000) range between 0.003 and 0.03.

The average storage coefficient values for the weathered aquifer in Wobulenzi are therefore slightly higher than estimates obtained else where.

5.7.3 Alluvial aquifers

Aquifer Diagnostic Methods (ADM) show that the aquifer in Rukungiri is unconfined, unconsolidated, homogeneous, highly permeable, limited in extent and exhibits linear flow characteristics. Interpretation of hydraulic test data from such an aquifer requires use of an unconfined aquifer analytical model that accounts for linear flow conditions due to the limited extent of the aquifer. Based on the assumptions of the various analytical solutions (Table 5.6) none of the commonly used solutions meets the above criteria because they are all based on the Theis theory. Although the Neuman method is an unconfined aquifer solution, it assumes that the aquifer is of infinite extent which is inconsistent with the conceptual model of the alluvial aquifer in Rukungiri.

If the commonly used methods are employed, the drawdowns due to pumping will be greater than those that would be predicted on the basis of Theis equation for an aquifer of infinite areal extent (Rushton, 2003; Freeze and Cherry, 1979). Use of an image well approach to interpret data from aquifers of limited extent (Freeze and Cherry, 1979; Kruseman and de Ridder, 2000; Rushton, 2003) can help to resolve the problems encountered using solutions based on the Theis theory. The image well approach is based on the principal of superposition, where image wells are introduced to transform an aquifer of finite extent into one of infinite extent and allow interpretation of the data using standard pumping test analysis methods (Kruseman and de Ridder, 2000; Freeze and Cherry, 1979).

According to the principle of superposition, the drawdown caused by two or more wells is the sum of the drawdown caused by each separate well. A recharge

(constant head) boundary is represented by an imaginary recharge well positioned at an equal distance beyond the boundary as the actual well and thus recharges the aquifer at a constant rate equal to the constant discharge of the real well. An impermeable (no flow) boundary is represented by an imaginary abstraction well which is positioned at an equal distance beyond the boundary as with the actual abstraction well (Kruseman and de Ridder, 2000). This enables the bounded system to be replaced with an equivalent system of infinite areal extent (Kruseman and de Ridder, 2000; Freeze and Cherry, 1979). The imaginary system has two wells, one real and another imaginary both discharging at the same constant rate. The image well induces a hydraulic gradient from the boundary towards the image well which is equal to the hydraulic gradient from the boundary towards the real well. The resultant real cone of depression is the sum of the depression cones of both the real and image well. Further details of this approach are presented in Kruseman and de Ridder (2000).

Through use of Wellbound program developed by Barker (2006), the Theis method was used to analyze the pumping test data after introduction of an impermeable boundary and images to transforms the aquifer from finite to infinite extent. The generated Theis plots are presented in Appendix 5 whereas the estimated aquifer properties are presented in Table 5.9.

Table 5.9. Aquifer hydraulic properties obtained using Theis method with and without boundaries for the alluvial aquifer in Rukungiri

Piezometer	T ($m^2 d^{-1}$)		S	
	Without boundary	With boundary	Without boundary	With boundary
P1	31	30	0.010	0.011
P2	26	25	0.012	0.012
P3	17	18	0.020	0.018
P4	29	30	0.040	0.035
P5	27	26	0.042	0.041
P7	25	24	0.005	0.005
P8	28	29	0.004	0.004
Ruk 8	40	39	-	-

The results of the analysis show that hydraulic properties derived from the image well approach using Theis Method are similar to those generated without the introduction of a boundary. The results suggest that the Theis theory can be used to interpret data from the alluvial aquifer in Rukungiri even though the aquifer is of limited extent. These findings suggest that despite the fact that some assumptions on which the various analytical methods are based are not met, these methods may still be used depending on the degree to which the various assumptions are violated. The appropriate analytical methods for estimating aquifer hydraulic properties in an alluvial aquifer could thus be selected based on aquifer geometry. For interpretation of pumping test data for the alluvial aquifer in Rukungiri the appropriate method is the Neuman which is an unconfined aquifer solution. However, as discussed earlier, when the observed drawdowns are very small compared to the aquifer thickness, the application of analytical solutions for a confined aquifer to the unconfined aquifer is possible without introducing significant inaccuracies (Marechal *et al.,* 2003). Since

the drawdowns in the alluvial aquifer in Rukungiri are very small (<10%) compared to the aquifer thickness confined aquifer analytical solutions (Theis and Cooper-Jacob) were used to estimate aquifer properties for the alluvial aquifer for purposes of comparison with Neuman method. The aquifer hydraulic properties derived from Theis, Cooper-Jacob and Neuman methods are presented in Table 5.10.

Table 5.10.Aquifer hydraulic properties obtained using appropriate analytical solutions methods for the alluvial aquifer in Rukungiri

Piezometer	Theis		Cooper - Jacob		Neuman	
	T ($m^2 d^{-1}$)	S	T ($m^2 d^{-1}$)	S	T ($m^2 d^{-1}$)	S
P1	31	0.010	29	0.0037	41	0.1
P2	26	0.012	29	0.0039	31	0.1
P3	17	0.020	29	0.0043	23	0.1
P4	29	0.040	29	0.0155	36	0.1
P5	27	0.042	29	0.0149	34	0.1
P7	25	0.005	29	0.0014	39	0.1
P8	28	0.004	29	0.0017	33	0.1
Ruk 8	40		13	0.001	-	-

Transmissivity estimates derived from Theis, Cooper-Jacob and Neuman methods are fairly similar although estimates from Neuman are slightly higher in all piezometers except P3. The average transmissivity estimates are 26, 29 and 34 $m^2 d^{-1}$ for Theis, Cooper- Jacob and Neuman respectively whereas average storage coefficient estimates are 0.019, 0.006 and 0.1 for Theis, Cooper- Jacob and Neuman respectively. The variations in the transmissivity estimates from the 3 methods are small but there is wide variation in estimates of storage coefficient. Consistent with the findings of ADMs, the average transmissivity and storage coefficient for the alluvial aquifer in Rukungiri have been estimated based on Newman method and are

34 m^2 d^{-1} and 0.1 respectively. The relatively lower storage coefficient values for the alluvial aquifer compared to those for the weathered aquifer suggest that the alluvial aquifer has lower drainage porosity. This is consistent with the high water level fluctuations in Rukungiri as a result of abstraction (20 m in 8 years). Low storage coefficient values (S_y = 5 x 10^{-3}) were also observed by Marechal *et al.* (2003) in a low drainage porosity unconfined aquifer in the weathered-fractured hard rocks of India.

5.8 Conclusions

This chapter has assessed aquifer geometry and models of groundwater flow in weathered crystalline rocks of Uganda, using Aquifer Diagnostic Methods, resulting in development of conceptual models of the weathered and fractured aquifer, and alluvial aquifer in Wobulenzi and Rukungiri towns respectively. The conceptual models have been used to select appropriate pumping test analysis solutions and to evaluate estimates of aquifer hydraulic properties. The conclusions of this chapter are discussed in the following sections.

5.8.1 Aquifer geometry and models of groundwater flow

Results of this study indicate that the weathered aquifer is unconfined whereas the fractured-bedrock aquifer is leaky and the two aquifers form a heterogeneous aquifer system. Groundwater flow in the fractured-bedrock aquifer is fairly complex but is generally linear at early pumping times and evolves to radial flow at pumping periods ranging between 600 and 1500 minutes whereas leakage from the overlying aquifer occurs after 1800 minutes of pumping. Similarly, groundwater flow in the weathered aquifer changes from linear through radial and finally becomes uni-dimensional after approximately 1800 to 2400 minutes of pumping, as a result of

induced downward gradient due to pumping in the fractured-bedrock aquifer. The evolution of the various flow mechanisms in the weathered and fractured-bedrock aquifer units are similar confirming that the two units are hydraulically connected and form one aquifer system with a flow dimension of 2.

The results further show that the alluvial aquifer in Rukungiri is unconfined, highly permeable and relatively homogeneous due to well sorted sediments associated with fluvial deposition. Groundwater flow in the fluvial aquifer has changed from radial to linear at a depth of 22 metres below ground level with a corresponding change of flow geometry from 2 to 1 due to the rapid decline in groundwater storage over the last 8 years.

The representativeness and applicability of these conceptual models has been verified though supplementary but limited studies in seven areas underlain by similar geological conditions. The results suggest that weathered and fractured-bedrock aquifers are characterised by large and sharp water level declines (normally >20 m after 72 hrs of pumping) and very fast recovery (full recovery normally in less than 3 hrs). Fast recovery is due to high storage in the weathered aquifer that recharges the deeper fractured-bedrock aquifer. Similarly, fluvial aquifers are characterised by small and gradual water level declines (normally less than 10 m after 72 hrs of pumping) and very slow recovery (full recovery normally achieved after over 10 hrs if at all it is achieved). Slow recovery is characteristic of low aquifer storage characteristics. Weathered and fractured-bedrock aquifers exhibit radial flow conditions with a flow dimension of 2 whereas the fluvial aquifer may exhibit radial flow conditions that gradually change to linear flow as the pumping proceeds due to dewatering of the aquifer and possibly due to reduction in the extent of the aquifer.

The flow dimension of the fluvial aquifer thus also changes from 2 to 1 as a result of dewatering and reduction in the extent of the aquifer.

5.8.2 Usefulness of ADM

Four ADMs (s versus t/r^2, log-log and semi-log plots, derivative and flow dimension) have been used together for the first time in sub-Saharan Africa to investigate the characteristics of weathered crystalline rocks. The ADMs have made it possible to assess aquifer geometry and models of groundwater in weathered, fractured-bedrock and alluvial aquifers of Uganda and to guide interpretation of pumping test data. The most useful and easy to use method is the log-log and semi-log plots as the comparison of the plots makes it possible to quickly diagnose the aquifer and obtain information on aquifer geometry and models of groundwater flow. The flow dimension plot method is particularly useful in differentiating between radial and linear flow although interpretation of the meaning of the obtained flow dimension may not be straight forward. The derivate plot method is quite diagnostic but is very sensitive to fluctuations in drawdown making it difficult to identify some characteristics of the aquifer. Plots of s versus t/r^2 are useful in identifying heterogeneity of the aquifer but can only be used where there are more than one piezometer. Use of aquifer diagnostic methods is therefore essential in characterizing aquifers and guiding appropriate analysis and interpretation of hydraulic test data for sustainable groundwater development and management.

5.8.3 Aquifer hydraulic properties

Seven commonly used analytical models (Theis, Cooper- Jacob, Theis recovery, Hantush, Neuman and PTFIT program) were employed to estimate aquifer hydraulic properties in order to assess the errors inherent in interpreting pumping test

data without knowledge of aquifer geometry and models of groundwater flow. The aquifer hydraulic properties estimated from the seven methods were highly variable for the weathered and fractured-bedrock aquifers but relatively consistent for the alluvial aquifer. The results suggest that available analytical solutions can be used to interpret pumping-test data from fairly homogeneous alluvial aquifers without introducing significant errors in the estimates. The results further indicate that the determined hydraulic properties of the weathered and fractured-bedrock aquifers are sensitive to the employed model. Using the appropriate analytical solution selected based on ADMs, the average transmissivity and storage coefficient values for the weathered aquifer in Wobulenzi are 16 m^2 d^{-1} and 0.21 respectively. The average transmissivity and storage coefficient values for the fractured-bedrock aquifer in Wobulenzi are 14 m^2 d^{-1} and 0.014 whereas the average transmissivity and storage coefficient values for the alluvial aquifer in Rukungiri are 34 m^2 d^{-1} and 0.1 respecitively. The results suggest that the commonly used analysis solutions for confined and leaky aquifer conditions (Theis, Cooper-Jacob and Hantush methods) overestimate transmissivity values for the leaky fractured-bedrock aquifer because they underestimate leakage from overlying layers. The inapplicability of these methods to the complex groundwater flow conditions in fractured-bedrock aquifers that has also been observed in fractured rocks of India imply that more appropriate methods are required for interpretation of data from such aquifers. The results further show that despite the fact that some assumptions on which the various pumping test analytical solutions are based are not met, the methods can still be employed to generate good estimates of aquifer hydraulic properties depending on the degree to which the various assumptions are violated. This assessment is possible though use of ADMs.

CHAPTER 6: ENVIRONMENTAL TRACERS AS INDICATORS OF RESIDENCE TIME

This chapter employs anthropogenic CFC gases (CFC-113, CFC-11, CFC-12) and tritium to assess groundwater flow, mixing and residence times in the weathered and fractured-bedrock, and alluvial aquifers in Uganda. The study represents the first application of CFCs in the humid tropics of Uganda and required the reconstruction of historical atmospheric input functions for CFCs and tritium in Uganda. The distribution of these environmental tracers in groundwater is considered using piston-flow, binary mixing and exponential models. Tritium is used to provide an independent test of groundwater residence times derived from CFCs.

6.1 Introduction to residence time indicators

6.1.1 Overview

Over the last few decades, use of environmental tracers to understand physical processes that affect movement of water and to determine residence time of water in various hydrological environments has greatly increased (Shapiro, *et al.*, 1997; Alley, *et al.*, 2002; Plummer, 2004). Environmental tracers are natural or anthropogenic compounds including isotopes that are widely distributed in the near-surface environment of the earth. Variations in their abundances can therefore be used to determine pathways and timescales of environmental processes (Plummer and Busenburg, 1999; Clark and Fritz, 1997; Cook and Bohlke, 2000). The period of time spent by groundwater between its entry to the water table, and exit from, an aquifer is called the 'residence time'.

Residence-time indicators such as chlorofluorocarbons (CFCs) and tritium (^3H) have been used in a number of studies to determine fractions of young components in groundwater, to estimate mean groundwater residence times and to constrain hydrological models of groundwater systems (e.g. Amin and Campana, 1996; Cook *et al.*, 2003; Zuber *et al.*, 2004; Viville *et al.*, 2006). Knowledge of transit times of groundwater, also sometimes called "age of groundwater", is essential to understanding the movement of groundwater and pollutants as well as evaluating vulnerability of groundwater systems to pollution. Residence-time indicators can provide both quantitative and qualitative information on hydrological systems and processes (IAEA, 2006; Viville *et al.*, 2006).

"Modern" groundwaters are often considered to be those recharged within the past few decades and as such, are part of an active hydrological system (Cook, *et al.*, 1995; Clark and Fritz, 1997). Though classical hydrogeological methods often provide the best indication of whether groundwater is actively recharged, environmental tracers are used when such hydrogeological information is ambiguous and more importantly, to constrain the age of recently recharged water. Tritium, for example, can be used to provide information on groundwater recharge and vulnerability of the aquifers to pollution (IAEA, 2006). Presence of tritium above a certain detectable concentration in a groundwater sample reflects the contribution of a component of modern recharge. If the occurrence of groundwater recharge is questionable, tritium can act as a qualitative indicator of recent replenishment. Tritium data can also contribute to an assessment of vulnerability of groundwater to pollution since high tritium concentrations indicate recent recharge and, hence, the vulnerability of the aquifer to pollution. Information about water

transit time and storage capacity of groundwater systems can also be obtained from tracers using various interpretation models based on the decay of radioactive tracers or concentrations of conservative tracers such as CFCs. Application of environmental tracers requires knowledge of the historical input function of each tracer to the atmosphere (Cook *et al.,* 1995; Alley *et al.,* 2002) which can then be correlated to measured tracer concentrations in water. The 'age' of groundwater can be misleading (Clark and Fritz, 1997; Alley *et al.,* 2002) for two reasons: (i) dating methods apart from tritium rely on dissolved constituents whose abundance in water is controlled by physicochemical and biological processes; and (ii) hydrodynamic mixing and convergence of groundwater flow paths may integrate a variety of recharge origins and ages. Thus, groundwater dating aims to constrain "mean residence time" (MRT) of groundwater rather than assign a particular "age". Constraining groundwater residence times is best achieved through use of a multi-tracer approach as demonstrated in this study of weathered crystalline rocks of Uganda.

6.1.2 Chlorofluorocarbons (CFC)

CFCs are excellent tracers of recently recharged groundwater (i.e., less than 50 years old) (Cook *et al.*, 1995; Plummer and Busenberg, 1999). Chlorofluorocarbons (CFCs) are stable, synthetic halogenated alkanes that were developed from the early 1930s as safe alternatives to ammonia and sulphur dioxide in refrigeration (Plummer and Busenberg, 1999). Large-scale "industrial" production of CFC-12 (dichlorodifluoromethane, CCl_2F_2) began in 1931 followed by CFC-11 (trichlorofluoromethane, CCl_3F) in 1936. Many other CFC compounds have since been

produced, most notably CFC-113 (trichlorotrifluoroethane, CCl_2FCClF_2) in 1961. Atmospheric concentrations of these three CFCs have increased since the 1930s but peaked in the late 1980s. No actual measurements of CFCs in the atmosphere are available before those of Lovelock (1971) but reconstruction of atmospheric concentrations have been made using industrial production and emission records for each compound in conjunction with their atmospheric residence times (Walker *et al.*, 2000).

Release of CFCs to the atmosphere and subsequent incorporation into the hydrologic system closely follows production (Plummer and Busenberg, 1999; Walker *et al.*, 2000). Production and release of CFCs to the atmosphere rose rapidly through the 1970s and 1980s and annual production of CFC-11 and CFC-12 peaked in 1987 and that of CFC-113 peaked in 1989. Release of CFC to the atmosphere started reducing from 1987 (Plummer and Busenberg, 1999, Walker *et al.*, 2000) when the Montreal Protocol on substances that deplete the ozone layer was signed by 37 nations. The protocol restricted the release of CFCs and sought to halve CFC emissions by the year 2000.

Using CFC measurements at 3 stations in both the northern and southern hemispheres (Tuluila in American Samoa, Cape Grim in Tasmania, Australia and Niwot Ridge in Colorado, USA), Plummer and Busenberg (1999) found that the mixing ratios in the southern hemisphere lag slightly behind those of the northern hemisphere. Walker *et al.* (2000) confirmed the observed lag using CFC measurements for 3 stations (Mace Head, Ireland; California, USA; Cape Grim, Tasmania). The tropics were excluded in their work since these latitudes are periodically subjected to air masses originating in the northern and southern hemispheres. The observed lag in CFC mixing ratios between the northern and southern hemispheres is due to the proportionately greater release of CFCs

to the troposphere in the northern hemisphere (Plummer and Busenberg, 1999). Although hemispheric gradients have started diminishing, Plummer and Busenberg (1999) and Walker *et al.* (2000) suggest that groundwater dating using CFCs in other parts of the world and especially the southern hemisphere requires reconstruction of the historical mixing ratios.

Estimation of groundwater residence times using CFC-11, CFC-12 and CFC-113 is possible because: the atmospheric mixing ratios of these compounds are known or have been reconstructed over the past 50 years; the solubilities of these gases in water are known; and the concentrations of CFCs in air and young water are measurable. If CFC concentrations of natural groundwater are solely of atmospheric origin, the absolute CFC concentrations in groundwater can, in principle, be used to indicate the time of isolation of the water from the atmosphere. In practice, there are several complicating factors which are discussed below in relation to new datasets compiled in Uganda.

6.1.3 Tritium

Tritium is a radioactive isotope of hydrogen (^3H), with a half-life of 12.43 years (IAEA, 2004) that is produced naturally by cosmic radiation. The tritium unit (TU) is the unit of measure of tritium in water and represents 1 tritium atom in 10^{18} hydrogen atoms. In SI units, one TU is about 0.118 Bequerels per liter (Bq/L), where the Bequerel is one decay per second. Prior to the release of a large pulse of ^3H into the atmosphere as a result of thermonuclear bomb testing mainly in the northern hemisphere from 1952 to the early 1960s, tritium was generated in very small quantities naturally. The tritium content of precipitation prior to the 'bomb pulse' is estimated to have been in the range of 2 to 8 TU (Kendall and Mcdonnel, 1998). Since 1952, tritium produced by thermonuclear

testing ("bomb tritium") has been the dominant source of tritium in precipitation. A peak concentration of over 5000 TU was recorded in early 1963 at Ottawa, Canada, in the northern hemisphere (IAEA, 2004). In the southern hemisphere, the magnitude of the bomb pulse was much smaller and there was a time lag in its appearance. For example, the peak ^{3}H concentration in rainfall recorded in Entebbe, situated close to the equator, was 290 TU in June 1963 (Fig. 6.1). Following cessation of atmospheric testing in 1963, tritium concentrations in precipitation declined through radioactive decay. By the 1990s most of the "bomb" tritium had been washed from the atmosphere and tritium concentrations in precipitation are close to natural levels in areas unaffected by continued radioactive fall-out.

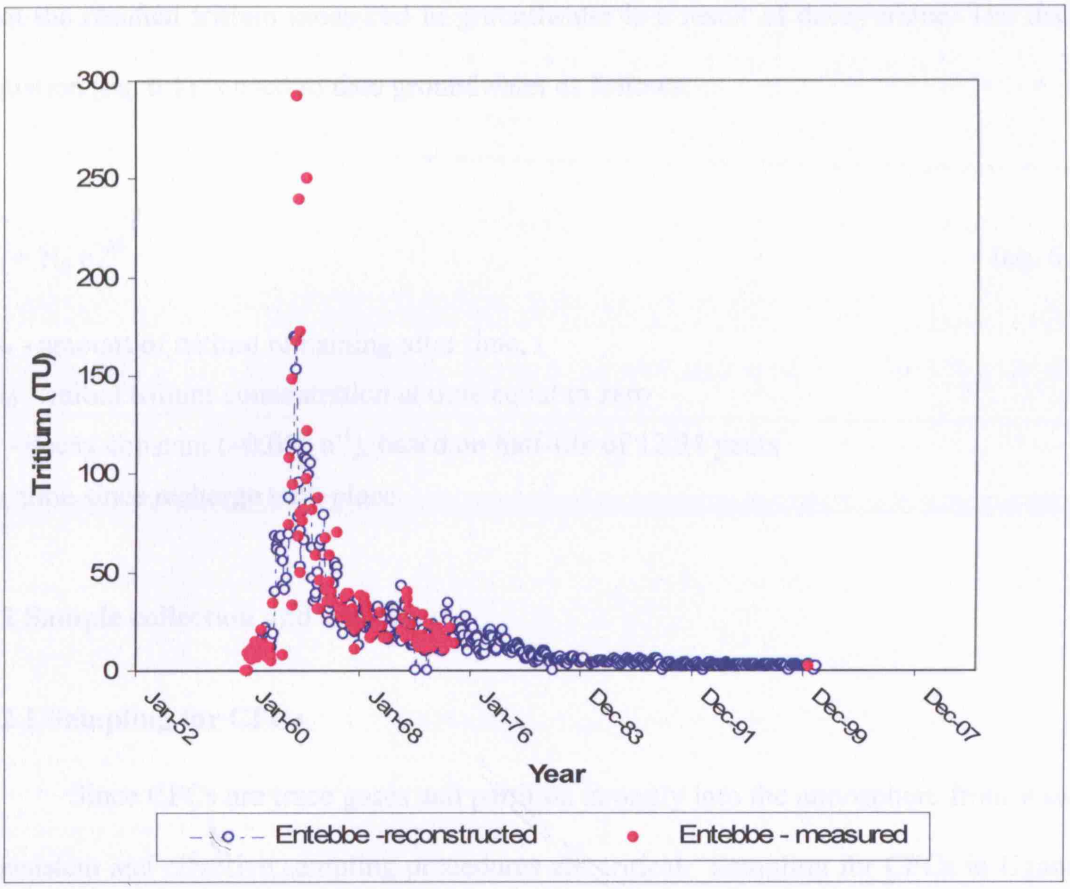

Figure 6.1. Measured and reconstructed tritium input function at Entebbe (0°N, 32°E)

Tritium concentrations in precipitation have been measured at a number of stations in the world since 1950s under the Global Network of Isotopes in Precipitation (GNIP) that is operated and maintained jointly by the International Atomic Energy Agency (IAEA) and the World Meteorological Organization (WMO). These datasets are widely used as reference values for determining the source concentrations of groundwater recharge (Celle-Jeanton *et al.*, 2001). Dating of groundwater by first-order decay of tritium is based on the assumption that the tritium input into groundwater is known and

that the residual tritium measured in groundwater is a result of decay alone. The decay equation (eq. 6.1) is used to date groundwater as follows:

$$N_t = N_0 e^{-\lambda t} \qquad \text{(eq. 6.1)}$$

N_t - amount of tritium remaining after time, t
N_0 - initial tritium concentration at time equal to zero
λ - decay constant (–0.056 a^{-1}), based on half-life of 12.34 years
t - time since recharge took place

6.2 Sample collection and analysis

6.2.1 Sampling for CFCs

Since CFCs are trace gases and partition strongly into the atmosphere from water, consistent and effective sampling procedures are critical. Sampling for CFCs in Uganda followed a technique developed at the IAEA Isotope Hydrology Laboratory (Groening *et al.*, 2004). A water sample is collected in a 50 ml glass bottle fitted with a metal foil-lined cap. An empty glass bottle is put in a metal container and the water for sampling is introduced directly to the bottom of the glass bottle (Fig. 6.2). The bottle is filled with water until it overflows. The bottle continues to overflow until the metal container overflows. While flushing the bottle with at least 2 litres of water the cap is filled with water in order to remove air bubbles underwater. The cap is loosely inserted in the cap holder and positioned close to the bottle so that it is rinsed with the overflowing water from the bottle. In this manner, the inner surface of the glass bottle and the cap are rinsed with plenty of water to remove any adsorbed CFCs derived from the atmosphere before

sampling. After this flushing period, the glass bottle is sealed underwater. The metal foil cap liner provides a tight seal and any CFCs initially adsorbed on the metal surface can be easily washed away by water.

Modifications to the usual sampling protocol had to be made at locations where sampled wells have handpumps. A stop cork with a delivery tube was fitted on the spout of the borehole and the water flowed through the tube into a bucket. The tube however led water through three copper outlets before finally pouring in the bucket. CFC sampling bottles were fitted on the three copper outlets and continuously filled with water until all the air bubbles were eliminated. The bottles were corked while within the water to avoid atmospheric CFC contamination. Three samples per source were collected in order to check reproducibility of results. Thirteen sources were sampled for CFC analysis in the River Kigwe catchment and nine in the Mitano catchment.

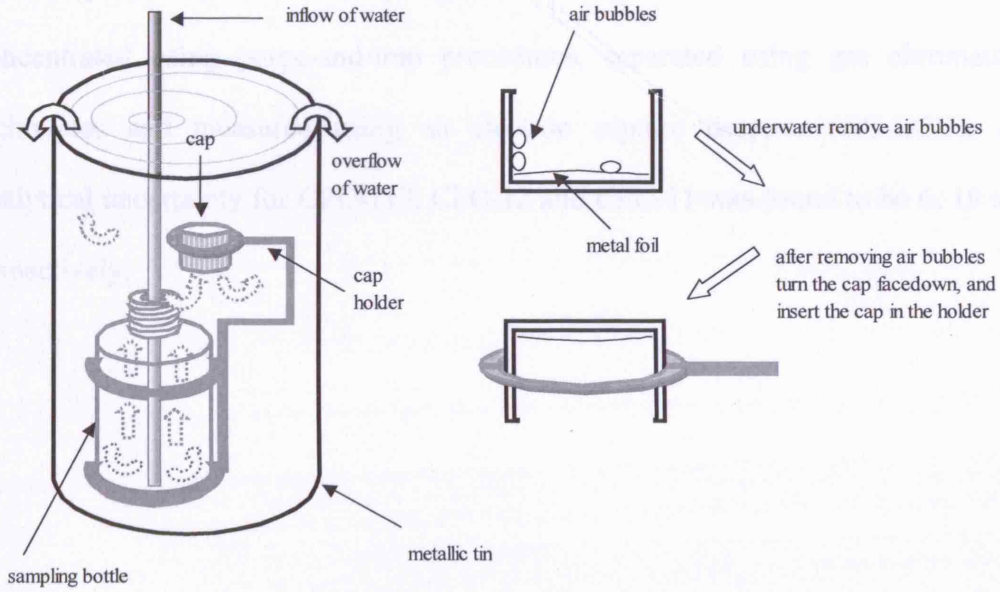

Figure 6.2. Apparatus for collecting CFC samples (Groening *et al.*, 2004)

6.2.2 Sampling for Tritium

As several groundwater sampling sites are boreholes fitted with handpumps, samples were collected after extended periods of pumping when wellhead parameters such as pH, electrical conductivity, and temperature had stabilized. Once the wellhead parameters stabilised, it was assumed that the water was drawn directly from the aquifer. Samples for tritium analysis were collected in 500 ml bottles. Fifteen sources were sampled for tritium analysis in the River Kigwe catchment and twelve in the Mitano catchment.

6.2.3 Sample analysis and analytical details

Samples for tritium were analyzed at the Schonland Research Center Isotope Laboratory in South Africa using the Liquid Scintillation Counting method after pre-concentration by electrolysis. Samples for CFCs were analyzed at the IAEA isotope laboratory in Vienna. In analyzing water samples for CFCs, the CFCs are pre-concentrated using purge-and-trap procedures, separated using gas chromatographic techniques and measured using an electron capture detector (GC-ECD). Average analytical uncertainty for CFC-113, CFC-12 and CFC-11 was found to be 6, 10 and 13% respectively.

6.3 Reconstruction of tracer input functions

6.3.1 CFC mixing ratios in global atmosphere and rainfall-fed recharge in Uganda

Atmospheric concentrations of CFCs over time were reviewed at three stations over a range in latitudes: Tasmania (41°S, 145°E), Ireland (53°N, 10°W) and Barbados (13°N, 59°W). The aim of the review was two-fold: (1) to investigate the suggestion that CFC mixing ratios in the southern hemisphere lag behind those of northern hemisphere (Plummer and Busenberg, 2000; Walker *et al.* 2000); and (2) to select the most appropriate monitoring station for use in the reconstruction of atmospheric CFC concentrations in Uganda. Consistency among all the stations in atmospheric CFC concentrations (< 5 % difference) despite preferential release of CFCs to the troposphere in the northern hemisphere (Fig. 6.3), implies very rapid tropospheric mixing of gases. Very close agreement in atmospheric CFC concentrations is observed in recent years (since 1990) for all three species whereas for earlier decades, when CFC levels were rising rapidly, there was a lag between hemispheres of approximately 1 year. The Barbados station in the northern tropics had values closest to those in Ireland, in the Northern hemisphere mid-latitudes. The observations confirm that differences in CFC mixing ratios between the southern and northern hemispheres have greatly diminished and the CFC mixing ratios in the tropics are similar to those in the mid-latitudes. Thus, atmospheric CFC measurements at any of the stations can be used in this study as long as appropriate temperatures are used to calculate the partitioning of anthropogenic gases between air and water following Henry's Law.

a)

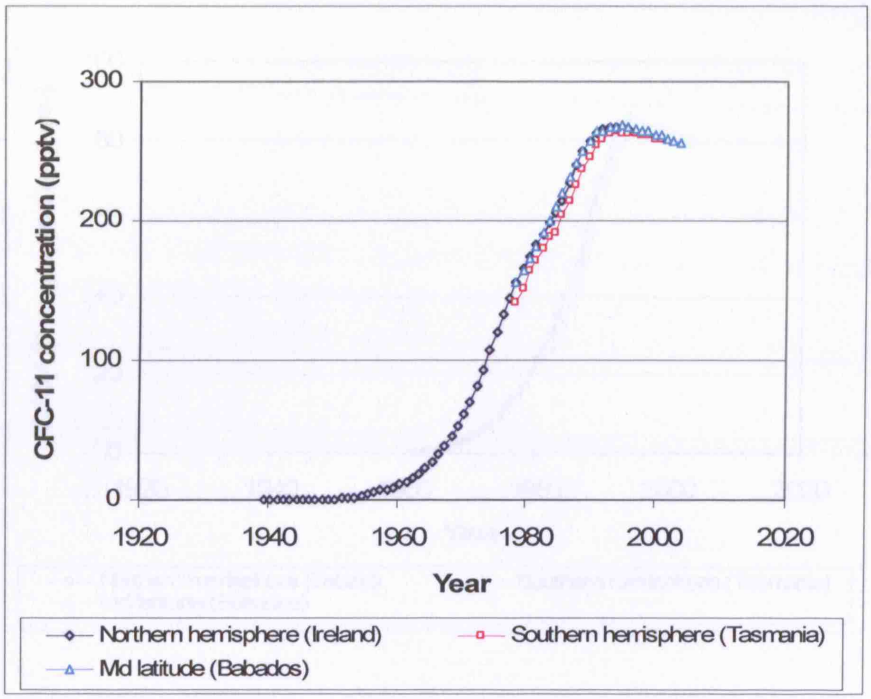
CFC-11 concentration (pptv)
300
200
100
0
1920
1940
1960
1980
2000
2020
Year
Northern hemisphere (Ireland)
Southern hemisphere (Tasmania)
Md latitude (Babados)

b)

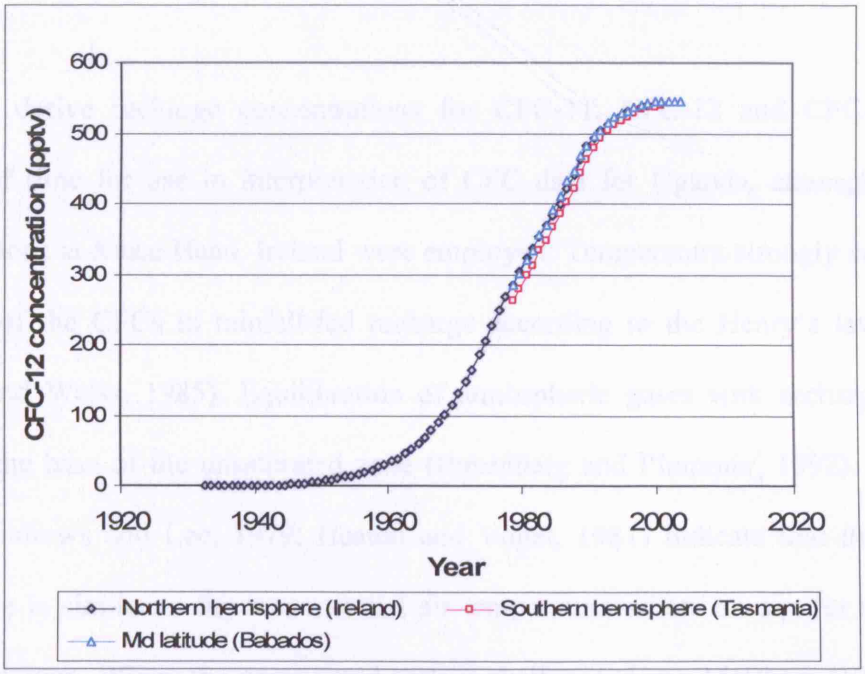
CFC-12 concentration (pptv)
600
500
400
300
200
100
0
1920
1940
1960
1980
2000
2020
Year
Northern hemisphere (Ireland)
Southern hemisphere (Tasmania)
Md latitude (Babados)

c)

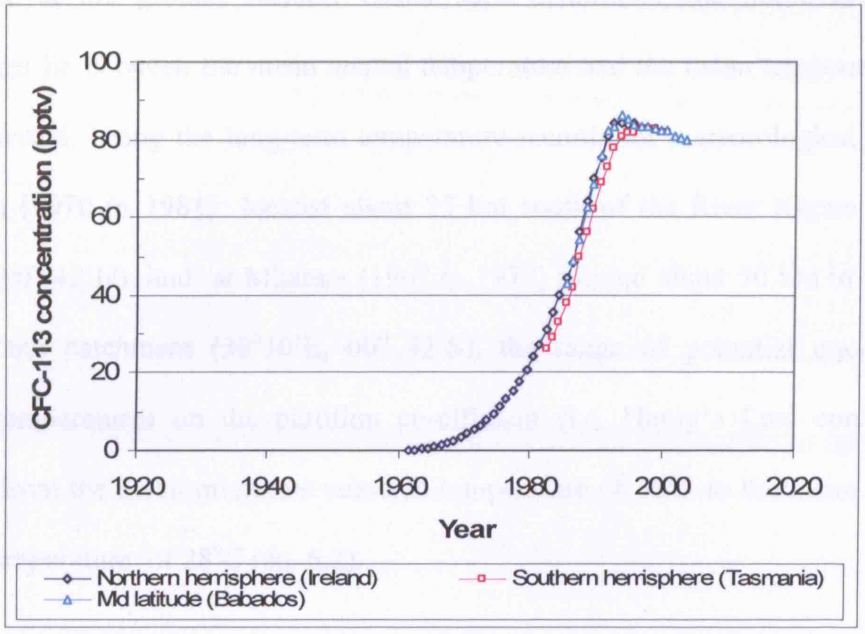

Figure 6.3. Atmospheric CFC concentrations observed at stations in Ireland, Barbados and Tasmania for a) CFC – 11, b) CFC – 12 and c) CFC-113

To derive recharge concentrations for CFC-11, CFC-12 and CFC-113 as a function of time for use in interpretation of CFC data for Uganda, atmospheric CFC concentrations at Mace Head, Ireland were employed. Temperature strongly controls the solubility of the CFCs in rainfall-fed recharge according to the Henry's law constant (Warner and Weiss, 1985). Equilibration of atmospheric gases with recharging water occurs at the base of the unsaturated zone (Busenberg and Plummer, 1992). Noble gas studies (Andrews and Lee, 1979; Heaton and Vogel, 1981) indicate that the recharge temperature is similar to the mean annual air temperature where an aquifer has a thick unsaturated zone. Where the unsaturated zone is shallow (<1 m), Matthess (1982) argues

that the temperature just above the water table responds to seasonal variations in air temperature at the ground surface. Under such conditions, the noble gas recharge temperatures lie between the mean annual temperature and the mean temperature of the recharge period. Using the long-term temperature records for meteorological stations at Kabanyolo (1970 to 1981) located about 25 km south of the River Kigwe catchment (32°30'E, 00° 42'N) and at Mbarara (1967 to 1977) located about 50 km to the east of River Mitano catchment (30°30'E, 00° 32'S), the range of potential uncertainty in recharge temperatures on the partition co-efficient (i.e. Henry's Law constant) was evaluated from the mean minimum seasonal temperature of 18°C to the mean maximum seasonal temperature of 28°C (eq. 6.2).

$$\ln K_{CFC} = a_1 + a_2(\frac{100}{T}) + a_3 \ln \frac{T}{100} \qquad \text{(eq. 6.2)}$$

K_{CFC}: Henry's law constant (mol kg^{-1} atm^{-1}) for a particular CFC gas
T: equilibrium temperature (degree Kelvin)
a_1, a_2, a_3: constants for CFC-11, CFC-12, and CFC-113

Table 6.1. Constants for calculation of Henry's law constant (Warner and Weiss, 1985)

	CFC-11	CFC-12	CFC-113
a_1	-136.269	-124.440	-136.243
a_2	206.115	185.430	206.475
a_3	57.281	51.638	55.8957

The Henry's law constant for CFC-11 is significantly more sensitive to changes in temperature relative to CFC-12 and CFC-113 (Fig. 6.4). For the range of recharge temperatures that occur in the tropics (> 18°C), the variation in Henry's law constant is low compared with the temperature effects in the temperate regions, particularly for CFC-113 and CFC-12. Taylor and Howard (1999) use stable isotope tracers (δ^2H, $\delta^{18}O$) and soil-moisture balance modelling to show that recharge under seasonally humid tropical conditions in Uganda occurs primarily during heavy (>10mm d^{-1}) rain events. Consequently, a slight bias toward colder air temperatures during heavy rainfall events might be expected but this makes <5 % difference to CFC input functions, especially for CFC-113 and CFC-12. Since the groundwater tables in the study areas are generally deeper than 10 m, the recharge temperature was assumed to be similar to the mean annual air temperature of 24°C, as considered elsewhere in the literature (Talma and Weaver, 2003).

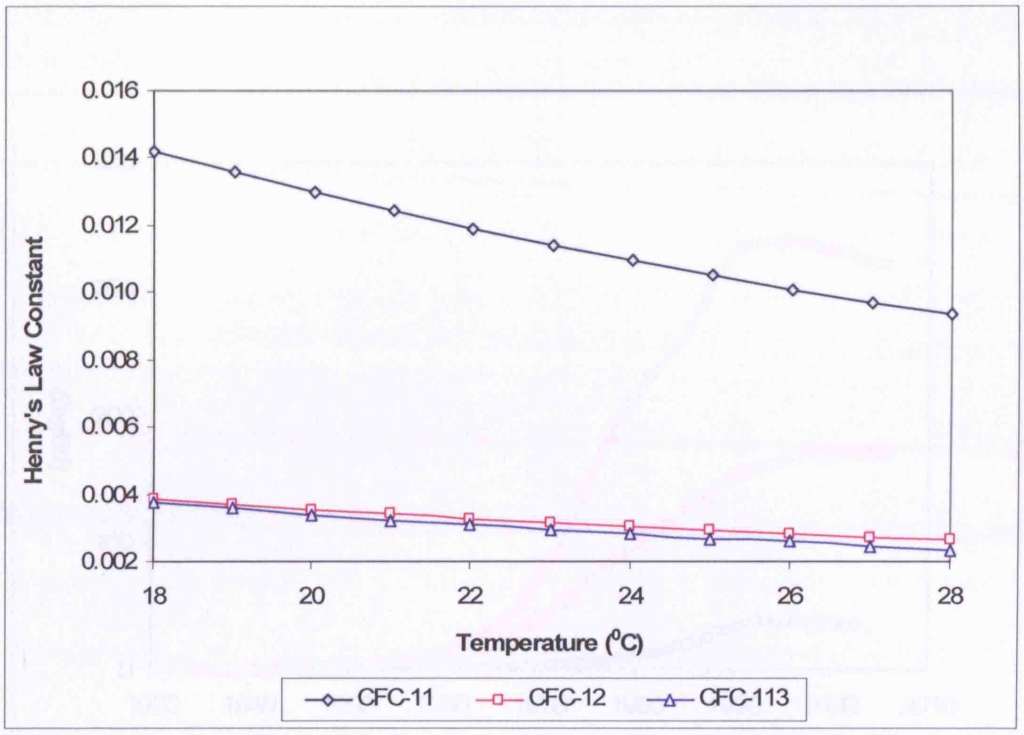

Figure 6.4. Variation in the Henry's law constant for applied CFC tracers with temperature

Concentrations of CFC species in rainfall-fed recharge, assuming equilibrium between the atmosphere and recharging groundwater were determined using eq. 6.3 (Busenberg and Plummer, 1992) and are plotted in Figure 6.5.

$$R_c = A_c \cdot M_{CFC} \cdot K_{CFC} \cdot (A_p - P_{(H2O)}) \qquad \text{(eq. 6.3)}$$

R_c : Recharge concentration (pg kg-1)

A_c : atmospheric concentrations (pptv)

M_{CFC} : molecular weight (g/mol)

K_{CFC} : Henry's law constant (mol kg^{-1} atm^{-1})

A_p : Total atmospheric pressure at recharge elevation (atm)

$P_{(H2O)}$: Water vapour pressure at time of recharge (atm)

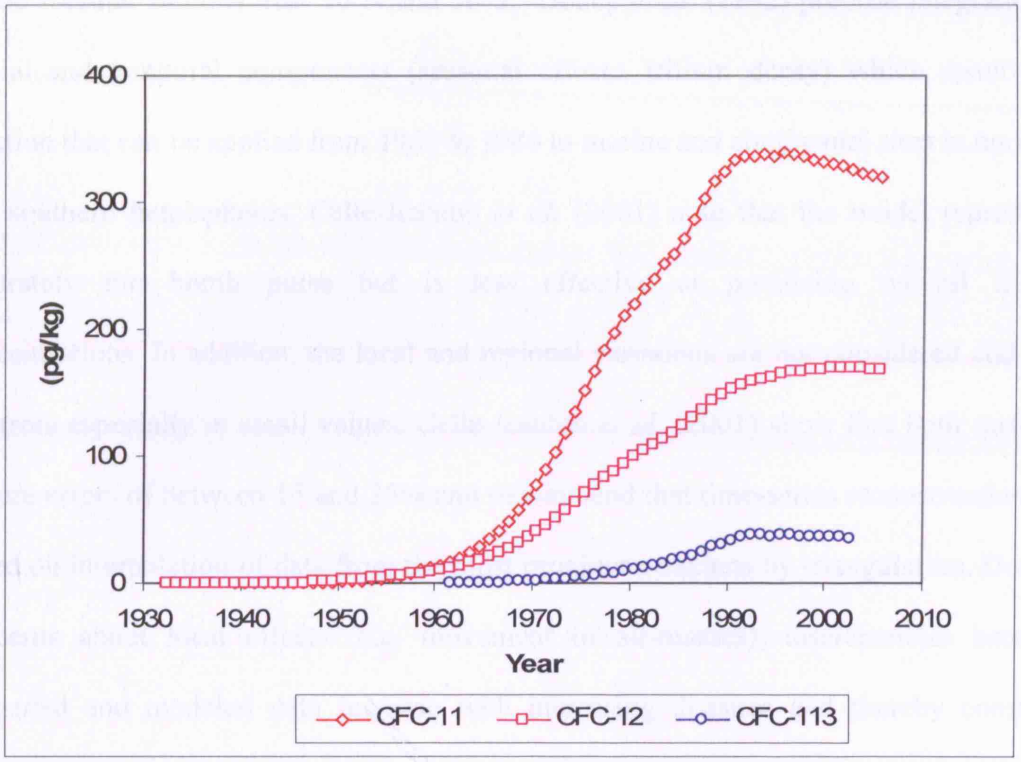

Figure 6.5. Estimated concentrations of CFC-11, CFC-12 and CFC-113 in groundwater recharge in Uganda from 1930 to 2005

6.3.2 Tritium concentrations in precipitation in East Africa

Monthly tritium measurements in precipitation were initiated in Uganda at Entebbe Airport in 1960 as part of the GNIP but ended in 1974 (Fig. 6.1). As a result, reconstruction of the time series of tritium concentrations in precipitation after 1974 was required. Several methods exist to reconstruct time series for atmospheric tritium concentrations (e.g. Weiss and Roether, 1980; Doney *et al.*, 1992; IAEA, 2002). Weiss and Roether (1980) provide an equation that combines various effects (latitude,

precipitation high, vapour exchange rate) but considers as reference, island, coastal and inland weather stations near 50°N and 50°S. Doney *et al.* (1992) propose integration of spatial and temporal components (seasonal effects, tritium decay) which result in a function that can be applied from 1960 to 1986 to marine and continental sites in northern and southern hemispheres. Celle-Jeanton *et al.* (2001) note that the model reproduces accurately the bomb pulse but is less effective at predicting natural tritium concentrations. In addition, the local and regional variations are not considered and lead to errors especially in small values. Celle-Jeanton *et al.* (2001) show that both methods feature errors of between 15 and 35% and recommend that time-series reconstructions be based on interpolation of data from the most proximate stations by triangulation. Despite concerns about local effects (e.g. movement of air-masses), discrepancies between measured and modeled data increase with increasing distance and thereby constrain application of this method in the southern hemisphere. For example, the most proximate stations to Entebbe (0°N, 32°E) are Addis Ababa (9°N, 39°E), Harare (18°S, 31°E) and Bamako (13°N, 8°W). Each possesses similarly limited records. A correlation method (IAEA, 2002) where station data (e.g. Entebbe) are reconstructed as a function of observations at another station (e.g. Vienna, Austria) (eq. 6.4) was, therefore, employed.

$$\log_{10} {}^{3}H_{Entebbe} = a \cdot \log_{10} {}^{3}H_{Vienna} + b \qquad \text{(eq. 6.4)}$$

${}^{3}H_{Entebbe}$: tritium concentration in precipitation at Entebbe (TU)

${}^{3}H_{Vienna}$: tritium concentration in precipitation at Vienna (TU)

a,b: correlation coefficients for reconstruction of tritium in precipitation which depend on the location of the station

The recommended values of *a* and *b*, applicable to Entebbe, are 0.54 and 0.08 respectively for reconstruction on an annual basis whereas values of a and b are 0.58 and 0.04 respectively for reconstruction on a monthly basis. Tritium in precipitation at Entebbe was reconstructed on a monthly basis. Comparison of the reconstructed tritium time series with measurements from 1960 to 1974 and spot measurements in 2000 reveals significant differences (Fig. 6.6). Calculated ^{3}H greatly exceeds observed ^{3}H during the bomb pulse of the early 1960s and overestimates ^{3}H by a factor of up to 2 in the year 2000. The calculated ^{3}H values were therefore normalized using a factor by which the observed values are overestimated as was done elsewhere during CFC modelling (Walker *et al.*, 2000; Michel Robert, pers. comm.). The spot measurements in 2000 were used for verification. The adjusted reconstructed ^{3}H time series are presented in Figure 6.1.

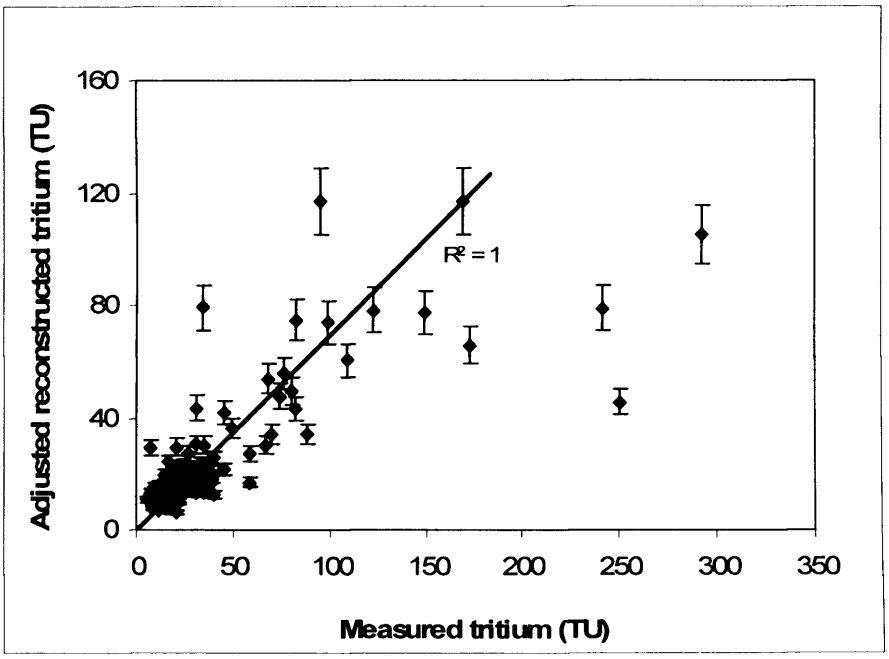

Figure 6.6. Final reconstructed versus measured tritium values in precipitation at Entebbe (0°N, 32°E)

6.4 Processes that affect tracer concentrations in groundwater

6.4.1 Overview

Apart from the fundamental control of temperature on CFC concentrations in rainfall-fed recharge, several processes can complicate the interpretation of groundwater residence times based on CFC concentrations in groundwater. These processes include microbial degradation, the entrainment of excess air, gas diffusion through the unsaturated zone, adsorption to organic matter, hydrodynamic dispersion and local contamination of groundwater. The concentrations of each CFC species is affected to a different extent and so the combined use of these tracers enables the effects of various processes to be evaluated (Cook *et al.*, 1995).

6.4.2 Microbial degradation

Microbial degradation of CFCs in groundwater has been observed under anaerobic conditions (Oster *et al.*,1996; Shapiro *et al.*,1997; Semprini *et al.*, 1990). Semprini *et al.* (1990) observed that some bacteria removed CFC-11 and CFC-113 in shallow anoxic aquifers whereas field and laboratory experiments by Oster *et al.* (1996) confirmed that anaerobic decomposition of CFCs occurs in natural groundwaters. Anaerobic conditions are, however, unlikely in the study areas where oxidising redox potentials are routinely observed in groundwater.

6.4.3 Excess air

'Excess air' describes the entrainment of air bubbles as water infiltrates through the unsaturated zone and the subsequent dissolution of these air bubbles in groundwater in the saturated zone (Heaton and Vogel, 1981). If groundwater residence times derived from CFCs are calculated without taking into account the dissolution of excess air, estimated recharge dates will be more recent than the actual values. Although entrainment of air bubbles by this mechanism will result in excess quantities of all atmospheric gases in a groundwater including CFCs, Busenberg and Plummer (1992) conclude that corrections for CFC-11 are very small even at high concentrations of excess air for young groundwater recharged under high temperatures. The effects of entraining excess air are more significant for CFC-12 especially for relatively young groundwaters recharged at high temperature because of the lower solubilities of this compound. Busenberg and Plummer (1992) suggest that fractured-rock aquifer systems like those in Uganda are favourable environments for the entrainment of excess air. Nevertheless, as highlighted below, CFC-12 concentrations in groundwater of the River Kigwe catchment reflect degradation (i.e. non-conservative conditions). As a result, groundwater residence times for this catchment are estimated from CFC species that are not affected by excess air.

6.4.4 Diffusion of gases through the unsaturated zone

An assumption that is central to the use of CFCs as residence-time indicators is that CFCs in the recharging water are in equilibrium with the atmosphere at the time of groundwater recharge. Cook and Solomon (1995) suggest that where groundwater recharge occurs through deep unsaturated zones, the air with which groundwater is

finally equilibrated may be substantially older than the contemporary atmosphere. If equilibration of infiltrating groundwater occurs with older air at depth, CFCs will overestimate groundwater residence times within the saturated zone. For water table depths of up to 20 m that occur in River Kigwe catchment, the maximum time lags derived from a diffusion based equation given by Cook and Solomon (1995) are 12, 6 and 11 years for CFC-11, CFC-12 and CFC-113 respectively. For water table depths of up to 30 m that occur in River Mitano catchment the maximum time lags based on Cook and Solomon (1995) are 15, 12 and 13 years for CFC-11, CFC-12 and CFC-113 respectively. Similarly, diffusion processes of gases are important at great depths but fluctuations in barometric pressure in fractured rocks may induce significant air to great depths making age corrections for diffusion unnecessary (Cook and Solomon, 1995)

6.4.5 Sorption (organic matter interactions)

Water recharging through a dry unsaturated zone can acquire CFC concentrations in excess of atmosphere-water equilibrium due to the release of CFCs adsorbed onto organic matter. CFC contributions from desorption are, however, considered to be important only in arid climates where shallow unsaturated zones dry out between recharge events (Plummer *et al.*, 1993).

6.4.6 Hydrodynamic dispersion

Hydrodynamic dispersion is a process through which CFC molecules that enter an aquifer at different times or different locations can be mixed (Plummer *et al.*, 1993). The

net effect of hydrodynamic dispersion on CFC as an age tracer depends on the magnitude of concentration gradients. Busenberg and Plummer (1992) conclude that longitudinal dispersion is not likely to be a significant factor in CFC dating especially in shallow groundwater. However, where there is strong convergence in a flow field such as towards a well, lateral dispersion may produce much more mixing.

6.4.7 Local contamination of groundwater

Groundwaters in which CFC concentrations are higher than water in equilibrium with contemporary atmosphere have likely been contaminated by an external (terrestrial) source such as a landfill (Bateman, 1998). Even where one of the CFC species is contaminated, dating may still be possible if concentrations suggest that contamination with respect to one or more of the remaining compounds has not occurred. However, where concentrations of CFCs are below the maximum possible from air-water equilibrium, the possibility still exists that some component of the measured concentrations may derive from a contaminated source. Plotting data on mixing diagrams and checking whether the relative CFC concentrations are achievable from air-water equilibrium can help identify contaminated groundwater (Cook *et al.*, 1995). A few samples that show obvious terrestrial contamination have been identified in this manner and have thus not been considered in the analysis.

6.5 Groundwater mixing processes

6.5.1 Groundwater mixing models

Mixtures of water occur when groundwater flow lines reaching a discharge point (e.g. pumping well) merge (Talma *et al.*, 2000; Plummer *et al.*, 2001; Burton *et al.*, 2002; Shapiro, 2002; Cook *et al.*, 2005; Gooddy *et al.*, 2006). Zinn and Konikov (2007) present evidence to show that intraborehole flow can lead to mixing of groundwater and substantially affect the determination of groundwater residence times. If waters of two distinct residence times mix, the mixing problem may be solved with measurement of CFC-11, CFC-12, and CFC-113, provided the CFC concentrations are representative of air–water equilibrium at recharge and have not been altered by any other physical or chemical process following recharge (Shapiro, 2002). The mixing problem becomes more complicated when more than two different waters mix as there are no known tracers that can be used for dating such water. Mean groundwater residence times in aquifers in which groundwater is highly mixed are better determined by use of distributed parameter models (Maloszewski and Zuber, 1982; Ozyurt and Bayari, 2005) but these models require detailed knowledge of the groundwater system which is normally unavailable. Use of "lumped-parameter" or "reservoir" models to interpret tracer data (Maloszewski and Zuber, 1982; Plummer *et al.*, 2001) is an option of lesser, intermediate complexity that is often the most feasible.

All the models which have been developed for investigating the dynamics of groundwater are based on two extreme theoretical cases namely piston flow (no mixing) and complete mixing (Amin and Campana, 1996; Plummer *et al.*, 2006). Four hypothetical models, are often used to describe variations in tracer concentrations

observed in groundwater: piston flow (PFM), exponential (complete) mixing (EM), exponential piston flow (EPM), and binary mixing (BM) (Cook and Böhlke, 2000). PFM consider that each recharge episode is stratified over the previous one and that flow moves without mixing between each of the successive contributions. PFM is analogous to water flowing through a pipe from the point of recharge to the point of discharge without mixing during transit (Gooddy *et al.,* 2006). EPM corresponds to a case in which an aquifer is recharged in an up-gradient unconfined area but the flow continues beneath a down-gradient unconfined area.

EM considers that each episode of recharge mixes completely and instantaneously within a homogeneous reservoir and flow is assumed to be continuous and constant so the outflow has a tracer concentration that corresponds to that of the reservoir. Maloszewski and Zuber (1982) suggest that EM can be used to describe discharge from an unconfined aquifer receiving uniform areal recharge. Although in reality, groundwater systems are never fully mixed and should thus be simulated using partial mixing models such as combined exponential and dispersion model (DM), these models have two fitting parameters and cannot consequently generate unique solutions. Single-parameter models are therefore appropriate for simulating mixing and estimating groundwater residence times especially where very limited measurements are available. Bockgard *et al.* (2004) suggest that binary mixing of young and old (pre-tracer) water is one of the simplest models to consider and is perhaps the most important in fractured-rock environments though Rademacher *et al.* (2003) suggest that this may not be the case in all fractured-rock environments.

In binary mixing, simple dilution occurs because the old fraction is assumed to be free of the tracer. Consequently, the age of the young fraction is calculated from the ratio of the two tracers. Multiple tracers can show whether simple models like those described above can explain ("fit") observations. A plot of one tracer against another can be used to distinguish the hypothetical mixing processes that may affect groundwater samples in addition to identifying anthropogenic contamination (Goody *et al.*, 2006). Comparison of the various tracers and identification of the mixing processes is described in the sections that follow.

6.5.2 Determining atmosphere–water equilibrium lines

Estimated CFC concentrations in recharge from 1950 to 2005 for different combinations of CFC gases are plotted in Figures 6.7 to 6.9 to determine their common atmosphere–water equilibrium lines (AWEL). Air-water equilibrium curves indicate trends in CFC concentrations of recharging water in equilibrium with the atmosphere over this period. A position on the AWEL represents concentrations of CFCs in a "single age" unmixed groundwater recharged in a particular year (Bateman, 1998). A straight line joining the AWEL and the origin is the mixing line and represents the location where groundwaters will plot if they are 2 component mixtures between a young water of recent composition and CFC free groundwater. A groundwater will plot within the area bounded by the AWEL and the mixing line if its composition has been determined solely from the dissolution of atmospheric CFCs and subsequent mixing with other air-water equilibrated groundwater.

Figure 6.7 shows the AWEL for CFC-12 and CFC-11. The AWEL is near linear and nearly regresses along the mixing line. The linearity of the AWEL (r^2 = 0.59) suggests that it is not possible to distinguish whether a groundwater which plots on the AWEL is (i) a single age, unmixed groundwater (ii) a two-component mixture or (iii) a complex mixture of groundwaters of different ages. Thus, it should be remembered that groundwaters will plot along this line even if they are multi-component mixtures of different ages or two-component mixtures of young water of recent composition and CFC-free groundwater.

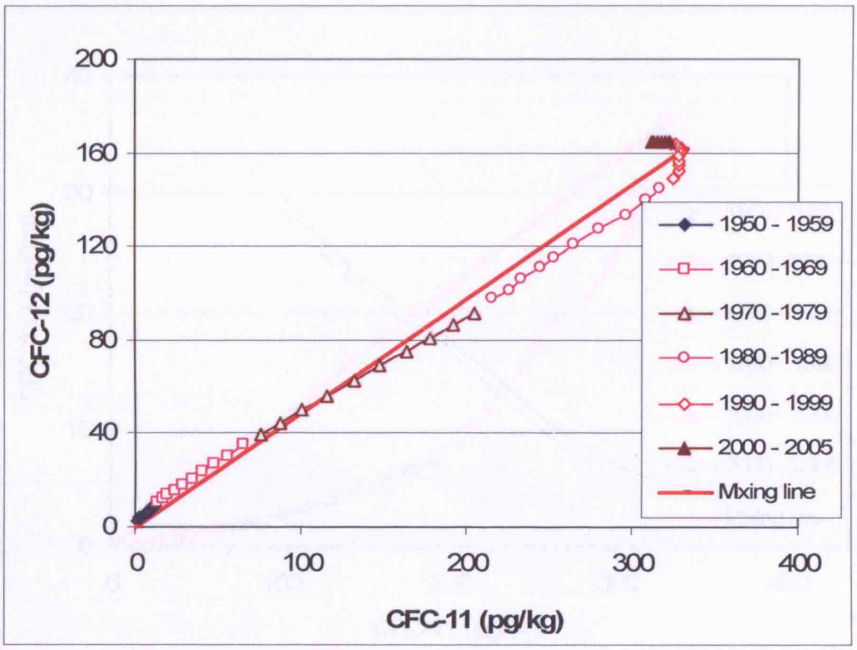

Figure 6.7. Common atmosphere–water equilibrium lines for CFC-12 and CFC-11

The AWELs for CFC-113 versus CFC-11 and CFC-113 versus CFC-12 (Figs. 6.8 and 6.9) are curved as a consequence of significant differences in the timing of the CFC releases into the atmosphere for each gas. Lines that join the AWEL to the origin in

Figures 6.8 and 6.9 represent groundwaters that are a mixture of recently recharged and CFC-free groundwater. The area defined by the AWEL curves and mixing lines delimits the region in which groundwaters with CFC concentrations determined by equilibrium between the atmosphere and recharging groundwater at 24°C and mixing, will plot (Bateman, 1998). Groundwater samples that plot outside the region bounded by the AWEL and the binary mixing line have been affected by other processes such as contamination or degradation that have altered the CFC concentrations from air-water equilibrium values (Plummer *et al.*, 1993)

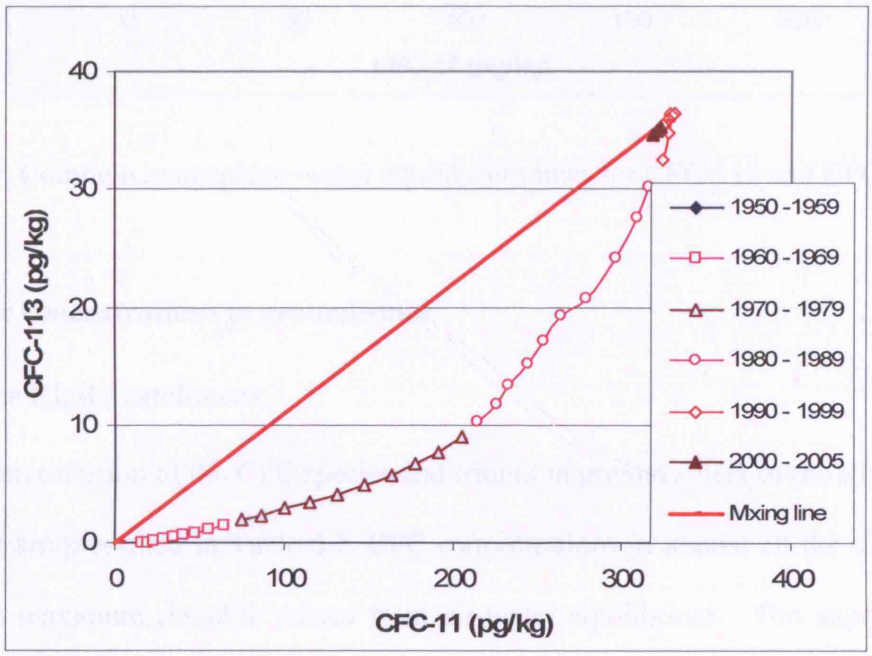

Figure 6.8. Common atmosphere–water equilibrium lines for CFC-113 and CFC-11

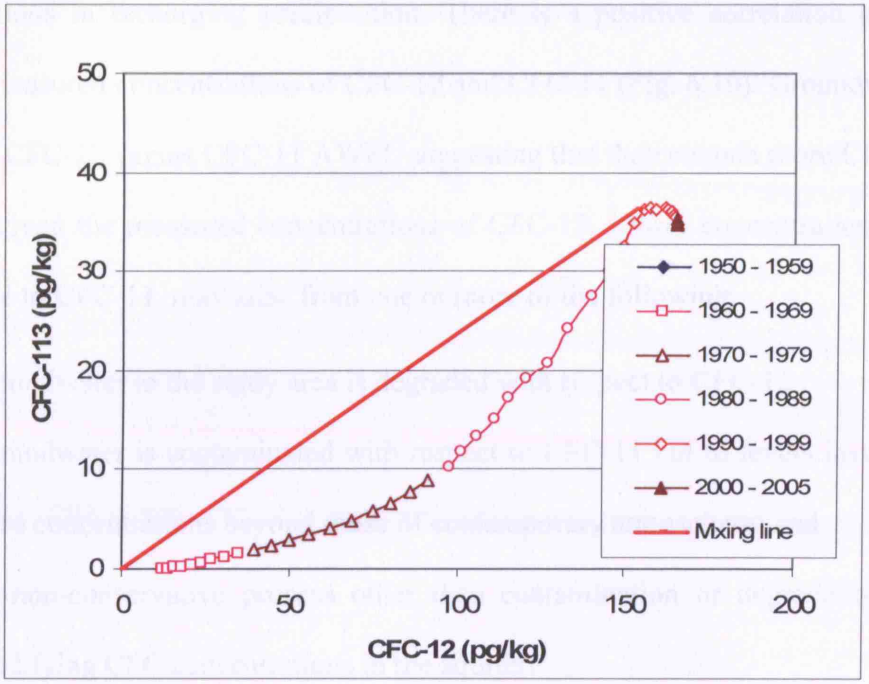

Figure 6.9. Common atmosphere–water equilibrium lines for CFC-113 and CFC-12

6.6 Tracer concentrations in groundwater

6.6.1 River Kigwe catchment

Concentration of the CFC species and tritium in groundwaters of the River Kigwe catchment are presented in Table 6.2. CFC concentrations in almost all the samples are below the maximum possible values from air-water equilibrium. The expected CFC concentrations in the atmosphere during the year 2000, when the sampling was carried out are 323, 165 and 35 pg kg^{-1} for CFC-11, CFC-12 and CFC-113 respectively and are above those found in all the samples except three sources (Sikanusu, Mosque spring and Wobulenzi Public School) which show obvious contamination of CFC-12.

Concentrations of CFCs in groundwater samples from the River Kigwe catchment are presented in relation to AWELs in order to assess their relationship to estimated CFC

concentrations in recharging precipitation. There is a positive correlation (r^2 = 0.59) between measured concentrations of CFC-12 and CFC-11 (Fig. 6.10). Groundwaters plot below the CFC-12 versus CFC-11 AWEL suggesting that they contain more CFC-11 than expected given the measured concentrations of CFC-12. Lower concentrations of CFC-12, relative to CFC-11, may arise from one or more of the following:

(i) groundwater in the study area is degraded with respect to CFC-12 ;

(ii) groundwater is contaminated with respect to CFC-11 but to levels insufficient to raise concentrations beyond those of contemporary atmosphere; and

(iii) a non-conservative process other than contamination or degradation may be modifying CFC concentrations in the aquifer.

Table 6.2. Concentrations of CFC species and tritium in groundwater along with details of the sampled boreholes for the River Kigwe catchment

Sample number	Sample location	Source Type	CFC-12 (pg kg^{-1})	CFC-11 (pg kg^{-1})	CFC-113 (pg kg^{-1})	Tritium (TU)	Casing depth (mbgl)	Well depth (mbgl)
1	Piezometer 1	Piezometer				1.7±0.2	N.A	39
2	Piezometer 2	Piezometer	52	163	30	1.7±0.2	N.A	32
3	Piezometer 3	Piezometer				0.4±0.2	49	71
4	Piezometer 4	Piezometer	12		26	0.1±0.2	48	65
5	Katik Com.Centre	Borehole	71	152	21	1.1±0.2	33	63
6	Kisule	Borehole		26		1.6±0.2	39	63
7	Bukeeka	Borehole		41	3.8	0.1±0.1	51	75
8	Mosque	Spring		398	32	1.4±0.2	N.A	N.A
9	Sikanusu	Spring	196	300	24	1.9±0.2	N.A	N.A
10	Nkonge	Borehole				1.0±0.2		
11	Sempa	Borehole				0.6±0.2	35	43
12	Monde	Borehole	68	313	19	0.3±0.1	20	61
13	Tweyanze	Borehole	36	180	15	1.0 ± 0.2	24	55
14	Kaliro-Katono	Borehole				1.0±0.2	23	53
15	Nsero	Borehole				0.8±0.2	30	71
17	Kikoma	Borehole	46	113	19	0.6±0.1	26	63
19	Busula	Borehole	9.7	84	17	1.5±0.2	21	51
22	Kaswa	Borehole	91	262	28	1.3±0.2	31	56
24	Saku S.S.	Borehole	34	137	15	2.7±0.2		
29	Wobu Public Sch	Borehole	121	334	39	0.4±0.1		75
30	Wobu Parents Sch	Borehole	35	81	5.6	1.3±0.2		
	Wobulenzi - May 2000	Rainfall				1.9±0.2		
	Wobulenzi -Jun. 2000	Rainfall				2.3±0.2		
	Entebbe - May 2000	Rainfall				2.1±0.2		
	Entebbe - Jun. 2000	Rainfall				2.3±0.2		

mbgl: metres below ground level; N.A.: Not applicable

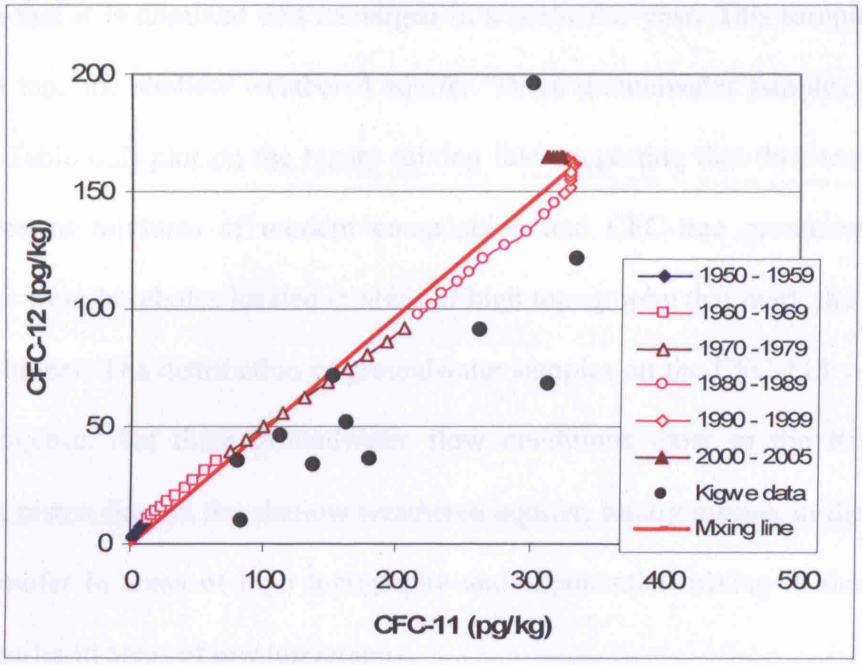

Figure 6.10. CFC-12 versus CFC-11 concentrations in groundwater of the River Kigwe catchment

The correlation between concentrations of CFC-113 and CFC-11 in groundwater in the River Kigwe catchment (Fig. 6.11) is roughly linear ($r^2 = 0.59$). Some groundwater samples plot to the left of the AWEL (above the binary mixing line) indicating relative enrichment in CFC-113. These results may reflect on-site degradation of CFC-11 and/or potentially land-based contamination of CFC-113. Contamination of CFC-113 in two samples is suggested as these data plot to the right of the AWEL beyond recently recharged groundwater. Two groundwater samples (nos. 13 and 30 in Table 6.2) plot between the AWEL and the binary mixing line so that their compositions may be determined by dissolution of atmospheric CFCs and mixing with other air-water equilibrated groundwater. One sample (No. 9 in Table 6.2) plots on the AWEL

suggesting that it is unmixed and recharged in a particular year. This sample is from a spring that taps the shallow weathered aquifer. Three groundwater samples (nos. 7, 22 and 24 in Table 6.2) plot on the binary mixing line suggesting that they may comprise two component mixtures of modern composition and CFC-free groundwater. These samples are from boreholes located in areas of high topography that mark the boundaries of the catchment. The distribution of groundwater samples on the CFC-113 versus CFC-11 plot suggests that three groundwater flow conditions exist in the River Kigwe catchment: piston flow in the shallow weathered aquifer, binary mixing in the fractured-bedrock aquifer in areas of high topography and exponential mixing in the fractured-bedrock aquifer in areas of low topography.

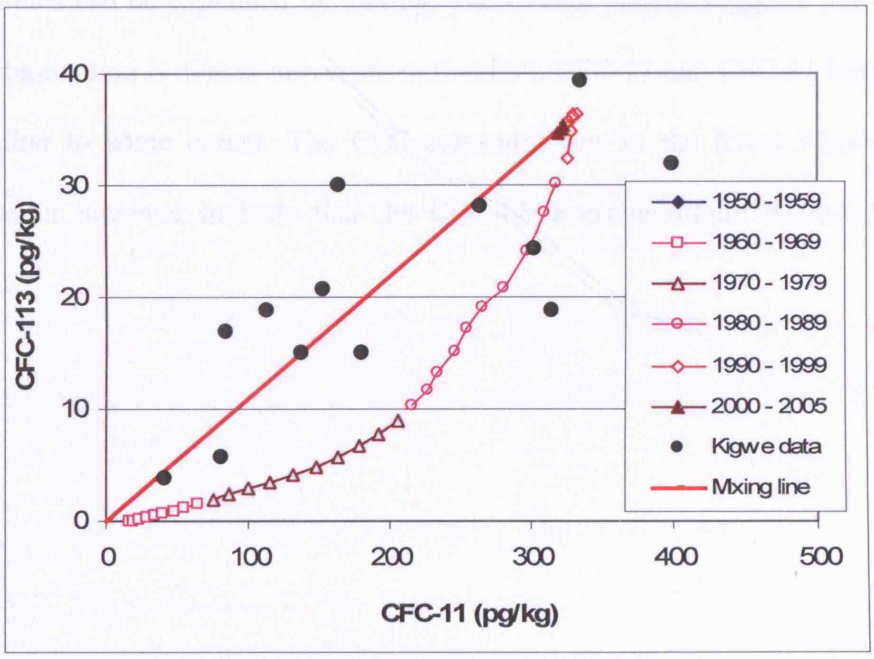

Figure 6.11. CFC-113 versus CFC-11 concentrations in groundwater of the River Kigwe catchment

In Figure 6.12, nearly all groundwater samples plot significantly to the left of the AWEL and beyond the mixing line suggesting enrichment in CFC -113 relative to CFC-12. The correlation between CFC-12 and CFC-113 concentrations is poor (r^2 = 0.22) implying that there is either degradation of CFC-12 or terrestrial contamination of CFC-113. Contamination of groundwater with respect to CFC-113 would result in groundwater samples plotting to the left and much above the AWEL in figures 6.11 and 6.12. If CFC-12 and CFC-11 were not degraded and there was excess CFC-113, all the water samples would plot to the left and above the AWEL in Figs. 6.11 and 6.12. In fact, this is not the case. Almost all the samples plot to the left of the AWEL for CFC-113 versus CFC-12. On the CFC-113 versus CFC-11 plot, four samples lie to the left of the AWEL whereas five samples can be explained by mixing. The overall pattern suggests that either CFC-113 contamination is almost universal, or that both CFC-12 and CFC-11 have undergone degradation to some extent. The CFC concentrations in the River Kigwe catchment groundwater however indicate that the CFC-12 is preferentially degraded relative to CFC-11.

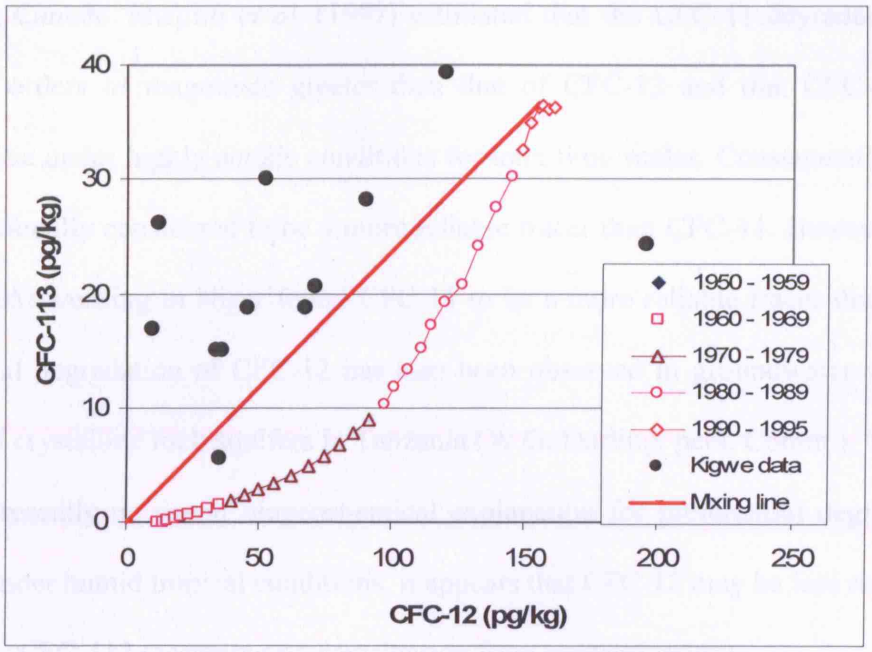

Figure 6.12. CFC-113 versus CFC-12 concentrations in groundwater of the River Kigwe catchment

The conclusion that CFC-12 is degraded under aerobic conditions in the River Kigwe catchment challenges the assertion that CFCs are stable under aerobic conditions (Khalil and Rasmussen, 1989; Semprini *et al.,* 1990). Furthermore, various studies established that, in temperate regions, CFC-11 and CFC-113 are more easily degraded by microbial activity than CFC-12 under anaerobic conditions (Oster *et al.,*1996; Shapiro *et al.,*1997; Semprini *et al.,* 1990). Oster *et al.* (1996) estimated that CFC-12 is approximately ten times less susceptible to degradation than CFC-11. Similarly, Khalil and Rasmussen (1989) found CFC-11, CFC-12 and CFC-113 to be degraded by approximately 12%, 4% and 2% respectively. Cook *et al.* (1995) showed that CFC-11 was nearly completely degraded whereas CFC-12 was stable in a sulphate-reducing

aquifer in Canada. Shapiro *et al.* (1997) estimated that the CFC-11 degradation rate is over two orders of magnitude greater than that of CFC-12 and that CFC-12 can be conservative under highly anoxic conditions for long time scales. Consequently, CFC-12 is conventionally considered to be a more reliable tracer than CFC-11. However, Rueedi *et al.* (2005) working in Niger found CFC-11 to be a more reliable tracer than CFC-12. Preferential degradation of CFC-12 has also been observed in groundwater sampled in weathered crystalline rock aquifers in Tanzania (W.G. Darling, pers. Comm.). Thus while there is presently no sound biogeochemical explanation for preferential degradation of CFC-12 under humid tropical conditions, it appears that CFC-12 may be less reliable than CFC-11 or CFC-113 (assuming no contribution from contamination).

6.6.2 River Mitano catchment

Concentrations of CFCs and tritium in groundwaters of the River Mitano catchment are presented in Table 6.3. CFC concentrations in groundwater at three sites (8, 10 and 11), exceed concentrations expected in recharging precipitation and suggest therefore that these samples are contaminated. The concentration of CFC-12 and CFC-113 in groundwater at sites 4 and 12, and 4 respectively also exceed concentrations expected in contemporary recharging precipitation. The expected CFC concentrations in recharging precipitation when the sampling was carried out in 2005 are 312, 165 and 35 pg kg-1 for CFC-11, CFC-12 and CFC-113 respectively. Five samples (4, 8, 10, 11 and 12) that show obvious contamination have been excluded from further analysis.

Table 6.3. Concentrations of CFC species and tritium in groundwater along with details of the sampled boreholes for the River Mitano catchment

Sample no.	Site name	Source type	CFC-12 (pg kg^{-1})	CFC-11 (pg kg^{-1})	CFC-113 (pg kg^{-1})	Tritium (TU)	Casing depth (mbgl)	Well depth (mbgl)
1 [a]	Ruk 5 (PW 1)	Alluvial aquifer PW	85	84	19	0.9±0.1	46	89
2 [a]	Ruk 8 (PW 2)	Alluvial aquifer PW	98	132	21	1.2±0.2	64	64
3 [b]	Kinyasano	Fractured aquifer borehole	7.3	9.6	1.9	0.5±0.2	22	43
4 [a]	Piezometer 3	Alluvial aquifer MW	191	288	75	1.4±0.1	35	35
5 [a]	Piezometer 1	Alluvial aquifer MW	114	161	28	1.2±0.2	45	45
6 [a]	Piezometer 4	Alluvial aquifer MW	53	71	24	1.0±0.1	61	61
7 [b]	Rwarubira	Fractured aquifer borehole	65	104	13	1.2±0.1	16	62
8 [a]	Piezometer 2	Alluvial aquifer MW	248	574	58	1.3±0.2	36	36
9 [a]	Piezometer 5	Alluvial aquifer MW	86	113	28	1.2±0.2	48	48
10 [a]	Piezometer 7	Fractured aquifer MW	323	398	49	1.6±0.2	36	48
11 [b]	Immaculate	Fractured aquifer borehole	167	312	41	2.1±0.1	15	42
12 [a]	Piezometer 8	Fractured aquifer MW	580	117	21	0.4±0.1	25	81

GW – groundwater; PW – production borehole; MW – monitoring well, 1[a]- samples from alluvial aquifer, 1[b] – samples from fractured-bedrock aquifer

Concentrations of CFCs in groundwater samples from the River Mitano catchment are presented in relation to AWELs in order to assess their relationship to

estimated CFC concentrations in recharging precipitation (Fig. 6.13). There is a positive correlation (r^2 = 0.96) between measured concentrations of CFC-12 and CFC-11. Groundwater samples plot in the centre above the CFC-12 versus CFC-11 AWEL, which is inconsistent with a simple atmospheric origin. The results suggest possible enrichment in CFC-12 or degradation of CFC-11. There is one sample with concentrations beyond those of the contemporary atmosphere which indicates contamination from a terrestrial source.

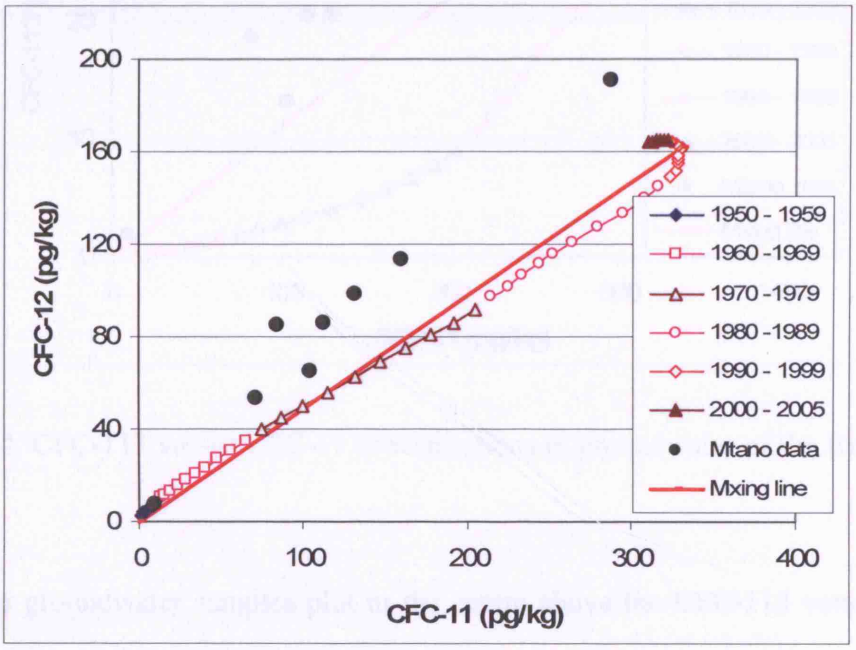

Figure 6.13. CFC-12 versus CFC-11 concentrations in groundwater of the River Mitano catchment

The correlation between concentrations of CFC-113 and CFC-11 in groundwater samples is roughly linear (r^2 = 0.60). All the groundwater samples plot to the left of the AWEL and above the mixing line indicating relative enrichment in CFC-113 (Fig. 6.14). However, when the CFC-113 versus CFC-11 plot is considered in relation to the CFC-12

versus CFC-11 plot (Fig. 6.13), the distribution of the samples appears to indicate degradation of CFC-11 rather than contamination of CFC-113. There are no groundwater samples that plot between the AWEL and the mixing line.

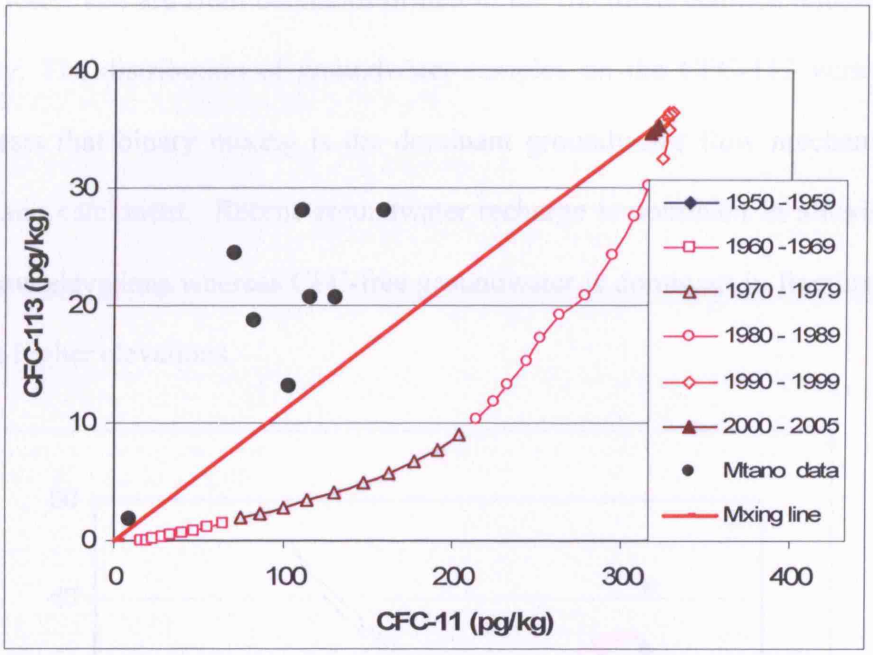

Figure 6.14. CFC-113 versus CFC-11 concentrations in groundwater of the River Mitano catchment

The groundwater samples plot in the centre above the CFC-113 versus CFC-12 AWEL (Fig. 6.15). There is a positive correlation (r^2 = 0.81) between measured concentrations of CFC-113 and CFC-12. Two samples lie significantly above the mixing line, suggesting that some degradation of CFC-12 relative to CFC-113 may have occurred. However, a single sample shows clear evidence of contamination in CFC-113, plotting at higher values than present atmospheric concentrations. It is therefore equally possible that samples are enriched in CFC-113 rather than degradation of CFC-12. Five groundwater samples lie along the mixing line between recent recharge and CFC-free

water on the CFC-113 versus CFC-12 plot. Three out of the five samples (Nos.1, 2 and 9 in Table 6.3) plot closer to recent recharge and are from boreholes drilled in the alluvial aquifer whereas the remaining two samples (Nos. 3 and 7 on Table 6.3) plot close to CFC-free water and are from boreholes drilled in the fractured-bedrock aquifer at higher topography. The distribution of groundwater samples on the CFC-113 versus CFC-12 plot suggests that binary mixing is the dominant groundwater flow mechanism in the River Mitano catchment. Recent groundwater recharge is dominant in alluvial aquifers found at low elevations whereas CFC-free groundwater is dominant in fractured-bedrock aquifers at higher elevations.

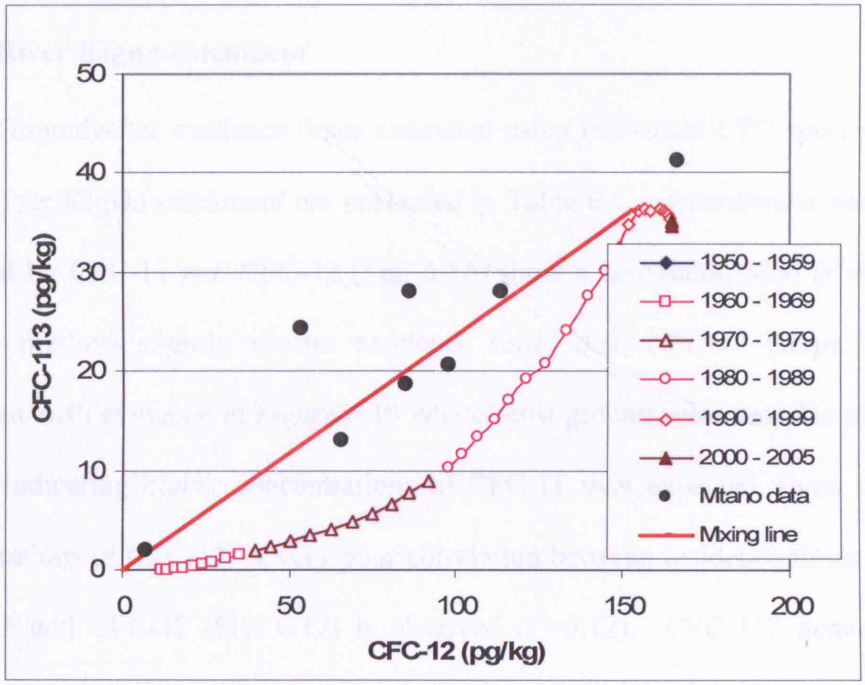

Figure 6.15. CFC-113 versus CFC-12 concentrations in groundwater of the River Mitano catchment

6.7 Modelling groundwater residence times

6.7.1 Estimation of groundwater residence time using CFCs (non – mixing model)

The most common assumption regarding tracing of atmospheric inputs to groundwater is piston flow. Estimated groundwater residence times assume for example, that the concentrations of CFC have remained unaltered by transport processes from the point of recharge to the point of capture in an aquifer. Following the approach of Busenberg and Plummer (1992), recharge dates are assigned by comparing measured concentrations in the samples to estimated recharge concentrations of each of the CFC species. This assumes that the groundwater is unmixed (i.e. of a single age).

6.7.1.1 River Kigwe catchment

Groundwater residence times estimated using individual CFC species and tritium in the River Kigwe catchment are presented in Table 6.4. Groundwater residence times indicated by CFC-11 and CFC-12 (Fig. 6.16) show a consistent trend (r^2=0.53) though CFC-11 predicts slightly shorter residence times than CFC-12 (slope >1). This is consistent with evidence in Figure 6.10 where most groundwater samples plot below the AWEL indicating higher concentrations of CFC-11 than expected given the measured concentrations of CFC-12. A very poor correlation between residence times predicted by CFC-113 and CFC-12 (Fig. 6.17) is observed (r^2=0.12). CFC-113 generally predicts shorter groundwater residence times than CFC-12 concentrations. A much better correlation between groundwater residence times predicted by CFC-113 and CFC-11 (Fig. 6.18) is observed (r^2=0.52) though CFC-113 consistently predicts shorter residence times than CFC-11 (slope <1).

Table 6.4. Estimated mean groundwater residence times from individual CFC species and tritium for the River Kigwe catchment

Sample No.	Sample Location	Source Type	CFC-12 residence times (years)	CFC-11 residence times (years)	CFC-113 residence times (years)	Tritium residence times (years)
2	Piezometer 2	Piezometer	30	25	13	
4	Piezometer 4	Piezometer	40		14	
5	Katik Com.Centre	Borehole	25	25	15	16
6	Kisule	Borehole		37		44
7	Bukeeka	Borehole		35	27	22
8	Mosque	Spring		13		4
9	Sikanusu	Spring	11	17	14	12
11	Sempa	Borehole				10
12	Monde	Borehole	28	16	17	51
13	Tweyanze	Borehole	32	25	17	22
15	Nsero	Borehole				32
17	Kikoma	Borehole	30	28	17	21
19	Busula B.	Borehole	42	31	18	5
22	Kaswa	Borehole	24	19	14	7
24	Saku S.S.	Borehole	33	27	19	3
29	Wobu Public Sch	Borehole	20	14	10	1
30	Wobu Parents Sch	Borehole	32	31	25	12

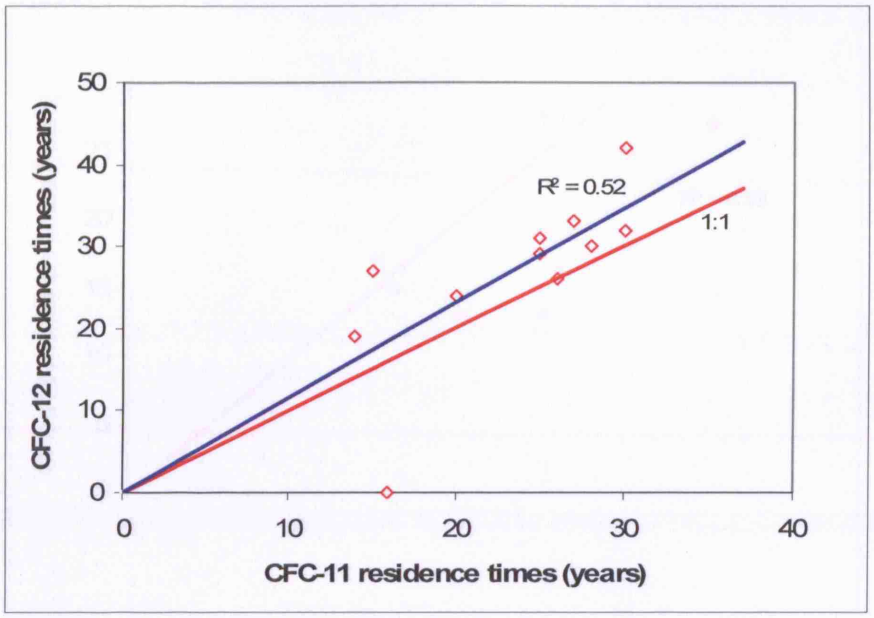

Figure 6.16. Plot of CFC-12 versus CFC-11 residence times for groundwater of the River Kigwe catchment

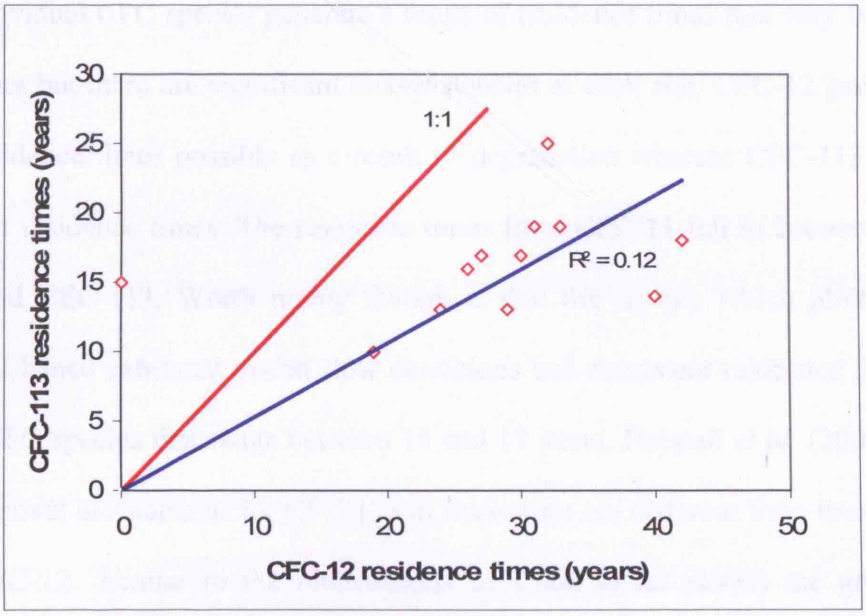

Figure 6.17. Plot of CFC-113 versus CFC-12 residence times for groundwater of the River Kigwe catchment

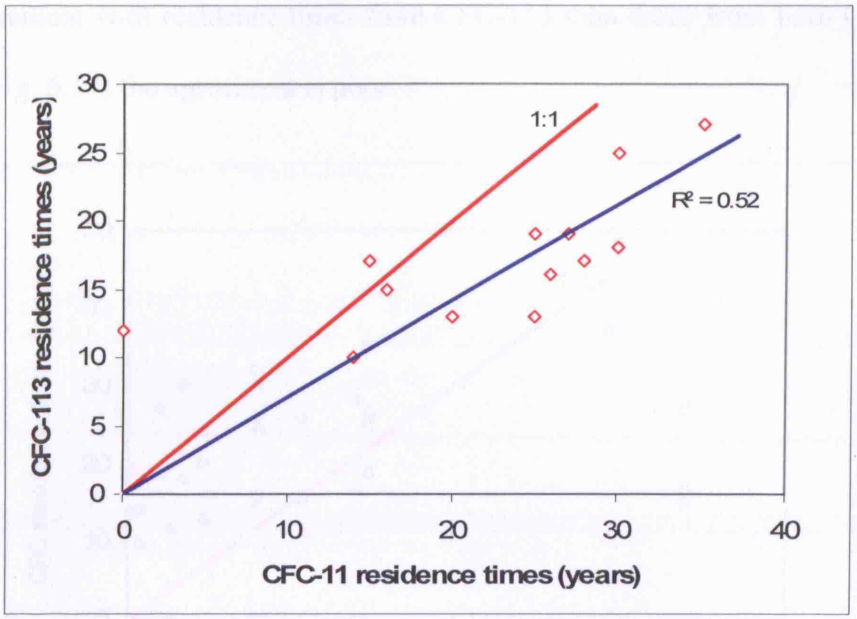

Figure 6.18. Plot of CFC-113 versus CFC-11 residence times for groundwater of the River Kigwe catchment

Individual CFC species generate a range of residence times that vary between 10 and 42 years but there are significant inconsistencies at each site. CFC-12 generates the longest residence times possibly as a result of degradation whereas CFC-113 generates the shortest residence times. The residence times from CFC-11 fall in between those of CFC-12 and CFC-113. Worth noting though is that the sample which plotted on the AWEL and hence exhibited piston flow conditions has consistent residence times from the three CFC species that range between 11 and 17 years. Happell *et al.* (2003) suggest that the removal mechanisms for CFC-113 in freshwater are different from those of CFC-11 and CFC-12. Similar to the observations by Cook *et al. (*1995) the groundwater residence times derived from CFC-113 appear the most reliable and range between 10 and 27 years. Residence times from tritium range between 3 and 51 years and are shorter than those from CFCs in almost all the samples. Although tritium residence times are in

closer agreement with residence times from CFC-113 than those from both CFC-11 and CFC-12 (Fig. 6.19) the agreement is poor.

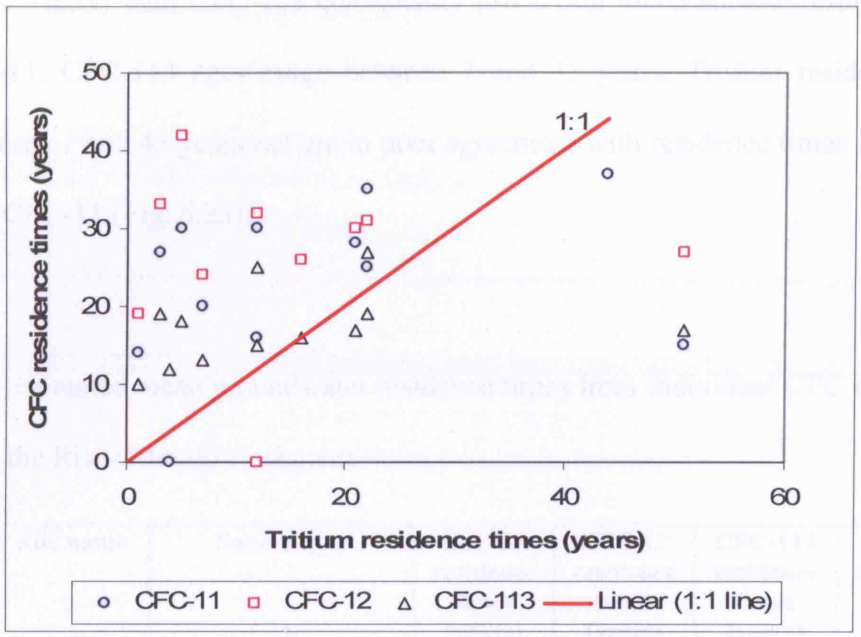

Figure 6.19. Plot of CFC versus tritium residence times for groundwater of the River Kigwe catchment

6.7.1.2 River Mitano catchment

Groundwater residence times estimated using individual CFC species and tritium for the River Mitano catchment are presented in Table 6.5. Groundwater residence times indicated by CFC-11 and CFC-12 (Fig. 6.20) show a consistent trend (r^2=0.60) though CFC-11 predicts slightly longer residence times than CFC-12. This is consistent with evidence in Figure 6.13 where all groundwater samples plot above the AWEL indicating slightly lower concentrations of CFC-11 than expected given the measured concentrations of CFC-12. The correlation between residence times predicted by CFC-113 and CFC-12 (Fig. 6.21) is fairly good (r^2=0.50). CFC-113 generally predicts slightly

shorter groundwater residence times than CFC-12 concentrations. A lower correlation between groundwater residence times predicted by CFC-113 and CFC-11 (Fig. 6.22) is observed (r^2=0.35) with CFC-113 consistently predicting much shorter residence times than CFC-11. CFC-113 ages range between 7 and 35 years. Tritium residence times range between 7 and 45 years but are in poor agreement with residence times from CFCs except for CFC-11 (Fig. 6.23).

Table 6.5. Estimated mean groundwater residence times from individual CFC species and tritium for the River Mitano catchment

Sample no.	Site name	Source type	CFC-12 residence times (years)	CFC-11 residence times (years)	CFC-113 residence times (years)	Tritium residence times (years)
1 [a]	Ruk 5 (PW 1)	Alluvial aquifer PW	27	34	20	44
2 [a]	Ruk 8 (PW 2)	Alluvial aquifer PW	25	31	19	7
3 [b]	Kinyasano	Fractured aquifer borehole	48	47	35	45
4 [a]	Piezometer 3	Alluvial aquifer MW		8		8
5 [a]	Piezometer 1	Alluvial aquifer MW	12	29	7	7
6 [a]	Piezometer 4	Alluvial aquifer MW	32	35	8	44
7 [b]	Rwarubira	Fractured aquifer borehole	33	33	13	7
8 [a]	Piezometer 2	Alluvial aquifer MW				8
9 [a]	Piezometer 5	Alluvial aquifer MW	27	32	7	7
10 [a]	Piezometer 7	Fractured aquifer MW				17
11 [b]	Immaculate	Fractured aquifer borehole				26
12 [a]	Piezometer 8	Fractured aquifer MW		32	9	45

GW – groundwater; PW – production borehole; MW – monitoring well, 1[a]- samples from alluvial aquifer, 1[b] – samples from fractured-bedrock aquifer

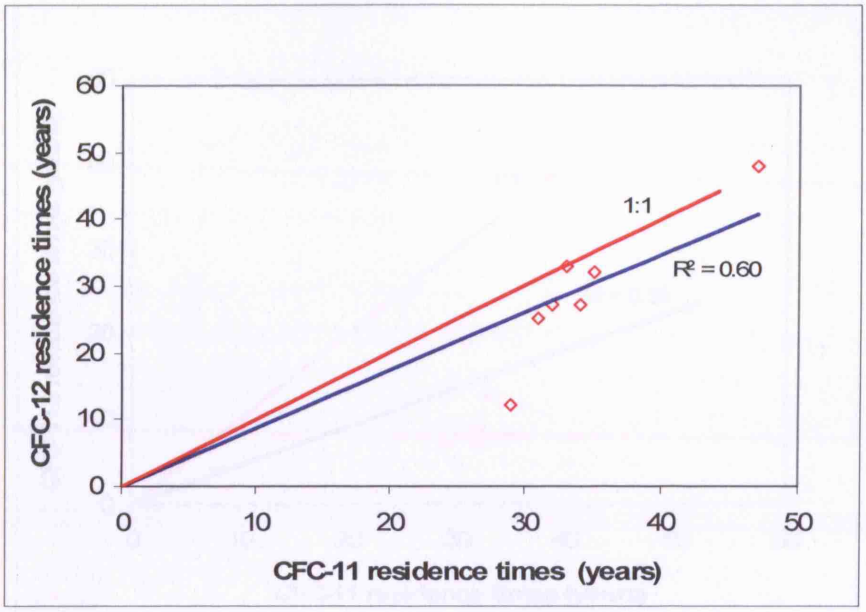

Figure 6.20. Plot of CFC-12 versus CFC-11 residence times for groundwater of the River Mitano catchment

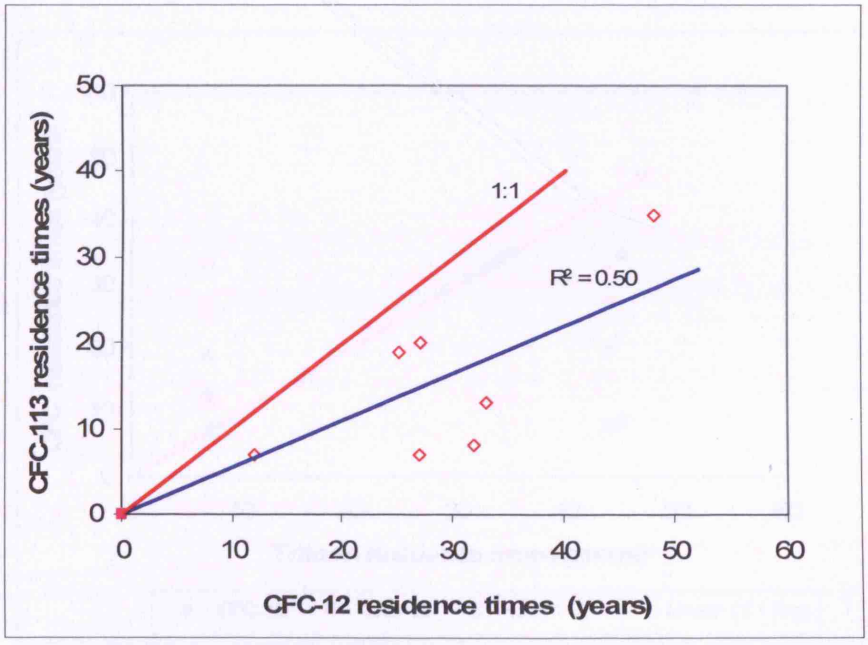

Figure 6.21. Plot of CFC-113 versus CFC-12 residence times for groundwater of the River Mitano catchment

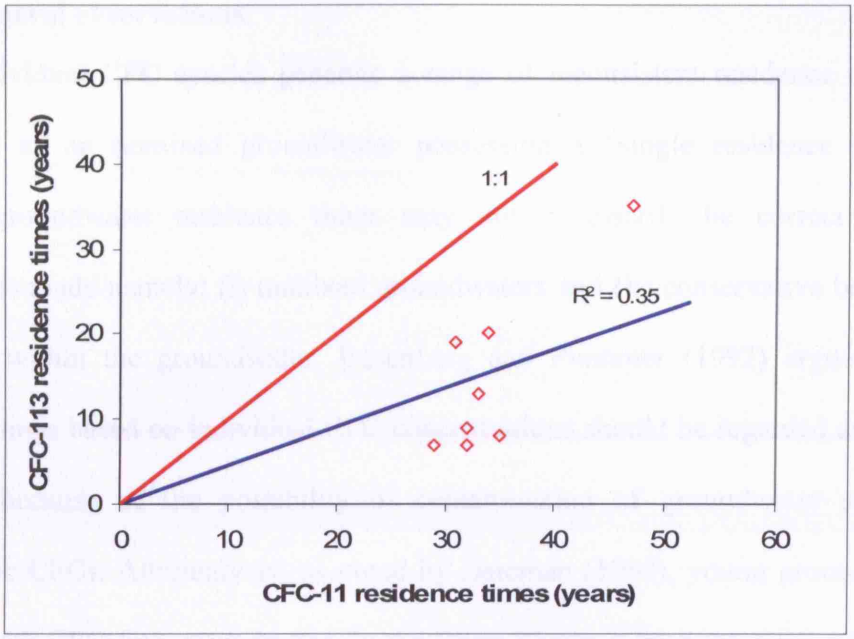

Figure 6.22. Plot of CFC-113 versus CFC-11 residence times for groundwater of the River Mitano catchment

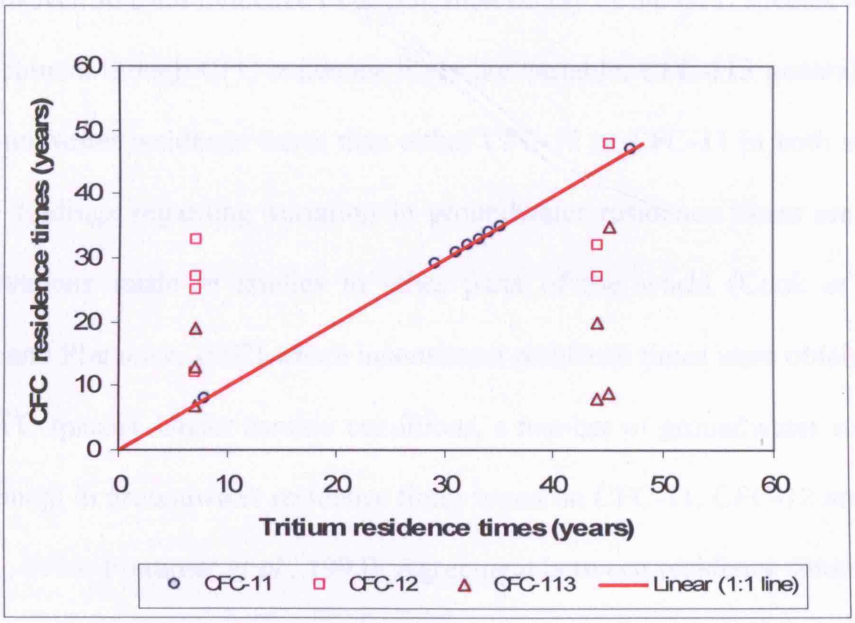

Figure 6.23. Plot of CFC versus tritium residence times for groundwater of the River Mitano catchment

6.7.1.3 General observations

Individual CFC species generate a range of inconsistent residence times when interpreted as an unmixed groundwater possessing a "single residence time". The assigned groundwater residence times may not necessarily be correct given the assumptions made namely; (i) unmixed groundwaters and (ii) conservative behaviour of the CFCs within the groundwater. Busenberg and Plummer (1992) argue that CFC residence times based on individual CFC concentrations should be regarded as minimum estimates because of the possibility of contamination of groundwater samples by atmospheric CFCs. Alternatively, as noted by Bateman (1998), young groundwater can also mix with CFC-free groundwater. In the River Kigwe catchment, CFC-12 and CFC-11 appear to be degraded relative to CFC-113 so that CFC-12 generates the longest groundwater residence times whereas CFC-113 generates the shortest residence times. There is however no clear evidence of degradation of any of the CFC species in the River Mitano catchment though CFC residence times are variable. CFC-113 generally predicts shorter groundwater residence times than either CFC-12 or CFC-11 in both study areas. The above findings regarding variation in groundwater residence times are consistent with observations made in studies in other parts of the world (Cook *et al.,* 1995; Busenburg and Plummer, 1992) where inconsistent residence times were obtained using a range of CFC species. Under aerobic conditions, a number of groundwater studies show good agreement in groundwater residence times based on CFC-11, CFC-12 and CFC-113 (Katz *et al.,* 1995; Plummer *et al.,* 1993). Agreement between residence times from CFC and those obtained with other environmental tracers indicate lack of degradation of CFCs under such conditions.

6.7.1.4. Testing groundwater residence times indicated by individual CFC species (non-mixing model) with ^3H

Groundwater residence times estimated from individual CFCs were tested against observed ^3H concentrations in precipitation and groundwater using tritium record in rainfall to predict tritium in groundwater at the time of sampling. Good agreement between predicted and measured tritium would demonstrate the validity of the single-age unmixed model that was assumed in deriving CFC residence times. ^3H concentrations in precipitation during recharge years predicted by CFCs were obtained from the reconstructed tritium time series for Entebbe. The non-mixing model assumes that the recharge of these groundwaters is of a single age and that the only process that has occurred since recharge, is radioactive decay. ^3H concentrations in precipitation were adjusted by first-order decay to the year 2000 and 2005 when groundwater was sampled in the River Kigwe and the River Mitano catchments respectively. The resulting tritium concentrations were assumed to represent the tritium concentrations that would be found in groundwater recharged by the various precipitation events. The reconstructed ^3H concentrations in precipitation were therefore considered as the input tritium concentration from precipitation.

a) River Kigwe catchment

Results for the River Kigwe catchment are presented in Table 6.6. There are significant discrepancies between predicted tritium derived from the non-mixing model and observed tritium in groundwater (Fig. 6.24). Only 21% of the 14 sources sampled

show agreement (<0.5 difference) between predicted and observed tritium. The results confirm that a 'single-age' unmixed model based on piston flow for groundwater residence times in the River Kigwe catchment does not adequately reconcile observed concentrations of CFCs and tritium. Interestingly, a reasonable agreement between predicted and observed tritium concentrations is obtained for groundwaters with a relatively short residence time. Agreement deteriorates for groundwaters with longer estimated residence times.

Table 6.6. Comparison of predicted (from CFC-113) and observed tritium concentrations in groundwater of the River Kigwe catchment

Sample no.	Site name	Tritium age (yrs)	CFC-113 age (yrs)	Expected ^{3}H in recharge precipitation (TU)	Predicted ^{3}H in GW (2005) (TU)	Observed ^{3}H in GW(2005)
2	Piezometer 2		13	4.1	2.0	1.7
4	Piezometer 4		14	4.0	1.8	0.1
5	Katik Com.Centre	16	15	4.2	1.8	1.1
7	Bukeeka	22	27	12.8	2.8	0.1
8	Mosque	4	13	4.1	2.0	1.4
9	Sikanusu	12	15	11.9	5.1	1.9
12	Monde	51	18	4.6	1.7	0.3
13	Tweyanze	22	19	5.3	1.8	1.2
17	Kikoma	21	18	4.6	1.7	0.6
19	Busula.	5	18	4.6	1.7	1.5
22	Kaswa	7	14	4.0	1.8	1.3
24	Saku S.S.	3	19	5.3	1.8	2.7
29	Wobu Public Sch	1	11	3.8	2.0	0.4
30	Wobu Parents Sch	12	25	17.3	4.2	1.3

GW – groundwater; PW – production borehole

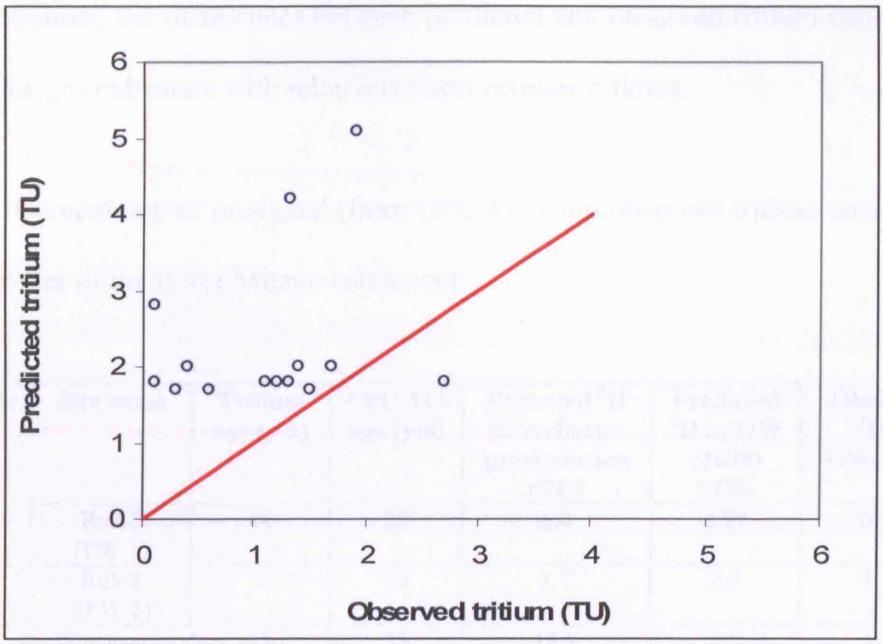

Figure 6.24. Predicted versus observed tritium in single-age groundwater in the River Kigwe catchment

b) River Mitano catchment

Results for the River Mitano catchment are presented in Table 6.7. The predicted tritium and observed tritium in groundwater in the River Mitano catchment differ but the discrepancy is less than observed in the River Kigwe catchment (Fig. 6. 25). 44 % of the 9 sources sampled show agreement (<0.5 difference) between predicted and observed tritium. Although the results show that a 'single-age' unmixed model does not fully reconcile observed concentrations of CFCs and tritium in the River Mitano catchment they suggest that the non-mixing model can provide reasonable estimates of groundwater residence times in this catchment. The above observations are consistent with findings by Morris *et al.* (2006) that tracer samples in an intergrannular aquifer system were most meaningfully interpreted as bulk ages assuming piston flow. As observed in the River

Kigwe catchment, the differences between predicted and observed tritium concentrations are small for groundwaters with relatively short residence times.

Table 6.7. Comparison of predicted (from CFC-113) and observed tritium concentrations in groundwater of the River Mitano catchment

Sample no.	Site name	Tritium age (yrs)	CFC-113 age (yrs)	Expected ^3H in recharge precipitation (TU)	Predicted ^3H in GW (2005) (TU)	Observed ^3H in GW(2005)
1 [a]	Ruk 5 (PW 1)	44	20	6.0	1.97	0.92
2 [a]	Ruk 8 (PW 2)	7	19	5.7	2.0	1.22
3 [b]	Kinyasano	45	35	18.9	2.6	0.51
4 [a]	Piezometer 3	8				1.38
5 [a]	Piezometer 1	7	7	1.8	1.24	1.23
6 [a]	Piezometer 4	44	8	2.3	1.47	0.99
7 [b]	Rwarubira	7	13	3.2	1.54	1.18
8 [a]	Piezometer 2	8				1.33
9 [a]	Piezometer 5	7	7	1.8	1.24	1.24
10 [a]	Piezometer 7	17				1.59
11 [b]	Immaculate	26				2.11
12 [a]	Piezometer 8	45	9	2.1	1.25	0.36

GW – groundwater; PW – production borehole, 1[a]- samples from alluvial aquifer, 1[b] – samples from fractured-bedrock aquifer

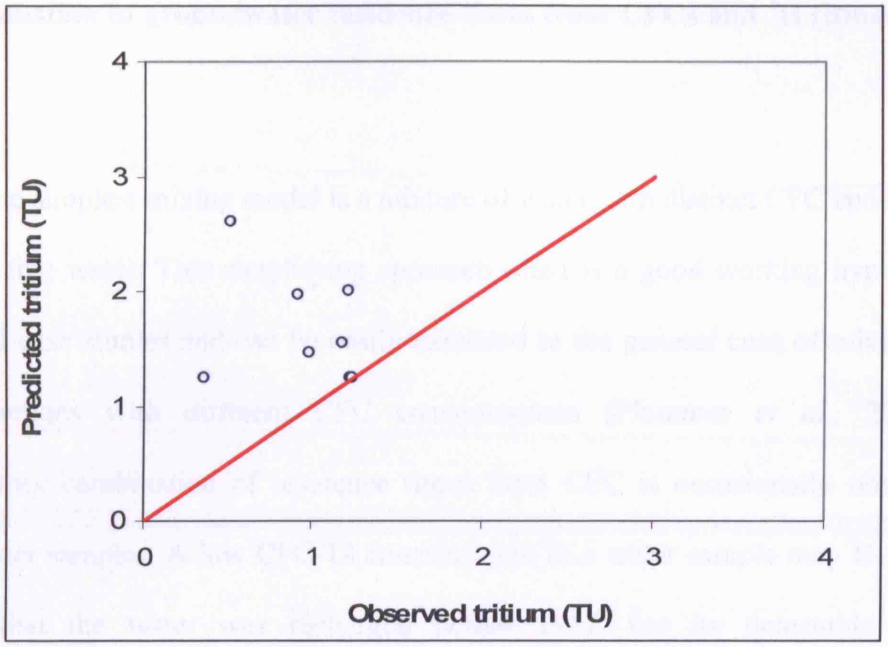

Figure 6.25. Predicted versus observed tritium in single-age groundwater in the River Mitano catchment

Discrepancies between predicted tritium derived from the non-mixing model and observed tritium in groundwater in both the River Kigwe and Mitano catchments confirm that a 'single-age' unmixed model is not well reconciled to observed concentrations of CFCs and tritium. However, the non-mixing model appears to provide more reasonable estimates of groundwater residence times in the River Mitano catchment than in the River Kigwe catchment. The characteristic pattern of shorter residence times for CFC-113 and longer residence times for CFC-12 or CFC-11 may quantitatively indicate mixing processes but does not provide information on actual residence times of different water fractions (Plummer *et al.,* 2006). Residence times from tritium are however generally higher than residence times from CFCs in the two study areas.

6.7.2 Estimation of groundwater residence times from CFCs and ^{3}H (Binary mixing model)

The simplest mixing model is a mixture of water with distinct CFC concentrations and CFC-free water. This simplifying approach often is a good working hypothesis for many real case studies and can be easily extended to the general case of mixing of two water fractions with different CFC concentrations (Plummer *et al.,* 2006). A contradictory combination of residence times from CFC is occasionally observed for groundwater samples. A low CFC-12 concentration in a water sample may for example, indicate that the water was recharged before 1957, but its detectable CFC-113 concentration indicates recharge after 1957. The contradicting combination of residence times from CFC species and tritium may point to and be reconciled by mixing (Plummer *et al.*, 2006; Gooddy *et al.,* 2006).

Based on extensive work in the fractured rocks of South Africa, Talma and Weaver (2003) noted that application of CFCs to estimate groundwater residence times is problematic because water encountered at discrete sampling points typically consists of water parcels that have moved along different pathways (e.g. fracture sets). Groundwater samples necessarily represent a mixture of water with different residence times. Talma and Weaver (2003) demonstrate using CFC with radioactive isotopes (^{3}H, ^{14}C) that additional tracers can be used to assess and quantify effects of mixing. Macdonald *et al.* (2003) however suggest that assumptions have to be made when interpreting CFC data as is done with all groundwater dating methods. They argue that groundwater in fractured aquifers, where flow within several fractures dominates, can be assumed to be a mixture of two members; modern water recharged within the last 10 years and old water with no

detectable CFC concentrations with a residence time greater than 50 years. This assumption enables CFC results to be presented in terms of the apparent percentage of modern water present.

Determination of mixing proportions of young and old water was carried out based on procedures proposed by Plummer *et al.* (1993). Straight lines were drawn through points representing water samples to cut the AWEL at 2 points. The lower point where the straight line cuts the AWEL marks the lower recharge date and hence represents old groundwater whereas the upper point where the straight line cuts the AWEL marks the upper recharge date and hence represents young groundwater. Based on the relative lengths between the water sample point and each of the points where the straight line cuts the AWEL, the relative proportions of the young and old components in the water sample were determined. In some cases, more than one straight line was drawn through a groundwater sample point indicating that there is more than one possible combinations of water mixtures that can generate a particular groundwater sample. The lower and upper recharge dates determined from the AWEL were used to determine the tritium concentrations in precipitation at the time of recharge during those particular years. The assumption was that tritium in those two years mixed in different proportions to generate a tritium concentration of groundwater represented by the measured sample. The resultant tritium concentrations for the young and old components were multiplied by the respective estimated proportions of young and old components to generate a predicted tritium concentration in a groundwater sample.

6.7.2.1 River Kigwe catchment

The CFC-113 versus CFC-11 tracer plot was used in the analysis for the River Kigwe catchment (Fig. 6.26) because results of this study suggest that CFC-12 is more degraded that CFC-11. The straight lines drawn through samples and cutting the AWEL at 2 points are shown in the plot. As many lines as possible can be drawn through each of the points to cut the AWEL at 2 points. For practical purposes, lines that would give recharge dates that vary by at least 2 years were drawn through the points. The relative lengths between the sample and each of the points where the straight line cuts the AWEL, the relative proportions of the young and old components in the water sample and the predicted and observed tritium contents are presented in Table 6.8.

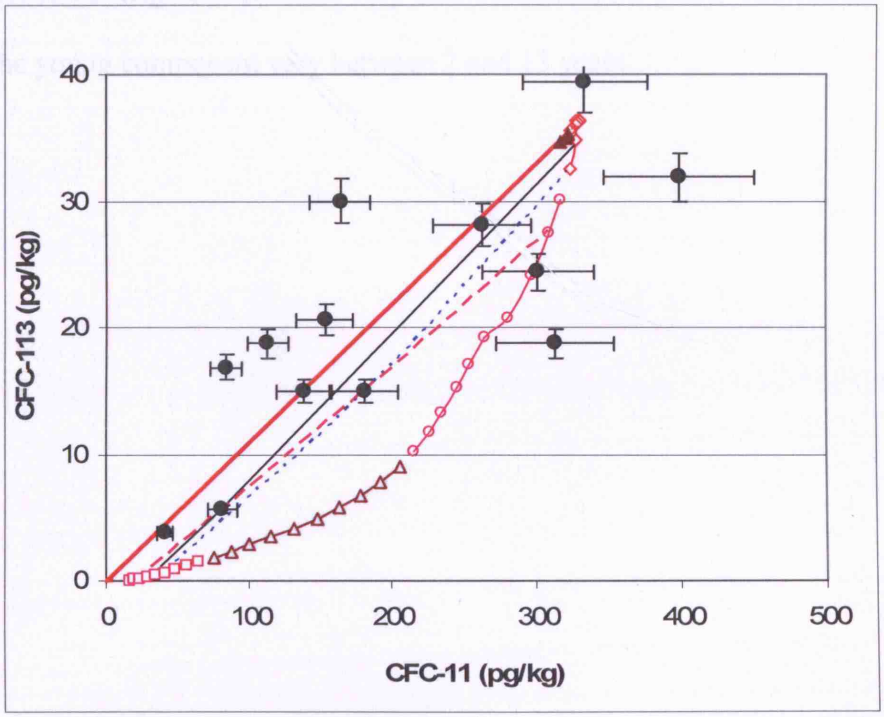

Figure 6.26. Groundwater mixing lines on CFC-113 versus CFC-11 plot for the River Kigwe catchment

Interpretations of CFCs based on the mixing model result in improved agreements between predicted and observed tritium in the River Kigwe catchment. Five of the nine sources analysed show good agreement (<0.5 difference) between predicted and observed tritium (Fig. 6.27). Best agreements between the predicted tritium and observed tritium concentrations were obtained in samples where shorter residence times (i.e. <12 years) represent the dominant component of the sample or is roughly equivalent to that of the water. This is further substantiated by the observation that the predicted and observed tritium contents are in reasonable agreement in the non–mixing model for groundwaters with short residence times. The percentage of young water in the samples ranged between 11 and 100 %. Based on the analysis using binary mixtures, the groundwater residence times in the River Kigwe catchment vary between 2 and 41 years whereas the residence times of the young component vary between 2 and 13 years.

Table 6.8. Comparison of predicted tritium with observed tritium in groundwater based on binary mixtures in the River Kigwe catchment. Straight lines drawn through each of the sample points give the sample number and subscript.

Sample and straight line nos.	Site name	Range of recharge dates (yrs)	Young proportion	Old proportion	Predicted ^{3}H in GW (2000) (TU)	Observed ^{3}H in GW(2000) (TU)
7	Bukeeka	1960 - 1995	0.11	0.89	0.97	0.1
8	Mosque	1988	1		1.5	1.4
9	Sikanusu	1987	1		1.4	1.3
13a	Tweyanze	1961 - 1988	0.56	0.46	1.5	1.2
13b	Tweyanze	1969 - 1990	0.48	0.52	2.4	1.2
22	Kaswa	1959 - 1998	0.78	0.22	1.6	1.3
24	Saku	1959 - 1998	0.42	0.58	1.5	2.7
30a	Wob. Par Sch	1962 - 1988	0.20	0.80	2.6	1.9
30b	Wob. Par Sch	1965 - 1997	0.16	0.84	8.2	1.9

GW – groundwater

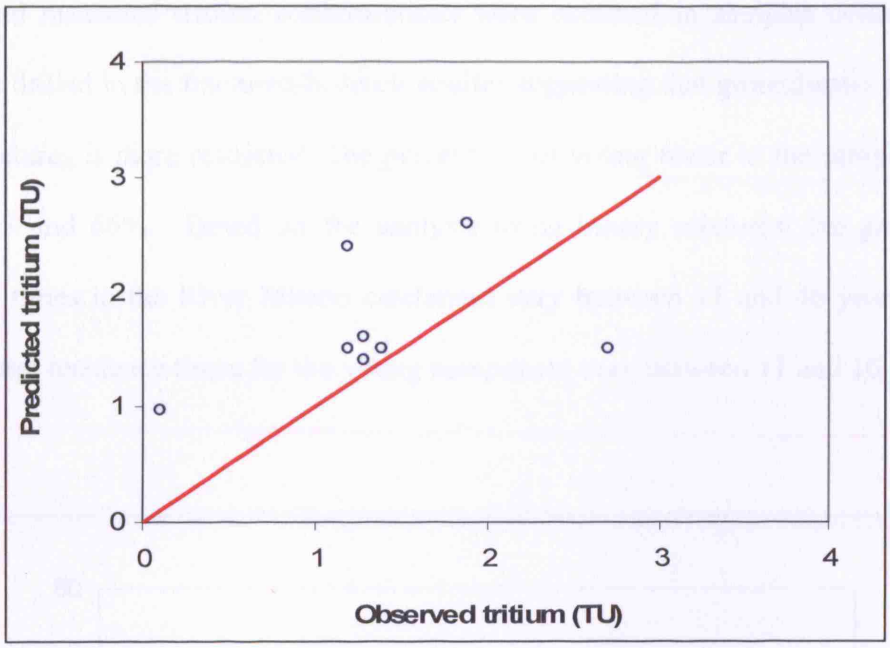

Figure 6.27. Predicted versus observed tritium in binary groundwater mixtures in the River Kigwe catchment

6.7.2.2 River Mitano catchment

The CFC-113 versus CFC-12 tracer plot was used in the analysis for the River Mitano catchment (Fig. 6.28). The relative proportions of the young and old components in the groundwater sample and the predicted and measured tritium concentrations are presented in Table 6.9. Interpretations of CFCs based on the mixing model in the River Mitano catchment also result in improved agreements between predicted and observed tritium. Four of the seven sources analysed show good agreement (<0.5 difference) between predicted and observed tritium (Fig. 6.29). Best agreements between the predicted tritium and observed tritium concentrations were obtained in samples collected from boreholes drilled in the fluvial aquifer. Poor agreements between the predicted

tritium and measured tritium concentrations were obtained in samples collected from boreholes drilled in the fractured-bedrock aquifer suggesting that groundwater circulation in the fractures is more restricted. The percentage of young water in the samples ranged between 5 and 66%. Based on the analysis using binary mixtures, the groundwater residence times in the River Mitano catchment vary between 11 and 46 years whereas groundwater residence times for the young component vary between 11 and 16 years.

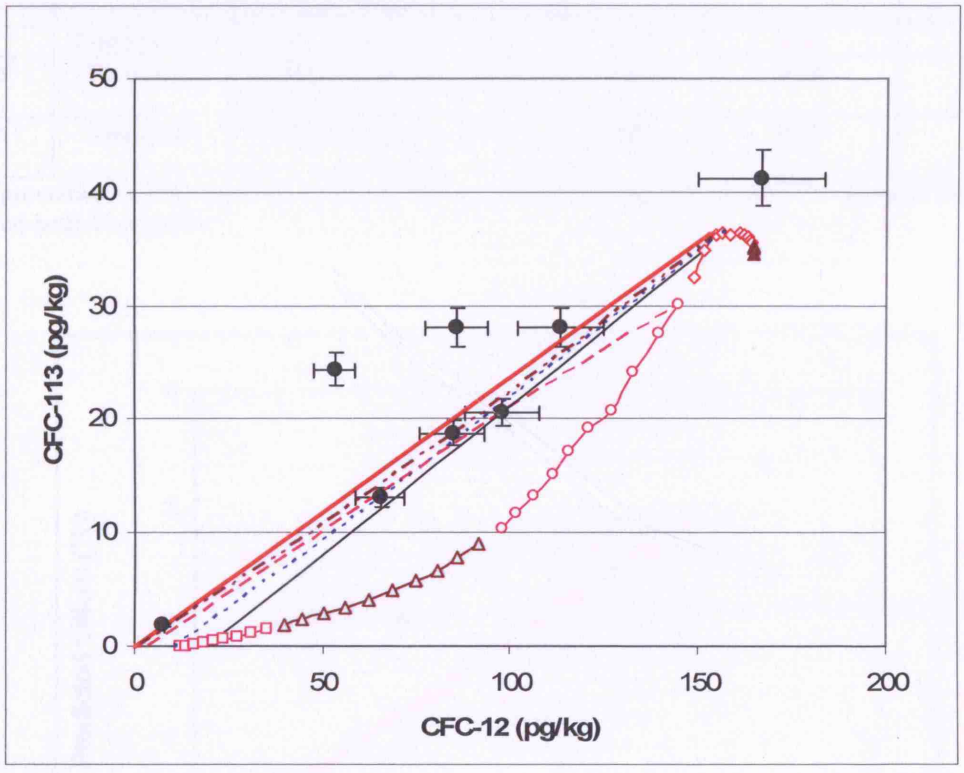

Figure 6.28. Groundwater mixing lines on CFC-113 versus CFC-12 plot for the River Mitano catchment

Table 6.9. Comparison of predicted tritium with observed tritium in groundwater based on a two-component mixture in the River Mitano catchment

Sample and straight line nos.	Site name	Range of recharge dates (yrs)	Young fraction	Old fraction	Predicted ^{3}H in GW (2005) (TU)	Observed ^{3}H in GW(2005) (TU)
1^{a}	Ruk 5 (PW 1)	1961 - 1992	0.53	0.47	1.00	0.92
2^{a} a	Ruk 8 (PW 2)	1965- 1991	0.58	0.42	2.01	1.22
2^{a} b	Ruk 8 (PW 2)	1961 - 1989	0.66	0.34	1.10	1.22
3^{b}	Kinyasano	1959 – 1993	0.05	0.95	0.68	0.51
5^{a}	Piezometer 1	1959 – 1994	0.25	0.75	1.10	1.23
7^{b} a	Rwarubira	1963 – 1990	0.38	0.62	4.78	1.18
7^{b} b	Rwarubira	1959 - 1988	0.46	0.54	0.85	2.18

GW – groundwater; PW – production borehole 1^{a}- samples from alluvial aquifer, 1^{b} – samples from fractured-bedrock aquifer

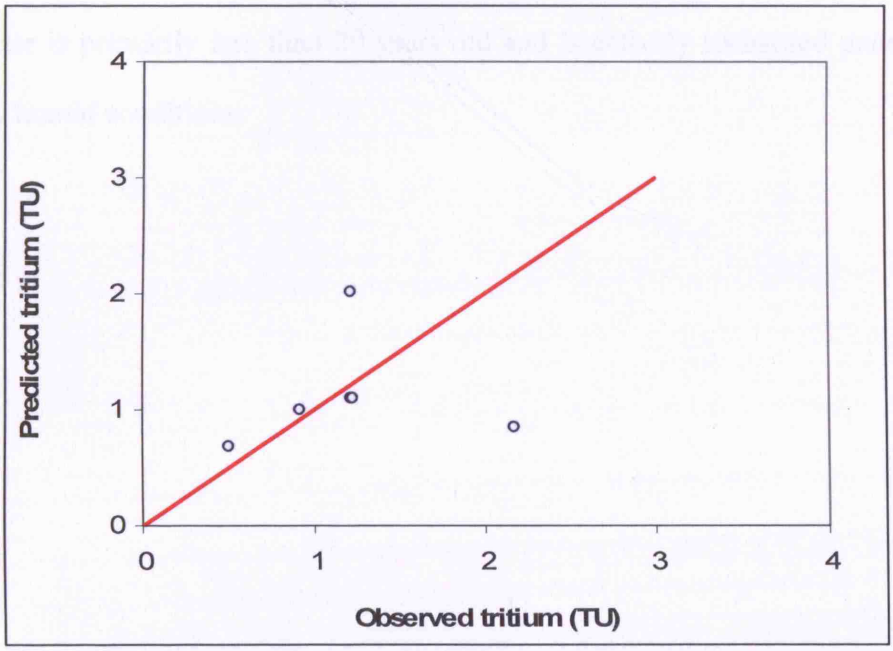

Figure 6.29. Predicted versus observed tritium in binary groundwater mixtures in the River Mitano catchment

Interpretations of CFCs based on the mixing model result in improved agreement between the predicted and the measured tritium in the River Mitano catchment with some notable exceptions from the fractured-bedrock aquifer. However for the River Kigwe catchment the predicted tritium values were improved over the single-age model but remain biased towards higher values than measured. The results obtained using the binary mixing model suggests that groundwater residence times in both study areas range between 2 and 46 years. Residence times in the River Mitano catchment are generally longer than in the River Kigwe catchment.

The binary mixing model yields estimates of the fraction of young water in the mixture and residence times of the young fraction. The percentage of young water in all the samples ranges between 5 and 100% whereas the groundwater residence times for the young water vary between 2 and 16 years. The results of this study therefore show that groundwater is primarily less than 20 years old and is actively recharged under current seasonally humid conditions.

6.7.3 Estimation of groundwater residence times from CFCs and tritium using Lumped Parameter Modelling

Lumped-parameter models have been used effectively for more than two decades to determine groundwater residence times from tracers such as CFCs and tritium (e.g. Maloszewski and Zuber, 1982; Cook *et al.*, 2003; Katz *et al.*, 2004; Viville *et al.*, 2006). Zuber *et al.*(2004) employed a lumped-parameter approach using several models that include Exponential model (EM), Exponential-Piston flow model (EPM) and Dispersion model (DM) in order to interpret ^{3}H concentrations in Jurassic limestone and Tertiary sand aquifers. Koh *et al.* (2006) employed lumped-parameter models to distinguish water recharged before the 1950s from young water using ^{3}H and CFC-12 concentrations. Comparison of measured concentrations of ^{3}H and CFC-12 with theoretical curves for the DM and EM showed that groundwater was highly mixed. Low concentrations of ^{3}H and CFC-12 were indicative of binary mixing of old groundwater with negligible ^{3}H and CFC-12 and young groundwater.

Lumped-parameter modelling ignores spatial variations in parameters and assumes that the system is homogeneous. All parameters affecting residence times are lumped into a single "system response function". Lumped-parameter models compare input and output signals of the concentrations of environmental tracers in groundwater systems assuming various residence time distribution models (Fig. 6.30) to estimate the mean residence time of water in the system (Maloszewski and Zuber, 1982; Amin and Campana, 1996; Cook and Böhlke, 2000; Ozyurt and Bayari, 2005). The relation between the input tracer concentration (C_{in}) and the tracer concentration in the sampled water (C) is given by the following convolution integral (eq. 6.5):

$$C(t) = \int_{-\infty}^{t} C_{in}(t')\, g(t-t') \exp[-\lambda(t-t')]\, dt' \qquad \text{(eq. 6.5)}$$

t : time of sampling
C(t') : input concentration
t' : time of entry
t-t' : transit time
g(t–t') : response function or residence time distribution of tracer.
λ : radioactive decay constant (for a non-radioactive tracer, λ= 0)

The response function represents the normalised output concentration (i.e. the concentration divided by the injected mass) which results from an instantaneous injection of a conservative tracer at the inlet. The response function defines the type of model whereas the parameters of the model are determined by calibration through fitting calculated concentrations to the observed concentrations. A good fit between the model produced and observed data means that the system response function represents satisfactorily the observed distribution in groundwater residence times (Ozyurt and Bayari, 2005).

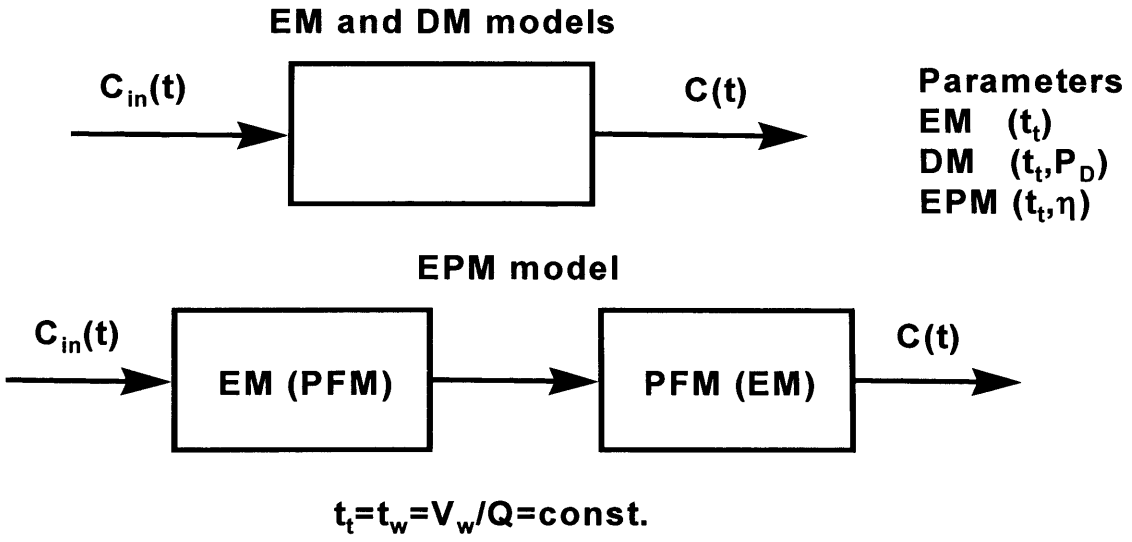

Figure 6.30. Schematic presentations of groundwater systems in the lumped-parameter approach (adapted from Maloszewski and Zuber, 1996)

Detailed information about lumped parameter models, their use, assumptions, fitting parameters and weighting functions are available from (Maloszewski and Zuber, 1982) and only brief description of the EM model is presented here.

Exponential model

The EM assumes groundwater flow lines have an exponential distribution of transit times (Maloszewski and Zuber, 1996). The shortest flow line has a theoretical transit time equal to zero and the longest flow line has a transit time equal to infinity. The EM assumes that there is no exchange of tracer between the flow lines, and that the following response function, mathematically equivalent to the response function of a well-mixed reservoir, is obtained (eq. 6.6):

$$g(t-t_*') = t_t^{-1} \exp(-(t-t_*')/t_t) \qquad \text{(eq. 6.6)}$$

t_t : earlier time
t : time of sampling
t_*' : time of entry
$t - t_*'$: transit time of tracer
$g(t - t_*')$: response function or residence time distribution of tracer.

Maloszewski and Zuber (1996) argue that if there are tracer exchanges between the flow lines with an exponential distribution of travel times, its distribution is described by a dispersion model. Maloszewski and Zuber (1996) suggest that understanding all effects that may lead to differences between the tracer response function and the distribution of flow lines is key to proper interpretation of tracer data. An EM further assumes that mixing occurs only at the sampling site. The mean transit time (age) of tracer is the only parameter of the EM, which defines the whole transit time distribution (Fig. 6.31). Maloszewski and Zuber (1996) argue that the response

function of the EM shows that the model is applicable only to systems in which there are short flow lines and hence, transit times. Thus, the EM is not applicable when samples are taken from very deep aquifers so that residence times obtained in such a situation are a rough approximation. Maloszewski and Zuber (1996) suggest that the real situation can be described more adequately by either the EPM or the DM although no unique solution is available.

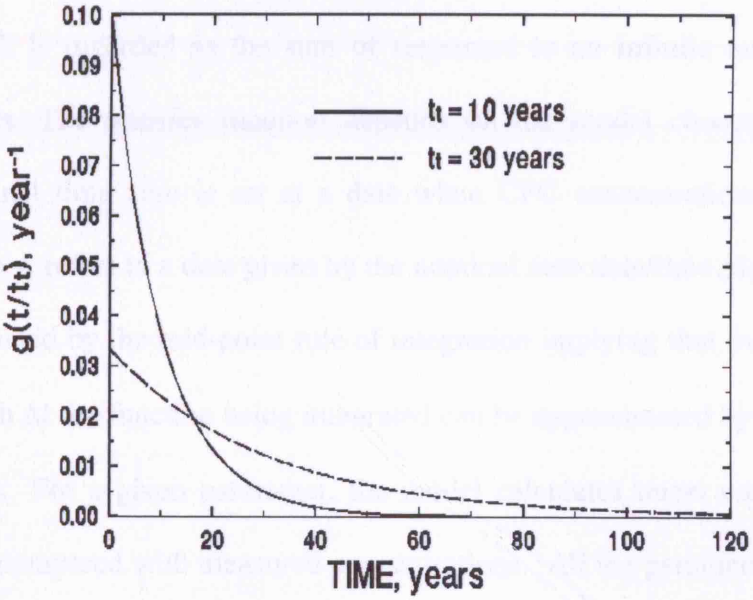

Figure 6.31. Examples of response functions of the exponential model (EM) (adapted from Maloszewski and Zuber, 1996)

Lumped parameter modelling was carried out using a DOS-based program, FLOWPC (Malosweski and Zuber, 1992) and Visual Basic Code in Microsoft Excel written by Barker (2006). The Excel macro program was used to test the results of FLOWPC. FLOWPC calculates output concentration as a function of time for a chosen environmental tracer, chosen model type, and assumed parameters using either a known input function or an input function determined from the available

precipitation rates, tracer concentration in precipitation and infiltration coefficient. The values of parameters are varied on a step by step basis until a best fit between the calculated and measured tracer concentrations are obtained.

The macro Excel program by Barker (2006) solves the exponential equation using tracer input functions. A groundwater system is considered as having a transfer function, which is the response to an instantaneous input at time zero (Barker, 2006). The output is determined for any input function as a weighted mixture (convolution) which is regarded as the sum of responses to an infinite number of instantaneous inputs. The transfer function depends on the model chosen. During modelling a nominal time zero is set at a date when CFC concentrations were still negligible. Time, t, refers to a date given by the nominal zero date/time plus t. The convolution is estimated by the mid-point rule of integration implying that over any time interval of length Δt the function being integrated can be approximated by the value at the central point. For a given parameter, the model calculates tracer concentrations which are then compared with measured concentrations. All the parameters were fixed and only the exponential decay constant was varied through trial and error until CFC concentrations that are similar to those measured in groundwater were obtained. Modelling of ^{3}H utilized the reconstructed ^{3}H concentrations in precipitation at Entebbe as described in Section 6.3.2. Modelling of CFCs utilized the calculated mixing ratios of the CFC species in rain-fed recharge in Uganda as input function as described in Section 6.3.1.

6.7.3.1 River Kigwe catchment

Groundwater residence times from tritium and CFC-113 for groundwaters in the River Kigwe catchment derived from modelling using FLOWPC and Excel Macro programs are summarized in Table 6.10. Groundwater residence times based on tritium using FLOWPC range between 24 and 44 years and are about double those from CFC-113 using FLOWPC in most of the samples. Residence times from tritium derived from FLOWPC are however less than twice those derived from Excel.

Residence times from CFC-113 based on FLOWPC range between 2 and 15 years whereas those based on Excel range between 9 and 31 years. The residence times from CFC-113 based on FLOWPC are lower than those based on Excel in all the samples except one which is from a spring (no. 9). Interestingly, this sample was the only one that plotted on the AWEL on the CFC-113 versus CFC-11 plot (Fig. 6.11) suggesting that it results from a single-age unmixed groundwater.

The residence times derived from FLOWPC are lower than those obtained from Excel possibly because they are based on the estimated proportions of the young component whereas those from Excel do not consider the mixing proportions. The similarity in the residence time estimate derived from FLOWPC and that derived from Excel for sample no. 9 appears to confirm the earlier observation that this sample results from unmixed groundwater. The estimated residence time of 15 years derived from EM is consistent with the earlier estimate of 14 years from the single-age unmixed model. However, this sample showed poor agreement between the predicted and observed tritium values when interpreted as a non-mixing model but showed very good agreement when interpreted as a binary mixing model.

The discrepancy between predicted and observed tritium in the non-mixing and binary mixing models may stem from uncertainty in the reconstructed ^{3}H input

function. Based purely on CFCs, the groundwater flow mechanism in the aquifer represented by sample no. 9 appears to be predominantly piston flow. Samples no. 13 and 30 which plotted in the zone of mixing on the CFC-113 versus CFC-11 plot have similar residence times (15 and 14 years) which are lower than those determined from the single-age model (17 and 25 years). These samples exhibit poor agreements between predicted and observed tritium values with the non-mixing but improved agreements with the binary mixing model. The results confirm the earlier observation from the CFC-113 versus CFC-11 plot (Fig. 6.11) that groundwater flow in the two samples can be explained by mixing. Samples no. 7 and 22 which plotted on the binary mixing line on the CFC-113 versus CFC-11 plot have groundwater residence times of 12 and 5 years respectively compared to residence times of 27 and 14 years respectively from the single-age unmixed model. These samples showed poor agreement between predicted and observed tritium with a single- age model but good agreements with the binary mixing model. It appears therefore that the groundwater flow in the two samples can be better explained by binary mixing than exponential model implying that the groundwater residence times from EM are slightly inaccurate. The results of EM modelling for the River Kigwe catchment are consistent with those of the binary mixing model which indicate that the residence times of the young component range between 2 and 13 years.

Table 6.10. Groundwater residence times from lumped parameter modelling for the River Kigwe catchment

Sample and straight line nos.	Site name	MRT from tritium (FLOWPC) (yrs)	MRT from CFC-113 (yrs)	
			FLOWPC	Excel
2	Piezometer 2	24	-	10
4	Piezometer 4	-	-	13
5	Katikamu Com.Centre	44	-	20
7	Bukeeka	25	12	-
8	Mosque	31	15	9
9a	Sikanusu	24	14	15
9b	Sikanusu	-	2	-
9c	Sikanusu	-	12	-
9d	Sikanusu	-	7	-
12	Monde	42	13	23
13	Tweyanze	-	15	31
17	Kikoma	35	-	23
19	Busula	-	-	27
22	Kaswa	27	5	12
24	Saku S.S	36	-	31
30	Wob Par Sch	30	14	-

MRT: mean residence time

6.7.3.2 River Mitano catchment

Groundwater residence times from tritium and CFC-113 for groundwaters in the River Mitano catchment derived from modelling using FLOWPC and Excel Macro programs are summarized in Table 6.11. Groundwater residence times from tritium derived from FLOWPC range between 31 and 48 years and are about twice those from CFC-113 using the same program but are in the same order of magnitude with those derived from Excel.

Residence times from CFC-113 based on FLOWPC range between 10 and 22 years whereas those based on Excel range between 15 and 47 years. The residence times from CFC-113 based on FLOWPC are about half those based on Excel in all the samples. As mentioned before the residence times derived from FLOWPC are lower than those obtained from Excel possibly because they are based on the estimated

proportions of the young component whereas those from Excel are not. Samples no. 1, 2, 3, 7 and 9 which plotted close to the binary mixing line on the CFC-113 versus CFC-12 plot have slightly different residence times. Samples no. 1, 2 and 9 have residence times that are predominantly less than 12 years whereas samples no. 3 and 7 have longer residence times (> 15 years). The clustering of the residence times is consistent with the plotting of the samples on the CFC-113 versus CFC-11 plot. Samples no. 1, 2 and 9 plotted closer to recent recharge whereas samples no. 3 and 7 plotted closer to the CFC-free water. The residence times derived from EM are lower than those derived from the single-age model except in samples no. 7 and 9 where they are higher (21 and 10 years).

Residence times from tritium using the single-age unmixed model are similar to residence times from CFC-113 using the same model for samples 7 and 9. These samples showed fairly good agreements between predicted and observed tritium values with the non-mixing model but poor agreements with the binary mixing model. The results appear to suggest that groundwater in samples no. 7 and 9 cannot be adequately explained by mixing. The apparent adherence of these samples to the binary mixing line may result from preferential degradation in CFC-12 or relatively small contamination in CFC-113. Samples 1, 2 and 3 show poor agreements between predicted and observed tritium based on the single-age unmixed model but good agreements with the binary mixing model. However, sample no 3 has longer residence time than samples no. 1 and 2, which is consistent with its location on the mixing line, closer to CFC-free waters. It appears therefore that the groundwater flow in the aquifers represented by the three samples can be explained by mixing but the proportion of the young component is lower in sample no.3 than in samples no. 1 and 2. This observation is consistent with the results of binary mixing which indicate that

the proportion of the young component in sample no. 3 is only 5% compared to 53 and 58% in samples no. 1 and 2. The results of EM modelling for the River Mitano are consistent with those of the binary mixing model which indicate that the residence times of the young component range between 11 and 16 years.

Table 6.11. Groundwater residence times from lumped parameter modelling for the River Mitano catchment

Sample and straight line nos.	Site name	MRT from tritium –(FlowPC) (yrs)	MRT from CFC-113 (yrs)	
			FLOWPC	Excel
1^a	Ruk 5 (PW 1)	47	12	29
2^a a	Ruk 8 (PW 2)	31	10	26
2^a b	Ruk 8 (PW 2)	41	19	26
3^b	Kinyasano	46	15	-
7^b a	Rwarubira	46	21	47
7^b b	Rwarubira	48	22	47
5^a	Piezometer 1	33	10	15
6^a	Piezometer 4	41	12	20
9^a	Piezometer 5	32	10	15
12^a	Piezometer 8	-	-	26

MRT: mean residence time; 1^a – samples from alluvial aquifer; 1^b- samples from fractured- bedrock aquifer

Interpretation of CFC concentrations using the EM based on FLOWPC generates lower groundwater residence times than those based on Excel possibly because FLOWPC considers mixing proportions whereas the Excel code does not. Residence time estimates from tritium are much higher than those derived from CFC-113. Lumped parameter modelling is used to verify groundwater flow processes earlier deduced from the CFC-113 versus CFC-11 and CFC-12 plots. Further evidence for the existence of three groundwater flow processes in the River Kigwe catchment: piston flow, binary mixing and exponential mixing has been provided using EM modelling. The residence times derived from EM range between 2 and 15

years and are consistent with those derived from binary mixing model which range between 2 and 13 years. Although CFC results from EM provide further evidence for the existence of binary mixing in the River Mitano catchment as exhibited in 3 samples, the results indicate that piston flow may exist although it was not indicated on the CFC plot. Residence times derived from EM for the River Mitano catchment range between 10 and 22 years and are consistent with those from the binary mixing model which range between 11 and 16 years. The consistency of the results of EM with those of the theoretical mixing models earlier deduced from the CFC plots suggests that the residence time estimates obtained through EM are representative of the aquifer systems in the two catchments.

6.8 Estimation of storage volumes of groundwater in the Rivers Kigwe and Mitano catchments

Groundwater residence times can be used to estimate the volume of water stored in aquifer (Ozyurt and Bayari, 2005; Viville *et al.*, 2006). In lumped parameter approach, output tracer concentrations are related to input concentrations using a convolution integral (eq. 6.5). The weighting function of the tracer is equal to the weighting function of the infiltrating water if the tracer is conservative and is injected and measured proportionally to the volumetric flow rate and there are no stagnant waters in the system (Zuber *et al.*, 2004). In the case of steady flow, the mean water transit time (T_{Water}) is defined by equation 6.7. Consistent with the procedures employed by Viville *et al.* (2006), eq. 6.7 has been used to estimate the volume of water stored in aquifer systems in both the Rivers Kigwe and Mitano catchments using baseflow estimates and the estimated mean groundwater residence times.

$$T_{Water} = \int_0^{\infty} tg(t)dt = \frac{v}{Q} \qquad \text{(eq. 6.7)}$$

v : volume of mobile water in the system
Q : volumetric flow rate through the system
t : time variable
g(t) : weighting function
T_{Water} : residence time of water

6.8.1 River Kigwe catchment

The catchment area of River Kigwe is 50 km^2, the mean annual baseflow from the catchment, considered to be equal to groundwater recharge is 160 mm (Tindimugaya, 2000), estimated mean groundwater residence time is 8 years and estimated porosity is 0.23. Based on the above parameters, the mean annual discharge from the catchment is estimated to be 8 million m^3 of water and this implies that the total volume of water stored in the aquifer is 64 million m^3. This is equivalent to 1.3 m of water depth and requires 8.5 m thick aquifer to store it. The amount of water stored in the River Kigwe catchment per square kilometre is approximately 1.3 million m^3.

6.8.2 River Mitano catchment

The catchment area of River Mitano is 2089 km^2, the mean annual baseflow from the catchment is 104 mm (Mileham *et al.*, in prep), estimated mean groundwater residence time is 16 years and estimated porosity is 0.10. Based on the above parameters, the mean annual discharge from the catchment is estimated to be 218 million m^3 of water and this implies that the total volume of water stored in the aquifer is 3.5 billion m^3. This is equivalent to 1.7 m of water depth and requires a 16.6

m thick aquifer to store it. The amount of water stored in the River Mitano catchment per square kilometre is approximately 1.7 million m^3.

The estimated water depths of 1.3 and 1.7 m and required aquifer thicknesses of 8.5 and 16.6 m in the Rivers Kigwe and Mitano catchments respectively are feasible and are supported by hydrogeological information (Chapter 4). The aquifers in the two catchments are more than 20 m thick and the estimated amounts of water can easily be stored. The calculated volumes of water stored in aquifers in the two catchments are therefore considered to be good estimates.

6.9 Conclusions

Combined use of the three CFC species and tritium in weathered crystalline rocks in Uganda has made it possible to assess groundwater mixing processes and estimate groundwater residence times as discussed in the sections that follow.

6.9.1 Groundwater mixing processes

The distribution of anthropogenic gases in sampled groundwater in the River Kigwe catchment indicates that three groundwater flow processes operate in the catchment: piston flow in the shallow weathered aquifer, binary mixing in the fractured-bedrock aquifer in areas of high topography and exponential mixing in the fractured-bedrock aquifer in areas of low topography. The existence of the three flow mechanisms has been substantiated through lumped parameter modelling using the exponential model. The distribution of anthropogenic gases in sampled groundwater in the River Mitano catchment suggests that binary mixing is the dominant process in the catchment and recent groundwater recharge is dominant in alluvial aquifers found at low elevations whereas CFC-free groundwater is dominant in fractured-bedrock

aquifers at higher elevations. Although exponential modelling provides evidence for the existence of mixing as earlier deduced, it suggests that piston flow mechanism might also exist.

6.9.2 Groundwater residence times

This study confirms the usefulness of residence-time indicators in investigation of groundwater flow in weathered crystalline basement aquifers. A multi-tracer approach involving use of the three species of chlorofluorocarbons and tritium has made it possible to estimate groundwater residence times and proportions of young water in the Rivers Kigwe and Mitano catchments in Uganda. This approach has involved use of individual CFC species and tritium, binary tracer mixtures and lumped parameter models to generate groundwater residence times. Tritium observed in groundwater was used to constrain inferences from individual CFC species using non-mixing, binary mixing and lumped parameter models although discrepancies between estimates from tritium and CFCs were observed.

Interpretations of CFCs based on the non- mixing model result in inconsistencies between the predicted and the observed tritium implying that a single age, unmixed model is inappropriate to explain the distribution in groundwater residence times in fluvial, weathered and fractured-bedrock aquifers. Interpretations based on the binary mixing model reduces discrepancies between the predicted and observed tritium. The results indicate that the groundwater in the Rivers Kigwe and Mitano catchment is a mixture between young water and CFC-free old water. The proportions of young water range between 5 and 100% and the young water is less than 20 years old. The results show that the mixing model better explains observed concentrations of environmental tracers in the groundwater than an unmixed single-age model. Groundwater residence times derived from lumped parameter modelling

of CFC are consistent with those derived from the binary mixing model but are younger than those generated using non-mixing. Results from the lumped parameter and the binary mixing models suggest that groundwater in the Rivers Kigwe and Mitano catchments is predominantly mixed with a few locations where the groundwater is of a single age. Mean groundwater residence times derived from CFC modelling using the binary mixing and exponential models in the River Kigwe catchment range between 2 and 15 years whereas those in the River Mitano catchment range between 10 and 22 years. Although the groundwater in the River Mitano catchment is slightly older than that in the River Kigwe catchment the fact that groundwater residence times are low (<22 years) suggests that groundwater in the two catchments is young. This is consistent with the big proportions of the young water (5 and 100%) determined through the binary mixing modelling.

Residence times based on CFC are much shorter that those based on ^{3}H. The high variation between residence times based on ^{3}H and those based on CFC could be due to a number of factors including; different input concentrations that are difficult to reconstruct especially for ^{3}H and possible effects on CFC concentrations such as contamination or excess air that may result in much younger ages (Viville, et al., 2006). Although ^{3}H concentrations may not be suitable for determination of groundwater residence times, the ^{3}H data are invaluable when combined with CFC concentrations as demonstrated in this study. Consistency between expected ^{3}H in groundwater, derived from residence times from CFC, and observed ^{3}H concentrations in groundwater has provided greater confidence in the results of CFC modelling.

Although groundwater residence times determined in this study using CFCs are approximate, the fact that they have been corroborated by ^{3}H suggests that they

reasonably represent the groundwater flow in the two catchments. The short residence times (2 to 22 years) suggest that groundwater in the two catchments is young and is actively recharged. The presence of appreciable concentrations of ^{3}H (>1 TU) that are closer to atmospheric concentrations combined with the relatively high proportions of a modern component (>50%) in most of the groundwater samples confirm the connection with an active flow system.

Mean groundwater residence times determined in the Rivers Kigwe and Mitano catchments have been used to estimate the amount of groundwater stored in the aquifers in the two catchments, which can potentially be available for abstraction. Based on a mean groundwater residence time of 8 years estimated in the River Kigwe catchment, the amount of groundwater circulating in the catchment is 64 million m^3, equivalent to 1.3 million m^3 per square kilometre. Similarly, the mean groundwater residence time of 16 years estimated in the River Mitano catchment implies that the amount of groundwater circulating in the catchment is 3.5 billion m^3, equivalent to 1.7 million m^3 per square kilometre. The calculated volumes of water stored in aquifers in the two catchments are considered to be good estimates and are substantiated by field hydrogeological information.

6.9.3 Implications for future use of environmental tracers in weathered crystalline rock aquifers.

There are two important findings of this study related to the use of environmental tracers in weathered crystalline rock aquifer systems. Firstly, although CFCs are normally degraded under anaerobic conditions this study found that CFC-12 in the River Kigwe catchment is degraded despite the groundwater being aerobic. Happell *et al.* (2003) provide evidence for removal of CFCs from recharging groundwater through unconsolidated carbonate marl sediments overlying a carbonate

aquifer, but the removal occurred at the groundwater-surface water interface with anoxic conditions and involved all the CFC species contrary to this study where only CFC-11 and CFC-12 are degraded. Happell *et al.* (2003) attribute the removal of CFCs to methanogenic bacteria. Cook *et al.* (1995) however cautions that the presence of oxygen in groundwater samples in not itself an indication that degradation of chlorofluorocarbons has not occurred somewhere along the flow line and suggest that further study is required to assess how the CFC species are degraded in aerobic conditions.

Similarly, contrary to studies elsewhere (Oster *et al.*, 1996; Shapiro *et al.*, 1997; Semprini *et al.*, 1990) which indicated that CFC-12 is the most stable species, CFC-12 in the groundwaters of the River Kigwe catchment appear to have been degraded and the least stable of the CFC species. Degradation of CFC-12 in tropical aquifers has also been reported in Niger and Tanzania and this finding suggests that preferential degradation of CFC-12 occurs in this environment although the causes of this degradation are currently unknown. CFC-12 will consistently overestimate groundwater ages due to the degradation. Based on the results of the River Mitano catchment, there is no evidence for degradation of any of the CFC species including CFC-12 in fluvial aquifers. The conservative nature of CFC-113 is observed in both the fluvial and weathered and fractured-bedrock aquifers possibly because of low organic content. Thus, use of CFC-12 to estimate groundwater residence times in weathered crystalline rock aquifers should consider the possible effect of degradation and the estimated ages should be compared with those from CFC-11 and CFC-113. Similarly, dating of groundwater should rely more on the other CFC species, most especially CFC-113 which has been found to be stable in both fluvial and weathered and fractured-bedrock aquifers.

Use of ^{3}H in estimating groundwater residence times is problematic. The tritium input function for groundwater is more complicated than that measured in precipitation due to attenuation of seasonal variations and mixing of contributions from more than one year. The groundwater residence times derived from ^{3}H are therefore subject to great uncertainly due to the problems with the input function.

CHAPTER 7: EVOLUTION OF WEATHERED, FRACTURED BEDROCK AND FLUVIAL AQUIFERS IN UGANDA

This chapter discusses the evolution of weathered and fractured, and fluvial aquifers in Uganda. Aquifer evolution is related to landscape development through cycles of deep weathering and stripping (surface erosion) driven by tectonic activity. The chapter correlates hydrogeological characteristics to geomorphic processes using historical information and data obtained from seven areas located within the intra-arch and inter-arch basins of Uganda. The study makes use of the large, and hitherto little used, National Borehole Database (NBD) to investigate regional trends in hydrogeologically significant parameters including regolith thickness, lithology, borehole yield and specific capacity. Field investigations identify, for the first time, a productive fluvial aquifer (borehole yields >5 m^3 h^{-1}) in palaeochannels of former river networks, truncated by the development of the western arm of the East African Rift System from the Miocene to mid-Pleistocene.

7.1 Tectonically controlled landscape and aquifer evolution in Uganda

7.1.1 Landscape evolution and drainage development

The contemporary landscape of Uganda and the whole Great Lakes Region of Africa was largely shaped during the mid-Miocene to Late-Pleistocene period when headwaters of westward flowing river systems were truncated by the western arm of the East African Rift System (Bishop and Trendall, 1967; de Swardt and Trendall, 1969; Doornkamp and Temple, 1966; Doornkamp, 1970). Prior to that, development of the South Atlantic Ocean in the mid-Cretaceous (Bishop and Trendall, 1967; de

Swardt and Trendall, 1969) was followed by eastward incision along a failed rift that resulted in the development of the Congo drainage which extended across equatorial Africa, though Uganda to Kenya. Ugandan rivers such as Kafu, Katonga and Kagera formed headwaters of the Congo basin that flowed in the east-west direction (Fig.7.1). During the Miocene, the proto- East African rift valley began to subside below the then level of the westward flowing streams (Doornkamp and Temple, 1966; Doornkamp, 1970) resulting in the severing of the riverine connection with the Congo Basin. Subsequent tectonic events radically altered the evolution of the regional topography and drainage in western Uganda (Doornkamp and Temple, 1966) with progressive surface upwarping continuing on the eastern flank of the subsiding rift valley from Miocene to early Pleistocene times. The rising warp progressively modified the drainage system, altering patterns of sediment transport and deposition along river channels east of the rift. During Tertiary and post Tertiary times (Doornkamp,1970), the rate of uplift parallel to, but 13 to 33 km east of the rift escarpment, exceeded the rate of river valley incision. This upwarping causing reversal and eastward flow of Kagera, Katonga and Kafu rivers away from a new regional north-south trending drainage divide.

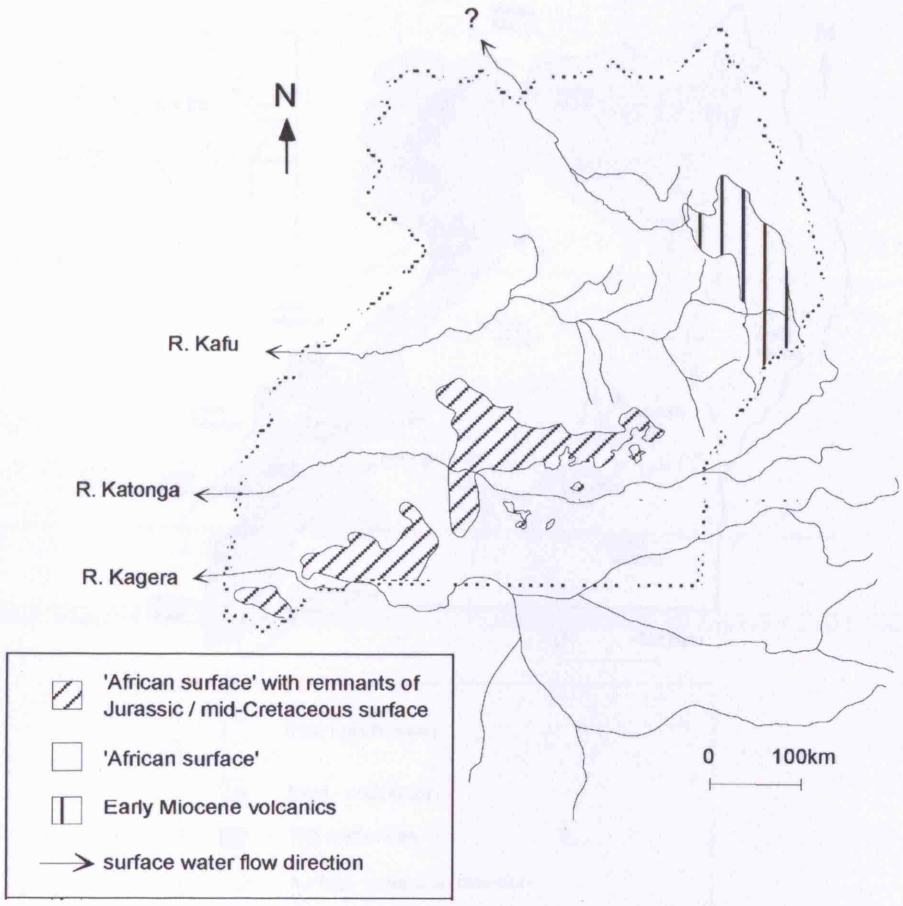

Figure 7.1. Drainage across Uganda before reversal (adapted from Taylor and Howard, 1998)

Due to drainage reversal, rivers between the axis of upwarp and the rift continue to flow westwards toward the rift valley, whereas those east of the axis of upwarp flow east wards towards the lowest points of the basin currently occupied by Lakes Victoria and Kyoga. Veevers (1977) classifies the area east of the axis of uplift (between the Albertine rift in Uganda and the Gregory rift in Kenya) the "inter-arch" basin and that between the axis of uplift and the rift escarpment the "intra-arch" basin (Fig. 7.2).

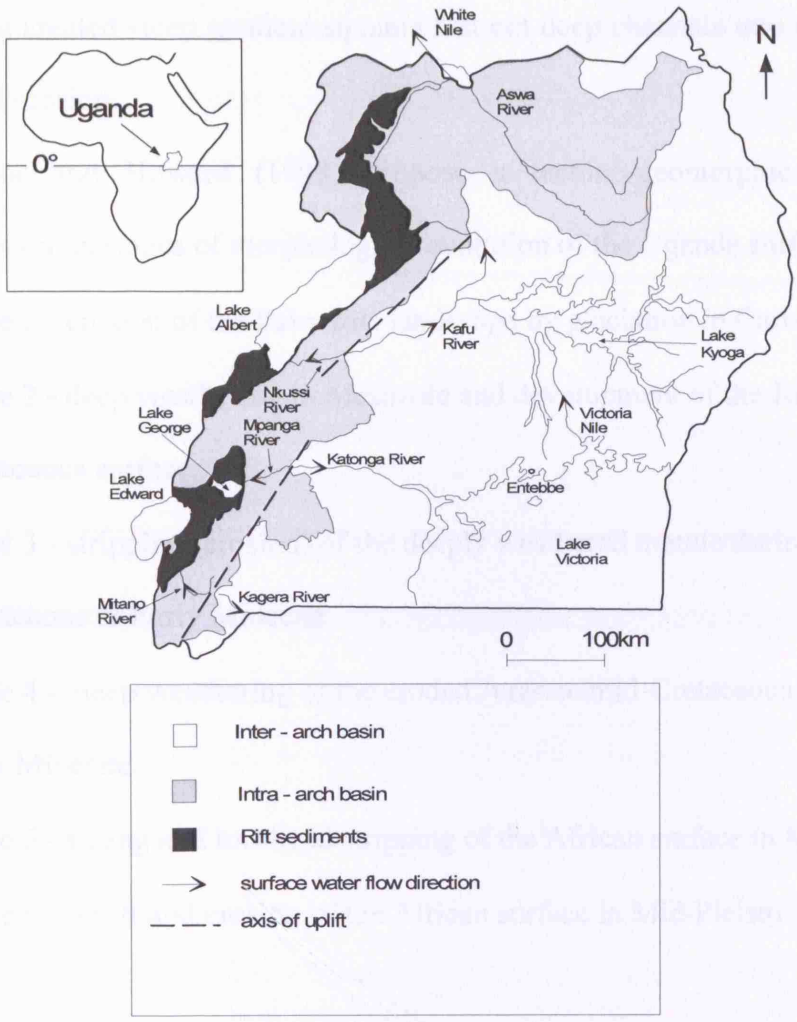

Figure 7.2. The reversed rivers in the intra-arch and inter-arch basins of Uganda (adapted from Taylor and Howard, 1999)

In the inter-arch basin, reduction in relief due to the reversal of the westward tilt led to flooding and sediment aggradation within the wide drainage channels associated with formerly westerly flowing rivers (Doornkamp and Temple, 1966). In the intra-arch basin, the increased relief and falling base levels led to rapid and deep incision of narrow drainage channels into the bedrock (Doornkamp, 1970). The consequential erosion stripped the regolith cover and highlights the polycyclic notion of soil development (Radwanski and Ollier, 1959). The sequence of events outlined above follows the model of Summerfield (1991) of passive margin development

where rifting created steep gradient streams that cut deep channels into rift walls and caused rapid erosion.

Taylor and Howard (1998) propose a tectono-geomorphic model that considers six broad stages of morphological evolution of the Uganda surface.

- Stage 1 - erosion of the Paleozoic landscape by glaciation in Carboniferous
- Stage 2 - deep weathering in Mesozoic and development of the Jurassic/mid-Cretaceous surface.
- Stage 3 - stripping (erosion) of the deeply weathered mantle during the late Cretaceous to Early Miocene
- Stage 4 - deep weathering of the eroded Jurassic/mid-Cretaceous surface in early Miocene.
- Stage 5 - rifting and localized stripping of the African surface in Miocene
- Stage 6 - uplift and erosion of the African surface in Mid-Pleistocene.

The various models of landscape development suggest that long-term evolution of the Ugandan landscape is a result of tectonically controlled cycles of deep weathering and stripping (Taylor and Howard, 1998). Stripping of colluvial and alluvial deposits occurs in areas of tectonically induced rise in relief whereas deep weathering occurs in areas of subsidence and low relief unaffected by tectonic activity.

7.1.2 Development of weathered and fractured-bedrock aquifers

Cycles of deep weathering of the bedrock yield a thick weathered regolith and induce sub-horizontal fissures though isostatic uplift (Taylor and Howard, 2000). Cycles of stripping partially erode the unconsolidated weathered overburden and give

rise to a discontinuous regolith. Stripping also leads to fluvial deposition of coarse-grained clasts in river channels. McFarlane (1992) argues that formation of weathered surfaces occurs through slow subsidence, wherein leaching and eventual collapse of the saprolite dominates over direct erosion by surface run off through these processes may occur together. McFarlane (1992) notes that during dry periods and in areas covered by sparse vegetation, direct soil erosion by surface run off may be significant and may be enhanced in areas with high topographic gradients and where the rainfall is substantial.

The rate at which deep weathering and stripping occur is controlled, in part, by climate (Taylor and Howard, 2000) as this determines the input of precipitation reaching the land surface either as surface runoff or as infiltration. Surface runoff and infiltration are also influenced by topography. The low relief of the inter- arch basin favours infiltration over surface runoff whereas the high relief of the intra-arch basin promotes surface runoff over infiltration. Thus, deep weathering in the inter-arch basin is facilitated by high infiltration whereas stripping in the intra-arch basin is facilitated by high surface runoff (Taylor and Howard, 1999).

The rate and product of weathering and stripping and hence the nature of the resultant aquifers are also controlled in part by geology. Doornkamp (1970) suggests that bedrock lithologies which are more resistant to weathering are less denuded by deep weathering and remain conspicuous by forming ridges. These rocks remain exposed during cycles of stripping whereas the surrounding less resistant and deeply weathered and unconsolidated overburden is eroded. The geology of the inter-arch basin in central Uganda is predominantly made up of granites, granitoid gneisses and gneisses which are commonly referred to as the 'Precambrian Basement Complex'. The long term weathering of these rocks, in the absence of stripping yields fine

grained overburden with low transmissivity but high storage that provides recharge to the underlying fractured aquifer. Land surfaces underlain by these formations have low relief except in a few areas where remnants of more resistant formations such as quartzites and inselbergs are found. In western Uganda, bedrock lithologies are more complex but consist of low-grade metasedimentary rocks composed of quartzites, schists, gneisses and granites of Buganda-Toro rock system and quartzites, shales, phyllites and gneisses of Karagwe- Ankolean rock system.

Gneisses, shales and phyllites are less resistant to weathering as opposed to granites but weather to fine grained weathered overburden. In the intra-arch basin, the weathered cover formations were eroded and deposited along river channels and valleys and form aquifers of variable yields depending on the transport processes. Surfaces of deep weathering in the inter-arch basin are characterised by low relief, a thick weathered regolith, dominance of infiltration over surface run-off, broad valleys with concave slopes and regionally extensive aquifers in the weathered overburden (Fig. 7.3a). Surfaces of stripping in the intra-arch basin are characterised by high and undulating relief, a thin weathered mantle, dominance of surface run-off over infiltration, narrow and highly incised valleys and channels, with convex slopes and localized aquifers (Fig. 7.3b). This evolution of weathered and fractured bedrock aquifers is generally well recognised and understood (McFarlane, 1992; Taylor and Howard, 1998; 2000) but development of fluvial aquifers in palaeochannels of deeply weathered terrains, implied by these models, in the humid tropics has remained largely ignored.

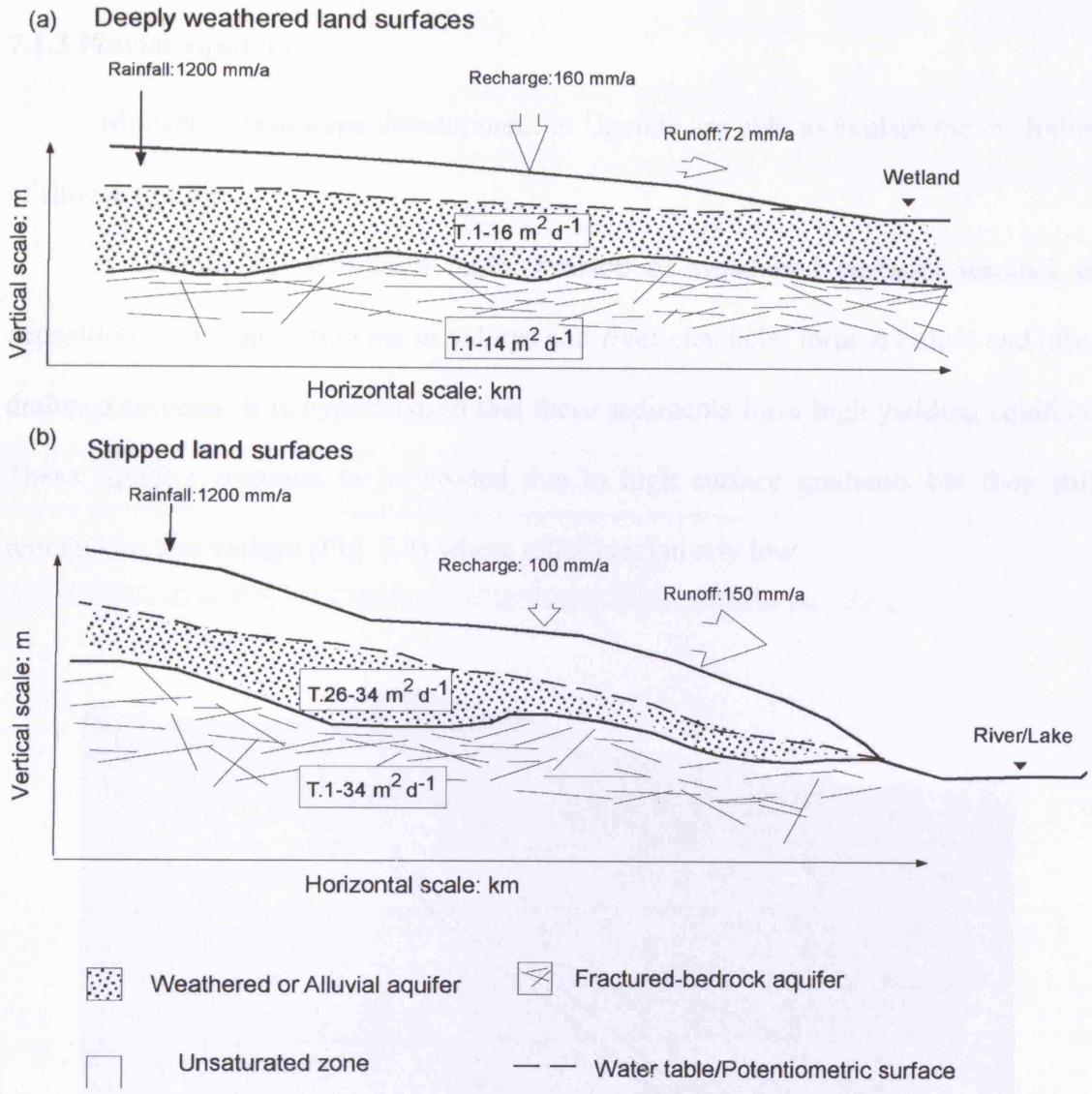

Figure 7.3. Conceptual cross-sectional models of surfaces of deep weathering and stripping based on studies in the Kigwe (Inter-arch) and Mitano (Intra-arch) catchments (modified based on Taylor and Howard, 1998)

7.1.3 Fluvial aquifers

Models of landscape development in Uganda are able to explain the evolution of fluvial aquifers.

a. Within the intra-arch basin, erosion of weathered surfaces resulted in deposition of fluvial sediments in valleys and river channels, formed before and after drainage reversal. It is hypothesised that these sediments form high yielding aquifers. These aquifers continue to be eroded due to high surface gradients but they still remain in a few valleys (Fig. 7.4) where relief is relatively low.

Figure 7.4. Photograph showing a valley floor filled with fluvial sediments in Rukungiri, north of River Mitano

b. Within the intra-arch, along the north-south running rivers and parallel to the rift wall, there is little sign of deep incision due to the slow drainage of the rivers to the rift. Stripping on these surfaces is minimal and areas underlain by these surfaces feature low lying broad valleys (Fig. 7.5) underlain by medium to coarse grained aquifers.

Figure 7.5. Photograph showing a low lying broad valley in Ntungamo, south of River Mitano

c. Within the inter-arch basin, the eastward flow became choked with infill of alluvium or papyrus vegetation or standing water in the valleys of the Kagera, Katonga and Kafu rivers. The lakes in the former valleys of Katonga and Kagera rivers later merged to form Lake Victoria due to further uplift while the lake in the valley of Kafu River formed Lake Kyoga. The headward extension of the old River Kagera drainage probably flowed across the area now occupied by Lake Victoria (de Swardt and Trendall, 1969) while the drainage system of River Katonga, may have risen east of Lake Victoria, and drained much of what is now the northern part of Lake Victoria (Fig. 7.6).

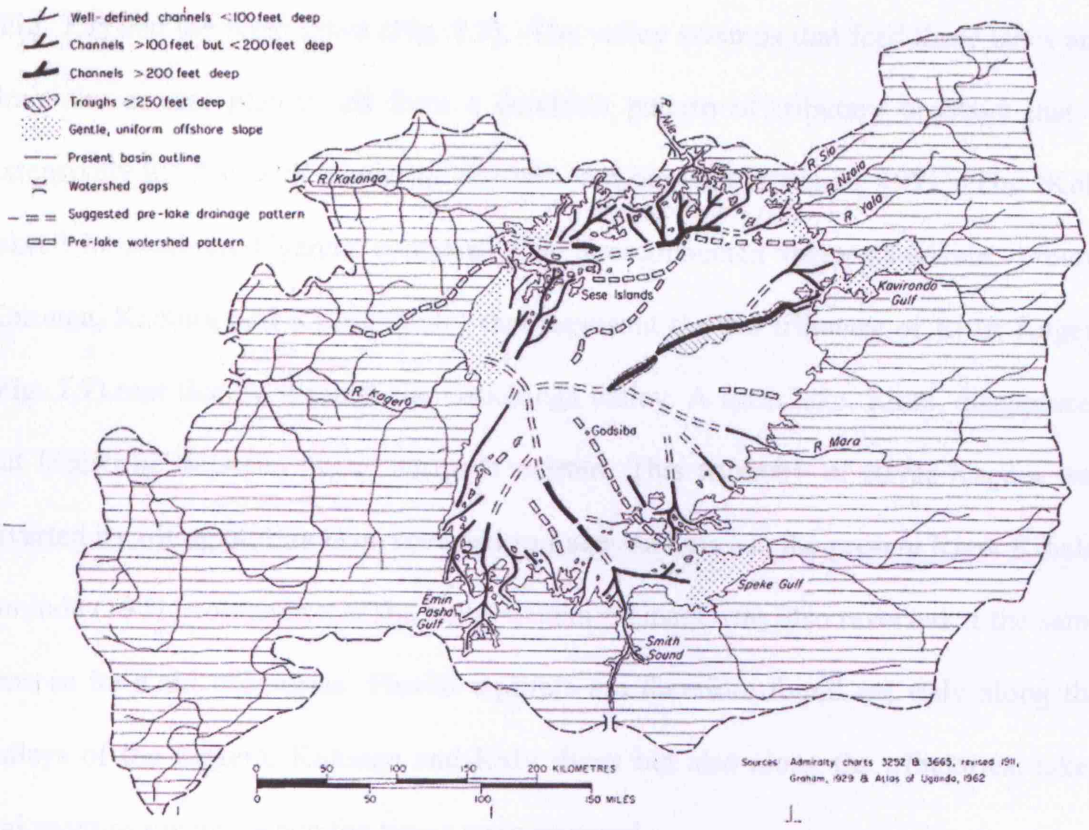

Figure 7.6. Pre-drainage over Lake Victoria (from Temple, 1966)

De Swardt and Trendall (1969) suggest that the lower part of Katonga drainage system, the Mpanga river (Fig. 7.2), was probably deflected to the south-west by early rise of the Rwenzori block. Kafu drainage system was redirected northwards along a low sediment-filled depression of the West Nile section of the Western Rift by tilting and upwarp. The upper sections of rivers Nkusi and the Kafu (Fig. 7.2) originated from these processes. De Swardt and Trendall (1969) postulate that River Kafu originally flowed west-north-west though what is now Hoima, but was deflected to a west-south-westerly course as a result of early warping along the Western Rift.

Tectonic activity not only reversed the main rivers to form lakes (Bishop and Trendall, 1967) but their tributaries were also affected resulting in a connected series

of major lakes in central and southern Uganda comprising Lakes Victoria and Kyoga (Fig. 7.2) and the Koki lakes (Fig. 7.7). The valley swamps that feed these lakes and drain the central plateau all form a dendritic pattern of tributary drainage that is extensively infilled with lacustrine deposits and papyrus (Ominde, 1971). The "Koki lakes" in southern Uganda comprise five interconnected lakes (Nakivale, Mburo, Karunga, Kachira and Kijanebalola) that represent the old tributary of River Kagera (Fig. 7.7) that flowed through the Oruchinga valley. A sixth lake, Ruizi, disappeared but lacustrine deposits occur where it existed. This tributary of River Kagera was diverted by tilting and its flow reversed to Lake Victoria via the present River Kibale. Ominde (1971) contends that the main Kagera drainage was also reversed at the same time as its Koki tributaries. Fluvial aquifers are therefore found not only along the valleys of the Kagera, Katonga and Kafu rivers but also along the tributaries, lakes and swamps created when the rivers were reversed.

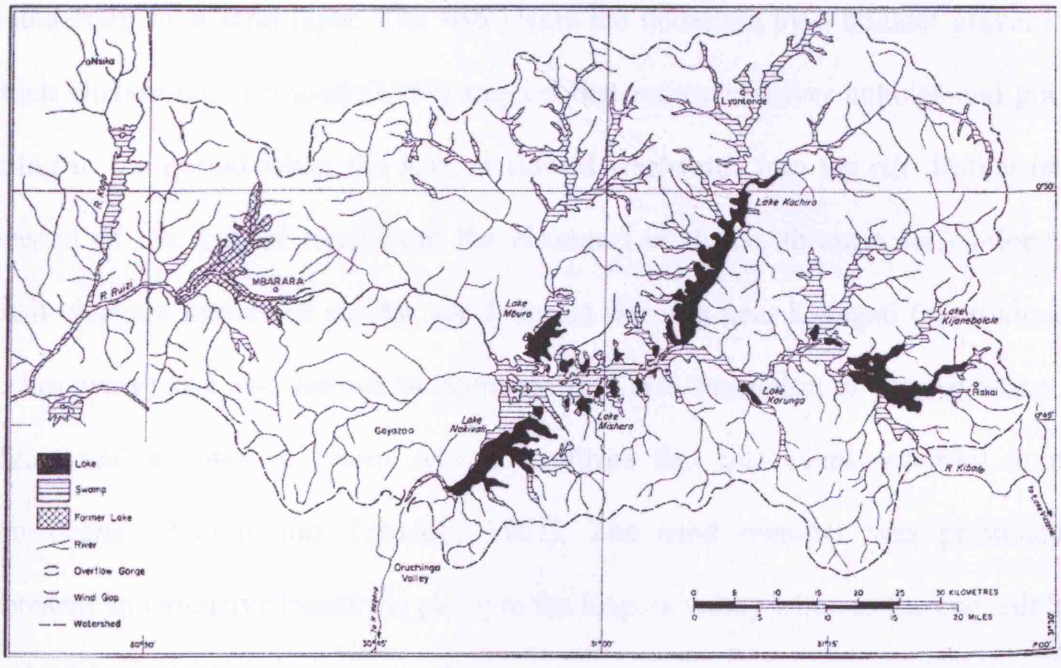

Figure 7.7. Flooded old river system associated with River Kagera in south-western Uganda occupied by the "Koki lakes" (from Temple, 1966)

The last phases of upwarping that formed the proto-Lake Victoria resulted in the regression eastward of the western lake margin (Doorkamp and Temple, 1966) in late Pleistocene, abandoning flats of lacustrine deposits unconformably overlapping parts of the pre-existing landscape slopes. Lacustrine plains are most extensive along the present lower sections of the Katonga and Kagera (Fig. 7.7) where the pre-existing topography was low. Continued tilting resulted in the exposure of the lacustrine sediments (Doorkamp and Temple, 1966) and the incision of the reversed streams due to tectonically induced changes in relief. Elevated lacustrine flats stretch inland in some places for more than 60 km from the present Lake Victoria shore line.

Evidence for the evolution of fluvial aquifers in drainage networks of the former westerly flowing rivers is found in unconsolidated deposits comprising of three distinct members (Bishop and Trendall, 1967) observed in the Kagera valley in south-west Uganda at Nsongezi (Fig. 7.8). The upper layer composed of clay and silt is underlain by a sand layer. The two layers are underlain by a boulder gravel layer which Bishop and Trendall (1967) suggest that represents river cobbles and gravels dating to the period when the Kagera flowed westwards into the rift. Dating of the reversal of the Kagera river from the Nsongezi evidence, through correlation with fossil elephant molars of similar age found at deposits near Kikagati (approximately 30 km away) and also known to occur in the Kaiso formation of the Albertine Rift Valley and at sites in North Africa, confirms that this event occurred in mid-Pleistocene (Bishop and Trendall, 1967). The sand member was presumed to represent an extensive lacustrine phase in the Kagera valley whereas the clay/silt layer marked the end of open- water conditions.

A summarised sequence of events that lead to the formation of the Nsongezi formation (Bishop and Trendall, 1967), based on fauna evidence, indicates that there

was an earlier Pleistocene event, westerly flowing Kagera river that was reversed by upwarping close to the rift valley resulting in deposition of the sand layer of the Nsongezi formation, by the end of mid- Pleistocene (Taylor and Howard, 1998). The lake that persisted in the Kagera valley until the beginning of late Pleistocene was converted into vegetated swamp with seasonal swamp sediments, by renewed uptilting in the west. Uplift finally resulted in the drying out of swamps and the progressive incision of the Kagera river below the top of Nsongezi formation deposits. Uptilting occurred by approximately 1.8 m per km westwards from the present Lake Victoria shore, and the Nsongezi sediments, found 110 km west of Lake Victoria shore, were uptilted (Doorkamp and Temple, 1966) by about 90 m.

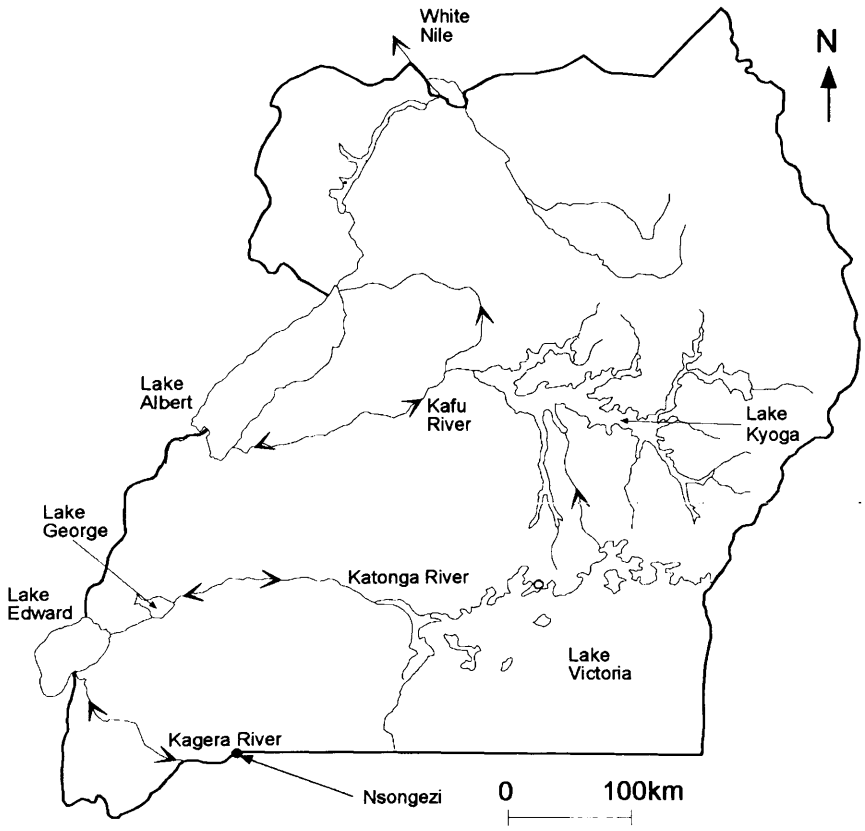

Figure 7.8. Location of Nsongezi along Kagera river valley

Field reconnaissance mapped the sediments described by Bishop and Trendall (1967) in the Kagera valley at Nsongezi (Fig. 7.9) which are currently mined for building sand. The different layers of the deposits as seen from the sand pits have been reworked in most places. The cobbles and gravels reported by Bishop and Trendall (1967) exist mixed with sand and clay (Fig. 7.10) all around the site and in some pits.

Figure 7.9. Photograph of the exposed Nsongezi sediments and surroundings

Figure 7.10. Photographs of Nsongezi sediments with cobbles and gravels, and layered sediments in pits.

Field reconnaissance also mapped the landform features observed by various workers along the Katonga and Kagera rivers. The lacustrine flats, approximately 3 km wide in Katonga valley and 2 km wide in Kagera valley, extend for approximately 20 km and 60 km from the present lake shore line along the two valleys respectively (Fig. 7.11).

Figure 7.11. Photograph of the extensive lacustrine flats along Kagera River valley

Lacustrine sediments along the Katonga valley were mapped and their composition assessed from a sand mining pit. The sediments are composed of fine grained sand with some clay (Fig. 7.12) and the thickness of the clay is less than 1 metre below which there is fine sand that probably originated from the regression of Lake Victoria.

Figure 7.12. Photograph of lacustrine sediments in the Katonga valley

Evidence from the Nsongezi deposits and field mapping along Katonga and Kagera valleys clearly indicate that the gravel/coarse sand and sand layers that originated from the former westerly flowing rivers exist along paleochannels and are overlain by lacustrine clayey sand. Continued uptilting of the sediments westwards exposed the lacustrine deposits especially in the upper reaches. The conceptual profile of Kagera valley (Fig. 7.13) showing the distribution of the various layers, reconstructed based on Bishop and Trendall (1967) and field mapping, indicates that

the depth to the gravel and coarse sand layer increases eastwards from Nsongezi to Lake Victoria.

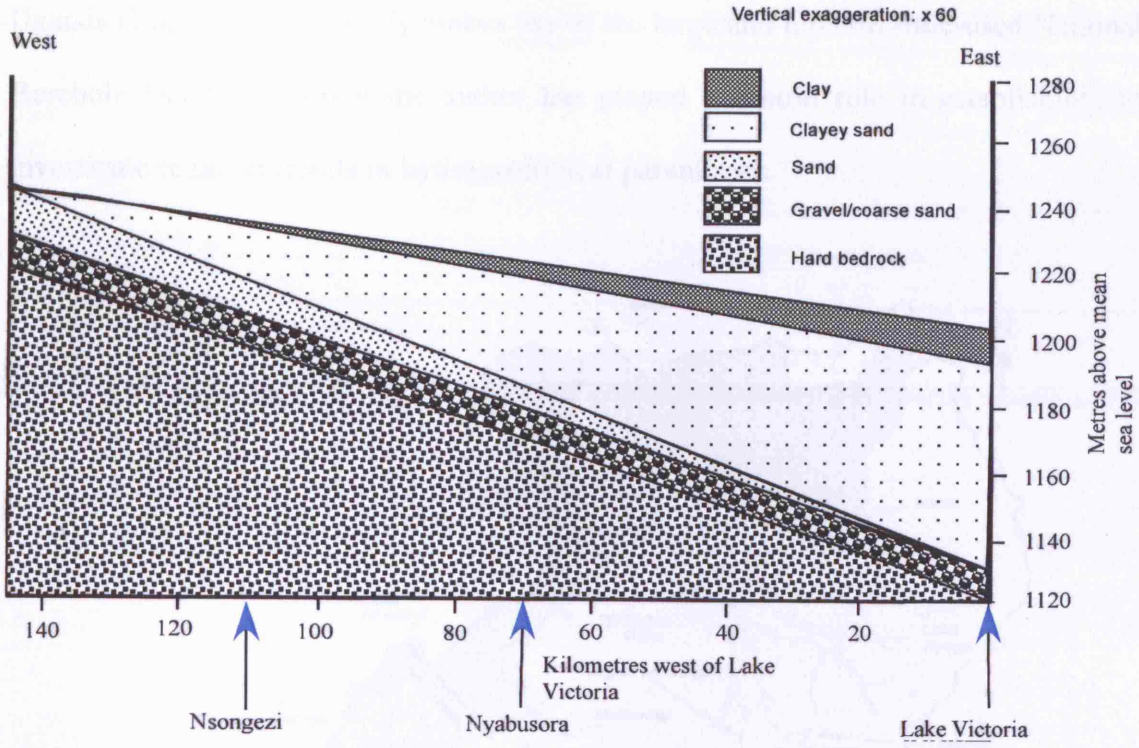

Figure 7.13. Conceptual profile of Kagera valley showing the distribution of the various formations (reconstructed based on Bishop and Trendall (1967) and field mapping).

7.2 Field evidence for evolution of aquifers

7.2.1 Overview

Field evidence for evolution of aquifers by tectonically controlled deep weathering and stripping is derived from a wide range of sources (topography, hydrology, regolith thickness, lithological units, well yields and specific capacity) at locations throughout the inter-arch (River Kigwe catchment in central Uganda, Hoima

in mid western Uganda, Lukaya and Mubende in central Uganda, Iganga in eastern Uganda and Aroca catchment in northern Uganda) and the intra-arch (River Mitano catchment, Ntungamo and Nyabisheki catchment in southwestern Uganda) basins of Uganda (Fig. 7.14). The study makes use of the large and hitherto little-used National Borehole Database, which the author has played a central role in establishing, to investigate regional trends in hydrogeological parameters.

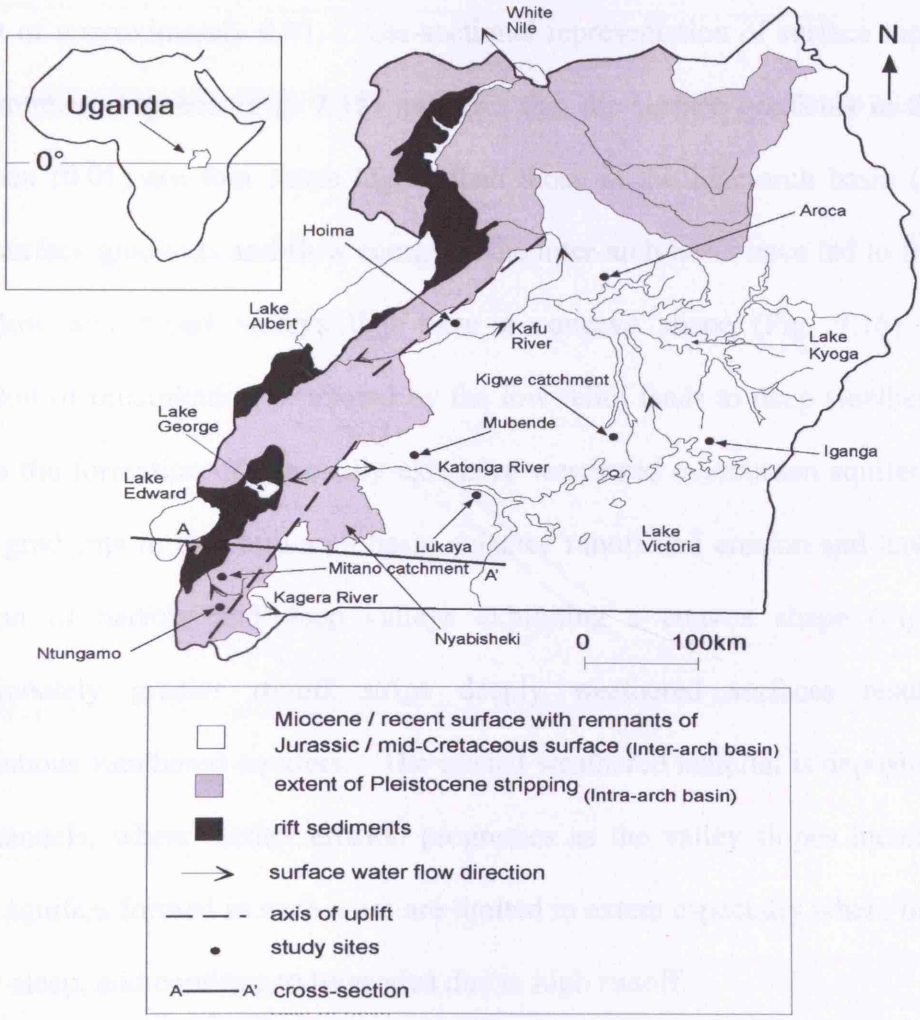

Figure 7.14. Location of sites where field evidence for evolution of aquifers was obtained.

7.2.2 Evidence from channel/surface gradients

Down-faulting of the western rift valley and uplift east of the rift created significantly greater relief in the intra-arch basin relative to the inter-arch basin (Fig. 7.14). Based on studies in River Kigwe catchment, the mean elevation of the inter-arch basin is 1100 m above mean sea level (mamsl) with an average surface gradient of approximately 0.003. The mean elevation of the intra-arch basin, based on studies in the River Mitano catchment, is approximately 1740 mamsl with an average surface gradient of approximately 0.01. Cross-sectional representation of surface topography across southern Uganda (Fig. 7.15) indicates that the surface gradients in the intra-arch basin (0.01) are four times higher than those in the inter-arch basin (0.0025). Lower surface gradients and flow energy in the inter-arch basin have led to formation of shallow and broad valleys that have a concave shape (Fig. 7.16). Greater infiltration of precipitation promoted by the low relief leads to deep weathering and supports the formation of regionally extensive weathered overburden aquifers. High surface gradients in the intra-arch basin enhance runoff and erosion and have led to formation of narrow and deep valleys exhibiting a convex shape (Fig. 7.16). Proportionately greater runoff strips deeply weathered surfaces resulting in discontinuous weathered aquifers. The eroded weathered material is deposited along river channels, where further erosion progresses as the valley slopes increase. The alluvial aquifers formed in such areas are limited in extent especially where the slopes are very steep, and continue to be eroded due to high runoff.

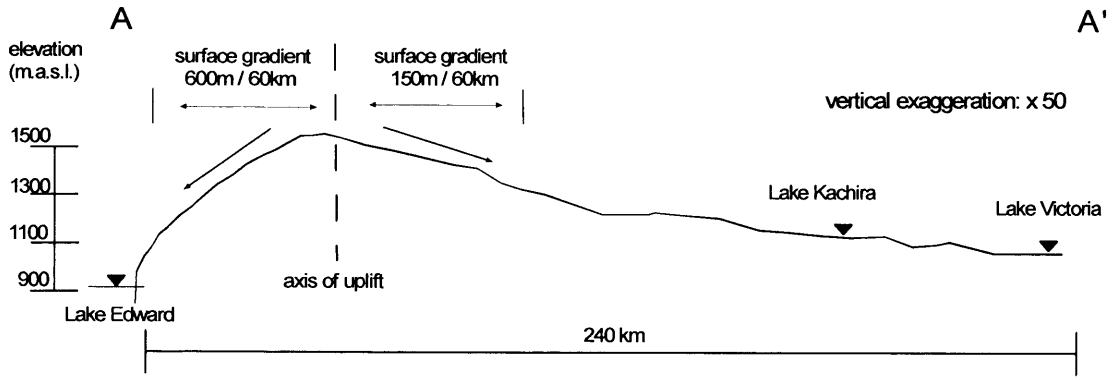

Figure 7.15. Cross-section representation of topographic expressions across southern Uganda. Locations of A and A' are indicated on Fig. 7.14.

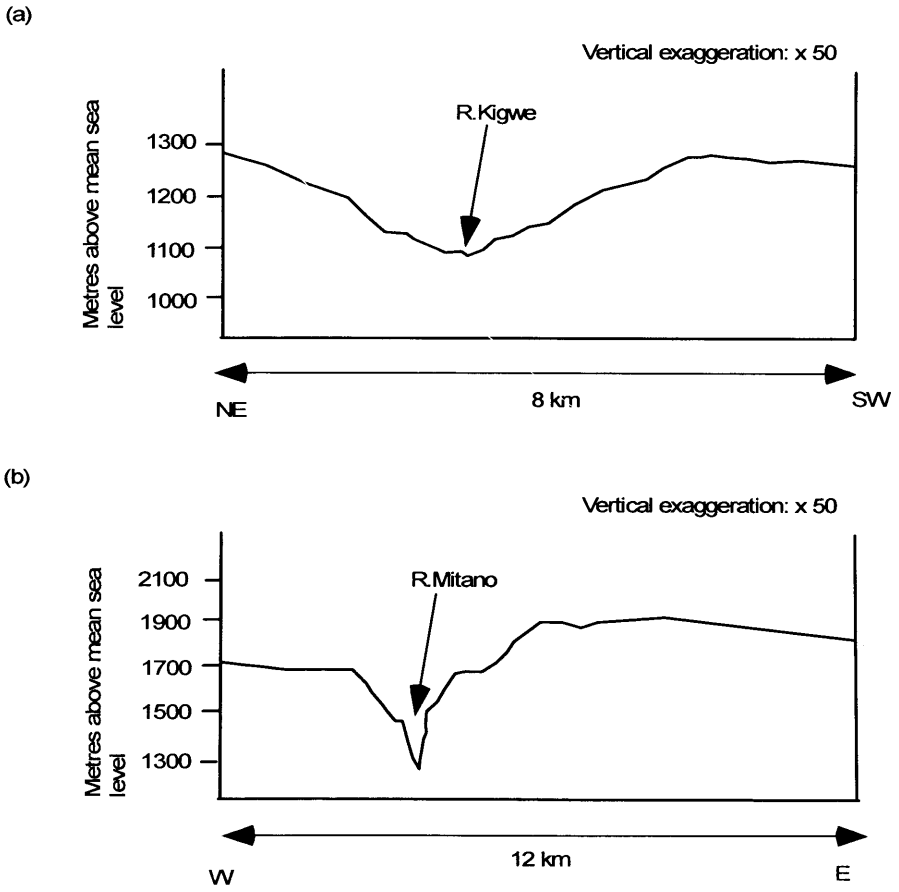

Figure 7.16. Valley shapes in inter and intra-arch basins of Uganda. a) Concave valley in River Kigwe catchment. b) Convex valley in River Mitano catchment.

7.2.3 Evidence from hydrological responses

Hydrology in the inter-arch (Kigwe and Aroca catchments) and intra-arch (Mitano and Nyabisheki catchments) basins of Uganda (Taylor and Howard, 1999; Tindimugaya, 2000; Mileham et al., in prep.) reflects the relationship between tectonic setting and aquifers. The discharge of the River Kigwe responds quickly to rainfall events (Fig. 7.17). However, during dry periods and particularly from January to March, river discharge ceases altogether. The low baseflow inferred from this observation is derived by previous water balance studies (Tindimugaya, 2000) indicating that groundwater recharge is more than double surface runoff (Table 7.1). Similar to the Aroca catchment (Fig. 7.14) that also occurs in the inter-arch basin, baseflow contributions are almost entirely consumed by evapotranspiration in the broad drainage channels covered by papyrus swamps (Taylor and Howard, 1999) that occur upstream of the gauging station. This is consistent with observations by Chilton and Smith-Carington (1984) in the humid tropics of southern Africa where groundwater seepage is lost by evapotranspiration from the green dambo vegetation in the dry season upstream of the gauging station resulting in significant underestimation of baseflow. The mean annual discharge averaged over the River Kigwe catchment is 72 mm.

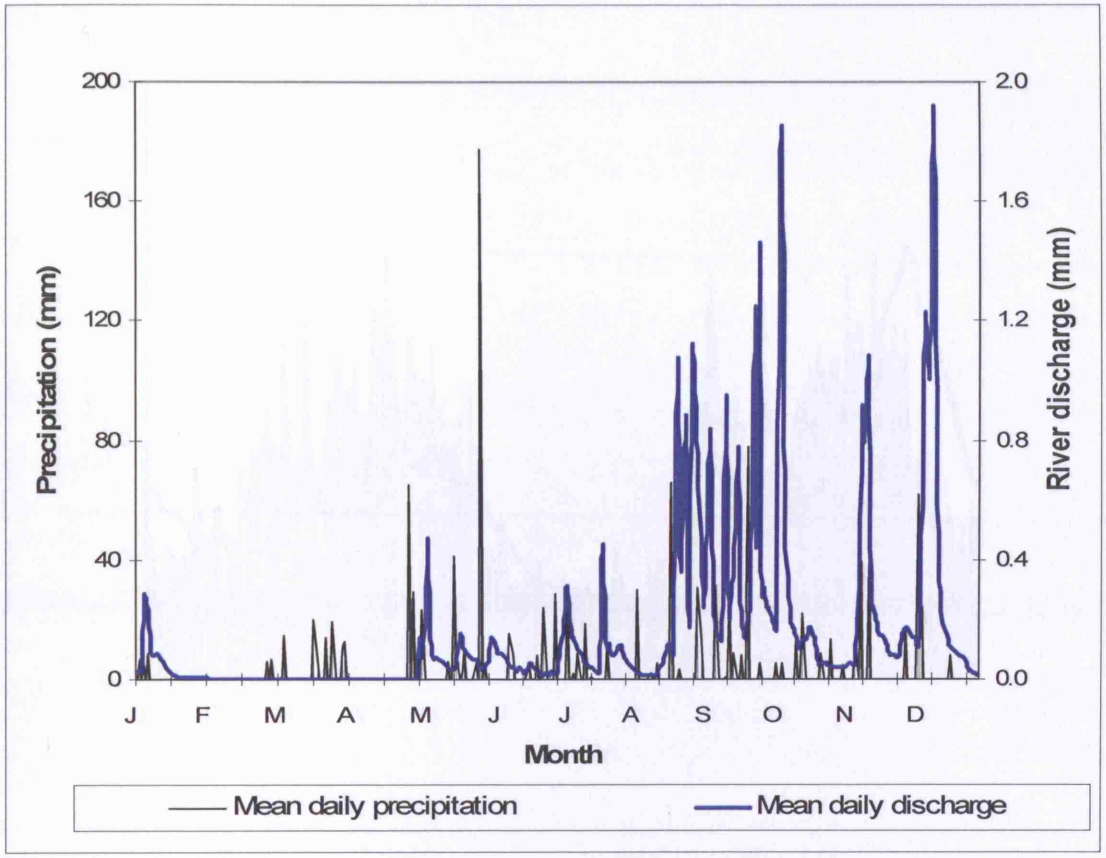

Figure 7.17. Mean daily precipitation and areally averaged river discharge in the River Kigwe catchment of Central Uganda (inter-arch basin)

The River Mitano discharge (Fig. 7.18) at the end of the dry season provides a rough indication of baseflow. Ongoing catchment studies show that runoff in the narrow and deeply incised drainage channels exceeds recharge by ~50% (Table 7.1). The recharge flux of 101 mm a^{-1} suggests that appreciable basin storage may exist in coarse-grained fluvial deposits in river channels and in areas of the catchment where incision has not yet occurred. The mean annual discharge averaged over the River Mitano catchment is 150 mm.

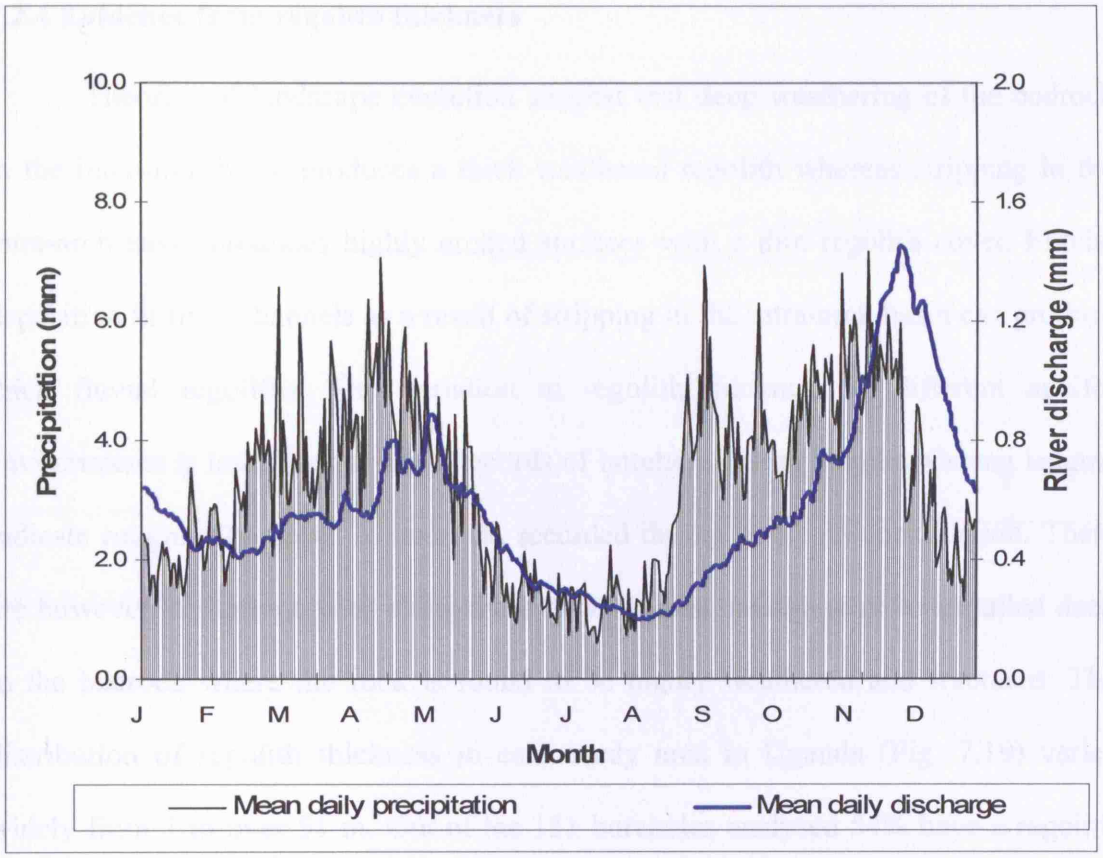

Figure 7.18. Mean daily catchment precipitation with areally averaged daily discharge for River Mitano in Western Uganda (intra-arch basin)

Table 7.1. Comparison of estimated recharge (R) and surface runoff (RO) in inter- and intra-arch basins of Uganda.

	Inter-arch basin		Intra-arch basin	
Catchment	Kigwe[1]	Aroca[2]	Mitano[3]	Nyabisheki[2]
R (mm/a)	161	120	101	15
RO (mm/a)	72	3	150	34
R/RO	**2.2**	**40**	**0.67**	**0.44**

1: Tindimugaya (2000); 2: Taylor and Howard (1999); 3: Mileham et al. (in prep.)

Variations in recharge and surface runoff in the Rivers Kigwe and Mitano catchments are consistent with conclusions drawn by Taylor and Howard (1999) for Aroca and Nyabisheki catchments.

7.2.4 Evidence from regolith thickness

Theories of landscape evolution suggest that deep weathering of the bedrock in the inter-arch basin produces a thick weathered regolith whereas stripping in the intra-arch basin produces highly eroded surfaces with a thin regolith cover. Fluvial deposition in river channels as a result of stripping in the intra-arch basin can produce thick fluvial regoliths. The variation in regolith thickness in different aquifer environments is investigated using records of borehole casing lengths. Casing lengths indicate roughly the depth to bedrock, recorded during borehole construction. There are however limitations with using these data because casings may be installed deep in the bedrock where the rock is found to be highly weathered and fractured. The distribution of regolith thickness in each study area in Uganda (Fig. 7.19) varies widely from 1 to over 51 m. Out of the 151 boreholes analysed 54% have a regolith thickness of between 21 and 40 m. The thinnest regoliths (<10 m) occur in the Rivers Mitano and Kigwe catchments and Hoima whereas thicker regoliths (>10 m) occur in all the study areas. Thicker regoliths (>10 m) are expected in deeply weathered surfaces (River Kigwe catchment, Hoima, Mubende and Iganga) and areas of fluvial deposition (River Mitano catchment, Hoima, Mubende, Ntungamo and Lukaya); the thin regoliths (<10 m) are expected in stripped surfaces (Rivers Mitano and Kigwe catchments and Hoima).

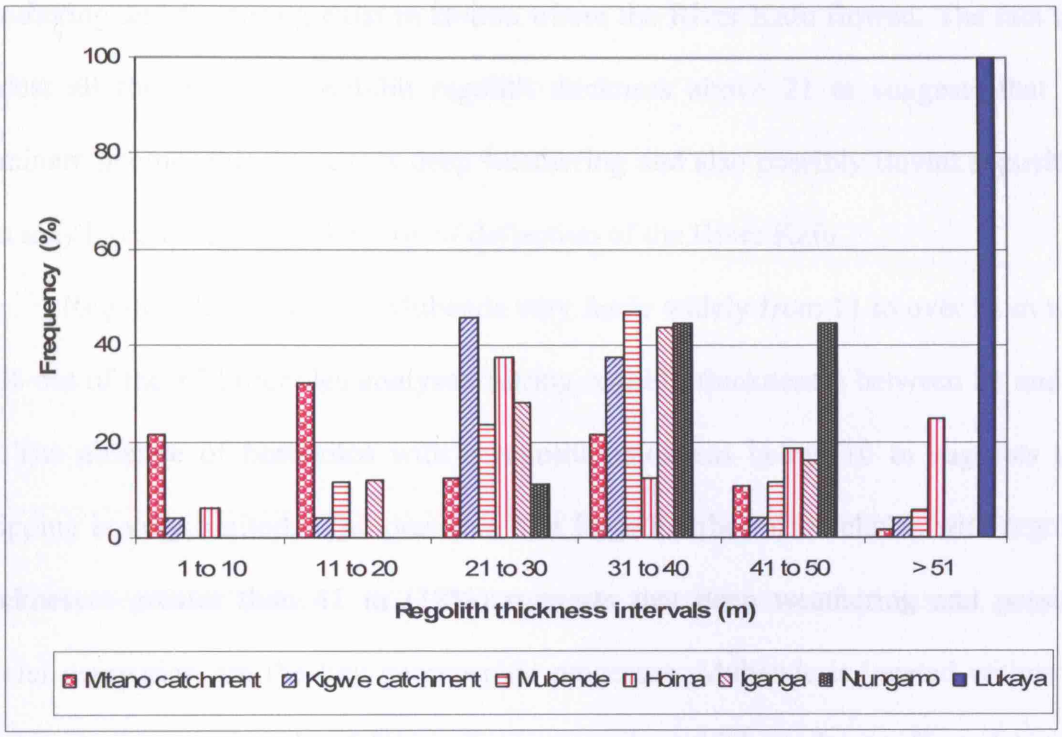

Figure 7.19. Distribution of regolith thicknesses in various areas in Uganda

Out of the 24 boreholes analysed for the River Kigwe catchment, 84% have regolith thicknesses between 21 and 40 m whereas only 8% have regolith thicknesses below 20 m. Out of the 56 boreholes analysed for the River Mitano catchment, 53% have regolith thicknesses below 20 m. 13 % of the boreholes have regolith thicknesses greater than 41 m possibly due to presence of *in situ* deeply weathered surfaces and fluvial deposits in low lying areas along river channels. Out of the 16 boreholes analysed for Hoima, 43% of the boreholes have regolith thicknesses below 30 m whereas 57% have regolith thicknesses above 31 m. The high variation in regolith thickness in a small area (< 25 km^2) with small variations in topographic elevation may reflect the consequences of geomorphic processes. According to de Swardt and Trendall (1969), the River Kafu (Fig. 7.2) originally flowed through Hoima but was deflected along a west-south- westerly course as a result of warping along the Western Rift. Based on this information, it appears that zones of preferential

weathering and fracturing exist in Hoima where the River Kafu flowed. The fact that almost all the boreholes exhibit regolith thickness above 21 m suggests that the dominant geomorphic process is deep weathering and also possibly fluvial deposition that may have occurred at the time of deflection of the River Kafu.

Regolith thicknesses in Mubende vary fairly widely from 11 to over 51 m with 70% out of the 17 boreholes analysed having regolith thicknesses between 21 and 40 m. The absence of boreholes with a regolith thickness below 10 m suggests that stripping is very limited. The presence of a large number of boreholes with regolith thicknesses greater than 41 m (18%) suggests that deep weathering and possibly fluvial deposition are the key geomorphic processes. Mubende is located within the former drainage network of River Katonga and could have been affected by the reversal of the Katonga drainage.

Regolith thicknesses in Ntungamo range between 21 and 50 m with 89% of the 9 boreholes having regolith thicknesses between 31 and 50 m. There are no regolith thicknesses below 10 m and above 50 m. The findings appear to suggest that deep weathering and drainage deposition are the dominant processes and that *in situ* weathered or fluvial materials deposited in river channels have not been greatly eroded though the area is situated in the intra-arch basin. Consistent with observations by Doorkamp (1967), the areas with south-north drainage have relatively low surface gradients and stripping has been minimal resulting in a thick regolith.

Regolith thicknesses exhibited by the 4 boreholes analysed in Lukaya are all > 51 m and indeed no hard rock was encountered in the boreholes drilled to the maximum depth of 69 m. Lukaya is located within the former drainage network of River Katonga and the thick regolith is a result of sediments deposited due to drainage reversal and regression eastwards of the western margin of Lake Victoria. Fluvial

deposition is therefore considered to be the dominant process in the formation of the regolith in Lukaya.

Regolith thicknesses in Iganga range between 11 and over 50 m with 72% of the 25 boreholes analysed having regolith thicknesses between 21 and 40 m. There are no regolith thicknesses below 10 m and above 50 m. The presence of thick regolith and absence of thin regolith suggest that deep weathering is the dominant process in the formation of weathered mantle in Iganga.

Variation in regolith thickness, inferred from borehole casing lengths, are consistent with the assertion that stripping is the dominant process in the intra-arch basin and is responsible for the comparatively thinner regolith. Deep weathering is inferred to be the dominant process in the inter-arch basin as the existence of thick weathered overburden suggests stripping has been minimal. In low lying areas and river channels in stripped surfaces, regolith thickness depends on the degree of deposition and the rate of erosion of the deposited sediments. Within the paleochannels in deeply weathered terrain, fluvial deposition leads to the formation of very thick regoliths.

7.2.5 Evidence from lithological units

Deeply weathered environments are characterised by clay, sand and bedrock that may or may not be weathered and fractured; stripped surfaces and surfaces of fluvial deposition are characterised by lithologies that depend on the sediment origin and degree of sorting. Fluvial sediments that have travelled for long distances (highly weathered and sorted) are characterised by gravel and coarse sand. Sediments that have travelled for short distances are generally not sorted and are thus dominated by fine grained clay and clayey sand. Taylor and Howard (1998) suggest that in situ weathered regoliths are bimodal due to presence of fine-grained material whereas

fluvial sediments are unimodal due to the removal of fine-grained material. Variation in lithology in areas of deep weathering, stripping and fluvial deposition is investigated using lithological logs recorded during drilling of boreholes in seven areas. Lithology of River Kigwe catchment (Fig. 7.20) is characteristic of deeply weathered environments and is typically composed of top soil, clay and clayey sand overlying quartz and sands and bedrock. The lithology that forms the main aquifers consists of quartz and sand, weathered bedrock and fractured bedrock.

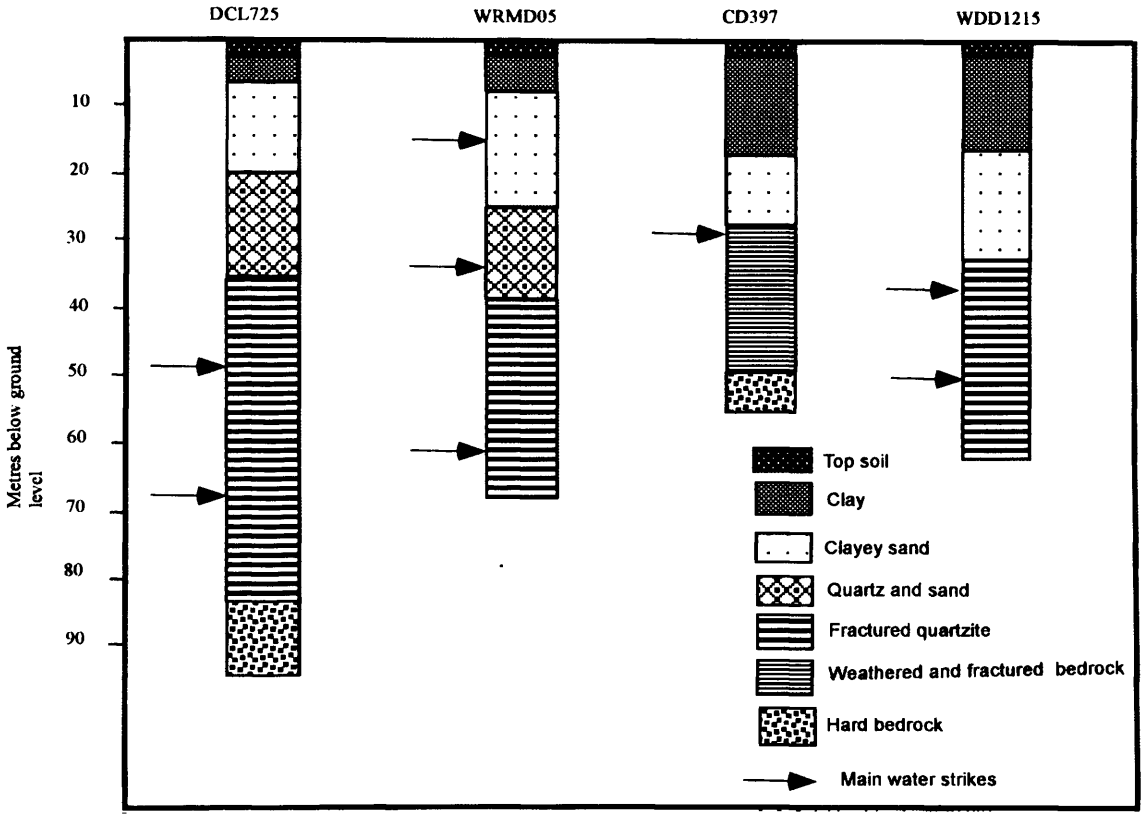

Figure 7.20. Lithological log for boreholes in the River Kigwe catchment

Lithology in the River Mitano catchment (Fig. 7.21) is variable. Some locations have lithology that is characteristic of fluvial deposition and composed of clay and fine sand overlying gravel and coarse sand and fractured bedrock (e.g. boreholes DCL1016, DWD20342 and DCL1011). Other locations have a lithology

that is characteristic of stripped weathered surfaces and composed of clay and clayey sand overlying the bedrock that may or may not be weathered and fractured (e.g. borehole WDD3878). Lithology therefore indicates that stripping with the resultant fluvial deposition of weathered material and deep weathering have been key to the formation of aquifers in the River Mitano catchment.

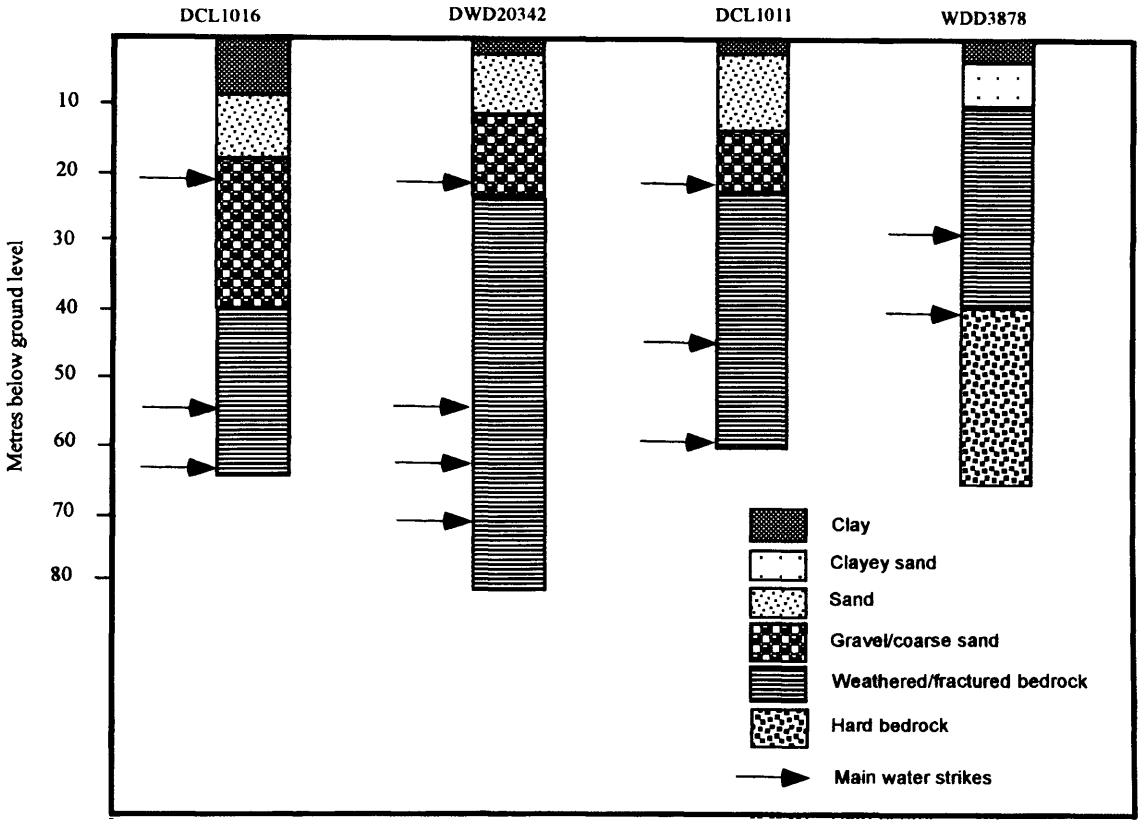

Figure 7.21. Lithological log for boreholes in the River Mitano catchment

Lithology of Hoima (Fig. 7.22) is highly variable and rather complex. The overlying lithology composed of laterite, clays and shales appears to be characteristic of a later deposition of deep weathered material whereas the underlying coarse and highly fractured formations are characteristic of fluvial deposition possibly due to deflection of River Kafu (Fig. 7.2). Lithology therefore indicates that fluvial

deposition and deep weathering are the main processes responsible for formation of aquifers in Hoima.

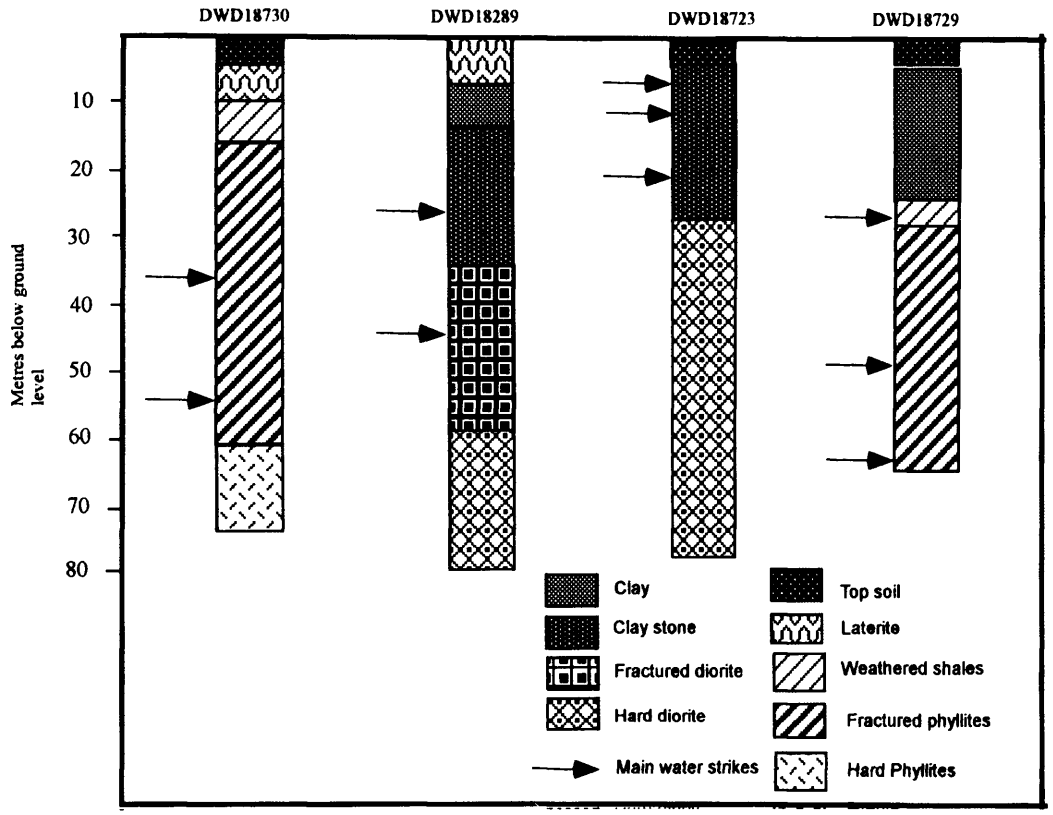

Figure 7.22. Lithological log for boreholes in Hoima

Lithology of Mubende (Fig. 7.23) is variable. Some locations have lithology that is characteristic of fluvial deposition and composed of clay, sand, gravels and coarse sand overlying fractured bedrock (e.g. boreholes DWD18836 and DWD18945). Other locations have lithology that is characteristic of deeply weathered surfaces and composed of clay, clay and sand, and bedrock that may or may not be fractured (e.g. boreholes DWD18936 and DWD18938). On the basis of lithology, fluvial deposition and deep weathering are the main processes responsible for formation of aquifers in Mubende.

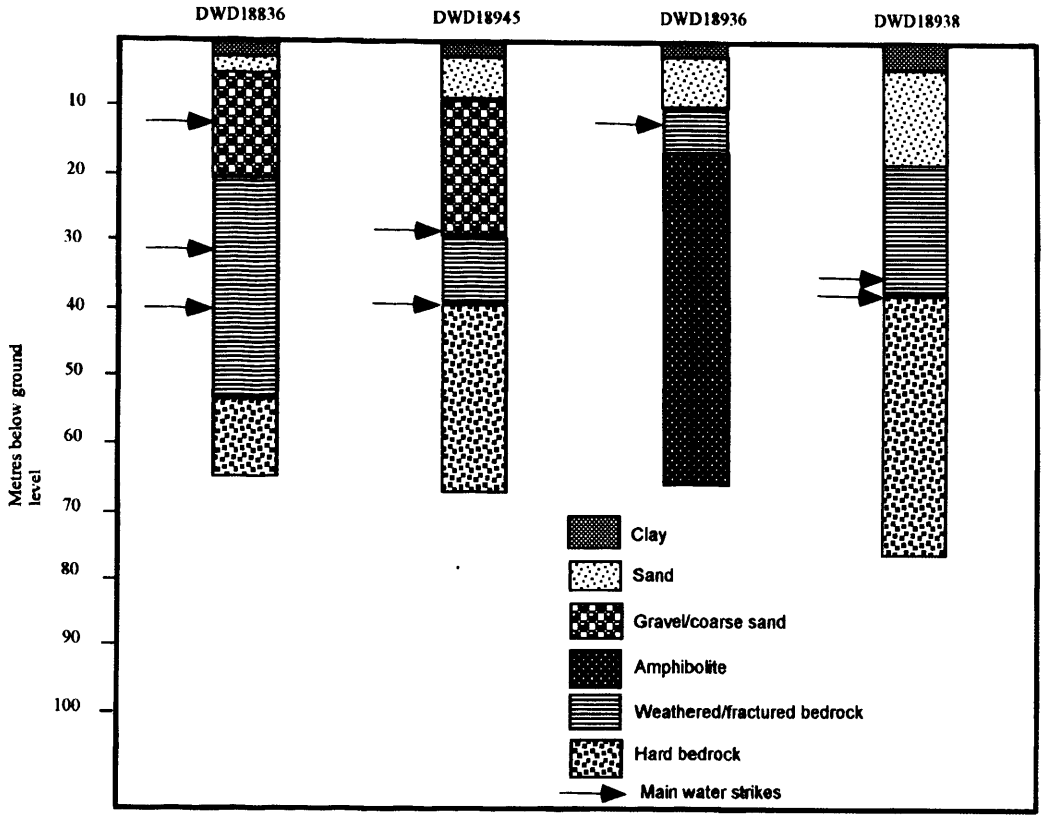

Figure 7.23. Lithological log for boreholes in Mubende

Lithology of Ntungamo (Fig. 7.24) is characteristic of deep weathering and stripping and fluvial deposition of the weathered material. Lithology is composed of murrum, clay, sand and gravel and coarse sand overlying weathered and fractured bedrock. The overlying formations composed of gravels and coarse sands and fine sediments result from stripping and fluvial deposition whereas the underlying weathered and fractured bedrock result from deep weathering.

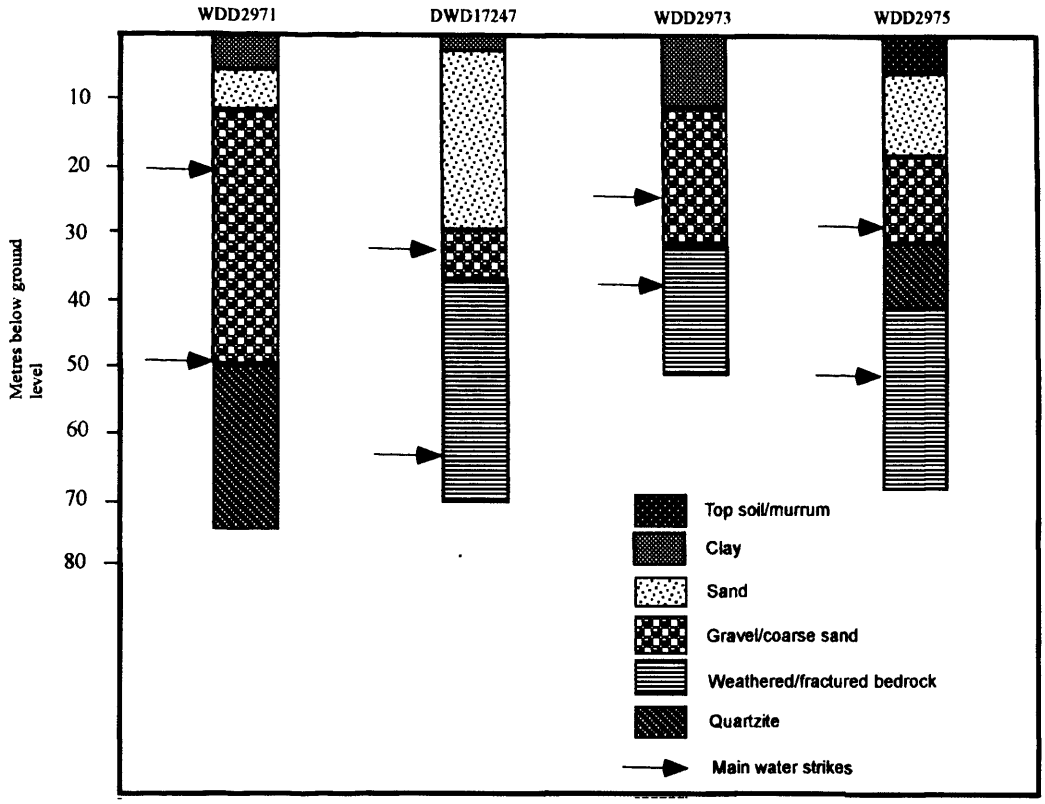

Figure 7.24. Lithological log for boreholes in Ntungamo

The lithology of Lukaya (Fig. 7.25) is characteristic of fluvial deposition and is composed of top soil, clay and sand. Some locations found on the edges of the valleys have weathered and fractured bedrock underlying the sand. Fluvial deposition is therefore considered to be the main process responsible for formation of aquifers in Lukaya.

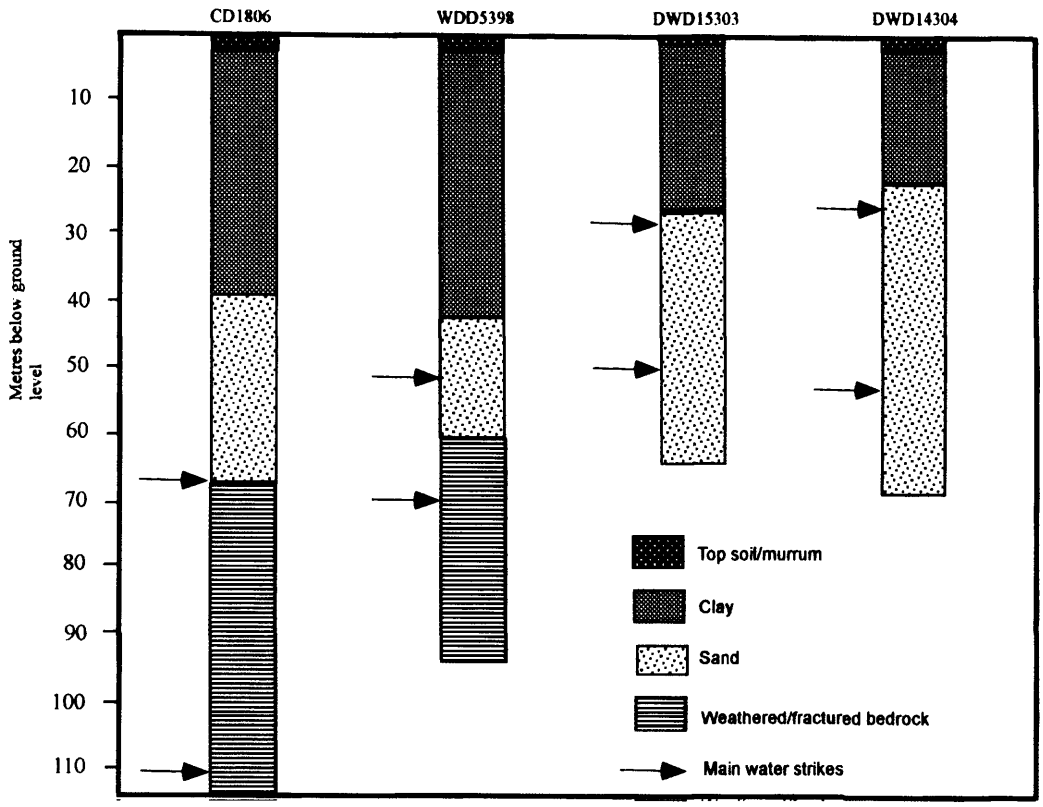

Figure 7.25. Lithological log for boreholes in Lukaya

Lithology of Iganga (Fig. 7.26) is characteristic of deep weathering and is composed of top soil, clay and clayey sand overlying bedrock that may or may not be weathered and fractured. The nature and grain size of the lithology suggests that deep weathering is the main process responsible for formation of aquifers in Iganga.

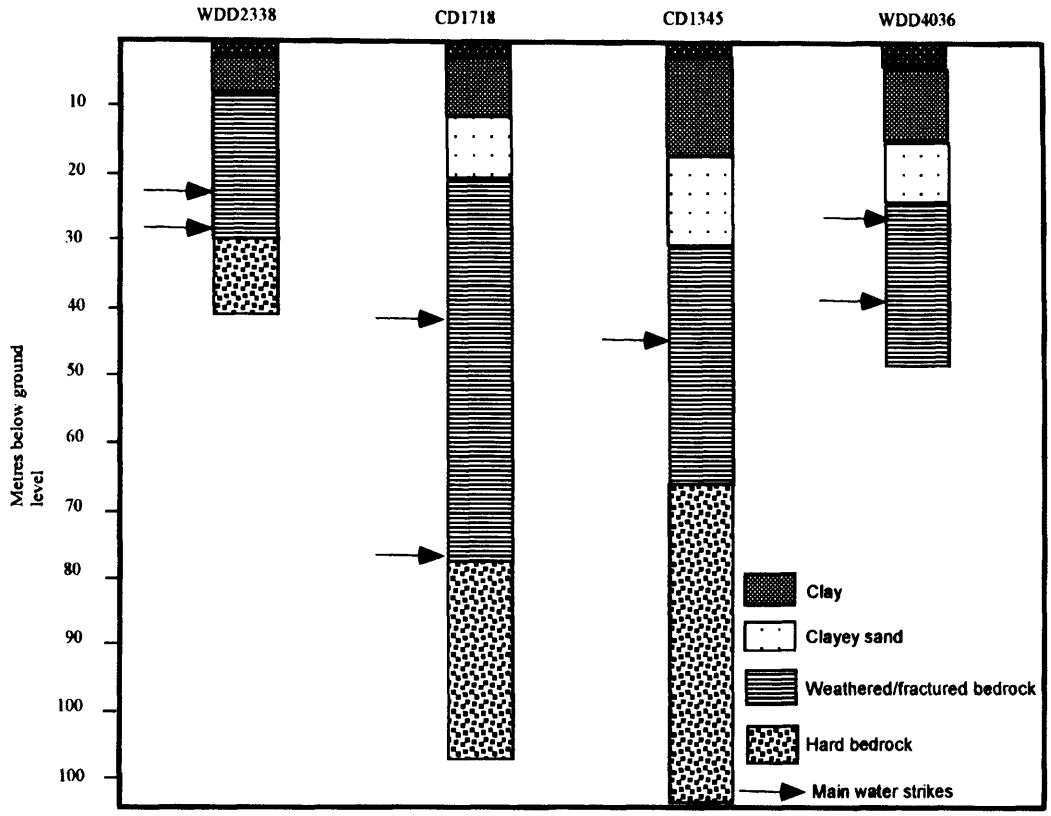

Figure 7.26. Lithological log for boreholes in Iganga

7.2.6 Evidence from borehole yields

Weathered crystalline rock aquifers are known to have highly variable but low yields (Taylor and Howard, 2000; Howard *et al.,* 1992; Houston and Lewis, 1988; Chilton and Smith-Carington, 1984) due to the fine-grained nature of the regolith and the limited extent of fractures in the bedrock whereas fluvial aquifers are expected to have yields that are much higher than those of weathered crystalline rock aquifers because the sediments are coarser. Variation in borehole yields in the various aquifers is investigated using airlift and pumping test data collected during the drilling of boreholes in the seven areas. The distribution of borehole yields in all the 7 areas

(Fig. 7.27) varies widely between 0.1 and >5.1 $m^3 h^{-1}$ with the individual borehole yields ranging between 0.1 and over 50 $m^3 h^{-1}$.

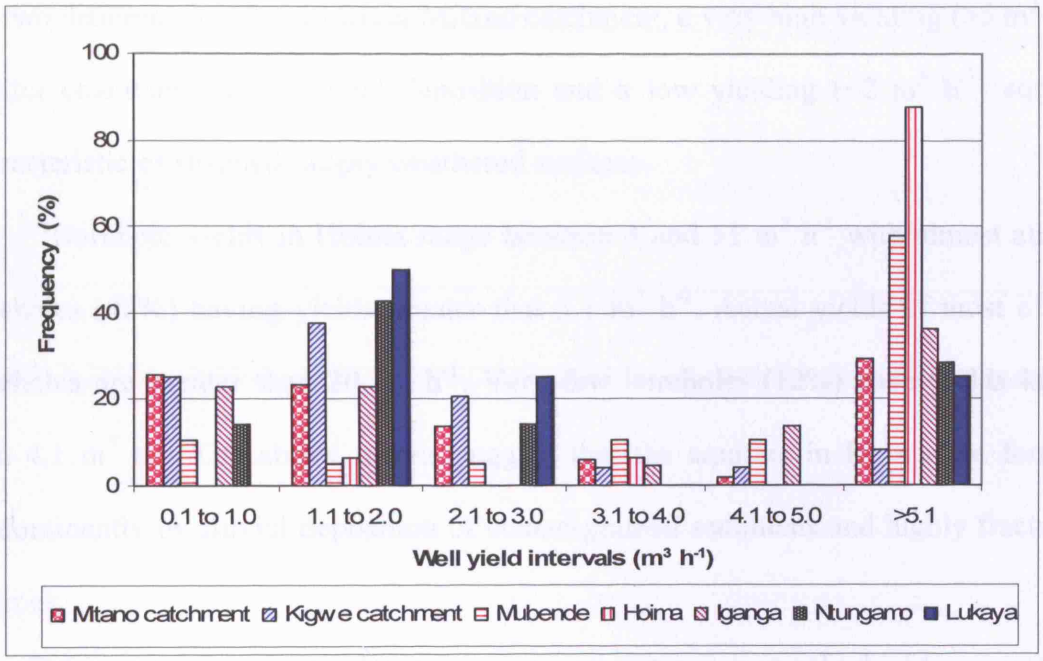

Figure 7.27. Distribution of borehole yields in studied areas in Uganda

57% out of the 141 boreholes investigated in the 7 areas have yields less than 3 $m^3 h^{-1}$. Boreholes with yields less than 3 $m^3 h^{-1}$ are found mainly in River Kigwe catchment and Iganga (i.e the inter-arch basin characterised by deep weathering). In selected areas of the intra-arch (River Mitano catchment and Ntungamo) and of the inter-arch (Mubende, Hoima and Lukaya) that are underlain mainly by fluvial sediments, boreholes have much higher yields (>5.1 $m^3 h^{-1}$). While all the 7 areas have some boreholes with yields greater than 5.1 $m^3 h^{-1}$, it is only Mubende and Hoima that have over 50% of their boreholes with such high yields.

Less than 10% of the boreholes in River Kigwe catchment have yields greater than 5 $m^3 h^{-1}$ suggesting that the aquifers are predominantly formed by deep weathering.

Borehole yields in River Mitano catchment range between 0.1 and 23 $m^3 h^{-1}$ with 49% of the boreholes having yields less than 2 $m^3 h^{-1}$ and 29% of the boreholes exhibiting yields greater than 5.1 $m^3 h^{-1}$. The distribution of yields suggests that there are two different aquifers in River Mitano catchment, a very high yielding (>5 $m^3 h^{-1}$) aquifer characteristic of fluvial deposition and a low yielding (<2 $m^3 h^{-1}$) aquifer characteristic of stripped deeply weathered surfaces.

Borehole yields in Hoima range between 4 and 51 $m^3 h^{-1}$ with almost all the boreholes (88%) having yields greater that 5.1 $m^3 h^{-1}$. Actual yields of most of the boreholes are greater than 20 $m^3 h^{-1}$. Very few boreholes (12%) have yields lower than 4.1 $m^3 h^{-1}$. The above results suggest that the aquifers in Hoima are formed predominantly by fluvial deposition of coarse-grained sediments and highly fractured bedrock.

Borehole yields in Mubende range between 0.1 and 43 $m^3 h^{-1}$ with most of the boreholes (57%) having yields greater that 5.1 $m^3 h^{-1}$. 64% of these boreholes have yields greater than 10 $m^3 h^{-1}$, 22% of the boreholes have yields between 3.1 and 5 $m^3 h^{-1}$, 11% have yields between 0.1 and 1 $m^3 h^{-1}$ whereas only 10% have yields between 1.1 and 3 $m^3 h^{-1}$. The distribution of borehole yields suggests that the characteristics of the aquifers in the areas vary greatly possibly due to differences in geomorphic processes and variation in grain sizes of the sediments. Presence of very high yielding boreholes (>40 $m^3 h^{-1}$) in this area indicates that the main aquifers are predominatly formed by well sorted coarse-grained sediments derived from fluvial deposition. Lower yielding boreholes are characteristic of fine-grained sediments derived from either deep weathering or fluvial deposition.

Borehole yields in Ntungamo range between 0.6 and 20 $m^3 h^{-1}$ with 57% of the boreholes investigated having yields less than 2 $m^3 h^{-1}$. 29% of the boreholes have

yields greater than 5.1 $m^3 h^{-1}$. There are no boreholes with yields between 3.1 and 5 $m^3 h^{-1}$ while only 14% of the boreholes have yields ranging between 2.1 and 3 $m^3 h^{-1}$. Similar to Mitano catchment, the distribution of yields suggests that there are two different aquifers in Ntungamo, a very high yielding (>5 $m^3 h^{-1}$) aquifer characteristic of fluvial deposition and a low yielding (<2 $m^3 h^{-1}$) aquifer characteristic of stripped deeply weathered surfaces. The percentage of boreholes with yields between 1.1 and 2 $m^3 h^{-1}$ in Ntungamo (43%) is much higher than that in Mitano catchment (24%) suggesting that the degree of weathering and fracturing is higher in Ntungamo than in Mitano catchment. This finding is consistent with the observations by Doorkamp (1967) that there is minimal stripping in areas of low gradients associated with south-north drainage. The low gradients and limited incision of the landscape in Ntungamo appear to facilitate deep weathering of the bedrock and formation of weathered and fractured aquifers. Low yielding boreholes appear to be located where there is bedrock weathering and stripping while the high yielding boreholes are located in river channels and low lying areas where the coarse grained material was deposited.

Only 4 boreholes are available for study in Lukaya and their yields range between 1.5 and 6 $m^3 h^{-1}$. Despite the fact that the number of boreholes studied is small, the results suggest that the yields of the aquifers in the area also vary greatly. Presence of variable borehole yields (1.5 to 6 $m^3 h^{-1}$), but lower than those of Rukungiri, Ntungamo, Mubende and Hoima indicates that the aquifer is composed of fine to medium-grained fluvial sediments. The boreholes are located where fluvial sediments were deposited due to reversal of Katonga drainage and regression of the western margin of Lake Victoria. The coarser gravel and sand deposits appear to be buried deeper below the lacustrine sediments due to the uptiliting westwards of the land surfaces by tectonic activity (Fig. 7.13).

Borehole yields in Iganga range between 0.1 and 10 $m^3 h^{-1}$ with only 35% of the 22 boreholes investigated having yields greater that 5.1 $m^3 h^{-1}$. Although 14% of the boreholes have yields between 4.1 and 5 $m^3 h^{-1}$, 46% have yields less than 2 $m^3 h^{-1}$. The wide variation in borehole yields suggest that the weathering and fracturing patterns are highly variable. Presence of many (35%) high yielding boreholes (>5 $m^3 h^{-1}$) in an area underlain by metamorphic rocks which normally have yields of less than 1 $m^3 h^{-1}$ indicates that deep weathering and fracturing of the bedrock are very intense.

The above results indicate that the lowest borehole yields are found in deeply weathered and stripped surfaces in River Kigwe catchment, Iganga, River Mitano catchment and Ntungamo whereas the highest borehole yields are found in River Mitano catchment, Hoima, Mubende, Ntungamo and Lukaya within fluvial sediments.

7.2.7 Evidence from specific capacity

Specific capacity is defined as the yield per metre drawdown and is a function of aquifer transmissivity. Deeply weathered and stripped surfaces have aquifers with low specific capacity due to the fine-grained lithology and the limited extent of the fractures whereas surfaces of fluvial deposition have aquifers whose specific capacities vary depending on the grain size and degree of sorting of the sediments but which are generally much higher. Low specific capacity values are therefore characteristic of deeply weathered environments, and palaeochannels underlain by fine-grained sediments whereas high specific capacity values are characteristic of coarse grained fluvial sediments. Specific capacity is investigated using long-term pumping test data collected in the towns of Wobulenzi (River Kigwe catchment), Rukungiri (River Mitano catchment), Hoima, Mubende, Ntungamo, Lukaya and

Iganga. Distribution of specific capacity in all the 7 areas (Fig. 7.28) varies widely between 0.1 and over 50 $m^2 d^{-1}$.

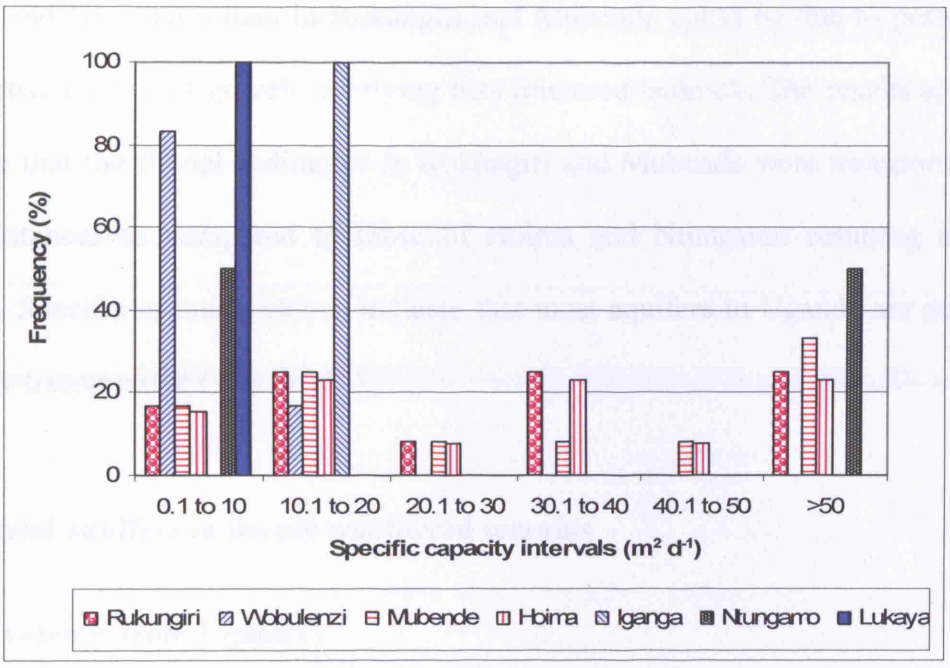

Figure 7.28. Distribution of specific capacity in various areas in Uganda

67% out of the 49 boreholes investigated in 7 areas have specific capacity values less than 20 $m^2 d^{-1}$. Although specific capacity values less than 20 $m^2 d^{-1}$ occur in all the 7 areas, they are common in Wobulenzi, Iganga and Lukaya where no borehole has specific capacity greater than this value. The results indicate that aquifers in Wobulenzi, Iganga and Lukaya are fine-grained and result from either deep weathering or fluvial deposition of fine-grained sediments. These results are consistent with information on lithological units.

Four areas (Rukungiri, Mubende, Hoima and Ntungamo) have specific capacity values that vary between 0.1 and over 50 $m^2 d^{-1}$. While high specific capacity values above 20 $m^2 d^{-1}$ and greater than 50 $m^2 d^{-1}$ are common in all the four areas, the highest values are found in Rukungiri and Mubende suggesting that the

aquifers in the two towns are more transmissive than those in Hoima and Ntungamo. The high specific capacity values in the four areas are characteristic of coarse-grained sediments and or very highly fractured bedrock. The lower specific capacity values in Hoima and Ntungamo than in Rukungiri and Mubende could be due to presence of less sorted sands and gravels overlying less fractured bedrock. The results appear to indicate that the fluvial sediments in Rukungiri and Mubende were transported over long distances as compared to those of Hoima and Ntungamo resulting in more sorting. Specific capacity values indicate that most aquifers in Uganda are generally not very transmissive ($<20\ m^2\ d^{-1}$).

7.3 Fluvial aquifers in deeply weathered terrains

7.3.1 Evidence from Uganda

Historical information and detailed investigations carried out in this study show that fluvial, weathered and fractured bedrock aquifers in Uganda have evolved by tectonically controlled weathering and stripping. Deep weathering of the bedrock yields a thick weathered regolith and induces sub-horizontal fissures whereas stripping partially erodes the weathered overburden, giving rise to a discontinuous regolith and fluvial deposition of coarse-grained clasts in river channels. Evolution of weathered and fractured bedrock aquifers has previously been recognised and characterised but existence of fluvial aquifers in deeply weathered terrains in humid tropics has largely been ignored. Field investigations have identified, for the first time, a highly productive aquifer comprising coarse-grained, fluvial sediments, in palaeochannels of river networks truncated by Miocene to Pleistocene rifting. Palaeochannel sediments are of limited extent on stripped surfaces but can feature

significant thicknesses along former river channels on deeply weathered surfaces (i.e. inter-arch basins).

Evidence for existence of fluvial aquifers with high specific capacities (> 20 m^2 d^{-1}) composed of gravels and coarse sands within palaeochannels has been compiled from 4 areas located in both the intra-arch and inter-arch basins. The aquifers have the highest yields in Uganda (>50 m^3 h^{-1}) and feature the thickest regoliths. Areas with the highest prospects for obtain high yielding boreholes in Uganda are therefore those that are associated with palaeochannels. Palaeochannels, are known to be good conduits for groundwater flow in arid and semi-arid areas but their existence in humid tropics has been reported only in a few areas with direct detailed studies in India and Australia (Mohammed *et al.*, 2003; Sinha *et al.*, 2000; de Broekert and Sandiford, 2005). There is no documented evidence for existence of palaeochannels in humid tropics of Africa and hence their role as conduits for groundwater flow within weathered terrain is unknown.

7.3.2 Evidence from Asia and Australia

Detailed studies in India (Mohammed *et al.*, 2003; Sinha *et al.*, 2000) and Australia (de Broekert and Sandiford, 2005) show that a network of palaeochannels can occur in deeply weathered environments. Studies carried out in Cauvery river basin in India (Mohammed *et al.*, 2003), where topographic and geological controls to the occurrence and movement of groundwater are apparent, show that palaeochannels characterised by extensive sedimentary deposits composed of pebbles, sand, silt and clay exist and form zones of preferential flow of groundwater. These form the main source of water in a number of locations and shallow wells drilled in the palaeochannels generally give high yields (179 to 236 m^3 d^{-1}) with good water quality

compared to the surrounding weathered and fractured gneiss. A hydrogeomorphological map prepared by demarcating geomorphic units favouring the occurrence and movement of groundwater shows that areas near or within palaeochannels have the highest well yields whereas the surrounding areas underlain by metamorphic rocks have much lower well yields. Studies in western India (Sinha *et al.*, 2000) use geological, geophysical and remote sensing techniques to identify river deposits dominated by coarse grained sand and gravels and prove the existence of palaeochannels. Although not mapped and delineated, the studies found that the palaeochannels form a thick sedimentary pile with significant groundwater flow and better prospects for water storage than the surrounding non-fluvial zones. De Broekert and Sandiford (2005) studied a network of fluvially incised valleys, referred to as "inset-valleys" filled with sediments, that are widespread in southwestern Australia. The studies found that the valleys are well preserved due to minimal denudation and tectonic deformation and can be traced in boreholes and open cut mines. In addition to providing significant insights into the geological history of the area, the studies identified the valleys as having a significant potential as source of minerals and groundwater.

7.3.3 Implications of the identification of the palaeochannel aquifer

Identification of the fluvial aquifer provides new and important targets for the development of groundwater for meeting urban, industrial and agricultural demand in Uganda and similar environments where groundwater resources are limited due to low permeability of the geological formations. However, as observed in the field, many valley flats were formed by meandering streams, and traces of the original river

courses have been removed by silting up of the channels and the growth of papyrus and other vegetation. Thus, identification of old river channels along which fluvial deposits may have been deposited is key to the search for groundwater.

Distribution of the palaeochannels (Fig. 7.29) has been demarcated based on the drainage network before and after tectonic uplift and drainage reversal in Uganda, to provide guidance for further work related to development and management of groundwater in the fluvial aquifers. Palaeochannels are also presumed to occur in other countries in Eastern and Southern Africa (Fig. 7.30) affected by rifting and the subsequent reversal of drainage. The existence, extent and potential of these aquifers therefore need to be assessed so that they can be targeted for large scale groundwater development.

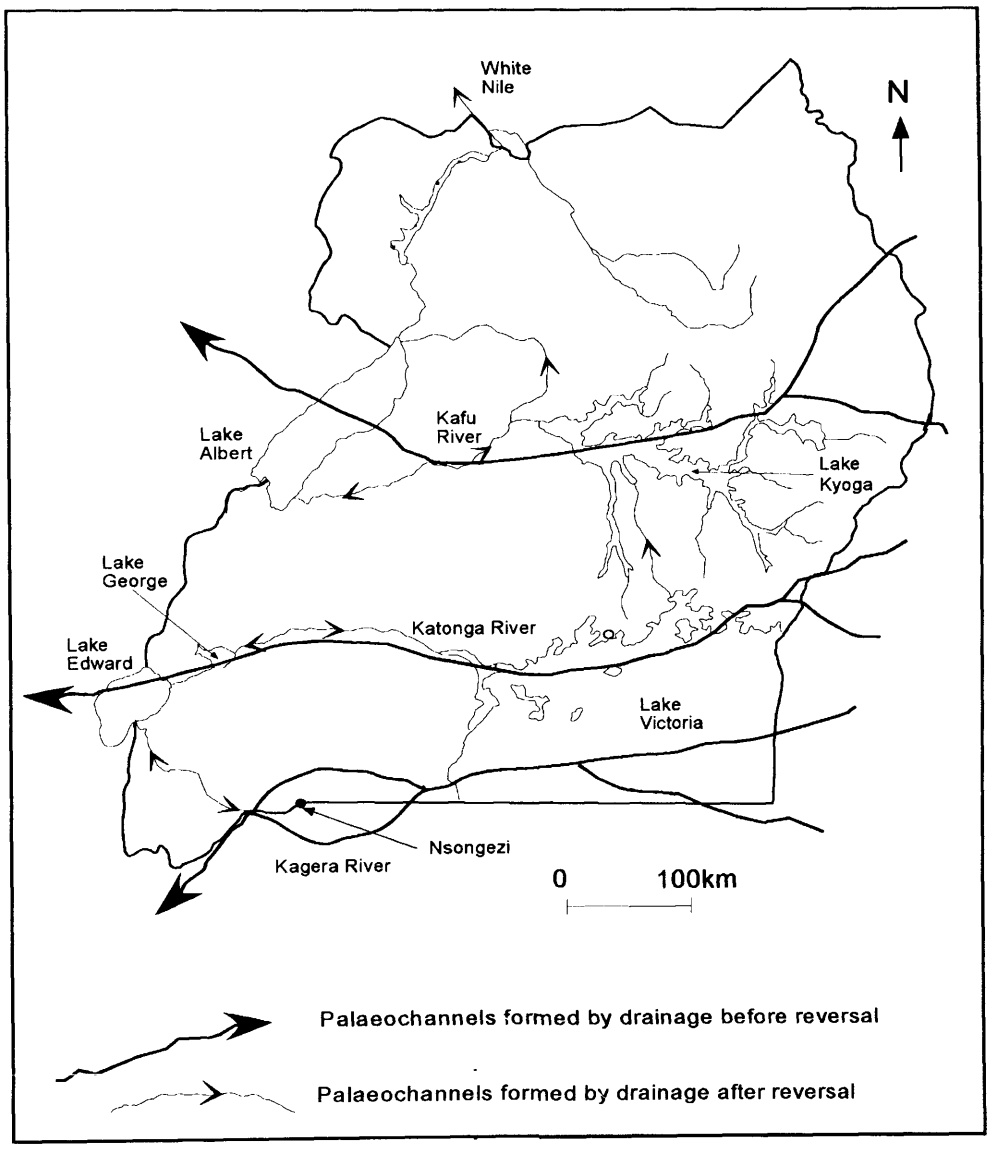

Figure 7.29. Distribution of palaeochannels in Uganda (based on Temple, 1970)

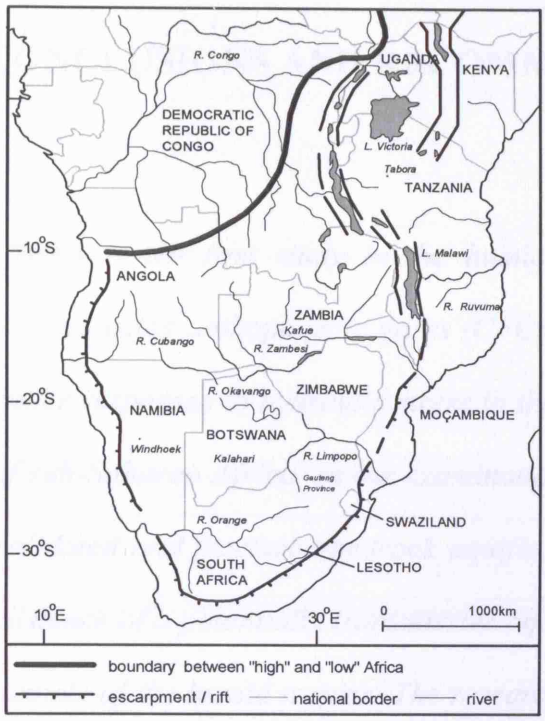

Figure 7.30. Areas affected by rifting in Eastern and Southern Africa (reproduced from Taylor, 2004). Palaeochannels are presumed to occur east of the western rift along former river channels within Uganda, Kenya, Tanzania, Malawi and Mozambique

CHAPTER 8: CONCLUSIONS AND RECOMMENDATIONS

8.1 Introduction

This doctoral thesis is the first study in the humid tropics that assesses groundwater residence times using anthopogenic gases (CFCs) and presents the first detailed analysis of aquifer responses to hydraulic stress in the weathered crystalline rock aquifer systems of sub-Saharan Africa. In the examination of groundwater flow and storage in unconsolidated and fractured-bedrock aquifers, this thesis identifies, for the first time, the existence of a potentially transmissive aquifer comprising fluvial sediments in palaeochannels of the humid tropics. The research was undertaken with three aims: (1) to assess the source, timing, and flow of recharge and groundwater residence times in weathered, fractured bedrock and fluvial aquifers; (2) to determine the flow of groundwater in weathered, fractured-bedrock and fluvial aquifers in response to hydraulic stress; (3) to relate observed hydrogeological characteristics to geomorphic evolution of the weathered, fractured bedrock and fluvial aquifers in Uganda. Conclusions including specific contributions to knowledge are presented and are followed by key recommendations arising out of this research.

8.2. Source, timing, and flow of recharge and groundwater residence times in weathered, fractured bedrock and fluvial aquifers

Aquifers are actively recharged by precipitation

Identical stable isotope ratios of oxygen and hydrogen in precipitation and groundwater strongly indicate that the aquifers in the humid tropics of Uganda are replenished by rainfall-fed recharge. Furthermore, groundwater levels in the weathered, fractured-bedrock and fluvial aquifers respond to seasonal (bimodal)

pulses of rainfall. The fast response (lag time ~ 2 weeks) of water levels observed simultaneously in the shallow weathered and deep fractured-bedrock aquifers to heavy rainfall events, indicates rapid vertical flow of recharge that necessarily bypasses the weathered matrix. Active recharge is confirmed by the similarity in tritium content and hydrochemistry of the weathered and fractured-bedrock aquifers, and short mean groundwater residence times described below.

Groundwaters comprise mixtures of residence times that are predominantly less than 50 years old.

A multi-tracer approach involving use of CFC gases (CFC-113, CFC-11, CFC-12) and tritium to assess mixing processes and estimate groundwater residence times, indicates that groundwater in Uganda is a mixture of young and old water. CFC results suggests that three groundwater flow conditions exist in aquifers in Uganda namely: piston flow in shallow weathered aquifers, binary mixing in fluvial aquifers and fractured-bedrock aquifers in areas of high topography, and exponential mixing in fractured-bedrock aquifers in areas of low topography. The results further show that the fraction of young water ranges from 5 to 100%. Mean residence times of the young groundwater range between 2 and 22 years. The short groundwater residence times and the presence of large proportions of modern water confirm that there is active groundwater recharge.

A necessary component of this pioneering application of residence-time indicators in the humid tropics of Uganda was the reconstruction of historical input functions for CFCs in tropical Africa and tritium in Uganda. These reconstructions facilitate future applications of these residence-time indicators in groundwater studies

in tropical Africa and Uganda. The consistency observed in atmospheric CFC concentrations in the northern hemisphere, southern hemisphere and mid-latitudes, despite preferential release of CFCs to the troposphere of the northern hemisphere, implies very rapid stratospheric mixing of gases. Reconstructions of historical input functions for CFCs can, therefore, be based on station data irrespective of its location without inducing errors of greater than 5%. Concentrations of CFC-12 in groundwater in weathered and fractured-bedrock aquifers were proportionately lower than CFC-113 and CFC-11, relative to their input function suggesting that this CFC species is degraded. This observation has also been reported in a similar hydrogeological environment in Tanzania and Niger and is considered to reflect preferential (natural) degradation of this anthopogenic gas in deeply weathered aquifer systems of the humid tropics.

Substantial amount of groundwater is stored in weathered and fractured-bedrock, and fluvial aquifers

Estimation of the amount of groundwater stored in the aquifers in the Rivers Kigwe and Mitano catchments, which can potentially be available for abstraction, based on mean groundwater residence times of 8 and 16 years respectively, indicates that 64 million m^3 and 3.5 billion m^3 of water is available in the two catchments respectively. This is equivalent to 1.3 million m^3 and 1.7 million m^3 of water per square kilometre for the River Kigwe and Mitano catchments respectively. The aquifer in the River Mitano catchment therefore stores more water per square kilometre than the aquifer in the River Kigwe catchment.

8.3. Flow of groundwater in weathered, fractured-bedrock and fluvial aquifers in response to hydraulic stress

Abstraction from fractured-bedrock aquifers is sustained by vertical leakage from the overlying weathered aquifer

Drawdown responses to pumping in the fractured-bedrock aquifers show that flow is complex and depends on the proximity to transmissive fractures but is generally linear through individual fractures at early pumping times but evolves to radial flow at pumping periods ranging between 600 and 1500 minutes. Leakage from the overlying aquifer occurs after approximately 1800 minutes of pumping. The similarity in the evolution of the various flow mechanisms in the weathered and fractured-bedrock aquifers confirms that the weathered and fractured-bedrock aquifers are hydraulically connected and form one aquifer system. Similar tritium content, hydrochemistry and residence times for groundwater in the weathered and fractured-bedrock aquifers are consistent with the observation of a hydraulically integrated aquifer system. Under active groundwater recharge, of the order of 160 mm a^{-1}, heavy groundwater abstraction in Wobulenzi (12 m^3 h^{-1}) has, over the last 9 years, not significantly depleted groundwater storage suggesting that abstraction from fractured-bedrock aquifers is sustained by vertical leakage from the overlying weathered aquifer.

Groundwater flow in the fluvial aquifer is more uniform and radial but becomes linear due to intensive groundwater abstraction

Groundwater flow response in the fluvial aquifer in Rukungiri is relatively homogeneous and is radial but changes to linear due to intensive groundwater

abstraction. This response suggests that dewatering of the fluvial aquifer occurs as pumping proceeds and the rate depends on the extent of the aquifer. The transition from a radial flow field to linear flow corresponds with a rapid decline in groundwater storage of ~2.5 m a^{-1} over the last 8 years. Dewatering of the aquifer is also indicated by drawdown responses and flow dimensions of boreholes installed in the fluvial aquifer in Ntungamo located in the intra-arch basin.

Graphical analysis of drawdown responses using aquifer diagnostic methods is an essential precursor to the selection of analytical and numerical models of groundwater flow in weathered, fractured bedrock and fluvial aquifers

Graphical analysis of drawdown responses using aquifer diagnostic methods (s versus t/r^2, log-log/log-linear, derivative, flow dimension) has been used for the first time in tropical Africa to characterise groundwater flow and aquifer geometry. Groundwater flow characteristics of the weathered, fractured bedrock and fluvial aquifers determined in this study show that there are two dominant flow regimes that occur in the geological formations of Uganda: (1) radial flow through a network of interconnected fractures; and (2) linear flow through coarse grained fluvial sediments and individual bedrock fractures at early pumping times. Diagnostic plots usefully inform conceptual models of groundwater flow in the various aquifer systems and hence use of analytical groundwater flow models.

Estimates of aquifer hydraulic properties in crystalline rock aquifers are sensitive to the employed analytical model

Determination of aquifer hydraulic properties using analytical methods results in highly variable estimates of transmissivity and storativity for the weathered and

fractured-bedrock aquifers but relatively consistent estimates for the fluvial aquifer. While available analytical solutions can be used to interpret pumping-test data from fairly homogeneous fluvial aquifers without introducing significant errors in the estimates, the determined properties of the weathered and fractured-bedrock aquifer are sensitive to the employed model. This observation confirms that selection of appropriate analytical solutions based on knowledge of aquifer geometry and groundwater flow is an essential first step in the interpretation of pumping-test data. Based on analytical solutions selected using aquifer diagnostic methods, the average transmissivity and storage coefficient values for the weathered aquifer in Wobulenzi are 16 m^2 d^{-1} and 0.21 whereas those for the fractured-bedrock aquifer in the same study area are 14 m^2 d^{-1} and 0.014 respectively. The average transmissivity and storage coefficient values for the fluvial aquifer in Rukungiri are however 34 m^2 d^{-1} and 0.1 respectively. The study findings suggest that the commonly used analysis solutions for confined and leaky aquifer conditions (Theis, Cooper-Jacob and Hantush methods) are inapplicable to the complex groundwater flow conditions in fractured-bedrock aquifers implying that more appropriate methods are required for interpretation of data from such aquifers.

8.4. Relationship between observed hydrogeological characteristics and geomorphic evolution of the weathered, fractured-bedrock and fluvial aquifers in Uganda

Revision of the tectono-geomorphic model to include fluvial aquifers

Historical observations and detailed investigations carried out in this study confirm that the evolution of weathered, fractured-bedrock and fluvial aquifers in

Uganda is closely related to development of landscapes though tectonically controlled cycles of deep weathering and stripping. Deep weathering of the bedrock yields a thick weathered overburden and induces sub-horizontal fissures whereas stripping partially erodes the weathered overburden, giving rise to a discontinuous regolith and fluvially deposited coarse-grained clasts in river channels. The evolution of homogeneous, well sorted unconsolidated fluvial aquifers in deeply weathered terrains in humid tropics is recognised explicitly for the first time and therefore necessitates revision of the tectono-geomorphic model of the hydrogeology of weathered crystalline rocks. The revised techono-geomorphic model of the hydrogeology of weathered crystalline rocks thus consists of weathered, fractured-bedrock and fluvial aquifers.

Highly transmissive fluvial aquifers exist in palaeochannels of major river networks truncated by Miocene to Pleistocene rifting

A highly productive aquifer comprising coarse-grained, fluvial sediments has been identified, for the first time, in palaeochannels of former westerly flowing river networks in Uganda. The fluvial aquifer has borehole yields (> 5 $m^3 h^{-1}$) and specific capacity values (>50 $m^2 d^{-1}$) that far exceed yields of less than 1 $m^3 h^{-1}$ and specific capacity values of less than 20 $m^2 d^{-1}$ that are typically observed in weathered and fractured-bedrock aquifers systems. Fluvial sediments can feature significant thicknesses in palaeochannels of major river networks truncated by Miocene to Pleistocene rifting but subsequent erosion in the intra-arch basin significantly constrains the extent and thickness of these aquifers and, hence, the sustainability of groundwater abstraction. Depletion of groundwater storage over the last 8 years as a result of abstraction (12 $m^3 h^{-1}$ per borehole), is indicated by water-level declines of

2.5 m a^{-1} in Rukungiri town found in the intra-arch basin. Identification of palaeochannel aquifers represents a key contribution to the understanding of the relationship between the geomorphology and hydrogeology of deeply weathered environments. Fluvial aquifers provide important new targets for the development of groundwater for meeting urban, industrial and agricultural demand in Uganda and similar environments where groundwater resources are limited by the low permeability and storage of weathered and fissured crystalline rock aquifers.

8.5. Recommendations emanating from improved understanding of crystalline rock aquifers

Establishment and operation of groundwater monitoring networks

This study clearly shows that groundwater level measurements remain the principal source of information on changes in groundwater storage whether natural or human induced. In order to understand the nature and causes of the change in groundwater storage, sustained measurements of groundwater levels are required. Monitoring groundwater levels has, however, received little attention especially in low-income countries. Although monitoring may be initiated, it is often not sustained. Monitoring may be discontinued because of operational costs or the perception that groundwater resources are unlimited and therefore do not need to be monitored like surface water. Intensification of groundwater development for urban, industrial and agricultural use combined with the effects of climate change, means that groundwater resources will in the future be under increasing pressure. It is, therefore, recommended that groundwater monitoring networks be established in weathered crystalline rock aquifer systems both in areas of intensive groundwater development

to monitor the impacts of abstraction on groundwater resources and in areas where there is no groundwater abstraction to monitor natural climatic impacts on groundwater. Such information provides critical guidance to the design of appropriate pumping regimes and management of well fields and in evaluation of the causes of any change in groundwater storage.

Conducting pumping tests and reporting of data

This study showed that drawdown responses to pumping in weathered and fractured-bedrock change over time. Linear flow via individual fractures at early pumping times evolves into radial flow between 600 and 1500 minutes of pumping through a dense network of fractures at late pumping times. To assess the yield of a well and determine aquifer transmissivity and storage it is therefore important that pumping tests are conducted for sufficient durations to ensure that the response of the aquifer has evolved from linear to radial flow. Based on results of this study, it is recommended that the durations of pumping tests should be as long as possible but should not be less than 600 minutes. In addition to monitoring drawdown during pumping, recovery should be monitored at the end of every test for a sufficiently long period or until over 90% of the drawdown has been recovered.

Assessment of well performance from specific capacity

This study has established that specific capacity (yield per unit drawdown) is a better means of assessing the performance of a well than borehole yield. Specific capacity can assist in estimating transmissivity of an aquifer and in determining pump installation depths, in the absence of pumping test data, which is usually not available in developing countries. Specific capacity can be easily estimated during drilling of

wells through dividing yield by drawdown created during the yield estimation. It is therefore recommended that for each well, an airlift yield estimate be made immediately after completion of development of a well, for at least one hour, and the drawdown created be immediately recorded and the results reported together with well yields.

Interpretation of aquifer hydraulics data using analytical and numerical models

The choice of an invalid conceptual model to interpret aquifer hydraulics data necessarily leads to erroneous conclusions regarding flow and storage subjecting groundwater development and management strategies to great uncertainty. It is therefore recommended that flow characteristics and aquifer geometry be determined before selecting analytical and numerical models for interpretation of aquifer hydraulics data. Plotting time-drawdown data on log scale and determining the characteristics of flow can usefully provide the required information.

Use of environmental tracers

This study has demonstrated that a multi-tracer approach in groundwater studies offers a possibility to assess mixing of groundwater, determine proportions of the young component, determine groundwater residence times, and assess the susceptibility of aquifers to pollution. It is therefore recommended that use of environmental tracers should employ a multi-tracer approach as it provides an opportunity to compare and corroborate the results of the various tracers.

Groundwater development and management in weathered, fractured-bedrock and fluvial aquifers

This study has established that groundwater abstraction from the weathered and fractured-bedrock aquifers is sustainable due to the vertical leakage of the overlying weathered aquifer to the fractured-bedrock aquifer. This therefore implies that pollution of the shallow weathered aquifer can lead to contamination of the fractured-bedrock aquifer. Furthermore, the study has found that sustainability of groundwater abstraction in fluvial aquifers is limited by the extent and thickness of fluvial sediments. Fluvial aquifers in intra-arch basin are therefore highly vulnerable to over abstraction due to their limited extent. It is therefore recommended that weathered, fractured-bedrock and fluvial aquifers be adequately protected from any potential sources of pollution, and groundwater abstraction be closely monitored and managed to avoid depletion of the aquifer and adverse effects on the environment. Lack of protection of groundwater may increase scarcity of water supply and escalate the water supply costs with potential impacts on human health.

While the existence of the fluvial aquifer with high yields has been confirmed, the understanding of the groundwater development potential of this aquifer is, however, still in its infancy. It is therefore recommended that further research be carried out to determine the extent, depth and recharge mechanism of the aquifer as well as sustainability of long-term intensive groundwater development. Possibilities of artificial recharge in palaeochannels for augmenting available water resources to meet the increasing water demands also need to be assessed. Despite the above observations, future intensive groundwater development should target palaeochannels underlain by fluvial aquifers in order to obtain high yielding wells.

REFERENCES

Acworth, R.I (1987). The development of crystalline basement aquifers in tropical environment. Quarterly Journal of Engineering Geology (London), Vol. 20, pp 265 – 272.

Alley, M.W., Healy, W.R., LaBaugh, W.J. and Reilly, E.T (2002). Flow and storage in groundwater systems. Science, Vol. 296, pp 1985 –1990.

Amin, I.E. and Campana, M. E (1996). A general lumped parameter model for the interpretation of tracer data and transit time calculation in hydrological systems. Journal of Hydrology, Vol. 179, pp 1 – 21.

Barker, J.A (1985). Generalized well-function evaluation for homogeneous and fissured aquifers. Journal of Hydrology, Vol. 76, pp143-154.

Barker, J.A (1988). A generalized radial flow model for hydraulic tests in fractured rock. Water Resources Research, Vol. 24, No. 10, pp1796-1804.

Barker, J.A (1991). Transport in fractured rock. In: "Applied Groundwater Hydrology", R.A. Downing & W.B. Wilkinson (Eds.), Oxford University Press, pp199-216.

Barker, J.A (2000). A manual for BGSPT: programs to simulate and analyse pumping test in large-diameter wells. Version 5. Unpublished report. University College, London, UK.

Barker, J (2006). Unpublished lecture material, University College London, UK.

Basalirwa, C.P.K (1995). Delineation of Uganda into Climatological rainfall zones using the method of Principal component analysis. International Journal of Climatology, Vol. 15, pp1161 - 1177.

Bateman, A (1998). Chlorofluorocarbons in groundwater. Unpublished PhD thesis, University of East Anglia, UK, pp253.

Birpinar, M.E (2003). Aquifer parameter identification and interpretation with different analytical methods. Water SA, Vol. 29, No. 3, pp251 -256.

Bishop, W.W. and Trendall, A.F (1967). Erosion-surfaces, tectonics and volcanic activity in Uganda. Journal of Geological Society, London, Vol. 122, pp385 - 420.

Bjørlykke, O. K (1975). Mineralogical and chemical changes during weathereing of acid and basal rocks in Uganda. Norsk Geologisk Tidsskrift, Vol. 55, pp81- 89.

Bockgard, N., Rodhe, A. and Olsson, K.A (2004). Accuracy of CFC groundwater dating in crystalline bedrock aquifer: data from a site in Southern Sweden. Hydrogeology Journal, Vol. 12, pp171-183.

Bourdet, D., Ayoub, J.A. and Pirard, Y.M (1989). Use of pressure derivative in well-test interpretation. SPE Formation Evaluation, pp293-302.

Brown, D.J (2007). Using a global VNIR soil spectral library for local soil characterisation and landscape modelling in a 2nd-order Uganda watershed. Geoderma, Vol.140, pp444 - 453.

Busenburg, E. and Plummer, L.N (1992). Use of chlorofluorocarbons as hydrological tracers and age dating tools: the alluvium and terrace system of central Oklahoma. Water Resources Research, Vol.28, No.9, pp 2257 –2283.

Celle-Jeanton, H., Gourcy, L. and Aggarwal, P (2001). Reconstruction of Tritium time series in precipitation. Unpublished report. Intentaional Atomic Energy Agency, Vienna, Austria.

Chilton P.J. and Smith-Carington A.K (1984). Characteristics of weathered basement aquifer in Malawi in relation to rural water supplies. In: Africa Hydrology and water resources, Proceedings of Harare symposium.

Chilton, P.J. and Foster, S.S.D (1995). Hydrogeological characterisation and water supply potential of basement aquifers in tropical Africa. Hydrogeology Journal, Vol.3, pp36 - 49.

Clark, I. and Fritz, P (1997). Environmental Isotopes in Hydrogeology. New York, Lewis Publishers, CRC Press LLC, pp 290.

Cook, P.G., Solomon, D.K., Plummer, L.N., Busenberg, E. and Schiff, S.L (1995). Chlorofluorocarbons as tracers of groundwater transport processes in a shallow, silty sand aquifer. Water Resources Research, Vol. 31, No.3, pp 425 – 434.

Cook, P.G. and Solomon, D.K (1995). Transport of atmospheric tracer gases to the water table: implications for groundwater dating with chlorofluorocarbons and krypton –85. Water Resources Research, Vol. 31, No.2, pp 263 – 270.

Cook, P.G. and Solomon, D.K (1997). Recent advances in dating young groundwater: chlorofluorocarbons, $^{3}H/^{3}He$ and ^{85}Kr. Journal of Hydrology, Vol. 191, pp 245 –265.

Cook, P.G., Favreau, G., Dighton, C.J. and Tickell, S (2003). Determining natural groundwater influx to a tropical river using, chlorofluorocarbons and ionic environmental tracers. Journal of Hydrology, Vol. 277, pp 74 – 88.

Cook, P.G., Love, J.A, Robinson, I.N. and Simmons, T.C (2005). Groundwater ages in fractured rock aquifers. Journal of Hydrology, Vol. 308, pp 284 – 301.

Craig, H (1961). Isotopic variations in meteoric waters. Science, Vol, 133, pp1702-1703.

Dansgaard, W (1964). Stable isotopes in precipitation. Tellus, Vol. 16, No.4, pp436 - 468.

Darling, W.G., Edmunds, W.M., Kinniburg, D.G. and Kotoub, S (1987). Sources of recharge to the basal Nubian sandstone aquifer, Butana Region, Sudan. Isotope Techniques in Water Resources Development, IAEA-SM-299/177. IAEA, Vienna, pp205 - 225.

Darling, W.G., Morris, L.B., Stuart, M.E. and Gooddy, C.D (2005). Groundwater age indicators for public supplies tapping Chalk aquifer of Southern England. Water and Environment Journal, Vol. 19, pp30-40.

De Broekert, P. and Sandiford,M (2005). Buried Inset-Valleys in the Eastern Yilgarn Craton, Western Australia: Geomorphology, Age, and Allogenic Control. Journal of Geology, Vol. 113, pp471 - 493.

De Swardt, A.M.J and Trendall, A.F (1969). The Physiographic development of Uganda. Overseas geology and Mineral Resources, Vol. 10.

Dietrich, P., Helmig, R., Sauter, M., Hotzl, H., Kongeter, J. and Teutsch, G (2005). Flow and transport in fractured porous media. Springer, Heidelberg, The Netherlands

Doney, S.C., Glover, D.M. and Jenkins, W.J (1992). A model function of the global bomb tritium distribution in precipitation 1960 – 1980. Journal of Geophysical Resources, Vol. 97, No. C4, pp5481 -5492.

Doornkamp, J.C. and Temple, P.H (1966). Surface, Drainage and Tectonic instability in part of Southern Uganda. The Geographical Journal, Vol. 132, part 2.

Doornkamp, J.C (1968). The role of Inselbergs in the Geomorphology of Southern Uganda. Transactions. Institute of British Geographers, No.44.

Doornkamp, J.C (1970). Geomorphology of the Mbarara Area Sheet SA-36-1. Geomorphology report No.1.

DWD (2001). Urban Towns Water and Sanitation Facilities: Data collection sheets. Unpublished report. Directorate of Water Development, Ministry of Water, Lands and Environment.

DWD (2002). Urban Towns Water and Sanitation Facilities: Data collection sheets. Unpublished report. Directorate of Water Development, Ministry of Water, Lands and Environment.

Edet, A. and Okereke, C (2005). Hydrogeological and hydrochemical character of the regolith aquifer, northern Obudu Plateau, Southern Nigeria. Hydrogeology Journal, Vol.13, No. 2, pp24-36.

Ekwurzel, B., Schlosser, P., Jr.W.M.S., Plummer, L.N., Busenburg, E, Michel, R.L., Weppernig and Stute, M (1994). Dating shallow groundwater: comparison of the transient tracers 3H/3He, chlorofluorocarbons and ^{85}Kr. Water Resources Research, Vol.30, No.6, pp1693-1708.

Foster, S.S.D., Lawrence, A. and Morris, B (1998). Groundwater in urban development. Assessing management needs and formulating policy strategies. World Bank Technical Paper No. 390, The World Bank, Washington D.C.

Gat, J.R (1987). Variability (in time) of isotopic composition of precipitation: Consequences regarding the isotopic composition of hydrologic systems. In: Isotope Techniques in Water Resources Development, IAEA-SM-299/177. IAEA, Vienna, pp551 - 563.

Gernand J.D. and Heidtman J.P (1997). Detailed pumping test to characterise a fractured bedrock aquifer. Groundwater, Vol. 35, No.4, pp345-365.

Gooddy, C.D, Darling, W.G, Abesser, C. and Lapworth, J.D (2006). Using chlorofluorocarbons (CFCs) and sulphur hexafluoride (SF_6) to characterise groundwater movement and residence times in a lowland chalk catchment. Journal of Hydrology, Vol. 330, pp 44-52.

Goodwin, A.M (1991). Precambrian Geology. Academic Press, pp666.

GoU (2001). Rural water supply and sanitation strategy and investment plan. Unpublished report. Directorate of Water Development, Ministry of Water, Lands and Environment.

GoU (2003). Urban water supply and sewerage strategy and investment plan. Unpublished report. Directorate of Water Development, Ministry of Water, Lands and Environment.

Gyau-Boakye, P. and Dapaah-Siakwan, S (1999). Groundwater: Solution to Ghana's rural water supply industry? The Ghana Engineer, May 1999.

Hamm, S. and Bidaux, P (1996). Dual porosity fractal models for transient flow analysis in fissured rocks. Water Resources Research, Vol. 32, No.9, pp2733 -2745.

Happell, J.D., Price, R.M., Top, Z. and Swart, P.K (2003). Evidence for the removal of CFC-11, CFC-12 and CFC-113 at the groundwater – surface water interface in the Everglades. Journal of Hydrology, Vol. 279, pp94 - 105.

Heaton, T.H.E. and Vogel, J.C (1981). Excess air in groundwater. Journal of Hydrology, Vol.50, pp201- 216.

Horne, R.N (1997). Modern Well Test Analysis. A computer-Aided Approach. Petroway Inc., California, USA.

Howard, K.W.F. and Karundu, J (1992). Constraints on the development of basement aquifers in east Africa - water balance implications and the role of the regolith. Journal of Hydrology, Vol. 139, pp183 - 196.

Howard, K.W.F., Hughes, M., Charlesworth, D.L. and Ngobi, G (1992). Hydrogeological evaluation of fracture permeability in crystalline basement aquifers of Uganda. Journal of Applied Hydrogeology, Vol. 1, pp55 – 65.

Hydrogeology - Uganda Phase II (1994). Hydrogeological and socio-economic examination of the regolith and fractured – basement aquifer systems of Aroca catchment in Apac District and Nyabisheki catchment in Mbarara District. Final report to the Directorate of Water Development of the Ministry of Natural Resources, Republic of Uganda (May, 1994).

IAEA (2002). Statistical treatment of data on environmental isotopes in precipitation. Updated version of Technical Report Series no. 331, International Atomic Energy Agency, Vienna, Austria.

IAEA (2004). New recommended half life for Tritium. International Atomic Energy Agency web page.

IAEA (2006). Use of Chlorofluorocarbons in Hydrology. A guidebook. International Atomic Energy Agency, Vienna, Austria.

Johnson, S. G., Cosgrove, M. D. and Frederick, B. D (2001). A Numerical Model and spreadsheet interface for Pumping test analysis. Groundwater, Vol. 41, No.3, pp333 - 341.

Katz, G.B., Chelette, R.A. and Pratt, R.T (2004). Use of chemical and isotope tracers to assess nitrate contamination and groundwater age, Woodville, Karst Plain, USA. Journal of Hydrology, Vol. 289, pp36 - 61.

Kendal, C. and Mcdonnell, J.J (1998). Isotope Tracers in Catchment Hydrology, Elseveir Science B.V., The Netherlands, pp816.

Khalil, C. and Rasmussen, R.A (1989). The potential of soils as a sink of chlorofluorocarbons and other man-made chlorocarbons. Geophysical Research letters, Vol.16, pp679-682.

Koh, C.D., Plummer, L.N, Solomon, K.D, Busenberg, E, Kim, J.Y. and Chang, W.H (2006). Application of environmental tracers to mixing, evolution, and nitrate contamination of groundwater in Jeju Island, Korea. Journal of Hydrology, Vol 327, pp258 - 275.

Kruseman, G.P. and de Ridder, N.A (2000). Analysis and Evaluation of Pumping test Data. International Institute for Land Reclamation and Improvement, Wageningen, The Netherlands.

Kuusela-Lahtinen, A., Niemi, A. and Luukkonen, A (2003). Flow Dimension as an Indicator of Hydraulic behaviour in site characterization of fractured rock. Groundwater, Vol. 39, No.4, pp582 - 592.

Leroux, M (1983). The climate of tropical Africa. Champion, Paris, pp274.

Lovelock, J. E (1971). Atmospheric fluorine compounds as indicators of air movements. Nature, Vol.230, pp379.

MacDonald, A (2001). Community water supplies from mudstones. Unpublished PhD Thesis submitted to the Department of Geological Sciences, University College London. pp36 - 40.

Macdonald, A., Darling, W.G., Ball, F.D., and Oster, H (2003). Identifying trends in groundwater quality using residence time indicators: an example from the Permian aquifer of Dumfries, Scotland. Hydrogeology Journal, Vol. 11, pp504 – 517.

Macdonald, A., Davies, J., Carol, R and Chilton, J (2005). Developing groundwater: a guide for Rural Water Supply. ITDG Publishing, Warwickshire, UK.

McFarlane, M.J (1992). Groundwater movement and water chemistry associated with weathering profiles of the African surface in parts of Malawi: In: Wright, E.P., Burgess, W.G. (Eds.), Hydrogeology of Crystalline basement Aquifers in Africa. Geological Society Special Publication No.66, pp101 - 130.

McFarlane, M.J., Chilton, P.J. and Lewis, M.A (1992). Geomorphological controls on borehole yields: a statistical study in an area of basement rocks in central Malawi: In: Wright, E.P., Burgess, W.G. (Eds.), Hydrogeology of Crystalline basement Aquifers in Africa. Geological Society Special Publication No.66, pp131 - 154.

Maloszewski, P. and Zuber, A (1982). Determining the turnover time of groundwater systems with the aid of environmental tracer data. Journal of Hydrology, Vol. 57, pp207 -231.

Maloszewski, P. and Zuber, A (1996). Lumped parameter models for the interpretation of environmental tracer data. Manual on Mathematical Models in Isotope Hydrogeology, IAEA-TECDOC 910, IAEA, Vienna, pp9 - 58.

Marchant, R. and Taylor, D (1997). Late Pleistocene and Holocene History of Mubwindi Swamp, Southwestern Uganda. Quaternary Research, Vol, 47, pp316 - 328.

Marechal, J.C., Dewandel, B. and Subrahmanyam, K (2004). Use of hydraulic tests at different scales to characterise fracture network properties in the weathered-fractured layer of a hard rock aquifer. Water Resources Research, Vol. 40, W11508, pp1 - 17.

Marechal, J.C., Dewandel, B., Subrahmanyam, K. And Torri, R (2003). Specific methods for the evaluation of hydraulic properties in fractured hard-rock aquifers. Current Science, vol. 85, No.4, pp11- 23.

Matthess, G. (1982). The properties of groundwater. John Wiley.

Mileham, L., Taylor, R.G., Todd, M., Thompson, J. and Tindimugaya, C (in prep). Impact of rainfall distribution on the parameterisation of a soil-moisture balance model of groundwater recharge in equatorial Africa. Journal of Hydrology.

Mohammed Aslam, A.M., Balasubramanian, A., Kondoh, A., Rokhmatuloh, A., and Mustafa, J.A (2003). Hydrogeomorphological mapping using remote sensing techniques for water resources management around palaeochannels. In: Proceedings of the symposium on Geosciences and remote sensing, Toulouse, France. Vol.5, pp3317 -3319.

Morris, L.B., Darling, W.G., Cronin, A.A., Rueedi, J., Whitehead, J.E. and Gooddy, C.D (2006). Assessing the impact of modern recharge on a sandstone aquifer beneath a suburb of Doncaster, UK. Hydrogeology Journal, Vol. 14, pp979- 997.

Mulligan, E.A., Evans, L.R. and Lizarralde, D (2007). The role of paleochannels in groundwater/seawater exchange. Hydrogeology Journal, Vol. 335, pp313 - 329.

MWE (2006). Water and Sanitation Sector Performance Report 2006. Unpublished report. Ministry of Water and Environment.
MWLE (2006a). Status of implementation of Urban Water and Sanitation Projects and Rural Growth Centres. Unpublished report. Ministry of Water, Lands and Environment, Directorate of Water Development.

MWLE (2006b). Water Authorities Division quarter four and annual inspection report. Unpublished report. Ministry of Water, Lands and Environment, Directorate of Water Development.

Njitchoua, R., Dever, L., Fontes, C.J. and Naah, E (1997). Geochemistry, origin and recharge mechanisms of groundwaters from the Garoua Sandstone aquifer, northern Cameroon. Journal of Hydrology, Vol, 190, pp123 - 140.

Ojany, F.F (1971). Drainage evolution in Kenya. In Ominde (editor): Studies in East African Geography and Development. Heinemann, London, UK, pp273.

Osiensky, J.L., Williams, R.E., Williams, B and Johnson, G (2006). Evaluation of drawdown curves derives from multiple well aquifer tests in heterogeneous environments. Technical Article, International Mine Water Association, pp30-55.

Oster, H., Sonntag, C., and Munnich, K.O (1996). Groundwater age dating with chlorofluorocarbons. Water Resources Research, Vol. 32, No.10, pp2989 –3001.

Owoade, A (1995). The potential of minimizing drawdowns in groundwater wells in tropical aquifers. Journal of African Earth Sciences, Vol. 20, No.3- 4, pp289 – 293.

Ozyurt, N.N. and Bayari, S.C (2003). Lumped unsteady: a Visual Basic code of unsteady-state lumped parameter models for mean residence time analyses of groundwater systems. Computers and Geosciences, Vol. 31, pp329 - 341.

Plummer, L.N., Michel, R.L., Thurman, E.M., and Glynn, P.D (1993). Environmental tracers for age dating young groundwaters. In: Regional Groundwater Quality (ed. Alley, W.M). Van Nostrand Reinhold. pp255 - 294.

Plummer, L.N. and Busenburg, E (1999). Chlorofluorocarbons. In: Cook, P. And Herczeg, A.L. (Eds.), Environmental Tracers in Subsurface Hydrology. Kluwer Academic Publishers, Amsterdam, pp441 – 478.

Plummer, L.N., Busenburg, E, Bohlke, J.K, Nelms, D.L, Michel, R.L and Schlosser, P (2001). Groundwater residence times in Schenandoah National Park, Blue Ridge Mt, Virginia, USA: a multi-tracer approach. Chemical geology, Vol. 179, pp93 - 111.

Plummer, L.N (2004). Dating of young groundwater with CFCs, SF6, 3H, and 3H/3He: Principles and examples. Paper presented at the Forensic Hydrology Workshop, Annapolis, MD.

Plummer, L.N., Busenburg, E. and Han, L.E (2006). Data interpretation in representative cases. In: Use of Chlorofluorocarbons in Hydrology: A guidebook. International Atomic Energy Agency Agency, Vienna, pp105-182.

Rademacher, L.K., Clark, J.K. and Boles, J.R (2003). Groundwater residence times and flow paths in fractured rock determined using environmental tracers in the Mission Tunnel; Santa Barbara county, California, USA. Environmental Geology, Vol. 43, pp557-567.

Radwanski, S.A. and Ollier, C.D (1959). A study of an east African catena. Journal of Soil Science, Vol. 10, No.2, pp149 - 170.

Renard, P (2005). The future of hydraulic tests. Hydrogeology Journal, Vol. 13, pp259 - 262.

RSA (2001). Launch of the South African Chapter of Vision 21 by Ronnie Kasrils, Minister of Water Affairs and Forestry and Mr Gourisankar Gosh, Executive Director of Water Supply and Sanitation Collaborative Council: Press release, 2001.

Rueedi, J., Brennwald, M.S., Purtschert, R., Beyerle, U., Hofer, M and Kipfer, R (2005). Estimating amount and spatial distribution of groundwater recharge in the Lullemmeden basin (Niger) based on 3H, 3He and CFC-11 measurements. Hydrological Proceses, Vol.19, pp3285-3298.

Rushton, K.R. and Weller, J (1985). Response to pumping of a weathered-fractured granite aquifer. Journal of Hydrology, Vol. 24, pp456 – 470.

Rushton, K.R (2003). Groundwater Hydrology: Conceptual and computational models. John Wiley & Sons Ltd, West Sussex, England.

Salati, E., Dall'Olio, A., Matsui, E. and Gat, J.R (1979). Recycling of water in the Amazon Basin: an isotopic study. Water Resources Research, Vol. 15, No.5, pp1250-1258.

Schlüter, T (1997). Geology of East Africa. Gerbrüder Borntraeger, Berlin- Stuttgart, pp484.

Semprini, L., Hopkins, G.D., Roberts, P.V., and McCarthy, P.L (1990). In situ biotransformation of carbon tetrachloride, 1,1,1, - trichloroethane, Freon –11 and Freon – 113 under anoxic conditions. Abstract Eos Transactions AGU, Vol.71, pp1324.

Serrano, S.E (1997). The Theis solution in heterogeneous aquifers. Groundwater, Vol. 35, No. 3, pp463-467.

Shapiro, S.D., Schlosser, P., Smethie Jn, W.M. and Stute, M (1997). The use of 3H and tritiogenic 3He to determine CFC degradation and vertical mixing rates in Framvaren Fjord, Norway. Marine Chemistry, Vol.59, pp141 - 157.

Shapiro, A.M (2002). Fractured –rock aquifers understanding an increasingly important source of water. United States Geological Survey Fact sheet 112 – 02.

Sinha, K.A., Raghav, S.K. and Sharma, A (2000). Palaeochannels and their recharge as drought proofing measure: study and experiences from Rajasthan, Western India. Unpublished report.

Sukhija, S.B., Reddy, V.D., Nagabhushanam, P., Bhattacharya, K.S., Jani, A.R. and Kumar, D (2006). Characterisation of recharge processes and groundwater flow mechanisms in weathered-fractured grante of Hyderabad (India) using isotopes. Hydrogeology Journal, Vol, 14, pp663- 674.

Summerfield, M.A (1991). Global Geomorphology: An introduction to the study of landforms. Prentice Hall. Pearson Education Limited, Essex, England

Talma, A.S. and Weaver, J.M.C (2003). Evaluation of groundwater flow patterns in fractured rock aquifers using CFCs and isotopes. Report to the Water Research Commission, South Africa. Report No. 1009/1/03.

Taylor, R.G and Howard, K.W.F (1996). Groundwater recharge in the Victoria Nile basin of East Africa: support for the soil moisture balance approach using stable isotope tracers and flow modelling. Journal of Hydrology, Vol. 180, pp31-53.

Taylor, R.G. and Howard, K. W.F (1998). Post Palaezoic evolution of weathered land surfaces in Uganda by tectonically controlled cycles of deep weathering and stripping. Geomorphology, Vol. 25, pp173 - 192.

Taylor, R.G. and Howard, K. W.F (1999a). Lithological evidence for the evolution of weathered mantles in Uganda by tectonically controlled cycles of deep weathering and stripping. Catena, Vol. 35, pp65 - 94.

Taylor, R.G. and Howard, K. W.F (1999b). The influence of tectonic setting on the hydrological characteristics of deeply weathered terrain: evidence from Uganda. Journal of Hydrology, Vol. 218, pp44 - 71.

Taylor, R.G. and Howard, K. W.F (2000). A tectono- geomorphic model of the hydrogeology of deeply weathered crystalline rock: evidence from Uganda. Hydrogeology Journal, Vol. 8, pp279 - 294.

Taylor, R.G., Barrett, M.H., Tindimugaya, C., Barker, J.A., Macdonald, D.M., Howard, A.G., Johal, K., Edwardmartin, R. and Nalubega, M (2001). A study of contaminant transport in deeply weathered crystalline rock in Uganda: results of forced-gradient tracer tests using chloride and bacteriophage φ-X174. Report to the Water Resources Management Department of Uganda.

Taylor, R.G., Barrett, M.H. and Tindimugaya, C (2004). Urban areas of sub-Saharan Africa; weathered crystalline aquifer system. International contributions to Hydrogeology, Vol. 24, pp155-179.

Taylor, R.G., Tindimugaya, C., Barker, J.A., Barrett, M.H., Macdonald, D.M., Howard, G., Kulabako, R., Nalubega, M., and Rwarinda, E.M (in prep.). Groundwater flow and storage in weathered crystalline rock:evidence from Uganda. Groundwater.

Temple, H.P (1971). The Lakes of Uganda. In Ominde (editor): Studies in East African Geography and Development. Heinemann, London, UK, pp273.

Tindimugaya, C (2000). Assessment of groundwater development potential for Wobulenzi town, Uganda. Unpublished Master's Thesis, International Institute for Infrastructural, Hydraulic and Environmental Engineering, IHE Deft, Netherlands.

Tumulinson, G. L., Osiensky, L. J. and Fairley, P. J (2006). Numerical evaluation of pumping well transmissivity estimates in laterally heterogeneous formations. Hydrogeology Journal, Vol. 14, pp21- 30.

Tweed, O.S., Weaver, R.T. and Cartwright, I (2005). Distinguishing groundwater flow paths in different fractured-rock aquifers using groundwater chemistry: Dendonong Ranges, southeast Australia. Hydrogeology Journal, Vol, 13, pp771- 789.

Vandenbohede, A. and Lebbe, L (2003). Combined interpretation of pumping and tracer tests: theoretical considerations and illustration with a field test. Journal of Hydrology, Vol. 277, No. 1, pp134-149.

van der Lee, J. and Gehrels, J.C (1990). Modelling Aquifer Recharge: Introduction to the Lumped Parameter model, EARTH. Unpublished Hydrological report. Free University of Amsterdam, The Netherlands.

van Tonder, G.J., Botha, J.F. and van Bosch, J (2001). A generalized solution for step-drawdown tests including flow dimension and elasticity. Water SA, Vol. 27, No. 3, pp345 - 354.

Veevers, J.J (1977). Rift arch basins and post-break up rim basins on passive continental margins. Tectonophysics, Vol. 41, ppT1 - T5.

Viville, D., Ladouche, B. and Bariac, T (2006). Isotope hydrological study of mean transit time in the granitic Strengbach catchment (Vosges massif, France) : application of the FlowPC model with modified input function. Hydrological processes, Vol. 20, pp1737 - 1751.

Walker, D. D. and Roberts, M. R (2003). Flow dimension corresponding to hydrogeologic conditions. Water Resources Research, Vol. 39, No. 12,1349, pp7-1 - 7-8.

Walker, S.J., Weiss, R.F. and Salameh, P. K (2000). Reconstructed histories of the annual mean atmospheric mole fractions for the halocarbons CFC-11, CFC-12, CFC-113 and carbon tetrachloride. Journal of Geophysical Research, Vol. 105, pp14,285 - 14,296.

Warner, M.J. and Weiss, R.F (1985). Solubilities of chloroflurocarbons 11 and 12 in water and sea water. Deep – Sea Research, Vol. 32, No. 12, pp1485 - 1497.

Weiss, W. and Roether, W (1980). The rates of tritium input to the world oceab. Earth Planet Science letter, Vol. 49, pp435 - 446.

Wilkes, M.S., Clement, T.P. and Otto, J.C (2004). Characterisation of the hydrogeology of the Augustus River catchment, Western Australia. Hydrogeology Journal, Vol, 12, pp209 - 223.

Wright, E. P. and Burgess, W. G. (Eds.) (1992). The Hydrogeology of Crystalline Basement Aquifers in Africa. Geological Society Special Publications, 66. London.

Wright, E.P (1992). The hydrogeology of crystalline basement aquifers in Africa. In: Wright, E.P. and Burgess, W.G. (Eds.), Hydrogeology of crystalline basement aquifers in Africa. Geological Society Special Publication No. 66, pp1 - 27.

Zinn, B.A. and Konikow, L. F (2007). Effects of intraborehole flow on groundwater age distribution. Hydrogeology Journal, Vol. 15, pp633- 643.

Zuber, A., Weise, M.S., Motyka, J., Osenbruck, K. and Rozanski, K (2004). Age and flow pattern of groundwater in a Jurassic limestone aquifer and related Tertiary sands derived from combined isotopes, noble gas and chemical data. Journal of Hydrology, Vol. 286, pp87- 112